Volume 46, December 2012

New Mexico

JOURNAL OF SCIENCE

New Mexico's Water Resources

Kurt S. J. Anderson
Editor

New Mexico Academy of Science

Volume 46, November 2012

NEW MEXICO JOURNAL OF SCIENCE

New Mexico's Water Resources

The *New Mexico Journal of Science* is intended to be the annual publication of the New Mexico Academy of Science. Each issue of the *Journal*, which began publication in 1960, contains research papers and review articles deemed of interest to the scientists, educators, and citizens of New Mexico. Some volumes have addressed topics of historical, social, or economic interest to those readers while others have emphasized scientific areas in which New Mexico is particularly active. Authors have usually been drawn from the universities, colleges and other research institutions of New Mexico.

This year's *Journal* is subtitled "New Mexico's Water Resources". Each of the papers in this volume has been examined by one or more expert reviewers and has undergone some revision before being accepted for publication. Our referees, as are our authors, are drawn from New Mexico's scientific, educational, and legal communities. Indeed, most of our reviewers were also contributors to this *Journal*. The Editor wishes to thank those anonymous referees for their efforts toward maintaining the quality of this publication. The research works presented here reflect their many helpful criticisms, comments and suggestions.

I also gratefully acknowledge the efforts of our Editorial Assistant, Ms. Amanda Medina, who helped to assemble the various pieces of this publication into a reasonably coherent whole.

As was the case with the previous volume of this *Journal*, "New Mexico's Water Resources" will not be published as a paper edition. This partly reflects the increasing costs of printing and distribution of paper copies - and the shortage of funds to cover such costs. This volume of the *Journal* will be available as an electronic version which can be downloaded from the New Mexico Academy of Science's web site at http://www.nmas.org Some earlier volumes of the *Journal* can also be found here in electronic format, and paper copies of some of these are also available for purchase. We intend to make "hard copies" of the *Journal* available in a CD format to members of the New Mexico Academy of Science.

Kurt S.J. Anderson, Editor
New Mexico Journal of Science
Department of Astronomy, New Mexico State University
kurt@nmsu.edu

The New Mexico Academy of Science

The New Mexico Academy of Science (NMAS) was founded in 1902, ten years before New Mexico became a state, and has been in continuous existence since 1915. The goals of the Academy are to promote science and science education within New Mexico; to improve communication among scientists, educators, students, public officials, and the general public; to recognize the achievements of scientists, science educators, and science students; to encourage scientific research; and to increase public awareness of the role of science in human progress and human welfare.

The NMAS is a non-profit organization registered with the New Mexico State Corporation Commission. It is a member of the National Association of Academies of Science (NAAS) and an affiliate of the American Association for the Advancement of Science (AAAS).

We serve as a public voice for science in New Mexico and support several programs and activities in support of our goals. These include

* The Junior Academy of Science
* Outstanding New Mexico Science Teacher Awards
* Public Lectures and Events
* New Mexico Journal of Science
* The NMAS Quarterly Newsletter
* Annual Meeting & Distinguished Lecturer Program

Membership in the New Mexico Academy of Science is open to anyone engaged in scientific research or science education or who has an interest in these activities. A membership applications as well as additional information about the Academy and its programs can be found at http://www.nmas.org.

Correspondence can be addressed to nmas@nmas.org or to

The New Mexico Academy of Science
c/o The New Mexico Museum of Natural History and Science
1801 Mountain Road NW
Albuquerque, NM 87104

The New Mexico Academy of Science

Officers and Executive Board 2012

Elected Officers

President: Mr. Jesse Johnson
President-Elect: Dr. Kurt S. J. Anderson
Vice President: Dr. Michaela Buenemann
Treasurer: Mr. David Duggan
Secretary: Mrs. Mona H. Pomeroy
Past President: Dr. Marvin Moss
Director at Large: Dr. Angela Wandinger-Ness
Director at Large: Mr. Hal Behl

Programs & Directors

NMAS Awards Program: Mr. Harry F. Pomeroy, Jr.
Junior Academy of Science: Mrs. Lynn Brandvold
Editor, NMAS Newsletter: Ms. Jayne C. Aubele
Editor, New Mexico Journal of Science: Dr. Kurt Anderson
Education Programs: Dr. Marshall Berman
Coordinator, National Youth Science Camp: Dr. Richard Nygren
Web Master: Mr. David Duggan
Publicity: Ms. Ruth Duggan
Legal: Dr. Melvin Eisenstadt, J.D.
Director Emeritus: Dr. David Hsi
SWARM, AAAS, and NAAS Delegate: Mrs. Lynn Brandvold
NMMNHS Representative: Ms. Jayne C. Aubele

CONTENTS

****

REMOTE SENSING OF AGRICULTURAL WATER USE IN NEW MEXICO: FROM THEORY TO PRACTICE

Z. Samani, R. Skaggs
A. Bawazir, M. Bleiweiss, V. Tran, and A. Piñon[1]

ABSTRACT

Irrigated agriculture in New Mexico is facing increased competition for use of scarce water resources as well as growing demands for water conservation. Irrigated areas in the state are undergoing water rights adjudication, varying degrees of urbanization, a changing structure of agriculture, and ongoing drought. As a result of recent remote sensing technological advances it is now possible to accurately and inexpensively assess crop water consumption on individual fields and farms. This technology is being used in New Mexico and is providing new insight into real-world on-farm water use in the state and has resulted in a dramatic increase in our understanding of and accountability for agricultural water use in New Mexico. Remote sensing research indicates there is great variability in crop water use in New Mexico, including for the same crops produced in the same area. Few farms in the state are irrigated at consumptive use levels considered theoretically optimal or consistent with potential or maximum yields. Under (or deficit) irrigation in the state is a function of technological, agronomic, and management constraints, and also influenced by crop quality and other farm-level objectives. Increased crop consumptive use would result in additional total depletion of New Mexico's ground and surface water supplies. Efforts to "conserve" water by promoting modern irrigation technologies have the potential to reduce the gap between New Mexico farms' actual and theoretically optimal levels of crop water use, but also will result in additional depletion which can jeopardize aquifer sustainability and downstream obligations. Adjudication of water rights consistent with theoretically optimal crop consumptive use rather than actual historical use has implications for long-run hydrologic sustainability, water resource equity, and conservation.

---

[1] Professor, Civil Engineering, zsamani@nmsu.edu; Professor, Agricultural Economics, rskaggs@nmsu.edu; Associate Professor, Civil Engineering; Science Specialist, Entomology, Plant Pathology, and Weed Science; Graduate Research Assistants, Civil Engineering; all with New Mexico State University, Las Cruces, NM, 88003. Corresponding authors are Samani and Skaggs.

THE NEED FOR WATER ACCOUNTABILITY

Water resource accountability in New Mexico has never been more important than it is today. It is critical that the state's residents have accurate data and information with respect to who uses water and how much water is used. Distribution of water consistent with existing legal entitlements is possible only in the presence of a functional accountability framework and the data to support it. At the current time, accounting for water use throughout much of New Mexico is inadequate or non-existent, owing to institutional and legal structures, lack of resources, as well as established, customary practices. Lack of water use accountability may be cheap in the short run, but it contributes to a naïve, informal, and shadowy water resource management structure. Lack of water accounting, data, and information encourages speculative water claims, contributes to the perpetuation of inadequately defined property rights, and incentivizes water use in excess of legal entitlements. Lack of water accounting and accountability imperils long-run hydrologic sustainability in the state.

Various methods have been developed for estimating crop evapotranspiration (e.g., the amount of water consumptively used by a crop). Evapotranspiration (ET) estimates can be made using commonly accepted crop coefficient techniques, eddy covariance methods incorporating data obtained using flux towers, by soil moisture monitoring, or with lysimeters. Crop coefficient methods provide standard ET estimates that are largely theoretical, while the other tools and methods provide a small number of point measurements of ET. ET estimates for a specific crop or vegetation type are usually scaled up to regional or basin scales from a handful of controlled research or data collection sites. In the past, estimation of ET at the broad scale, for multiple sites, at different times, under different crop production regimes or irrigation technology and infrastructure has not been possible due to resource constraints. Thus, assumptions regarding agricultural water use incorporated into regional water planning, adjudications, policies, and disputes have been based on hypothetical information.

It is conventionally assumed that agriculture "wastes" water due to inefficient irrigation practices and obsolete technologies. It is also further assumed that farmer adoption of modern irrigation practices and technologies would "conserve" significant quantities of water in New Mexico, as well as "release" water for other uses and users. The public policy response has been programs that subsidize farmer and irrigation district modernization and technology adoption. Another conventional notion about farmers who produce irrigated crops is that they are similarly motivated as farm owners or operators and all seek to produce the highest potential yields. Irrigation development and policy throughout the western United States have been founded on the notion that there is some standard level of crop ET which defines "successful" crop production and which characterizes most farmers' production and management objectives and conditions. While standardized assumptions about farm-level water use based on optimal or near-optimal conditions are cheap and easy, their continued use in New Mexico water planning, adjudications, policies, and disputes is dangerous, misleading, and not necessary at the current time.

The objective of this paper is to provide an overview of research using remote sensing technology to assess crop water use in New Mexico's Lower Rio Grande Valley (LRGV). This research is providing data and information that challenge many conventional assumptions regarding agricultural water use in New Mexico. The research has been underway for almost ten

years and has received financial support from numerous sources.[2] Due to space limitations, complete discussion of research methods and results will not be presented here, but can be found in the authors' original publications cited in this article. The potential for improved water accountability and hydrologic sustainability in New Mexico is greatly increased as a result of this research and the public investments which have supported it.

REMOTE SENSING OF CROP WATER USE

Techniques for estimating crop evapotranspiration using remotely-sensed data have been under development for several years and applied throughout the world. The Regional ET Estimation Model (REEM) developed at New Mexico State University has been used to measure crop ET on thousands of fields in the LRGV over the last decade (Samani *et al*. In Press; Samani *et al*. 2009; Samani *et al*. 2007a; Samani *et al*. 2006). REEM is based on the surface energy balance similar to that presented by Bastiaannssen (1995) and Allen *et al*. (2007) with the latent heat flux (LE) determined as a residual of the surface energy equation:

$$LE = R_n - G - H \quad (1)$$

where, LE is the latent heat flux, R_n is the net radiation flux at the surface, G is the soil heat flux and H is the sensible heat flux.

Daily net radiation (R_n) over a crop canopy is calculated using methodology developed by Samani *et al*. (2007b) as:

$$R_n = R_{ni}\left(\frac{R_s}{R_{si}}\right)\left(\frac{T_a}{T_i}\right)^4 \quad (2)$$

where, R_n is the daily net radiation in MJ/m^2/day, R_{ni} is instantaneous clear sky net radiation (W/m^2), R_s is daily short wave solar radiation (MJ/m^2/day), R_{si} is the instantaneous short wave solar radiation (W/m^2), T_a is average daily temperature in Kelvin (K), and T_i is the instantaneous air temperature (K).

Instantaneous net radiation (R_{ni}) is calculated after Campbell (1977):

$$R_{ni} = (1-\alpha)R_{si} + RL\downarrow - RL\uparrow \quad (3)$$

where, R_{ni} is instantaneous net radiation (W/m²), R_{si} is instantaneous incoming short wave radiation (W/m²), RL↓ is instantaneous effective incoming long wave radiation (W/m²), RL↑ is instantaneous outgoing long wave radiation (W/m²), α is surface albedo (dimensionless). Effective incoming long wave radiation (RL↓) is calculated using Stefan-Boltzmann Law (Unsworth and Monteith 1975) as:

[2] Funding sources include the "Efficient Irrigation for Water Conservation in the Rio Grande Basin" project (a joint project of the Texas A&M University System Agriculture Program and New Mexico State University), the New Mexico Governor's Water Innovation Fund, the New Mexico Agricultural Experiment Station, Western Pecan Growers' Association, the U.S. Environmental Protection Agency, the U.S. Geological Survey, and the New Mexico Water Resources Institute.

$$RL\downarrow = \varepsilon_{eff} \times \sigma \times T_i^4 \quad (4)$$

where, ε_{eff} is effective atmospheric emissivity, σ is Stefan-Boltzman constant (5.67×10^{-8} $W/m^2/K^4$), T_i is instantaneous near surface air temperature (K). Effective atmospheric emissivity (ε_{eff}) is calculated using the product of atmospheric emissivity and surface emissivity ($\varepsilon_a x \varepsilon_o$). Atmospheric emissivity (ε_a) is calculated using an equation by Bastiaanssen (1995) as:

$$\varepsilon_a = 0.85 \times \left(-\ln \tau_{sw}\right)^{0.09} \quad (5)$$

where, τ_{sw} is the atmospheric transmissivity calculated from elevation (Allen *et al*. 1998). Surface emissivity (ε_o) is calculated after Tasumi (2003) where, $\varepsilon_o = 0.95 + 0.01$ LAI when LAI < 3 and $\varepsilon_o = 0.98$ when LAI ≥ 3, where LAI is leaf area index. The LAI is the ratio of total upper leaf surface area of vegetation divided by the surface area of the land on which the vegetation grows (m^2/m^2).

The instantaneous outgoing long wave radiation ($RL\uparrow$) is calculated using Stefan-Boltzmann Law:

$$RL\uparrow = \varepsilon_o \times \sigma \times T_s^4 \quad (6)$$

where, T_s is surface temperature (in K).

Satellite data from Landsat-5 and Landsat-7 are used to calculate Normalized Difference Vegetation Index (NDVI, equation 7), albedo, and surface temperature for the study site in the LRGV. The LANDSAT sensor makes multispectral observations in seven wavelength regions, with usable images varying by year. The remote sensing software package ENVI®, by Research Systems Inc., Boulder, Colorado and its many tools are used for REEM data processing.

NDVI is calculated using the following equation:

$$NDVI = \frac{\rho_{nir} - \rho_{red}}{\rho_{nir} + \rho_{red}} \quad (7)$$

where, ρ is surface reflectance for Landsat-5 Thematic Mapper (TM) and Landsat-7 Enhanced Thematic Mapper Plus (ETM+), the near-infrared (nir) band is band 4 and the red band is band 3.

Albedo (α) is calculated using the methodology described by Liang *et al*. (2002):

$$\alpha = 0.356\rho_1 + 0.13\rho_3 + 0.373\rho_4 + 0.085\rho_5 + 0.072\rho_7 - 0.0018 \quad (8)$$

where, ρ_i is the reflectance in band i.

The thermal radiation observed by satellite is converted to T_s using a methodology proposed by Barsi *et al*. (2005):

$$L_{TOA} = \tau\varepsilon_o L_T + L_u + \tau\left(1-\varepsilon_o\right)L_d \quad (9)$$

where, L_{TOA} is the space-reaching or top of atmosphere (TOA) radiance measured by the satellite instrument, τ is the atmospheric transmissivity, L_T is the target radiance with a blackbody surface emissivity of 1, L_u is the upwelling or atmospheric path radiance, and L_d is the downwelling or sky radiance. Radiances are in units of W/(m^2 sr μm) and the transmissivity and emissivity are unitless. The web-based calculator (http://atmcorr.gsfc.nasa.gov/) is used to determine the atmospheric correction parameters necessary to complete the process. The calculator provides the necessary parameters for equation 9 with the exception of surface emissivity, ε_o. The L_T is determined by rearranging equation 9 as follows:

$$L_T = \left[L_{TOA} - L_u - \tau\left(1-\varepsilon_o\right) L_d \right] / \tau\varepsilon_o \tag{10}$$

L_T is then converted to radiometric temperature at the surface (T_s) using the Planck equation:

$$T_s = K_2 / \ln\left(1 + K_1 / L_T\right) \tag{11}$$

where, K_1 equals to 666.09 and 607.76 for Landsat-7 and Landsat-5, respectively, and K_2 equals 1282.71 and 1260.56 for Landsat-7 and Landsat-5, respectively (Barsi *et al*. 2005).

Using ground heat flux data ranging from 35 W/m² to 150 W/m² and NDVI ranging from 0.20 to 0.85, Samani *et al*. (2006) developed the following equation to estimate instantaneous soil heat flux (G_i) at the time of satellite overpass:

$$\frac{G_i}{R_{ni}} = 0.26e^{(-1.97\,NDVI)} \tag{12}$$

The instantaneous sensible heat flux (H_i) is calculated by combining the bulk aerodynamic equation with Monin-Obukhov similarity theory (Foken 2006). The bulk aerodynamic equation is defined as:

$$H_i = \rho_a C_p \frac{T_o - T_a}{r_{ah}} = \rho_a C_p \frac{dT}{r_{ah}} \tag{13}$$

where, ρ_a is the air density (kg/m^3), C_p is specific heat of air (1004 J/kg/K), T_o is the aerodynamic surface temperature in Kelvin (K), T_a is the air temperature (K), r_{ah} is the aerodynamic surface resistance, and dT is the air temperature gradient calculated using a linear function described by Bastiaanssen (1995):

$$dT = aT_s + b \tag{14}$$

where, a and b are calibration constants that are empirically determined by using reference extreme points on the ground. Calibration of equation 14 requires a minimum of two points on the ground where dT values can be calculated from sensible heat (H_i) fluxes using equation 13. In LRGV REEM studies, two sensible heat values have been used. One sensible heat value is measured using a one-propeller eddy covariance (OPEC) system in a well-watered field, while the other sensible heat value is estimated for a dry fallow field with no vegetation by setting instantaneous latent heat (LE_i) equal to zero and estimating instantaneous R_{ni} and ground flux G_i

from equations 3 and 12. The H_i value for the dry field is then calculated as a residual of the energy balance as:

$$H_i = R_{ni} - G_i \quad (15)$$

The aerodynamic resistance (r_{ah}) in equation 13 is calculated using wind speed extrapolated from blending height of 200 m and an iterative stability correction based on Monin-Obukhov similarity theory (Bastiaanssen 1995; Allen *et al*. 2007).

Once the values of "a" and "b" in equation 14 are estimated, the sensible heat flux at the time of satellite overpass is calculated for each pixel using equations 13 and 14. During the calculation of sensible heat flux, each pixel's r_{ah} value is calculated iteratively as described earlier. The other components of the energy, R_{ni} and G_i, for the time of satellite overpass are calculated using equations 3 and 12.

The evaporative fraction (E_f) for each pixel is defined as the ratio of the latent heat flux to the available energy and is calculated using the values of H_i, G_i, and R_{ni}:

$$E_f = \frac{R_{ni} - G_i - H_i}{R_{ni} - G_i} \quad (16)$$

Once the evaporative fraction is calculated and assuming the evaporative fraction is constant over the 24-hour period, daily ET is calculated by multiplying E_f by daily available energy as:

$$ET = E_f (R_n - G) \quad (17)$$

Assuming negligible daily G (Allen *et al*. 1998), daily ET is calculated by multiplying E_f by daily net radiation (R_n).

ET for individual fields and farms in New Mexico's LRGV for year 2011 and locations of eddy covariance flux towers and weather stations are shown in figure 1. Annual ET amounts for fields in the region range from 200 mm (equivalent to rainfall for a non-cultivated field) to 1500 millimeters (equivalent to ET for a mature well managed pecan field) are illustrated in figure 1. Annual or seasonal ET totals for individual fields are calculated through estimating daily ET with REEM and interpolating around clear days for which satellite images are available. REEM-estimated ET results compare favorably with site-specific ET measured using eddy covariance methods and flux tower technology (Samani *et al*. 2009)

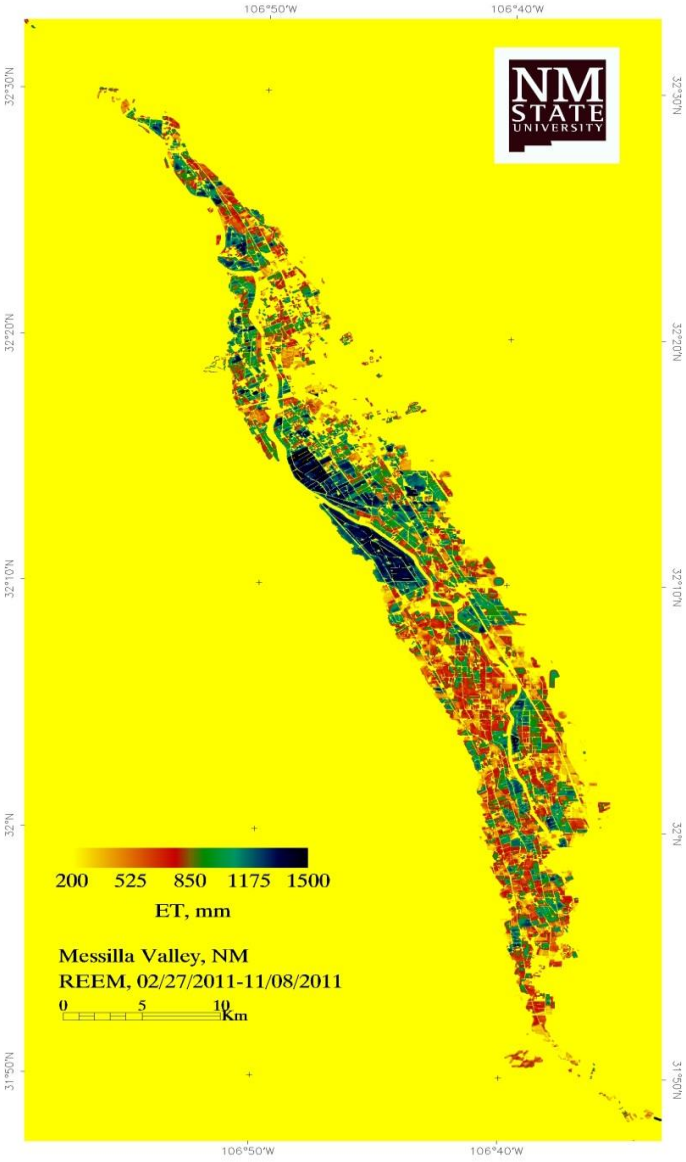

Figure 1. ET distribution in New Mexico's Lower Rio Grande Valley (LRGV) for year 2011 and location of eddy covariance flux towers and weather stations.

ASSUMPTIONS VS. REALITY

REEM has been used to estimate annual ET for all major agricultural crops grown in the LRGV for several different years between 2002 and 2011; however, REEM research has focused on pecans and alfalfa because those crops are produced on a majority of the region's irrigated acreage. The standard crop coefficient approach for estimating ET for these two crops in the LRGV results in consumptive use values of 55.2 acre-inches/acre (4.6 acre-feet/acre) for alfalfa and 51.6 acre-inches/acre (4.3 acre-feet /acre) for pecans (figure 2). These ET values are for healthy, disease-and-insect-free, actively growing, well-watered, and overall well-managed crops. These ET values are typically assumed for farms and farmers who are properly irrigating and successfully producing these crops (Skaggs *et al*. 2011). Theoretical ET values shown in

figure 2 were estimated using methods outlined by Allen *et al*. (1998), and are based on textbook assumptions infrequently present on actual farms and fields. Such theoretical ET values are the foundation of water duties (e.g., the quantities of water attached to water rights) throughout the western United States, including in New Mexico.

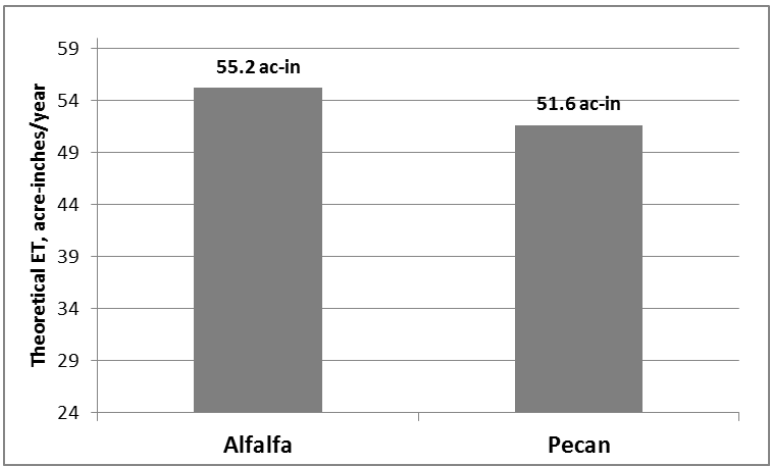

Figure 2. Theoretical annual ET for alfalfa and pecans
in New Mexico's LRGV, 2002, calculated using crop coefficient method.

As noted above, there are many conventional assumptions about agricultural water use in New Mexico. One of the principle assumptions is that crop ET is relatively homogeneous between farms and farmers, and thus theoretical ET, or ET measured at a specific farm or site, is representative of most farms. REEM results for major LRGV crops do not support this assumption and instead show widespread deficit irrigation. Figures 3-6 show remotely-sensed estimates of annual ET for 423 alfalfa fields and 246 pecan orchards in 2002 (a full allotment year in the Elephant Butte Irrigation District). These results illustrate the diversity of farms, fields, and farmers in the LRGV, as well as the folly of assuming a "standard" ET for any crop in the region.

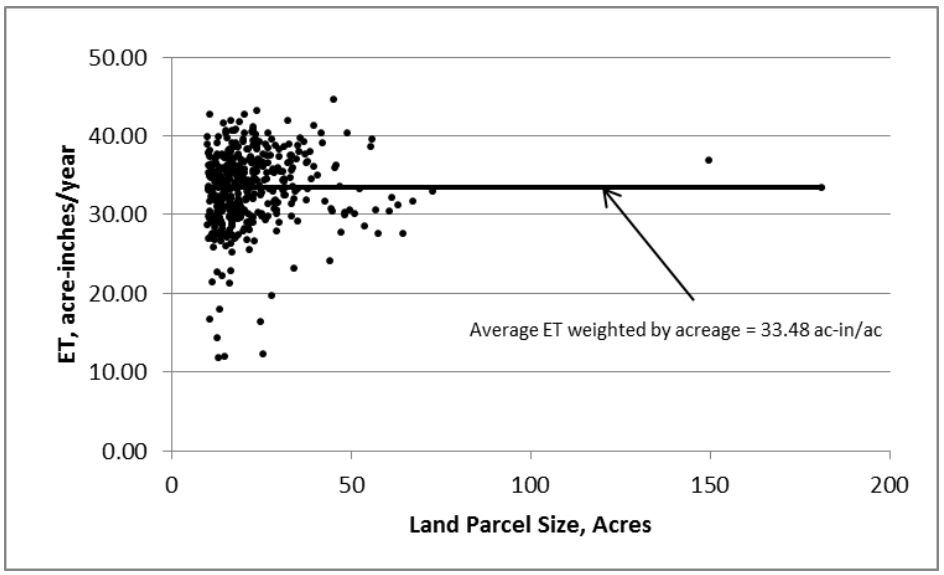

Figure 3. Remotely-sensed estimates of annual alfalfa ET (acre-inches) for 423 LRGV fields (>10 acres) by field size, 2002.

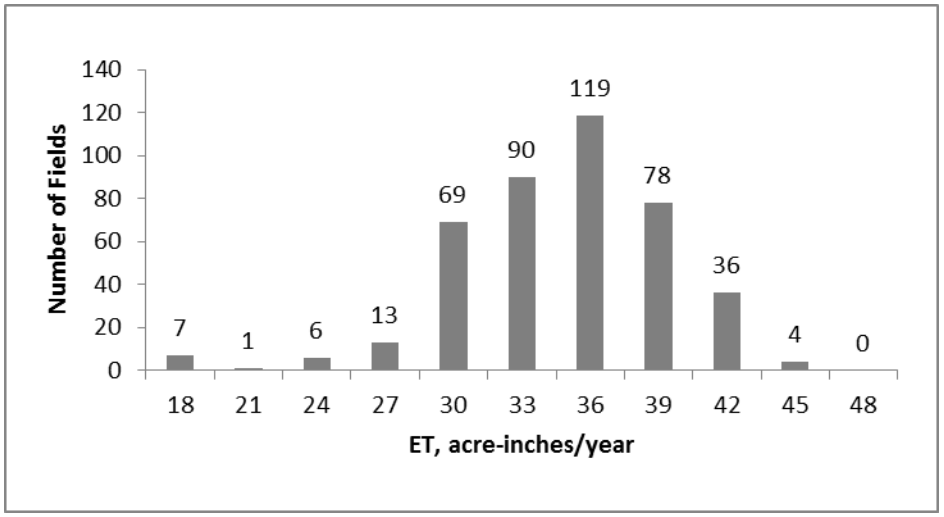

Figure 4. Distribution of remotely-sensed estimates of annual alfalfa ET (acre-inches) for 423 LRGV fields (>10 acres), 2002.

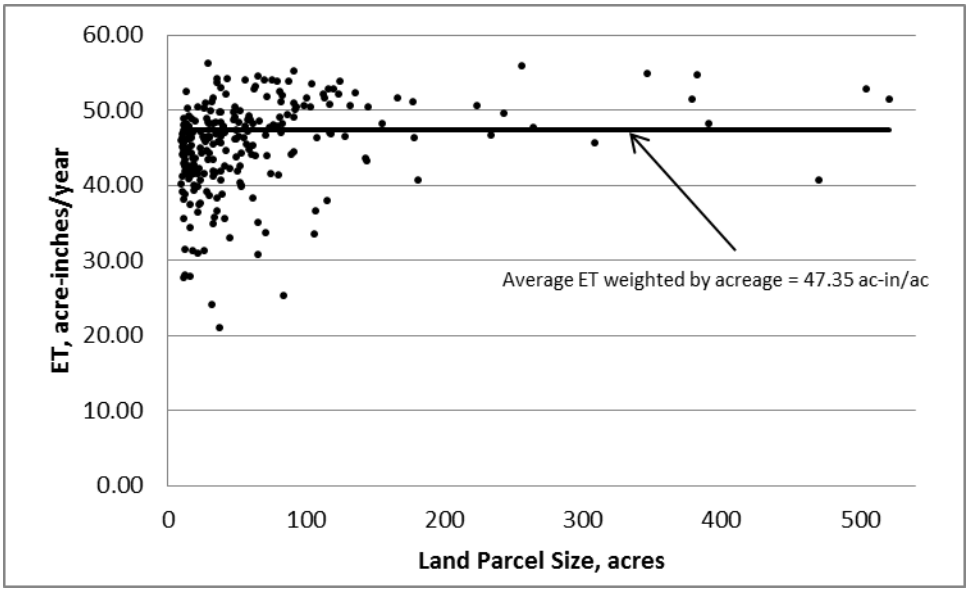

Figure 5. Remotely-sensed estimates of mature annual pecan ET (acre-inches) for 246 LRGV orchards (>10 acres) by orchard size, 2002.

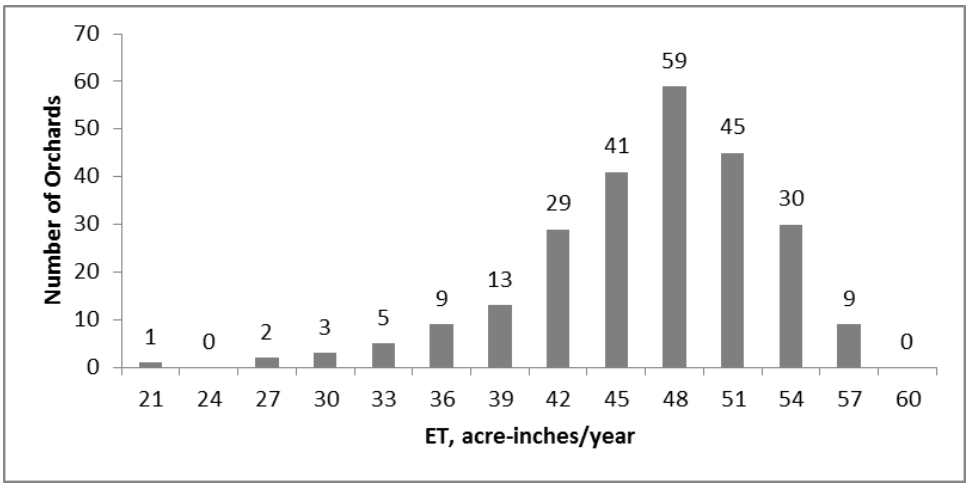

Figure 6. Distribution of remotely-sensed estimates of pecan annual ET (acre-inches) for 246 mature LRGV orchards (>10 acres), 2002.

Real-world production and management conditions in the LRGV are heterogeneous and rarely result in crop consumptive use at the theoretical (e.g., optimal or near-optimal) levels shown in figure 2. Comparison of figure 2 with the distributions of ET in figures 4 and 6 shows that few LRGV fields have ET levels consistent with the theoretical annual ETs calculated using crop coefficient methods and that most fields are deficit irrigated. The other key conclusion from figures 3-6 is the extreme variability in ET for the region's two largest crops. There are several reasons for the variability in annual crop ET (and thus yields) in the LRGV. The fundamental reason has to do with the random nature of farming and crop production. Farmers' abilities, objectives, resources, and resource constraints vary; thus, not all farmers can or seek to do a "perfect" job of growing a crop and achieve theoretical or potential ET and thus theoretical

or potential yield (Skaggs *et al*. 2011; Skaggs and Samani 2005). A few farmers grow their crops under optimal or near optimal conditions while most farmers produce under different, sub-optimal conditions. These differences will manifest in a range or distribution of ET and yield outcomes, with a majority of farmers achieving approximately average ET, crop yield, crop quality, and economic outcomes. The histograms of alfalfa and pecan ET shown here for hundreds of fields are, therefore, normally distributed due to variable farmer abilities, objectives, resources, and constraints.

The real-world crop water use illustrated in figures 3-6 for the LRGV varies due to several factors, including:

- Lack of sufficient groundwater to supplement surface water supplies on individual farms;
- Limited or no access to groundwater of adequate quality on many farms;
- Lack of knowledge of crop water consumptive use, soil-water-plant relationships, and associated benefits of irrigating to meet consumptive use demands at different stages of crop growth;
- Inability of the existing canal system to delivery surface water in a timely manner;
- Poor irrigation practices (e.g., non-uniformity of water application);
- Low volume of inflow and poor on-farm water distribution systems;
- Variability in soil physical and chemical properties
- Issues related to agronomic practices such as timing of flood irrigations and harvest operations;
- Crop quality objectives that supersede crop yield objectives;
- Non-commercial farmer economic motivations which preclude investments in and adoption of improved irrigation technology and practices and changes in overall farm management.

As noted above, it is commonly assumed that inefficient agricultural irrigation in New Mexico wastes water, and New Mexico irrigators must modernize their water delivery and on-farm irrigation technologies in order to conserve the state's water resources. However, remote sensing results indicate that most fields and farms in the LRGV are deficit-irrigated. This means that consumption of water by crops in the region is below levels that would achieve yields which could be obtained at higher, potential ET levels. Improvements to the region's canal system or adoption of efficiency-enhancing on-farm irrigation practices and technologies would likely increase farm-level crop consumptive use. Thus, given the variability of current crop ET, water conservation investments in the LRGV are likely to increase total agricultural water depletion in the region because "sloppy" or inefficient upstream water management is a source of downstream water users' supply (Samani and Skaggs 2008). There is little room in the LRGV for dramatic reductions in agricultural consumptive use unless irrigated acreage is significantly reduced or crop yields are further reduced. On-farm irrigation or water delivery system efficiency improvements designed to "conserve" water and release it for other uses will instead sustain or increase total agricultural depletion.

IMPLICATIONS

These results show that the ET of virtually all alfalfa and pecan fields in the LRGV is lower than potential ET. Results presented here are for 2002, the last full allocation year before the current drought period began. Remote sensing estimates of pecan and alfalfa ET in the LRGV for years since 2002 consistently show the same variability and distribution for hundreds of fields and orchards. Few LRGV fields and orchards have been or are currently irrigated at theoretically estimated potential ET levels. Theoretical equations for calculating crop ET are for crops growing under optimal conditions where there are no limiting factors such as nutrient and water deficiency, salinity, disease, or pest problems. In addition to agronomic and technical factors, marginal economic returns diminish as crops approach peak yield and further influence irrigation below theoretically optimal ET levels. Alfalfa's cutting and baling schedule also influences yield and overrides the irrigation schedule. Furthermore, alfalfa fields harvested to meet dairy hay quality requirements will not be the highest yielding fields given the tradeoff between hay quality and yield, with the yield sacrifice reducing alfalfa ET (Orloff and Putnam 2007).

In the LRGV there are many factors which influence irrigation and ET at the field-level. A variety of constraints and farmer objectives influence ET and yields in the region (as well as in other irrigated basins). The assumption that farmers can and will use their resources (specifically, irrigation water) to achieve maximum potential (or theoretically optimal) yields is not consistent with economic behavior, although it may be appealing from engineering and agronomic perspectives. Under-irrigation is economically rational when irrigation water is limited in supply and not free. Recommendations, public policy, and investments for building new irrigation systems as well as improving existing irrigation systems are founded on the notion that individual farmers should and do want to achieve potential ET and yields and that society will be better off with irrigation systems that meet full crop water demands. However, engineering and agronomic criteria for optimal irrigation are likely to be inconsistent with farm level economic decisions, irrigation practices, and irrigation outcomes.

Under-irrigation in the LRGV is also a function of resource limitations and constraints related to the nature of the crop being irrigated; however, dealing with these limitations and constraints presents hydrologic as well as economic dilemmas. For example, because of frequent drought-induced water shortages in the LRGV and growing demands to transfer water out of agriculture to other uses, it is often speculated that the implementation of modern drip and sprinkler irrigation systems would result in water savings by ending "wasteful" surface irrigation practices. The results of this study show that the majority of alfalfa and pecans are produced under water deficit conditions. Thus, widespread adoption of modern "water saving" irrigation technologies would most likely result in additional consumptive use by crops. This would further stress the LRGV's limited water resources, reduce groundwater recharge, and impair downstream flows, even though it could increase individual farmers' incomes if their crop yields and quality increased.

Basin adjudications are frequently founded on the notion that water rights should be established for the potential ET of full crop water demand. For example, the LRGV is currently undergoing adjudication, and claims for farm delivery requirements are being made on the basis of theoretical annual potential ET (Skaggs *et al*. 2011). The results reported here for alfalfa and pecans are significant with respect to the LRGV adjudication process. If basin-wide water rights

are adjudicated based on crop coefficients for optimally managed fields, this would most likely result in over-allocation of water resources with serious consequences for groundwater depletion and downstream water delivery obligations. Water rights adjudication based on theoretical crop water use rather than a basin's historical, long-run average water use could result in extreme water deficits, groundwater overdraft, reduced downstream deliveries, further divergence between wet and paper water quantities in already over-appropriated basins, and compromised hydrologic sustainability. A more realistic approach would be to determine the average historical consumptive use using consistent remote sensing techniques applied to historical satellite images.

Historic beneficial use of surface and groundwater determines non-tribal water rights in New Mexico. Water rights are defined both in terms of consumptive irrigation requirements and farm delivery requirements. Long-term sustainability of the state's hydrologic system is a function of the state's actual past water use. Using remotely sensed data, we now have the ability to accurately estimate historic and current basin-wide water use across the spectrum of crop production conditions, rather than rely on the fiction of widespread, optimal, consistent, well-watered crop production conditions.

In previous articles we asserted that accurate accounting of basin-wide water use is essential in New Mexico and elsewhere in order to get serious about water conservation and equitably distribute water resources based on existing legal entitlements (Samani and Skaggs 2007, 2008). Both short and long-run hydrologic sustainability require accurate basin-wide water accounting. Over-appropriation is exacerbated by continued use of crop ET theories disconnected from reality. We have stated that hydrologic ignorance resulting from the lack of rigorous water measurement and accounting undermines water equity and efficiency (Samani and Skaggs 2008). Much of our ignorance about water is disappearing as new technologies become available that can cheaply and quickly measure consumptive use. Remote sensing research at New Mexico State University is generating data that challenge conventional assumptions about crop water use in the LRGV. This research is contributing to the reality-based assessment and discussion of how water is used in New Mexico, as well as basin-level hydrologic sustainability. Crop production is subject to nature, farm-level resources vary (including supplemental ground water, soil type, labor, time, money, knowledge, etc.), water delivery systems have constraints, and farmers have diverse objectives. Remotely-sensed estimates of alfalfa and pecan ET in the LRGV show great variability in crop water use. Application of theoretical ETs in irrigation system design or rehabilitation, in recommendations for improved irrigation practices or technology, or in water rights adjudications will result in overestimation of crop water use.

Most LRGV alfalfa and pecan producers are unlikely to ever make major investments in modern irrigation technology or significantly change their irrigation management and cultural practices due to the changing structure of the region's agriculture (Skaggs *et al*. 2011). Farm-level economic decisions clearly involve mental models at odds with engineering or agronomic "best practices" and reflect the diversity of outcomes inherent in any complex system. Incorporating this reality into current water resource policy, public and private investments, programs, and adjudications is strongly recommended.

Our primary concern as New Mexico residents and water resource researchers is that water over-appropriation or over-allocation not be made any worse than it already is in the state

(Skaggs *et al*. In Press). Historical and actual beneficial use of water in agriculture in New Mexico is unlikely to ever align with theoretical notions of how much crops should or can consume. Hydrologic balances founded on long-run historically average agricultural water use are likely to be disturbed by higher levels of depletion, and LRGV hydrologic sustainability is at risk if fantastical, hypothetical estimates of agricultural ET in the region continue to be used in water planning, policy, and adjudications.

RESOURCES

Allen, R.G., L.S. Pereira, D. Raes, and M. Smith (1998). Crop evapotranspiration: Guidelines for computing crop water requirements. Food and Agriculture Organization. FAO Irrigation and Drainage Paper No.56. Rome, Italy.

Allen, R.G., M. Tasumi, and R. Trezza (2007). Satellite-Based Energy Balance for Mapping for Evapotranspiration with Internalized Calibration. ASCE J. Irrig. and Drain. Engrg. 133(4): 380-394.

Barsi, J.A., J.R. Schott, F.D. Palluconi, and S.J. Hook (2005). Validation of a web-based atmospheric correction tool for single thermal band instruments. In J.J. Butler (Ed.), Earth observing systems X; proceedings of SPIE Conference, 5882, San Diego, July 31-Aug. 2, 2005. Bellingham, WA: Society of Photo-optical Instrumentation Engineers (SPIE), pp.136-142.

Bastiaanssen, W.G.M. (1995). Regionalization of surface flux densities and moisture indicators in composite terrain: A remote sensing approach under clear skies in Mediterranean climates. Ph.D. dissertation, Landbouwuniversiteit te Wageningen, The Netherlands. Published as Report 109 of DLO Win and Staring Centre, Wageningen, The Netherlands.

Campbell, G.S. (1977). An introduction to environmental biophysics. Springer, New York. 159 p.

Foken, T. (2006). 50 years of the Monin-Obukhov similarity theory. Boundary-Layer Meteorology 119: 431-447.

Liang, S., C.J. Shuey, A.L. Russ, H. Fang, M. Chen, C.L. Walthalk, C.S.T. Daughtry, and R.Hunt (2002). Narrowband to broadband conversions of land surface albedo: I. Algorithms. Remote Sensing Environ. 76: 213-238.

Orloff, S.B. and D.H. Putnam (2007). Harvest Strategies for Alfalfa. University of California Division of Agriculture and Natural Resources Publication 8299. Available online: http://alfalfa.ucdavis.edu/IrrigatedAlfalfa/pdfs/UCAlfalfa8299HarvestStrategies_free.pdf?prevver=search#.

Skaggs, R.K. and Z. Samani (2005). Farm size, irrigation practices, and on-farm irrigation efficiency. Irrigation and Drainage 54: 43-57.

Samani, Z. and R.K. Skaggs (2007). The unintended consequences of water conservation. In: Water Resources of the Middle Rio Grande: San Acacia to Elephant Butte, Eds. L.G. Price, P.S.

Johnson, and D. Bland. Pages 112-115. New Mexico Bureau of Geology and Mineral Resources, New Mexico Institute of Mining and Technology, ISBN 978-1-883905-24-9.

Samani, Z. and R.K. Skaggs (2008). The multiple personalities of water conservation. Water Policy 10: 285-204.

Samani, Z., A.S. Bawazir, M. Bleiweiss, R. Skaggs, and T. Schmugge (2006). Estimating riparian ET through remote sensing. American Geophysical Union Fall Meeting, San Francisco, CA, Dec. 8, 2006.

Samani, Z., A.S. Bawazir, R. Skaggs, M. Bleiweiss, A. Piñon, and V. Tran (2007a). Water use by agricultural crops and riparian vegetation: An application of remote sensing technology. J. of Contemporary Water Research & Education 137: 8-13.

Samani, Z., A.S. Bawazir, M. Bleiweiss, and R. Skaggs (2007b). Estimating net radiation over vegetation canopy. ASCE J. Irrig. and Drain. Engrg. 133(4): 291-297.

Samani, Z., A.S. Bawazir, M. Bleiweiss, R. Skaggs, J. Longworth, V.D. Tran, and A. Piñon (2009). Using remote sensing to evaluate the spatial variability of evapotranspiration and crop coefficient in the Lower Rio Grande Valley, New Mexico. Irrigation Science 28:93-100.

Samani, Z., R. Skaggs and J. Longworth (In Press). Alfalfa water use and crop coefficients across the watershed: From theory to practice. ASCE J. Irrig. and Drain. Engrg.

Skaggs, R., Z. Samani, A.S. Bawazir, and M. Bleiweiss (2011). The convergence of water rights, structural change, technology, and hydrology: A case study of New Mexico's Lower Rio Grande. Natural Resources Journal 51(1): 95-117.

Skaggs, R., Z. Samani, A.S. Bawazir, and M. Bleiweiss (In Press). Response and Discussion: The convergence of water rights, structural change, technology, and hydrology: A Case Study of New Mexico's Lower Rio Grande. Natural Resources Journal.

Tasumi M. (2003). Progress in operational estimation of regional evapotranspiration using satellite imagery. Ph.D. dissertation, University of Idaho.

Unsworth, M.H. and Monteith, J.L. (1975). Geometry of long-wave radiation at the ground. I. Angular distribution of incoming radiation, Q.J. Roy. Meteorol. Soc. 101: 13-24.

A GIS-BASED ESTIMATE OF NET EROSION RATE FOR SEMI-ARID WATERSHEDS IN NEW MEXICO

Richardson, C.P.[1]; Gallegos, J.B.[2]; Ealey, J.[3]; Cal, M.P.[4]

ABSTRACT

A GIS-based algorithm of transport limited sediment accumulation provides a means to estimate an annual net erosion rate for a gridded watershed. The method requires specification of a transport capacity coefficient (K_{TC}) and gridded values of the five Universal Soil Loss Equation (*USLE*) factors (*R, K, LS, C,* and *P*). An estimate of K_{TC}, reflecting the vegetation impact on the transport capacity, may be obtained by calibrating the modeled sediment yield with reported average annual sediment yield. However, specific watershed soil erosion data for the State of New Mexico is limited. Data for the Volcano Hill Wash sub-basin of the Rio Puerco basin to the Rio Grande has been reported and was used herein to estimate a K_{TC}. Evaluation of K_{TC}, where data exist, may lead to better understanding of soil erosion and sediment transport issues from semi-arid rangeland watersheds. This research was supported by the New Mexico Department of Transportation (*NMDOT*).

ESTIMATING SOIL EROISION

A characteristic of watersheds in southwest arid and semi-arid regions is that, during rainfall events, large quantities of sediments are transported from upland regions and deposited into the lower reaches of the drainage catchment. The quantity and size of material transported depends on the transport capacity of runoff water. However, if transport capacity is less than the amount of eroded soil material available, then the amount of sediment exceeding the transport capacity gets deposited. If the converse is true, then the amount of sediment load passing the outlet of a catchment is known as sediment yield.

Monitoring of source areas via erosion pins and suspended sediment sampling, and fingerprinting using physical, chemical, or radiological properties are two approaches to evaluating net erosion rates within a watershed. Erosion pins were used by Ludwig *et al*. (2000) along six transects within the Otero Mesa desert grasslands in southern New Mexico to evaluate soil erosion. From 1982-1995, soil surfaces along these transects eroded an average of 0.4 mm/yr. This equates to approximately 5.2 mt/ha/yr at a soil bulk density of 1.3 mt/m^3. Nearing *et al*. (2005) used ^{137}Cesium fallout fingerprinting to evaluate erosion and deposition rates within the 3.7 ha shrub-dominated Lucky Hills sub-watershed within the Walnut Gulch Experimental Watershed near Tombstone, Arizona. Rates ranged from a soil loss of 9.83 mt/ha/yr to a

[1]Clinton P. Richardson, P.E., BCEE, Professor, Dept. of Civil and Environmental Engineering, New Mexico Tech 801 Leroy Place Socorro, NM, 87801, h2odoc@nmt.edu *corresponding author*

[2]Jose B. Gallegos, Environmental Engineer, ARCADIS US, Inc., 630 Plaza Drive, Suite 100 | Highlands Ranch, CO, 80129, jose.gallegos@arcadis-us.com

[3]Jaime Ealey, Graduate Research Assistant, Dept. of Civil and Environmental Engineering, New Mexico Tech, 801 Leroy Place Socorro, NM, 87801, jealey@nmt.edu

[4]Mark P. Cal, P.E., BCEE, Chair and Professor, Dept. of Civil and Environmental Engineering, New Mexico Tech, 801 Leroy Place Socorro, NM, 87801, mcal@nmt.edu

deposition gain of 5.74 mt/ha/yr with an average of 4.27 mt/ha/yr net soil loss for the total watershed. This latter average was similar to soil loss calculated from suspended sediment loads (5.8 mt/ha/yr) obtained via an instrumented fume.

Such studies provide insight into soil erosion and deposition as a phenomenon that directly impacts soil quality, water quality, and overall watershed condition and its subsequent management for beneficial use. *GIS*-based modeling and evaluation is another tool to evaluate and quantify potential soil erosion. A procedure is presented to estimate net soil erosion based on specification of a transport capacity coefficient, which reflects the impact of vegetative cover on eroded soil transport. The methodology is applied to reported soil loss data from the Volcano Hill Wash sub-basin of the Rio Puerco basin to the Rio Grande.

OBJECTIVE

The objective of this work is to utilize a *GIS* platform to estimate total annual net erosion from a given watershed using available or derivable raster-based attributes. To facilitate this, the procedure and method by Jain *et al*. (2010) is utilized. The Universal Soil Loss Equation (*USLE*), introduced later, estimates gross annual soil loss and is based on five empirical input variables: rainfall erosivity (*R*-factor), soil erodibility (*K*-Factor), length slope (*LS*-factor), land use cropping factor (*C*-Factor), and erosion prevention practice (*P*-factor). *GIS* provides the means to compute soil erosion in individual grids based on the *USLE*, and to determine catchment sediment yield, or net erosion, by using the concept of transport limiting sediment delivery.

AVAILABLE *GIS*-BASED WATERSHED ATTRIBUTES

In order to better understand sediment transport within a given watershed, foundational information and data must be collected:

Terrain: A Digital Elevation Model (*DEM*) is the most commonly used tool for terrain investigation. The National Elevation Dataset (*NED*) is the primary elevation data product produced and distributed by the United States Geological Survey (*USGS*). The *NED* provides seamless raster elevation data of the conterminous United States. Primary attributes that can be generated from a *DEM* include, but not limited to, slope, flow-path length, flow direction, and upslope contributing area.

Rainfall Erosivity: This metric reflects the erosion capacity of rainfall and is the product of total rainfall energy and the highest 30-minute intensity (EI_{30}). Hastings *et al*. (2005) reported that sediment yield from four micro-watersheds near Los Alamos National Laboratory exhibited a stronger positive correlation to rainfall erosivity than rainfall depth for 14 convective thunderstorms.

Vegetative Index: The Normalized Difference Vegetation Index (*NDVI*) is a thematic image of estimated vegetation density derived using multi-spectral satellite imagery. *NDVI* values range between -1 and +1. Non-vegetated areas typically produce small or slightly negative values, while vegetated areas produce values starting around 0.4 and approaching 1.0 (Shank 2006). *NDVI*-images have been scaled to approximate the crop management factor (*C*-factor) as defined in Eq. 1, or

$$C = e^{-\alpha\left\{\frac{NDVI}{\beta - NDVI}\right\}} \quad (1)$$

where

α and β = unitless parameters that determine the shape of the curve.

The *C*-factor integrates a number of factors that affect erosion including vegetative cover, plant litter, soil surface, and land management. van der Knijff *et al*. (2002) found that an α of 2 and β of 1 gave the most reasonable results when applied to the above relationship.

Soil Erodibility: Soil erodibility depends on organic matter content, soil texture, soil permeability, profile structure, as well as other factors, and is embodied in the soil erodibility factor (*K*-factor) of the *USLE*. The *K*-factor is a measurement of the inherent susceptibility of soil particles to detachment and transport by rainfall and runoff. It typically ranges from 0.10 to 0.45 (Renard *et al*. 1991), wherein a lower value constitutes to a stable soil, and a higher value represents a highly fragile soil. A GIS compatible map of *K*-factors for the State of New Mexico is available from the *NRCS* Soil Survey Geographic (*SSURGO*) database and *NRCS* State Soil Geographic (*STATSGO*) database.

National Hydrography Dataset: The National Hydrography Dataset (*NHD*) is the surface water component of the *USGS* National Map. More specifically, the *NHD* contains a flow network (flow-lines) that allows for tracing water downstream or upstream.

MATERIALS AND METHODS

Detailed and supplemental information for materials and methods described herein, including internet sources for downloads, may be found in Gallegos (2012).

Digital Elevation Models: *DEM* datasets for New Mexico were uploaded from the *USGS* National Elevation Dataset (*NED*) website (http://ned.usgs.gov/ned/). A 10-m resolution *DEM* raster for each county was acquired for watershed specific calculations.

Rainfall Erosivity: A raster grid of the *R*-factor is available based on a digitized USDA iso-erodent map of the US (http://invest.ecoinformatics.org/shared/Erosivity-US.zip/). A statewide raster for New Mexico was clipped from this grid. The resolution is low; however, it is currently the only available GIS-compatible dataset.

SSURGO and *STATSGO* Soil Datasets: *ArcGIS*® shapefile data was uploaded from the *NRCS* web site (http://soils.usda.gov/). With the uploaded soil data a complete countywide database was generated focusing primarily on the highly detailed *SSURGO* data and filling in the missing data locations with the less detailed *STATSGO* data. The result was a raster dataset of the *K*-factor.

NDVI: A *NDVI* raster layer based on a maximum seasonal *NDVI* average of 16 years of accumulated data for New Mexico (Bulut, 2011) was utilized to evaluate the *C*-factor used in the *USLE* via Eq. 1. An α of 2 and β of 1 were used (van der Knijff *et al*. 2002). The resultant statewide map of cropping factor ranged between 0.09 (low soil loss potential) and 0.82 (high soil loss potential).

National Hydrography Dataset: *NHD* high resolution (1:24,000-scale) topographic mapping data was uploaded from a specialized hydrography *USGS* portal (http://nhd.usgs.gov/).

DERIVED WATERSHED ATTRIBUTES

All watershed characteristics calculations were performed using *ArcGIS*® coupled with the extensional program *Arc Hydro*. For basic characteristics such as delineating a given

watershed boundary; calculating a watershed's area, slope, flow direction, flow accumulation, and stream linkage; and sub-watershed delineation, the *Arc Hydro* program extension calculates and generates raster grid and shapefile data.

Length-Slope Factor (*LS*-Factor): For a given watershed, a 2-dimensional *LS*-factor raster grid was developed using the TauDEM (Terrain Analysis Using Digital Elevation Models) *ArcGIS*® extension based on a *D-inflinity* flow direction and upland contributing area, or

$$LS = \left\{\frac{A}{22.13}\right\}^{0.4}\left\{\frac{S}{0.0896}\right\}^{0.6} \quad (2)$$

where A is the specific catchment area per contour length (m^2/m) and S is the slope (^{o}). A 2-dimensional *LS*-factor accounts for flow accumulation convergence (Moore and Burch, 1986).

WATERSHED NET SOIL EROSION

The eroded sediment from each watershed follows a defined drainage path for a particular cell to the catchment outlet as shown in Figure 1. The sediment outflow from each cell is equal to the soil erosion in the cell plus the contribution from upstream cells, if transport capacity is greater than this sum. However, if transport capacity is less than the sum of soil erosion in the cell and the contribution from upstream cells, the amount of sediment exceeding the transport capacity gets deposited in the cell and the sediment load equal to transport capacity is discharged to next downstream cell.

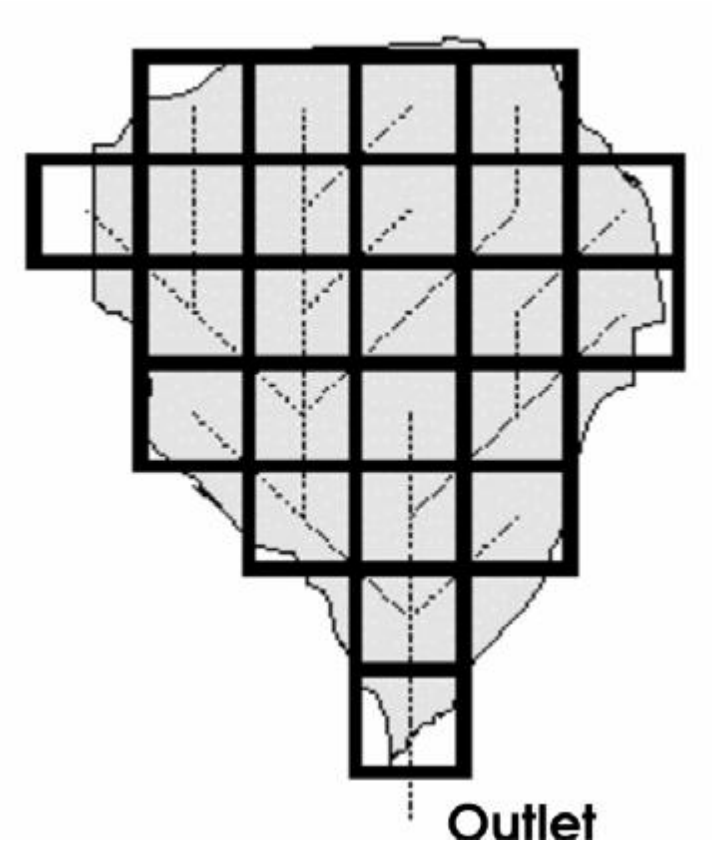

Figure 1: Schematic showing discretized grid cells in a catchment (Jain *et al.*, 2005).

The mean annual sediment transport capacity (*TC*) is computed using a relationship based on catchment physiographic parameters, such as soil erodibility, upslope contributing area, and slope gradient (Verstraeten *et al.*, 2007) as given below:

$$TC_i = K_{TC} R_i K_i A_i^m S_i^n \quad (3)$$

where TC_i is the transport capacity (Mt/ha/yr) of cell i, K_{TC} is the transport capacity coefficient (reflecting the vegetation impact on the transport capacity), R is the rainfall erosivity factor (MJ mm ha^{-1} hr^{-1} yr^{-1}), K_i is soil erodibility (Mt ha h ha^{-1} MJ^{-1} mm^{-1}), A_i is the upslope contributing area per unit of contour length for cell i (m^2/m), S_i is the slope gradient of cell i (m/m), and m and n are empirical or theoretical derived exponents. Prosser and Rustomji (2000) made a review of flume, laboratory plot, and field plot data and found that the median value is 1.4 for both exponents. Based on their review, values of $1.0 \leq m \leq 1.8$ and $0.9 \leq n \leq 1.8$ are recommended for use in sediment transport modeling. However, there was no strong evidence for one exponent to outweigh the other.

Eroded sediment is routed along the runoff paths towards the outlet taking into account the local transport capacity, TC_i of each pixel. If the local *TC* is smaller than the sediment flux, then sediment deposition occurs. This approach assumes that sediment transport is not necessarily restricted to a transport limited system. If *TC* is higher than the sediment flux, then sediment transport will be supply limited. For the grid-based discretization system adopted herein, transport limited accumulation can be computed as (Jain *et al.*, 2010):

$$T_{out_i} = min\left(SE_i + \sum T_{in_i}, TC_i\right) \quad (4)$$

$$D_i = SE_i + \sum T_{in_i} - T_{out_i} \quad (5)$$

where SE_i is the annual gross soil erosion in cell i, T_{in_i} is the sediment inflow in cell i from upstream cells, T_{out_i} is the sediment outflow from the cell i, and D_i is the deposition within cell i. All variables have units of Mt/ha/yr. An estimation of the annual gross soil erosion for a grid (or cell) is expressed by the *USLE* as

$$SE_i = R_i K_i L S_i C_i P_i \quad (6)$$

where R_i is the rainfall erosivity factor (MJ mm ha^{-1} hr^{-1} yr^{-1}), K_i is the soil erodibility factor (Mt ha h ha^{-1} MJ^{-1} mm^{-1}), LS_i represents a 2-dimensional length slope topographic factor (unitless), C_i is a cover-management factor (unitless), and P_i is the support practice factor (unitless). The latter factor is generally assumed to be unity for cell i.

Using Eqs. 3-6 results in different maps of erosion, sediment transport, and sediment deposition rates, whereby a distinction can be made between gross erosion, net erosion, and sediment deposition. With additional *ArcGIS*® processing within spatial analyst, different values of total gross and net erosion and total sediment deposition can be defined as follows:

$$Total\ Gross\ Erosion = \sum SE_i \quad (7)$$

$$Net\ Erosion\ (NE_i) = SE_i - D_i \quad (8)$$

$$Total\ Net\ Erosion = \sum NE_i \quad (9)$$

A low value of the transport coefficient, K_{TC}, indicates a strong influence of vegetative cover on reduction of transport capacity (Jain *et al.*, 2010); thus, resulting in lower total net

erosion flux within a given watershed. Jain and Das (2010) coupled the transport coefficient, K_{TC}, to the vegetative status in a watershed by hypothesizing it as an exponential function of the *NDVI*, or

$$K_{TC} = \beta * exp\left[\frac{-NDVI}{1-NDVI}\right] \quad (10)$$

where β is a scaling factor determined through calibration of observed sediment yield.

APPLICATION OF METHOD

To use the concept of transport limited accumulation to evaluate annual net soil erosion for a given watershed requires that a transport coefficient, K_{TC}, be specified, based on calibration of observed data or simply an engineering assumption based on professional judgment. Specific watershed soil erosion data for the State of New Mexico is limited. However, the Volcano Hill Wash sub-basin of the Rio Puerco basin to the Rio Grande was evaluated for erosion and sediment yield over a period of three years by Gellis *et al.* (2001). Figure 2 delineates the location of this 930 ha watershed. Note that while the Rio Puerco does not contribute significantly to the average annual runoff of the Rio Grande at its confluence, it does heavily impact the sediment burden to the Rio Grande due to its high average annual suspended sediment concentration.

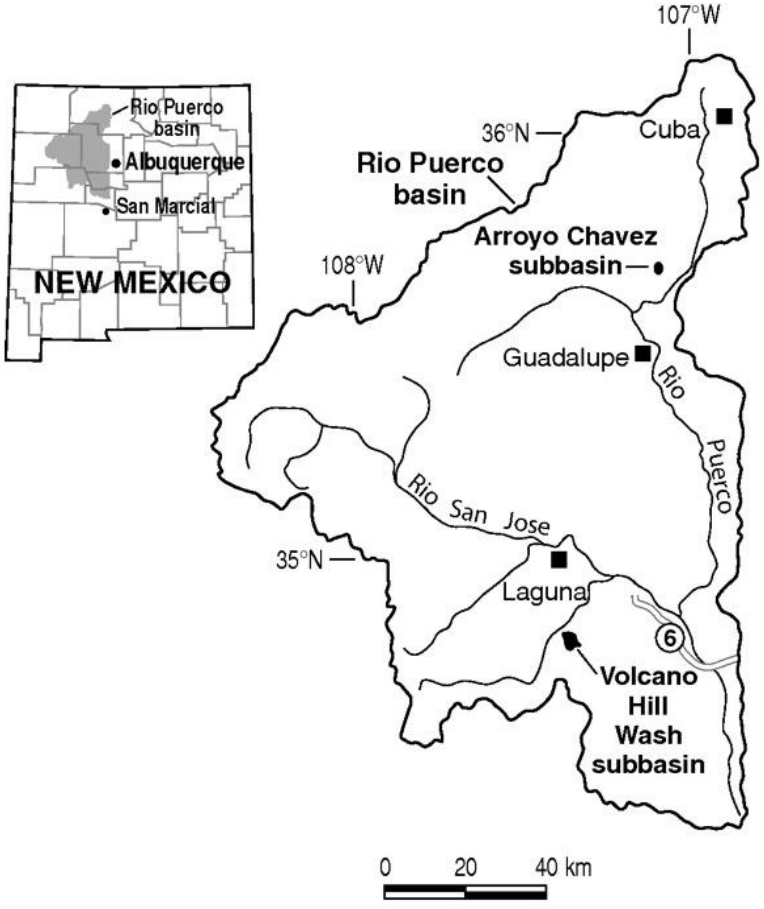

Figure 2: Volcano Hill Wash Sub-basin (Gellis *et al.* (2001).

The average annual sediment yield based on streamflow and suspended sediment measurements at gaging stations for water years 1996-1998 was 4.05 Mt/ha/yr. Upland erosion from sediment dams and traps throughout the basin's five geomorphic surfaces collected over a period of 797 days totaled 3630 Mt. This equates to an upland erosion of 1.79 Mt/ha/yr based on the reported total contributing area of the geomorphic units and duration of study. As the authors point out, the difference between measured estimates of sediment yield and upland erosion (unaccounted sediment) may be contributions of sediment from bed erosion and bank erosion, or sources of upland erosion not measured by sediment traps and dams.

The total net erosion rate was estimated for the Volcano Hill Wash sub-basin using the limited accumulation-based algorithms outlined in Eqs. 3-9 and clipped statewide rasters developed for *R*, *K*, *C*, and *S*. The upland contributing area raster and 2-dimensional *LS*-factor raster were evaluated based on the watershed *DEM*. Watershed *USLE* average attributes were as follows: R = 340 MJ mm ha^{-1} hr^{-1} yr^{-1}, K = 0.31 Mt ha hr ha^{-1} MJ^{-1} mm^{-1}, C = 0.46, and LS = 0.94. The average watershed slope was S = 0.13 m/m. The support practice factor (P) was taken as 1.0. The transport coefficient, K_{TC}, was then manually adjusted until a reasonable match of the Gellis *et al.* (2001) upland erosion data was realized. A K_{TC} of 2.0 x 10^{-8} gave a net soil erosion of 1.69 Mt/ha/yr.

DISCUSSION

The calculated net soil erosion rate depends upon a number of inputs.

NDVI: The *NDVI* metric upon which the *C*-factor raster is estimated via Eq. 1 was based on a sixteen-year average of the maximum growing season vegetative index. Selection of an appropriate *C*-factor raster directly impacts the cell *i* gross soil erosion rate via Eq. 6 and indirectly the cell *i* net soil erosion through the transport limited accumulation of Eqs. 4, 5, and 8. The maximum NDVI, or lowest erosive potential, was selected to correspond with the monsoonal precipitation period of high rainfall erosivity, or high erosive potential. However, the available *R*-factor raster employed herein is an annual average and of low resolution.

LS-factor: The *LS*-factor decreases when estimated with upslope contributing area as compared with the 1-dimensional *LS*-factor (Rodriguez and Suárez, 2010). The resultant annual upland soil erosion estimate would decrease based on Eq.6. The choice of topographic factor would affect the magnitude of the estimated K_{TC}. This effect was not evaluated herein.

K-factor: The *NRCS* soil data sets specify two soil erodibility factors for each soil component layer*:* *KFFACT* and *KFACT*. The latter is described as a soil erodibility factor which is adjusted for the effect of rock fragments. Interspersed rock fragments provide armoring and significantly reduce soil detachment. The *K*-factor raster used herein was developed from the un-adjusted *KFFACT* data.

Ogungbade (2012) implemented this method for eight sub-watersheds within the Walnut Gulch Experimental Watershed (*WGEW*) in southeastern Arizona. A 1-dimensional LS factor, however, was used along with a constant value for the *R*-factor and *C*-factor for all sub-watersheds (*versus* pixel by pixel values based on raster grids). Final estimates of K_{TC} were evaluated by calibrating the modeled sediment yield with reported average annual sediment yield determined from stock pond sediment accumulation (Nichols, 2006). Although these sub-watersheds had similar vegetation cover characteristics, a single value of K_{TC} could not be

determined for the set of 8 sub-watersheds. Calibrated K_{TC} ranged from approximately 10^{-5} to 10^{-3}.

Recall that this coefficient reflects the impact of vegetative cover on reduction of transport capacity within the watershed. The analysis herein does show that an order of magnitude increase in the specification of K_{TC} does result in an order of magnitude increase in calculated net soil erosion. Ritchie *et al*. (2005) observed, however, that vegetative cover was not related to soil redistribution at the aforementioned Lucky Hills sub-watershed within the *WGEW*. Cover within the shrub-dominated landscape was estimated at 26%; such low coverage did not appear to influence or capture transporting soils. Additionally, soil erosion rates were significantly correlated to the percent of rock fragments in the surface soil layer, with erosion decreasing as rock fragments increased.

In summary, careful specification and selection of the input variables based on the specifics of each watershed are needed as the calculated net erosion rate may be highly sensitive to one or more variables expressed in Eqs. 3 and 6. A sensitivity analysis is currently ongoing for selected watersheds.

CONCLUSION

Although only one example is provided herein, the method used is easily applied within an *ArcGIS*® environment to analyze similar sediment transport data, where available, and develop a database of K_{TC} values for semi-arid watersheds. Evaluation of K_{TC} may lead to better understanding of sediment transport data, where available, for rangeland watersheds with similar characteristics to that of the Volcano Hill Wash sub-basin and the *WGEW*. Additionally, an analysis of soil erosion risk as formulated by Bulut (2011) coupled with a net erosion estimate, based on the concepts and framework presented, could provide valuable information for local Natural Resources Conservation Service (*NRCS*) districts within the State of New Mexico involved in soil erosion management issues.

REFERENCES

Bulut, G.G. (2011). Potential Soil Erosion Risk for New Mexico and Sensitivity Analysis of Contributing Factors, MS Thesis, New Mexico Institute of Mining and Technology.

Gallegos, J.B. (2012). A *GIS*-based Characterization of Eight Small Watersheds in New Mexico with Emphasis on Development and Correlation of a Sediment Load Hydraulic Bulking Factor, MS Thesis, New Mexico Institute of Mining and Technology.

Gellis A.C., Pavich, M.J. and Ellwein, A. (2001). "Erosion and sediment yields in two subbasins of contrasting land use, Rio Puerco, New Mexico", Proceedings of the Seventh Federal Interagency Sedimentation Conference, March 23-29, Reno, NV.

Hastings, B.K., Breshears, D.D., and Freeman, M.S. (2005). " Spatial variability in rainfall erosivity *versus* rainfall depth: Implications for sediment yield", *Vadose Zone Journal*, 4, 500-504.

Jain, M. K., and Das, D. (2010). "Estimation of sediment yield and areas of soil erosion and deposition for watershed prioritization using GIS and remote sensing", *Water Resources Management*, 24, 2091-2112.

Jain, M. K., Kothyari, U.C. and Rangaraju, K.G. (2005). "*GIS* based distributed model for soil erosion and rate of sediment outflow from catchments", *ASCE Journal Hydraulic Engineering*, 131(9), 755-769.

Jain, M.K., Mishra, S. K. and Shah, R.B. (2010). " Estimation of sediment yield and areas vulnerable to soil erosion and deposition in a Himalayan watershed using GIS", *Current Science*, 98(2), 213-231.

Ludwig, J. A., Muldavin, E., and Blanche, K.R. (2000). "Vegetation change and surface erosion in desert grasslands of Otero Mesa, Southern New Mexico: 1982 to 1995", *The American Midland Naturalist,* 144(2), 273-285.

Moore, I.D. and G.J. Burch (1986). "Physical basis of the length-slope factor in the Universal Soil Loss Equation." *Soil Sci. Soc. Am. J.*, **50**(5), 1294-1298.

Nearing, M.A., Kimoto, A., Nichols, M.H., and Ritchie, J.C. (2005). "Spatial patterns of soil erosion and deposition in two small, semiarid watersheds", *J. Geophysical Research,* 110, F04020.

Prosser, I.P. and Rustomji, P. (2000). "Sediment transport capacity relations for overland flow", *Progress in Physical Geography*, 24 (2), 179-193.

Ogungbade, O.A. (2012). "Sediment Transport Capacity and Transport-Limited Deposition Using ArcGIS®: An Estimation of the Transport Capacity Coefficient for Eight Sub-watersheds within the Walnut Gulch Experimental Station", MS Thesis, New Mexico Institute of Mining and Technology.

Renard, K.G., Foster, G.R., Weesies, G.A., Porter, J.P. (1991). "RUSLE: Revised Universal Soil Loss Equation". *J. Soil and Water Cons.*, 46(1), 30-33.

Ritchie, J.C., Nearing, M.A., Nichols, M.H., and Ritchie, C.A. (2005). "Patterns of soil erosion and redeposition on Lucky Hills Watershed, Walnut Gulch Experimental Watershed, Arizona", *Catena,* 61, 122-130.

Rodriguez, J.L. and M.C.G. Suárez, (2010). *Historical Review of Topographical Factor.* Aqua LAC, 2(2), 56-61.

Shank, M. (2009), "Mapping vegetation change on a reclaimed surface mine using Quickbird", *Revitalizing the Environment: Proven Solutions and Innovative Approaches*, 2009 National Meeting of the American Society of Mining and Reclamation, May 30-June 5, Lexington, Kentucky.

van der Knijff, J., Jones, R.J.A., Montanarella, L., (2002*).* "Soil erosion risk assessment in Italy". *Proceedings of the Third International Congress Man and Soil at the Third Millennium. Geoforma Ediciones*, Logrono, Italy. 1903-1913.

Verstraeten, G., Prosser, I.P. and Fogarty, P. (2007). "Predicting the spatial patterns of hillslope sediment delivery to river channels in the Murrumbidgee catchment, Australia", *Journal of Hydrology,* 334(3-4): 440-454.

A GIS-BASED SOIL EROSION RISK MAP FOR NEW MEXICO

Bulut, G.G.[1]; Cal, M.P.[2]; Richardson, C.P.[3]; Gallegos, J.B.[4]

ABSTRACT

A soil erosion risk map was developed for the State of New Mexico using the Universal Soil Loss Equation (*USLE*), a fuzzy logic model (*FuzzyCell*) and *ArcGIS Desktop 9.3* software. Soil erosion was examined as a function of length-slope (*LS*) gradient, normalized difference vegetation index (NDVI), 2-yr, 6-hr precipitation levels ($_2P_6$), and soil erodibility (*K*). A color-coded erosion risk for New Mexico was developed showing that erosion risk varied between 0.05 and 0.87 on a scale of 0 (minimum) to 1 (maximum). This soil erosion risk map provides a visual perspective of potentially problematic areas for soil erosion within New Mexico. Although the data used in this study is specific to the State of New Mexico, the methodologies could be applied to other geographic regions.

Wischmeier (1959) developed the *Universal Soil Loss Equation* (*USLE*). Due to its ease of use and limited data input requirements, it is still a leading model for the estimation of soil erosion. *USLE* estimates soil erosion based on five empirical input variables: rainfall erosivity, soil erodibility, slope, land use cropping factor, and erosion prevention practice factor.
For this study, *USLE* is integrated into a Geographic Information System (GIS) along with publicly available data to generate a soil erosion risk map for New Mexico. Part of the difficulty with converting discrete data into a soil erosion risk map relates to the how discrete and ambiguous data are processed by computational systems. While the real world consists of fuzziness (ambiguous data), conventional GIS software only uses crisp data (yes/no choices or discrete data) as inputs. Shades of gray are present in the physical world (fuzzy logic), but only discrete data are used in traditional GIS environments (crisp logic). Both discrete data and fuzzy logic were used together to produce a soil erosion risk map.

SOIL EROSION MODEL – UNIVERSAL SOIL LOSS EQUATION (USLE)

USLE estimates annual soil loss, and it is based on five empirical input variables: rainfall erosivity, soil erodibility, length slope, land use cropping factor, and erosion prevention practice factor (Wischmeier, 1959). *USLE* is represented as:

$$A = K \times L \times S \times C \times R \times P \quad (1)$$

where A is average annual soil loss in metric ton/ha/yr, K is soil erodibility factor (metric ton·ha·hr/ha·MJ·mm), L is slope length factor (dimensionless), S is slope steepness factor

[1]Gaye G. Bulut, gayegul@gmail.com

[2]Mark P. Cal, P.E., BCEE, mcal@mac.com, Department of Civil and Environmental Engineering, New Mexico Tech, 801 Leroy Place, Socorro, NM, 87801 *Corresponding Author*

[3]Clint P. Richardson, P.E., BCEE, h2odoc@nmt.edu, Department of Civil and Environmental Engineering, New Mexico Tech 801 Leroy Place, Socorro, NM, 87801

[4]Jose B. Gallegos, jose.gallegos@arcadis-us.com

(dimensionless), *C* is cover-management factor (dimensionless), *R* is rainfall erosivity factor (MJ mm/ha·hr·yr), and *P* is soil erosion prevention practice factor (dimensionless).
Four attributes were selected to represent the *USLE* parameters in Equation 1: soil erodibility (*K*), 1-dimensional length slope factor (*LS*), vegetative coverage (NDVI), and average precipitation ($_2P_6$). The soil erosion prevention practice factor (*P*) was not considered, and therefore assumed to be equal to 1.

FUZZY SET THEORY

Fuzzy logic allows for the management of uncertainty by simulating the human thinking process within a physical world. It provides a formal framework to process linguistic knowledge and its corresponding numerical data through membership (characteristic) functions. Membership certifies that a variable belongs to a class and the overall linguistic knowledge summarizes complex phenomenon, concepts, and outputs of human thinking process, while the numerical data are used for processing (Yanar and Akyürek, 2006).
Fuzzy logic is implemented within the *ArcGIS* environment as an extension to process uncertainty, and to imitate the human thinking process. An *ArcGIS* extension, *FuzzyCell*, was used to estimate the potential soil erosion risk within the State of New Mexico by processing the relationships between the contributing factors and soil transport.
Fuzzy set theory has been used for decades to reflect real physical world vagueness and uncertainty into binary systems. Fuzzy refers to computational vagueness and it represents any uncertain, imprecise, or ambiguous real world knowledge. Since most systems are designed to work with classic data sets, which denote a belonging to a set by 1 and not belonging to a set by 0; they are unable to reflect fuzzy information, which falls in between 1 and 0. Fuzzy logic was derived from the fuzzy set theory and is able to define vague linguistic forms of the memberships such as *high*, *medium* and *low*. Zadeh (1965) introduced fuzzy sets as classes of objects with a continuum of grades of memberships. His fuzzy set theory was based on the fact that the classes of objects encountered in the real physical world usually do not have precisely defined criteria of membership.
Kainz (2008) explained the human thinking process and language, stating that there are many uncertain and vague concepts, because human language is not binary, i.e., 0 or 1, black or white. The values in between, for example, 0.6 or gray, are said to be fuzzy. Fuzziness is an indication to what degree something belongs to a class. Any phenomenon that shows a degree of vagueness or uncertainty is in need of a proper expression, which is not possible using crisp sets of class boundaries.
According to Yen and Langari (1999) fuzzy models are capable of incorporating knowledge from human experts naturally and conveniently, while traditional models fail to do so. Fuzzy models are also capable of handling nonlinearity.
Liu (2009) argued that traditional multi-criteria decision-making methods do not provide the best decision support because they are ineffective at the modeling of qualitative human-thinking process. Fuzzy logic is broadly recognized as a tool that has the ability to compute with words, which is useful for modeling qualitative human thought process in the analysis of complex systems and decisions.

FUZZY LOGIC COMBINED WITH ***USLE***

Soil erosion can show a significant difference when linguistically formulated using fuzzy logic instead of estimated using classical soil erosion models. Yanar and Akyürek (2006) introduced

fuzzy set theory into GIS. This integration allows users to obtain more flexibility and capability to effectively handle and process imprecise information about the real world. Using fuzzy logic, as a linguistic approach, they developed a fuzzy rule-based system called *FuzzyCell*.
As Tayfur (2003) stated, fuzzy rules, also known as *IF-THEN* rules, include two parts: the antecedent part of the rule, the part starting with *IF* up to *THEN*, and a consequent part, the part starting with *THEN* up to the end. For instance, *IF* the precipitation amount is high; the slope is very steep (high); the soil is compact (high); and NDVI is sparse (low), *THEN* the potential erosion risk is very significant (high).
Kainz (2008) defined membership function as an assignment to every element of the universe and a degree of membership to a fuzzy set. This membership value must be between 0 (no membership) and 1 (full membership), indicating to which degree an element belongs to the fuzzy set.
Mitra et al. (1998) developed a fuzzy logic model to study soil erosion in a relatively large watershed using a limited number of indicators. They worked on two different fuzzy logic rule bases. The first rule base included slope angle and land cover data as variables and the second rule base consisted of slope length, soil erodibility, and vegetation cover as input indicators. They came to the conclusion that fuzzy logic based soil erosion predictions were more successful than the USLE based calculations alone and the study based on three indicators was more accurate compared to the study with two indicators.
Tayfur et al. (2003) also claimed that experiments indicated the fuzzy model as a reliable sediment transport model. Ahamed (2000) compared soil loss calculated by the *USLE* and a *USLE* adapted fuzzy class membership approach. The comparison indicated that *USLE* based fuzzy approach showed more spatial variation in the regions with a soil erosion problem, while it showed no significant difference in areas without a soil erosion problem.

SOFTWARE

The GIS-based software package used throughout this study is the Environmental Systems Research Institute's (ESRI) *ArcGIS Desktop 9.3*, as well as extensions, such as *ArcToolbox* and *ArcScene*. This *ArcGIS* application performs data-based manipulations such as spatial analysis, raster calculations, geoprocessing, and data merging. The fuzzy inference system that is implemented within *ArcGIS* was *FuzzyCell* (Yanar and Akyürek 2006). *FuzzyCell* allows eight possible membership functions, inference methods for rule aggregation, operators for set operations, and defuzzification methods.

SITE DESCRIPTION

The study area is the State of New Mexico located in the southwest region of the United States. New Mexico has a surface area of 121,412 square miles, is approximately 350 miles square, and lies between latitudes 32° and 37° N and longitudes 103° and 109° W.
New Mexico has a range of altitudes changing between 861-m and 4012-m with an average of 1749-m. The altitudes result in terrain slope values between 0 degrees and 77.2-degrees with an average of 6.5-degrees. On average, the level of precipitation within New Mexico ranges from a minimum of 0.77-inches to a maximum of 2.19-inches for a $_2P_6$ precipitation duration (2-yr frequency, 6-hr duration).

DATA SETS

Four publicly available data sets for the State of New Mexico were used in this study: 1) United States Geological Survey (USGS) digital elevation maps (DEM); 2) USGS normalized difference vegetation index (NDVI); 3) 2-yr, 6-hr precipitation levels; 4) and soil erodibility (*K*). The soil erodibility (*K*) and DEM maps are 30 × 30-m resolution. The precipitation data is 800 × 800-m resolution and the vegetative index (NDVI) is 1000 × 1000-m resolution. When working with the GIS data sets, larger resolutions were downscaled to 30 × 30-m.

DIGITAL ELEVATION MODEL (DEM) AND LS FACTOR

For this macro-scale project, a 30-m DEM was used to quantify the topographical characteristics of New Mexico. The DEM data rendered in 3-D using *ArcScene* is presented in Figure 1.

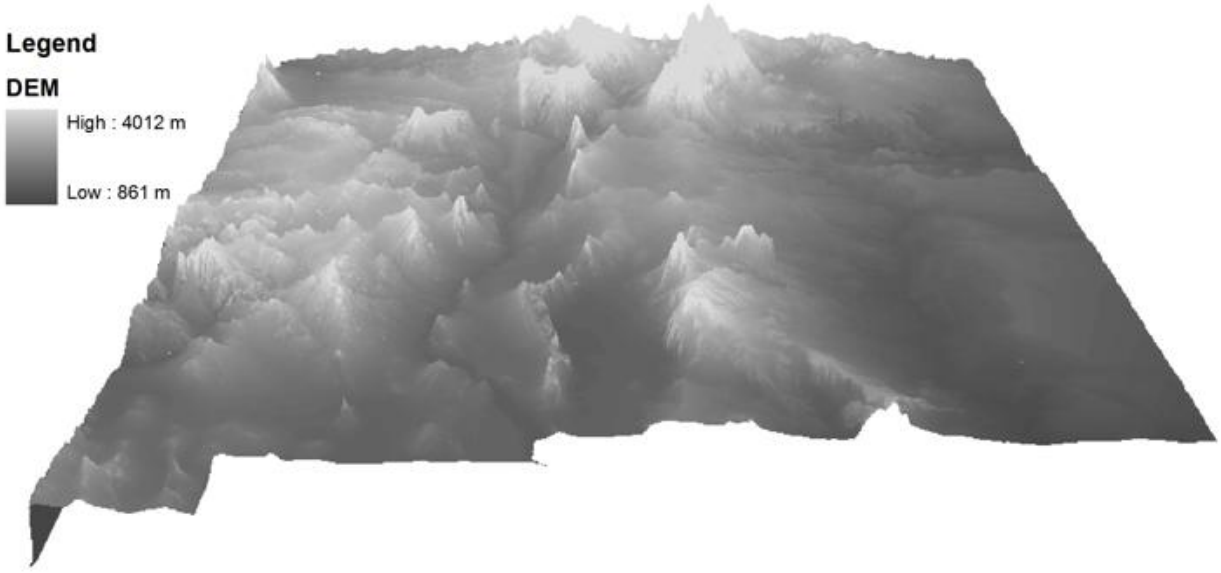

Figure 1. New Mexico Digital Elevation Map (DEM).

In this study, a 1-dimensional length-slope (*LS*) factor is evaluated and used as one of the contributing factors soil erosion risk rather than slope (Figure 2). *LS* provides a better identification of problematic areas affecting soil erosion risk. Detailed procedures for converting terrain slope into a length-slope factor are presented in Bulut, 2011.

Figure 2. Length-Slope (***LS***) Factor for New Mexico

NORMALIZED DIFFERENCE VEGETATIVE INDEX (NDVI)

The USGS defines the normalized difference vegetative Index (NDVI) as a standardized index of greenness. The differential in the reflections of different land coverage types under two spectral bands, red and infrared (IR), is monitored and the data are used to produce the NDVI data set. NDVI calculations are based on the fact that green plants absorb radiation in the visible range and they reflect radiation in the near IR range. Water stressed, diseased, or dead leaves become more yellow and reflect less radiation in the near IR range. Clouds, water, and snow reflect more radiation in the visible range than in the near IR range. Rock and bare soil show almost the same reflection in both the red and the near IR ranges. NDVI values vary between -1 and 1, where -1 represents clouds, water, and snow and 0 represents rock and bare soil. The NDVI process in the GIS environment creates a one-band, 8-bit image scaling output values of -1 to 1 to a scale from 0 to 255 (Lillesand and Kiefer, 1987). The NDVI raster data set representing the average maximum annual NDVI values from 1995-2009 is shown in Figure 3 based on this scaling. The lighter green shade represents the sparsely vegetated regions, while the darker shades of green represent heavily vegetated areas.

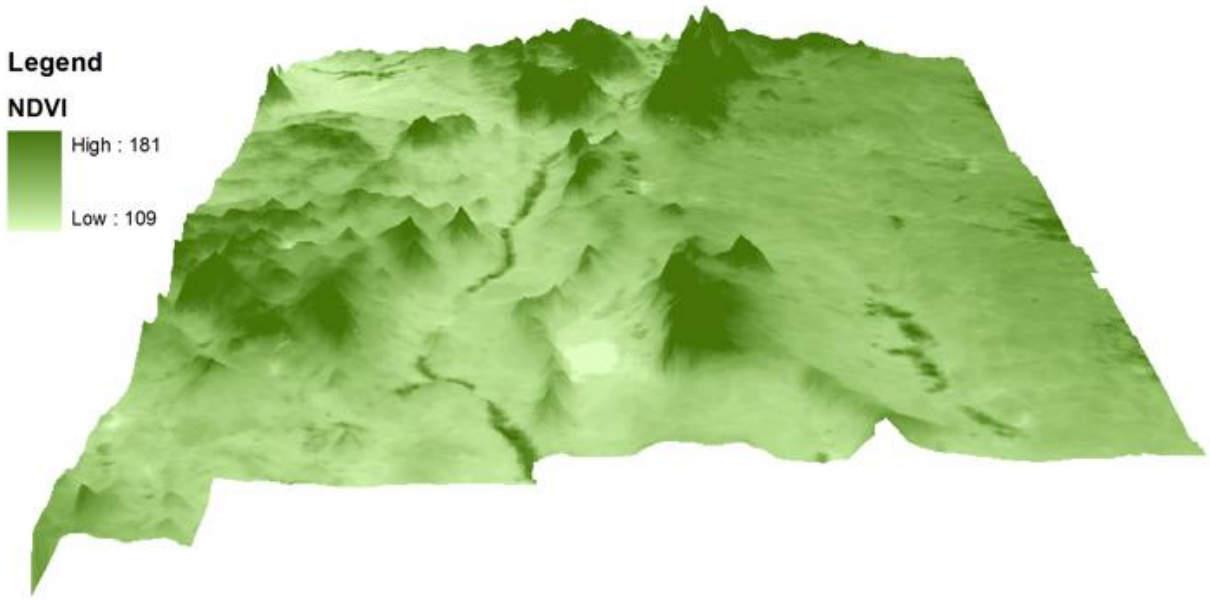

Figure 3. New Mexico Normalized Difference Vegetative Index Distribution.

PRECIPITATION

Precipitation frequency data are prepared by the Hydrometeorological Design Studies Center (HDSC), a division of the National Oceanic and Atmospheric Administration (NOAA)'s National Weather Service. The related data set, including the New Mexico region, is obtained from the NOAA Atlas 14 (Volume 1) map of the semiarid southwest. Wischmeier and Smith (1978) suggested that the 2-yr, 6-hr precipitation ($_2P_6$), which is a 6-hour duration precipitation with a 2-year return period, represents a reasonable accuracy for rainfall erosivity for the western states. Rainfall erosivity indicates the erosion capacity of rainfall. The statewide $_2P_6$ precipitation map is displayed in Figure 4.

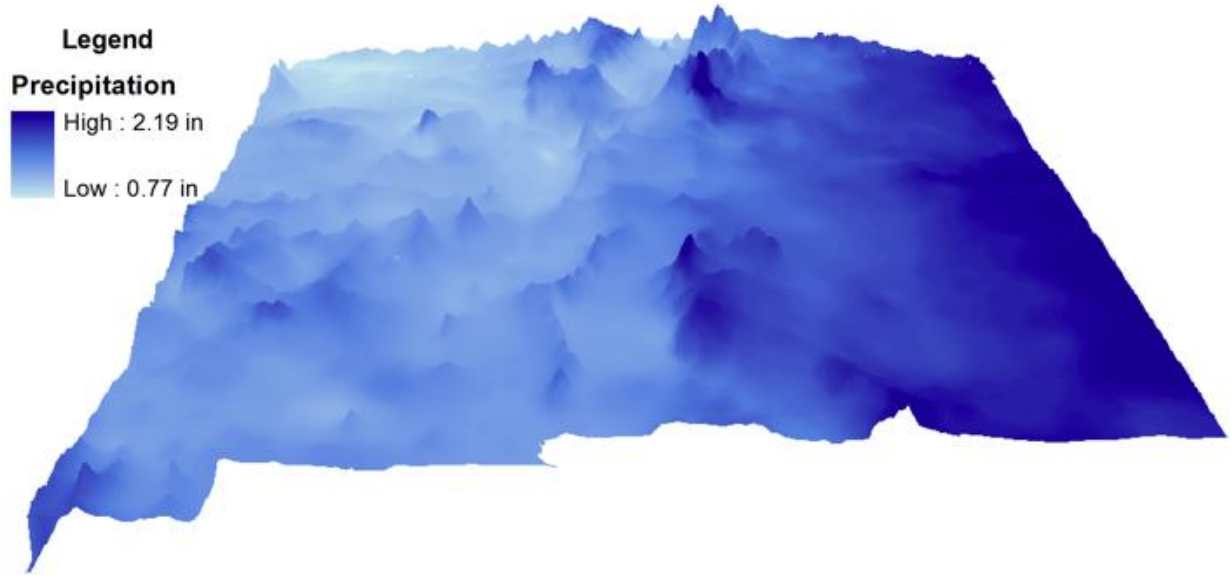

Figure 4. New Mexico 2-yr, 6-hr ($_2\boldsymbol{P}_6$) Precipitation Distribution.

SOIL ERODIBILITY

The Soil Survey Geographic (SSURGO) and State Soil Geographic (STATSGO) are soil property databases produced by the Natural Resources Conservation Service (NRCS). Since the SSURGO data for New Mexico is not complete, the STATSGO data at a resolution of 30-m was selected for this study. The *K*-factor, or soil erodibility, is available in STATSGO, and for New Mexico, the values range between 0 and 0.64. Low *K*-values between 0.05 and 0.15 represent fine-textured soils which are resistant to detachment due to a high clay ratio. Coarse-textured soils, such as sandy soils, have also low *K*-values ranging from 0.05 to 0.2. The particles in coarse-textured soils are easily detached; however, these soils have high infiltration capabilities resulting in low runoff. Moderate *K*-values ranging from 0.25 to 0.45 correspond to medium-textured soils such as silty loam. This type of soil is moderately susceptible to particle detachment and generates moderate runoff rates. High silt content soil is particularly susceptible to erosion and has higher *K*-values in the range of 0.45 and 0.69. These particles are easily separated, causing large volumes of runoff (Weesies,1998). A soil erodibility distribution for New Mexico is shown in Figure 5. The outlined areas are for a *K*-factor equal to zero, denoting rock outcrops, or water (Soil Info, 2001). Hypothetically, a *K* equal to 0 is a totally resistant soil layer to erosion.

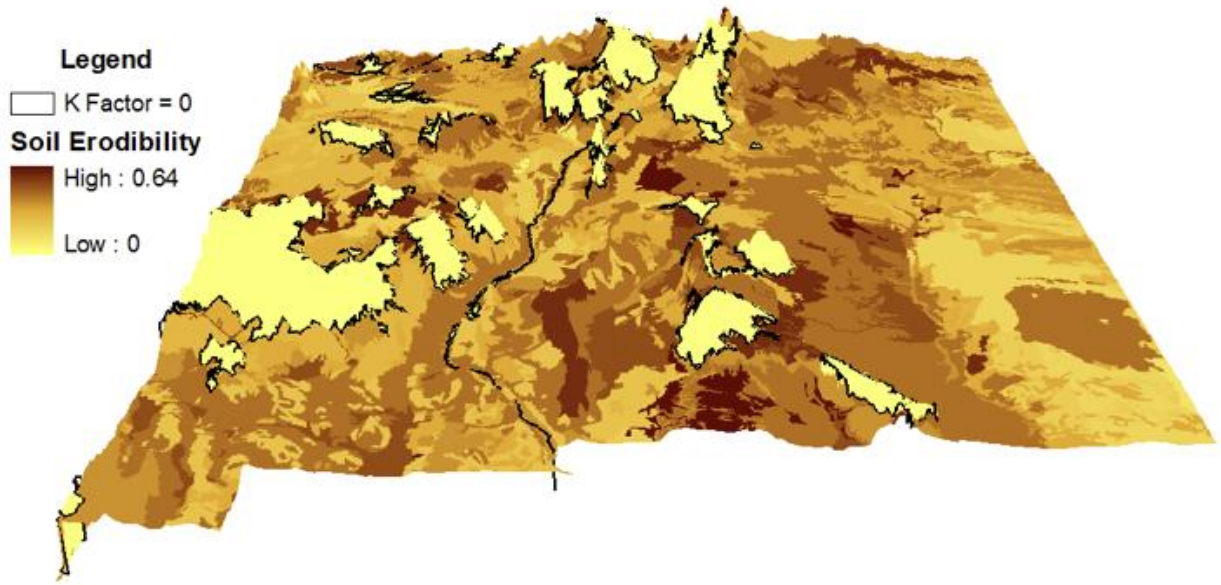

Figure 5. New Mexico Soil Distribution.

DEVELOPMENT OF THE SOIL EROSION RISK MAP

The data sets for length-slope (*LS*), normalized difference vegetative index (NDVI), soil erodibility (*K*), and the 2-yr, 6-hr precipitation ($_2P_6$) were manipulated in the *ArcGIS* environment and supplied to *FuzzyCell* to generate a potential soil erosion risk map.

APPLICATION OF FUZZY LOGIC AND FUZZYCELL

Liu et al. (2009) outlined the four main steps necessary for fuzzy reasoning: computing compatibilities, truncating conclusions, aggregating truncated conclusions, and the defuzzification process.

The first step of fuzzy reasoning is compatibility computation, which designates a crisp value to each antecedent (the part starting with *IF* up to *THEN*). *FuzzyCell* operates on the input raster datasets pixel by pixel to generate an output. For each input variable (contributing factor) the tool reads its raw value for that pixel from the raster data and uses its membership function to calculate a membership value. After determining all four membership values, a fuzzy operator is applied to them to produce a single membership value. For this study, the trapezoidal-norm (t-norm) operator product is used, which forces the tool to draw conclusions sensitive to every input. *FuzzyCell* repeats this procedure and calculates a compatibility value for each rule.
Each indicator is considered to have three different membership functions (low, medium, and high) that quantify the grade of its membership. Since there are four indicators each having three different possible memberships, there are 3^4 or 81 *IF-THEN* rules that must be constructed. For instance: *IF* slope gradient is high (steepness), soil erodibility is high, NDVI is medium, and precipitation depth is high, *THEN* risk is very significant.
The second step of fuzzy reasoning is truncating conclusions. Once the compatibility for a rule is calculated, the membership function of the consequent part (from *THEN* up to end) is truncated by the compatibility value using a fuzzy implication operator, which is minimum (*MIN*) for this study.
The next step is aggregating truncated conclusions, which generates a new single fuzzy set representing the truncated conclusions for each rule. For this study, the maximum (*MAX*) aggregation operator is used to truncate the conclusions.
The last step is defuzzifying the overall conclusion to convert a fuzzy set back into a crisp (numerical) value. There are several defuzzification methods, such as the weighted average, maximum membership, average maximum membership, and center of gravity. In this study, the center of gravity method is employed (Tayfur et al. 2003), which takes the centroid of the area under the membership function curve of a fuzzy set as the result (Liu, 2009).

FUZZY MEMBERSHIP AND PARAMETER CUTOFFS

A partially overlapping trapezoidal membership function was used for each indicator. Based on the study by Ahamed et al. (2000), cutoff values of 0.1, 0.3, and 0.5 were chosen for the soil erodibility distribution. Ahamed et al. (2000) also evaluated the *LS*-factor cutoff values for fuzzy memberships and suggested cutoff values as 0.5, 3.5, 9 and 16, respectively, for slope gradient classes of 0-5, 5-15, 15-30, and greater than 30%.
In order to calculate the NDVI cutoff values, *C*-factor cutoff values were assigned 0.2, 0.5, and 0.8 (Ahamed et al., 2000). NDVI values were then back calculated as 110, 125, and 145 using a NDVI-*C* factor relationship developed by van der Knijff et al. (1999).
The $_2P_6$ membership cutoff values were assigned as 0.63, 1.32, and 1.73 inches using the relationship developed by Wischmeier and Smith (1978) and *R*-factor cutoffs of 10, 50, and 90 as hundreds of ft·tonf ·in /ac·hr for low, medium, and high rainfall erosivity. This inverse method closely matched the minimum, average, and maximum $_2P_6$ data for New Mexico.
The soil erosion risk membership was defined so that it would scale the outcome from 0 to 1. A partially overlapping triangular membership function with cutoff values spanning seven fuzzy ranges was assumed. These soil erosion risk consequences were defined as *very insignificant (vi), insignificant (i), slightly insignificant (si), neutral (n), slightly significant (ss), significant (s) and very significant (vs)*. An example fuzzy reasoning process is presented in Figure 6, and the entire set of rules and membership classes are presented in Bulut (2011).

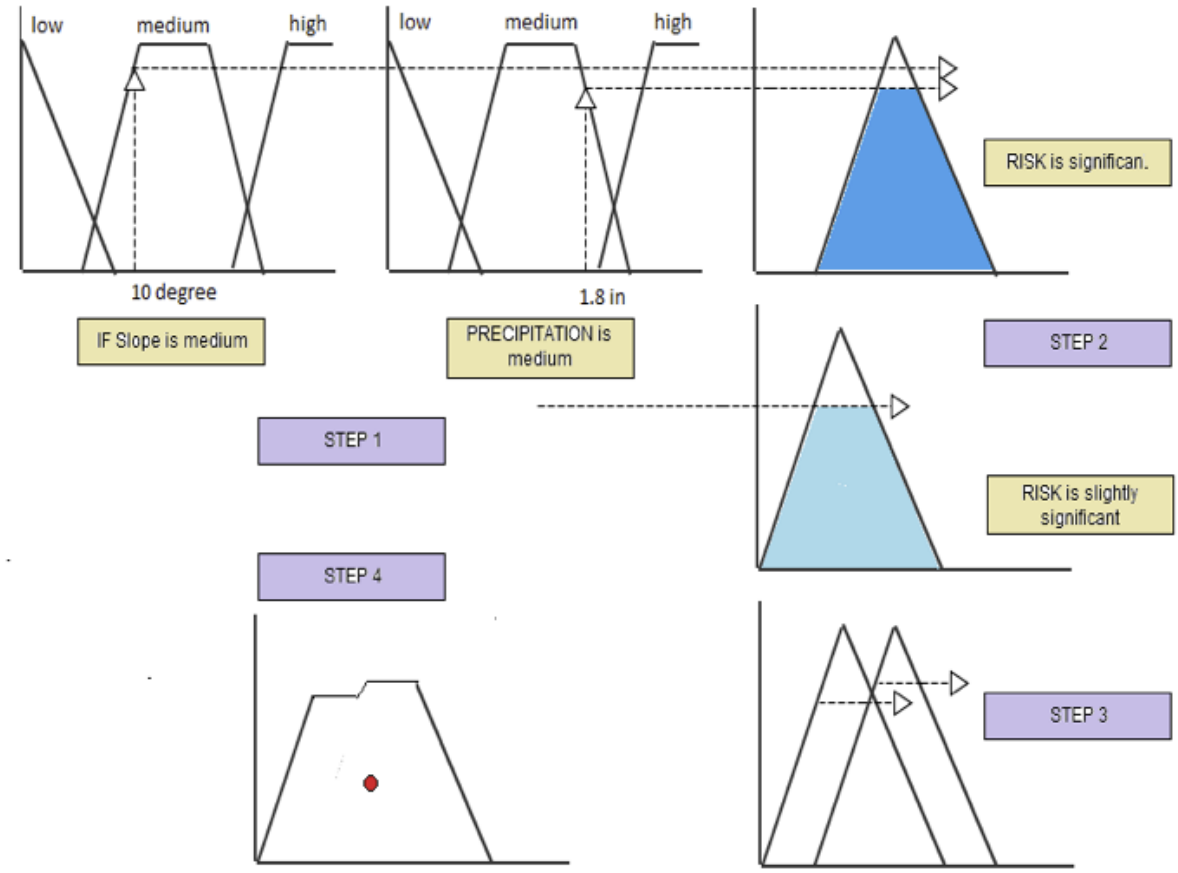

Figure 6. Fuzzy Reasoning Steps.

SOIL EROSION RISK MAP

The resulting soil erosion risk map based on the *LS*-factor is presented in Figure 7. The risk varied between 0.05 and 0.87 on a scale of 0 to 1. The red (high risk) to blue (low risk) color scale provides a visual perspective of potentially problematic areas.

With the superposition of individual rasters for NDVI, *LS*, *K*, and ${}_2P_6$, the combinations of one or more indicators can be interpreted that contribute to a given high or low erosion risk. For example, far northeast section of New Mexico shows moderate to high soil erosion risk. In this region, precipitation is high, soil erodibility is high, vegetative coverage is medium, and the terrain is flat. Along the eastern border, the soil erosion risk is low. Soil erodibility is low; however, the other three indicators are the same as above. The mid-south and southern regions show the highest erosion risk, having erodible soils, medium to dense vegetative cover, and low precipitation.

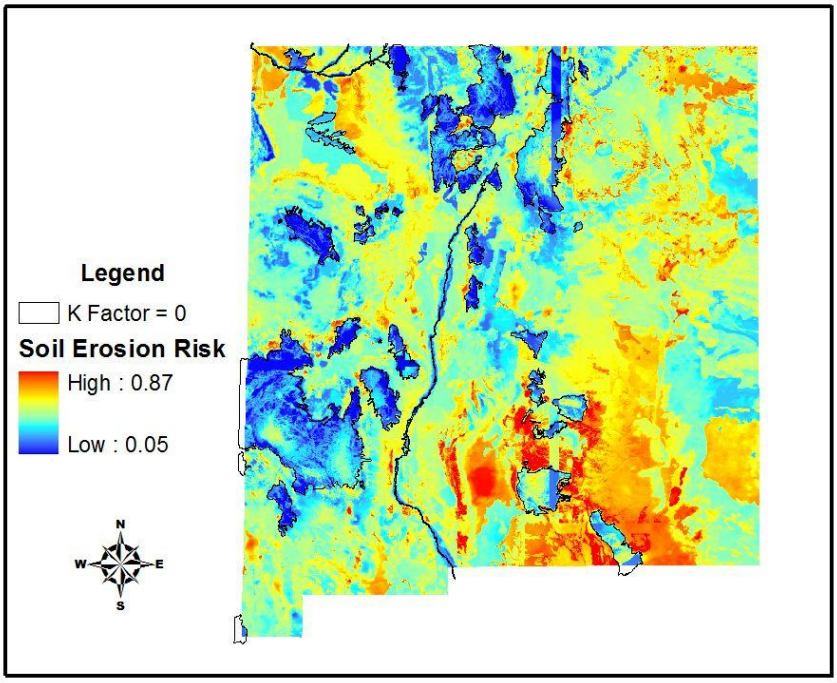

Figure 7. Soil Erosion Risk Map for New Mexico.

It is expected that low NDVI values result in high soil erosion risk, because there is not enough vegetation or land cover to inhibit soil movement. Steep slope gradients generally result in high soil erosion risk. Erodible soils are prone to detachment and movement by water during intense precipitation. The combinations of indicators and their dominance are complex and difficult to interpret, or generalize on a region by region basis.

The black framed areas in Figure 7 delineate areas there is either no soil erodibility data or the value is zero. This tends to bias those areas to have lower defuzzified soil erosion risk values. When the *K*-factor is zero, the membership function automatically becomes 1 (full belonging to low soil erodibility range). Since the defuzzification method used in this study is center of gravity, the outcome tends to be lower when one factor is zero. In addition, when soil erodibility is low, there are only 27 (3^3) rules left that can be applied to impact the outcome, depending on the pixel values of *LS*, NDVI and ${}_2P_6$. As evident in Figure 7, the black framed areas tend to have lower soil erosion risk (blue).

CONCLUSION

Quantifying the risk of soil erosion within a geographic region provides a useful engineering management and design tool. To this end, a soil erosion risk map was generated for the State of New Mexico. The method assumed that soil erodibility, precipitation, vegetation, and topography were primary factors that contribute to soil erosion. Areas for soil erosion were identified based on a color scale from 0 (low risk) to 1 (high risk). The potential soil erosion risk map identified the most problematic areas are present in the south, northeast, and southeast of New Mexico.

REFERENCES

Ahamed, T.R., K. Gopal Rao, and J.S.R. Murthy. 2000. Fuzzy Class Membership Approach to Soil Erosion Modelling. Agricultural Systems. 63:2, 97- 110.

Bulut, Gaye Gül. 2011. Potential Soil Erosion Risk for New Mexico and Sensitivity Analysis of Contributing Parameters. Thesis. New Mexico Institute of Mining and Technology.

Liu, K.F.R., Liang, H. H., Yeh, K. and Chen, C. W. 2009. A Qualitative Decision Support for Environmental Impact Assessment Using Fuzzy Logic. Journal of Environmental Informatics, 13:2, 93-103.

Kainz, W. 2008. Fuzzy Logic and GIS. http://homepage.univie.ac.at/wolfgang.kainz/Lehrveranstaltungen/ESRI_Fuzzy_Logic/File_2_Kainz_Text.pdf.

Lillesand, T.M. and Kiefer, R.W. 1987. Remote Sensing and Image Interpretation, 2nd edition.

Mitra, B., H.D. Scott, J.C. Dixon, and J.M. McKimmey. 1968. Applications of Fuzzy Logic to the Prediction of Soil Erosion in a Large Watershed. Geoderma. 86:3-4, 183-209.

Soil Information for Environmental Modeling and Ecosystem Management. 2001. http://www.soilinfo.psu.edu/index.cgi?soil_data&conus&data_cov&k&methods.

Tayfur, G., Ozdemir, S., and Singh, V.P. 2003. "Fuzzy Logic Algorithm for Runoff-induced Sediment Transport from Bare Soil Surfaces." Advances in Water Resources, 26:12, 1249-1256.

van der Knijff, J.M., Jones, R.J.A, and Montanarella, L. 1999. Soil Erosion Risk Assessment in Italy. European Soil Bureau, European Commission Joint, L.Research Centre Institute for Environment and Sustainability.

Weesies, G.A. 1998. K Factor. Soil Erodibility. Guidelines for the Use of the Revised Universal Soil Loss Equation (RUSLE).

Wischmeier, W.H. 1959. A Rainfall Erosion Index for a Universal Soil- Loss Equation. Soil Sci. Soc. Am. J, 23:3, 246-249.

Wischmeier, W.H. and Smith, D.D. 1978. Predicting Rainfall Erosion Losses: A Guide to Conservation Planning. U.S. Dept. of Agriculture, Science and Education Administration and Purdue University, Washington, D.C.

Yanar, T.A. and Akyürek, Z. 2006. The Enhancement of the Cell-based GIS Analyses with Fuzzy Processing Capabilities. Information Sciences, 176:8, 1067-1085.

Yen, J.and Langari, R. 1999. Fuzzy Logic: Intelligence, Control, and Information. Pearson Education, Inc.

Zadeh, L.A. 1965. Fuzzy Sets. Information and Control. Information and Control. 8, 338-353.

Acknowledgements

This research was funded in part by the New Mexico Department of Transportation (NMDOT)-Research Division in an effort to better understand typical soil erosion scenarios present along New Mexico highways.

CORRESPONDENCE SHOULD BE ADDRESSED TO:
Dr. Mark P. Cal, P.E., BCEE
New Mexico Tech
Department of Civil and Environmental Engineering
801 Leroy Place, Jones Annex 111
Socorro, NM 87801
mcal@mac.com

MODELING ACEQUIA WATER USE IN THE RIO HONDO WATERSHED

Sandeep Sabu[1]
William Fleming[2]
Jose Rivera[3]
Bruce Thomson[4]
Vince Tidwell[5]

ABSTRACT

Acequias are canals that channel water from higher to lower elevation to be used for flood irrigation of agricultural fields, which can result in the phenomenon of recharging local aquifers. In this study, a computer model was constructed to quantify the effects of agricultural water use in the Rio Hondo watershed, north of Taos, New Mexico. The watershed is home to 13 regional acequias, which flow through three separate communities. The Rio Hondo simulation aggregates water use in all 13 acequias to provide a general characterization of the impact of flood irrigation on the local aquifer. The simulation is constructed in STELLA® 9.1, a generalized system dynamics modeling platform that uses stocks, flows, and converters to map out interrelated components of any system. The Rio Hondo simulation models surface and groundwater availability, crop productivity, and crop market value across five climate change scenarios, five crop distributions, and three irrigation methods. The model is based on publically available data and a range of assumptions. The simulation was constructed to display dynamic trends that occur between surface and groundwater flows and show how these trends may respond to changes in crop distribution, irrigation practices and stream flow within the watershed. The simulation does not purport to project actual values for surface and groundwater yields across these scenarios. Based on an estimated hypothetical volume, the local aquifer stabilizes under flood irrigation, while its volume diminishes by as much as 20% under drip irrigation. Surface water flows in the Rio Hondo are projected highest to lowest in the drip irrigation scenario where water saved from drip was returned to the river, then the flood irrigation scenario where no water savings took place, and finally the drip scenario where water savings from drip were re-allocated for agricultural use. Again, these projections are not meant to represent hard and fixed predictions of future water availability or crop productivity within the watershed. Rather, they are meant to highlight how various components of this manmade-natural system may respond to future

[1]S. Sabu, Dept. of Community and Regional Planning and Water Resources, University of New Mexico, MSC04 2530, Albuquerque, NM 87131
[2]W. Fleming, Dept. of Community and Regional Planning and Water Resources, University of New Mexico, MSC04 2530, Albuquerque, NM 87131
[3]J. Rivera, Center for Regional Studies, University of New Mexico, MSC05 3020, Albuquerque, NM 87131
[4]B. Thomson, Dept. of Water Resources and Civil Engineering, University of New Mexico, MSC01 1070, Albuquerque, NM 87131
[5]V. Tidwell, Earth Systems Dept., Sandia National Laboratories, PO Box 5800, Albuquerque, NM 87185

changes, with the ultimate goal of engaging a broad range of stakeholders in envisioning alternative management strategies for future water use within the watershed.

Acequia communities have existed in northern New Mexico for more than 400 years (Brown & Rivera 2000). These communities practice subsistence agriculture and participatory water management where water is collectively allocated amongst parciantes, or irrigators, under the supervision of mayordomos, or canal managers. Home to one cluster of such communities, the Rio Hondo watershed drains an area of 194 square kilometers, with headwaters originating in Wheeler Peak, New Mexico's highest peak at more than 3,962 meters. Winding down the western face of Wheeler Peak, the Rio Hondo flows into the valley of Valdez, where it is eventually channeled into 13 regional acequias irrigating approximately 2870 acres (1,161 hectares) within the watershed. (Johnson 1998) After Valdez, the Rio Hondo flows near the village of Des Montes and through the village of Arroyo Hondo to join the Rio Grande at an elevation of 1,972 meters.

The hallmark of acequia communities is the fact that management of land and water resources remains embedded within the social structure of the community at a human scale. During times of water plenty, more parcels of land may be brought under immediate cultivation, while in times of drought, agricultural activity shrinks just as quickly (Palemon Martinez, personal communication, October 4, 2010). Most farmers within the watershed grow a range of crops that can be altered based on regional demand. In the Rio Hondo, pasture grass is grown for livestock that is sold at nearby auctions, as well as stored and used for winter hay. Fruit and vegetables are grown for household consumption. Extra pasture grass, fruit, and vegetables are traded with neighbors or sold at nearby farmers markets.

As the first users of snowmelt water, acequia communities are particularly vulnerable to changes in future climate that may include fluctuations in snowpack, precipitation, and resulting stream flow, increases in surface temperatures, and prolonged periods of drought (New Mexico Office of the State Engineer, 2006). Given the fact that, as an institution, acequia communities have functioned in one form or another for approximately 400 years in New Mexico, these communities have already withstood a range of historic, climatologic, economic, and social changes. They already demonstrate a high degree of resiliency.

Resiliency can be defined as the ability to adapt to change (Holling 2000, Meadows 2008). Relying on close-knit social networks to manage land and water resources, acequia communities are able to respond directly and efficiently to changes in their environment, whether these are social or natural. In contrast to large-scale, industrialized practices for resource management, acequia communities display a much higher degree of adaptability due to immediate socio-cultural responsiveness to changes in the environment. The Rio Hondo simulation was conceptualized to experiment with a

series of leverage points within this human-nature system and how intervening at these points may affect the system as a whole.

A system can be defined as any set of components interacting with each other based on structure, relationships, and a purpose (Meadows 2008). Systems abound; we can see them everywhere. The simplicity or complexity of a system is defined largely by how it is bounded and how many variables are included in this boundary. Clearly delineating a system is crucial in any modeling exercise as it focuses the modeling exercise on a manageable number of variables. Modeling human-nature systems is particularly relevant for natural resource managers as it helps to explicate broader trends that may not be directly perceptible regarding the functioning of the system. Systems modeling can enhance our understanding of how the overall system functions, how its various components interact with each other, which components have a greater impact on the system, and finally, points to intervene to encourage greater efficiency. As a participatory water planning tool, system dynamics modeling can also help to create a decision support structure to engage a broad range of stakeholders, inform the public on how human-nature systems function, and assist natural resource managers in presenting a range of options to policymakers in a cohesive, palpable format (Tidwell 2004).

System dynamics modeling relies on stocks, flows, and converters to visually map out a system and assign mathematical relationships to its various components. Stocks can be defined as an accumulation of a salient variable, such as water or money. Flows are a transfer between two stocks. Flows must be expressed as a rate and may be affected by numerous other factors. All of these factors must be unified based on a series of mathematical relationships to maintain consistency with the units of the stocks. For example, a stream flowing into a lake would collect water from precipitation and the surface area of the stream or perhaps even the whole catchment. By assigning a relationship between the precipitation in inches and the surface area of the catchment in square feet, these two influencing variables can be multiplied to determine a volume of water being added to the river, which is flowing into the lake. In systems modeling terminology, these influencing variables are called converters. See Figure 1.

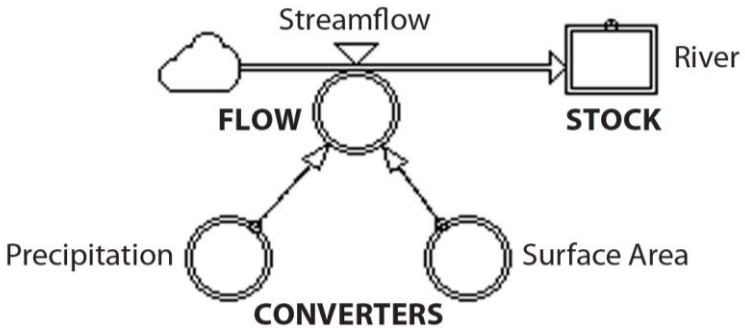

Figure 1: Example of building blocks of system dynamics models

The Rio Hondo simulation is constructed with these basic building blocks to produce outputs for surface and groundwater volumes, crop production, and crop market value across five climate change scenarios, three irrigation methods, and five alternate crop distributions. The simulation relies on basic mathematical relationships amongst a host of variables. All data for the simulation was taken from publically available reports published by academic researchers and government agencies.

OBJECTIVE AND MODEL CONCEPTUALIZATION

Flood irrigation has been shown to replenish shallow aquifers due to deep percolation from agricultural fields. Water in canals or atop agricultural fields seeps into shallow groundwater sources (Fernald 2006, Ochoa 2007, 2009). Water flowing in rivers and canals also promotes the growth of riparian vegetation along riverbanks and canal banks. Aptly termed a *paisaje del agua* by Rivera, this "water landscape" serves as a buffer to keep water within the riparian landscape. This is a particularly crucial ecosystem service in New Mexico's arid climate. Temperatures in these riparian corridors are cooler due to this vegetation, which in turn lowers surface water evaporation rates. However, these riparian corridors increase overall evapotranspiration of water due to water requirements for the vegetation. Given projections for reductions in spring runoff that may be as high as 43 percent by the end of this century (Coonrood & Hurd 2007, Reclamation 2011), the replenishment of local aquifers via flood irrigation and the riparian buffer created from water flowing through acequias might make an appreciable difference in available water resources for future inhabitants of New Mexico's high desert.

On the other hand, flood irrigation is a basic irrigation technique with a potential irrigation efficiency of only about 45 to 55 percent in New Mexico (Wilson & Lucero 2003, Fisher 2008). Developed in Israel, drip irrigation relies on PVC tubes to direct water onto the roots of crops where it is released in a small trickle, contributing to a potential irrigation efficiency of as high as 90 percent (Fischer 2008). Given the increasing scarcity of water resources in the region, drip irrigation could be an attractive, water-saving investment for farmers in New Mexico's acequia communities. This opportunity represents a possible leverage point to encourage more efficient use of water resources in these communities. The Rio Hondo simulation was conceptualized to see how switching from flood to drip irrigation would affect crop production rates as well as surface and groundwater flows within the watershed.

The United States Geological Survey (USGS) has established two gages within the watershed. Once the Rio Hondo enters the valley of Valdez it flows through USGS gage 8267500, Rio Hondo near Valdez, at 2,331 meters. The Rio Hondo then starts getting diverted into a series of 13 ditches irrigating a total of 2,870 acres (1,161 hectares) within the villages of Valdez, Des Montes, and Arroyo Hondo. See Map 1. Irrigated crops include alfalfa, hay and pasture, orchards, grain, and some vegetables (Hydrographic Survey 1969; Johnson 1998; Daniel B. Stephens & Assoc., 2008). See Table 1. Just before joining the Rio Grande at mile 1677.5 (Johnson 1998), water flows through USGS gage 8268500, Arroyo Hondo at Arroyo Hondo, at 2,033 meters (USGS

website, http://www.waterdata.usgs.gov/nwis/rt, last accessed October 20, 2011). Gage 8268500, Arroyo Hondo at Arroyo Hondo, was installed in 1913 and decommissioned in 1985, while gage 8267500, Rio Hondo near Valdez, was installed in 1935 and continues to collect data (Johnson 1998).

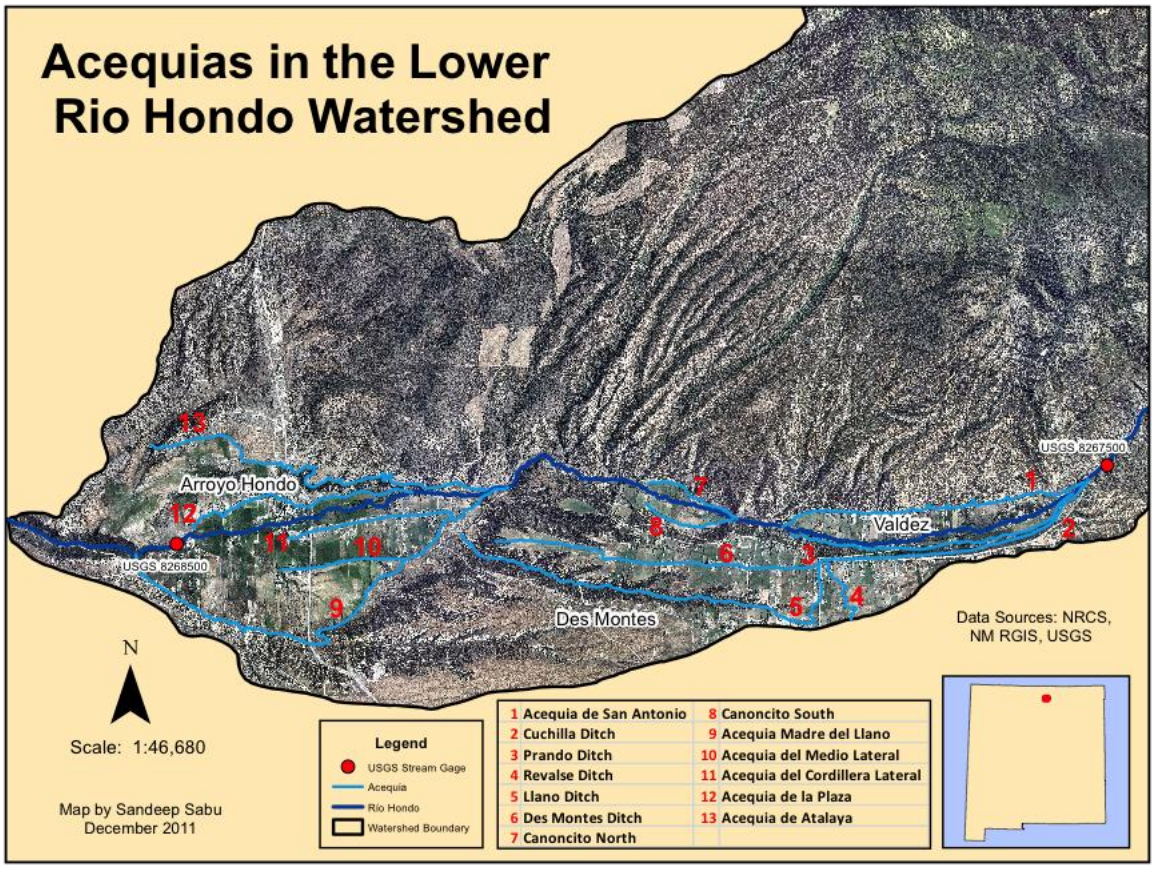

Map 1: Acequias in the Lower Rio Hondo Watershed

Crop Type	Percentage of Total Acreage	Acres (Hectares)
Alfalfa	24.6	706 (285)
Planted Pasture	10.2	293 (118)
Pasture & Hay	36	1,033 (418)
Native Pasture	12.4	356 (144)
Orchard	2.2	63 (25)
Vegetables	2.2	63 (25)
Grain	5.5	158 (64)
Fallow	6.9	198 (80)

Table 1: Distributions of crops in the Rio Hondo Watershed (Source: NMOSE, Hydrographic Survey 1969)

MODEL STRUCTURE AND DATA SOURCES

The primary input of the Rio Hondo simulation is stream flow data from USGS gage 8267500, Rio Hondo near Valdez. Current and historic stream flow as well as river stage measurements are available on the USGS website, "USGS Real-Time Water Data for the Nation" found at http://www.waterdata.usgs.gov/nwis/rt (last accessed October 20, 2011). The model is set to run on a yearly time step with stream flow input as a graphical function to capture natural fluctuations. Stream flow for the growing months of April to September was used since this is the period of substantial flow in the river, ie 229 cfs as compared to average of 81 cfs during the rest of the year based on USGS monthly data (accessed at http://www.waterdata.usgs.gov/nwis/rt).

Once stream flow data is input into the simulation water is diverted into a flow titled acequia inflow. Acequia inflow aggregates water flow for all 13 regional acequias and is calculated based on the New Mexico Office of the State Engineer's allocation of 3.9 acre-feet per irrigated acre (Daniel B. Stephens & Assoc., 2008).

Acequia inflow is calculated according to the equation:

$$\textit{Acequia inflow} = 3.9\ \textit{acre-feet per acre} * 2870\ \textit{acre} \quad (1)$$

From acequia inflow, diversions occur for agricultural consumptive use, incidental depletions, canal seepage, deep percolation, canal surface evaporation, and canal riparian evapotranspiration. Each of these diversions is based on studies of the demand profile of water used for irrigation. The Rio Hondo simulation uses percentages for each of these components. While there are obvious limitations to this generalized approach, the simulation is meant to provide a descriptive analysis of hydrologic trends in the watershed rather than fixed values of surface and groundwater availability.

Wilson and Lucero (2003) provide an example of the various components of the demand profile for water under flood irrigation. In their report, they refer to the figure below as a "computational aid…for quantifying irrigation withdrawls and depletions [and] addresses many facets of irrigation that are often overlooked" (Wilson and Lucero, 2003). In this example, agricultural consumptive use is valued at 60% of the total farm delivery. Total farm delivery is valued at 70% of the total canal diversion. This yields an agricultural consumptive use or consumptive irrigation requirement of 42% of water flowing through the channels.

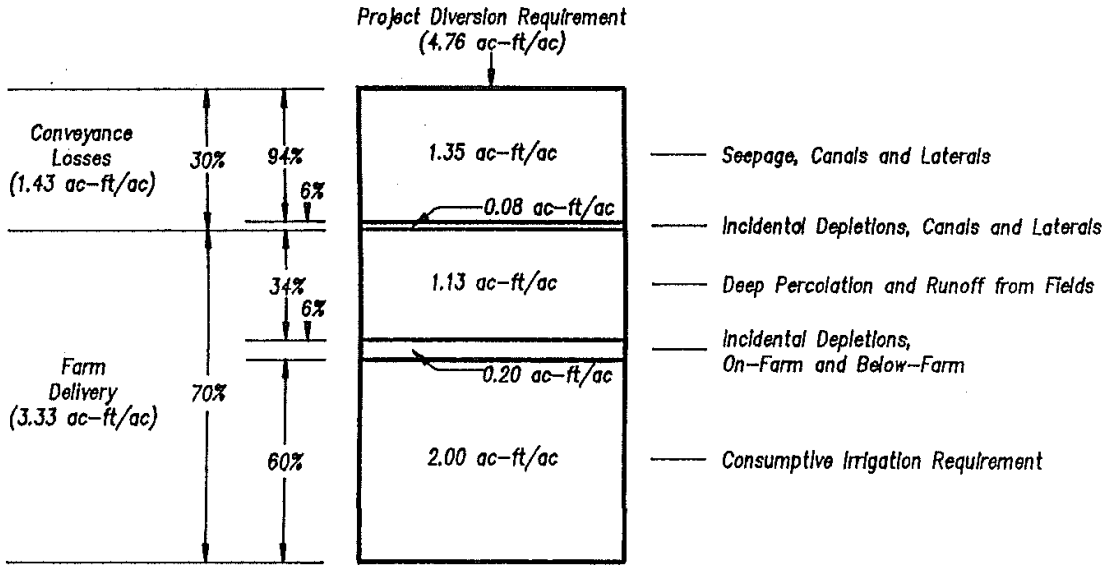

Figure 2: Water demand profile under flood irrigation (Wilson & Lucero 2003)

In contrast to this generalized approach, Fernald, et al. (2010) conducted studies wherein the specific components of the demand profile for flood irrigation were actually measured. In this study, conducted at the Alcalde Agricultural Science Center, a demand profile for components of flood irrigation is offered as percentages of total canal diversion. The largest discrepancy between the demand profile from Wilson & Lucero and Fernald et al. study is in agricultural consumptive uses. See Table 2. This is due to the fact that the Wilson & Lucero study does not account for canal outflows, but only for agricultural consumptive use based on a proportion of farm delivery requirements. Also, the two demand profiles rely on different methods for calculating agricultural consumptive requirements for crops. The Alcalde study calculates agricultural consumptive use based on weather data, which was used to calculate crop ET using the Penman-Monteith equation (Fernald et al., 2010). The sample demand profile offered by Wilson & Lucero is based on applying the Blaney-Criddle method and seasonal consumptive use coefficients to a hypothetical cropping pattern for a flood irrigated agricultural field (2003).

	Wilson & Lucero (2003)	Fernald, et. al (2010)
Canal Seepage	28.2%	12.1%
Incidental Depletions	6%	8.9%
Irrigation Seepage/ Deep Percolation	23.8%	21.2%
Consumptive Uses	42%	7.4%
Turnouts		9.5%
Canal outflow		40.9%

Table 2: Comparison of water demand components in flood irrigation in Wilson & Lucero (2003) and Fernald et. al., (2010) study

The Rio Hondo simulation uses these two studies as a launching point for assigning hypothetical values to the various components of the demand profile for flood irrigation. Normalized seasonal consumptive requirements minus effective precipitation as calculated by Blaney and Hanson (1965) are applied to the crop distribution of the Rio Hondo watershed. See Table 3. While this is a simplistic way of accounting for agricultural consumptive use, given the fact that the Rio Hondo simulation is an aggregated systems model, it is necessary to have a normalized value of crop consumptive use that can be applied to the watershed as a whole. The total consumptive requirement of 3,693 acre-feet is 33% of the total canal diversion of 11,193 acre-feet based on the State Engineer's allocation. The other components of the demand profile in the Rio Hondo simulation more or less follow the percentages found in the Alcalde study. See Figure 3.

Crop Type	Consumptive Irrigation Requirement (m. (in.))	Total Water Use based on irrigated acreage (acre-feet)
Alfalfa	0.46 m. (18.3 in.)	1077
Pasture	0.42 m. (16.77 in.)	2350
Orchard	0.32 m. (12.73 in.)	67
Vegetables	0.28 m. (11.03 in.)	58
Grain	0.27 m. (10.7 in.)	141
Total		3693

Table 3: Normalized seasonal consumptive use requirements for crops grown within the watershed (Source: Blaney and Hanson 1965)

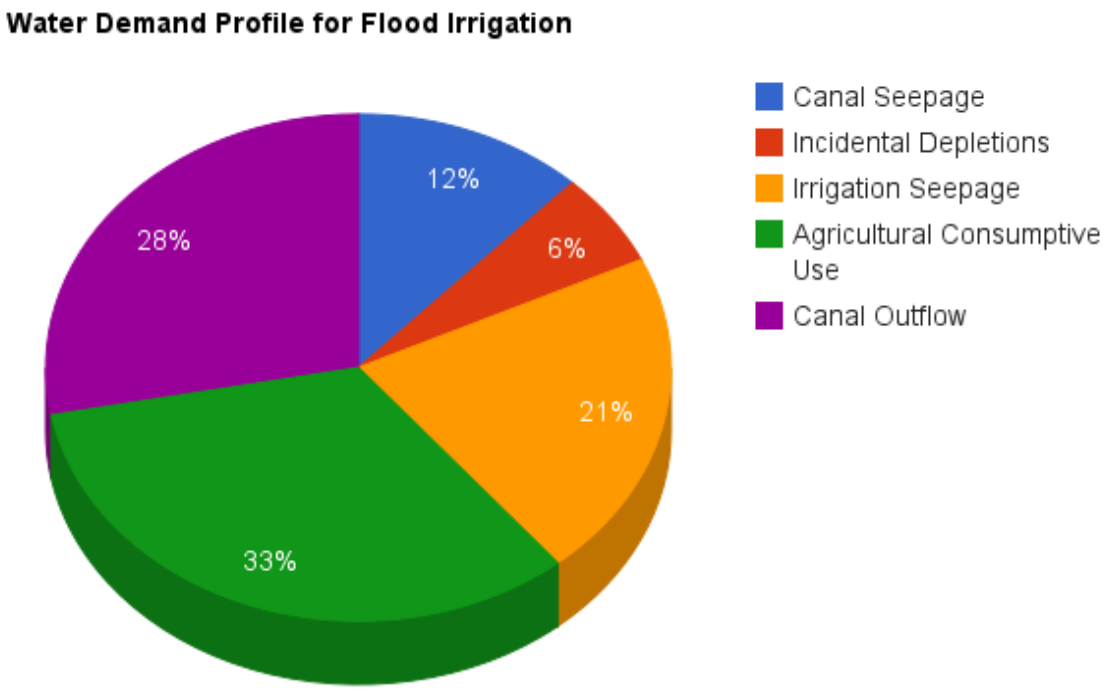

Figure 3: Values of water demand profile used in the Rio Hondo simulation

Surface water evaporation for the region is estimated at 2.2 acre-feet per year per acre while riparian evapotranspiration is about 3.75 acre-feet per year per acre (Daniel B. Stephens, 2008). The distance between USGS gage 8267500 and 8268500 is approximately 1.45 kilometers with a surface channel width of approximately 6.1 meters based on path measurement tool in Google Earth 6.1. This yields a channel surface area of 21.8 acres. The riparian buffer around the river and the canals is assumed to be approximately three feet on both sides of the canal or riverbank. Based on this demand profile and water lost through surface evaporation and canal riparian ET, acequia outflow is calculated with the formula:

Acequia outflow = acequia inflow – canal surface water evaporation – canal riparian evapotranspiration – incidental depletions – consumptive use – canal seepage – irrigation seepage or deep percolation (2)

From acequia outflow, the diversions for canal seepage and deep percolation are added to groundwater recharge that feeds into the shallow alluvial aquifer. An estimate for tributary inflow is also added to groundwater recharge on an annual basis. In the simulation, these inflows contribute directly to groundwater recharge. Groundwater depletion is an outflow from the shallow alluvial aquifer based on an approximate per capita pumping rate and population growth for the watershed (Alcantara 2008; Daniel B. Stephens 2008).

Surface and groundwater interactions are characterized with a bi-flow titled groundwater flow. A bi-flow allows flow to occur between two stocks, rather than

simply from one stock to another. Depending on the direction of the hydraulic gradient, water either moves from the aquifer to the river or from the river to the aquifer. Aquifer characteristics used in the simulation are based on studies of the regional hydrogeology (Johnson et al., 2009) as well as estimates and assumptions made to allow something as complicated as an aquifer to be characterized in the basic terms of stocks, flows, and converters.

The majority of the lower portion of the Rio Hondo watershed has an underlying geology of a shallow alluvial water bearing formation. This shallow alluvial aquifer ends at Airport Fault located at the western end of Arroyo Hondo (Johnson et al., 2009). See Map 2. At Airport Fault, a deep, volcanic water-bearing formation begins, creating conditions of anisotropic flow of water from the shallow alluvium to the deep volcanic formation, with a difference in head pressure measured at as much as 91 meters (Johnson et al., 2009).

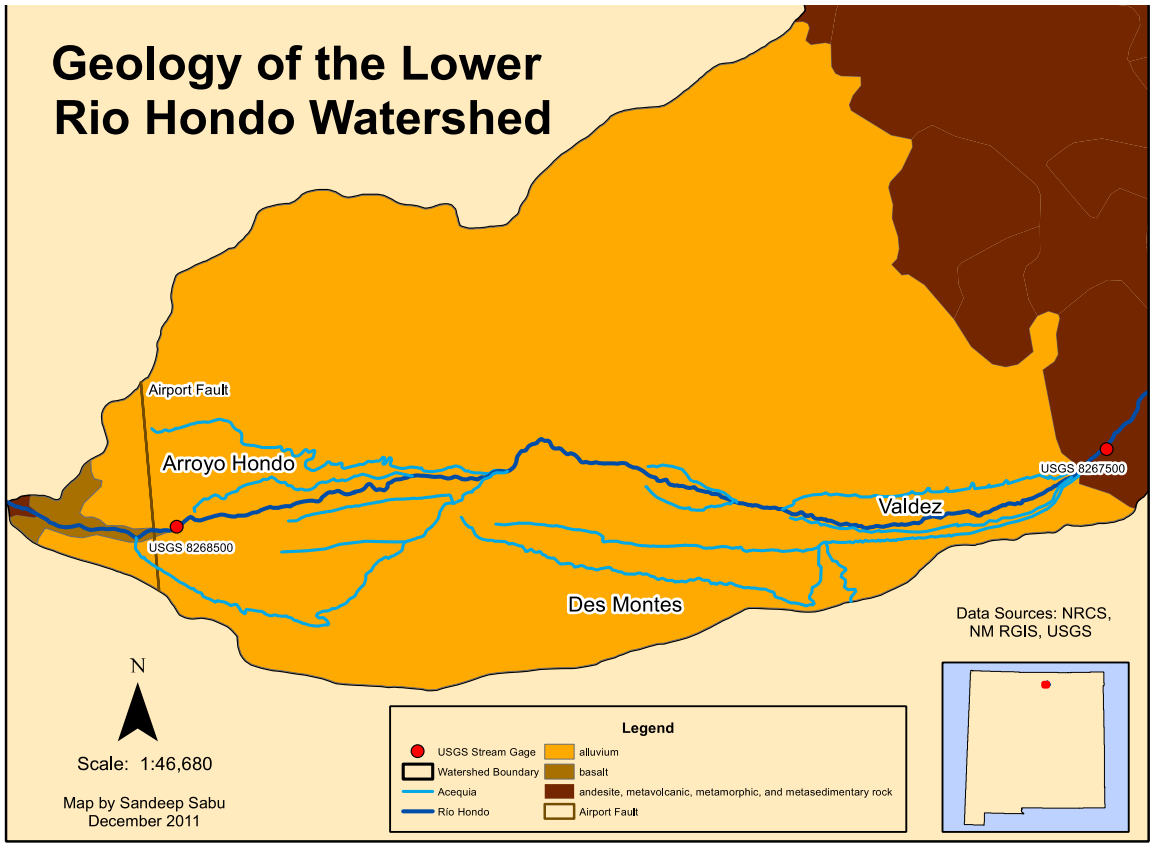

Map 2: Geology of the Lower Rio Hondo Watershed

Based on pump tests, hydraulic conductivity is measured to be 0.12 meters/day (Drakos 2004; Johnson 2009). Aquifer surface area is 124 square kilometers based on measuring the lower portion of the watershed in Google Earth® 6.1. The porosity of the alluvium is estimated to be 15% (V. Tidwell, personal communication, October 4, 2011),

while the depth of the aquifer is set at 30 meters based on a transmissivity of 3.72 square meters/day and a conductivity of 0.12 meters/day. This results in a calculated initial aquifer volume of 460,800 acre-feet.

Aquifer head interacts with Rio Hondo stage height to create a hydraulic gradient that is used to calculate flow through a porous medium based on Darcy's Law. USGS gage 8267500, Rio Hondo near Valdez, has an elevation of 2,331 meters while USGS gage 8268500, Arroyo Hondo near Arroyo Hondo, has an elevation of 2,033 meters. Due to the need to simplify certain physical characteristics of the system so it can be modeled in STELLA® 9.1, the channel bed of the Rio Hondo is assumed to remain at one constant elevation. Ignoring the 2% slope of the Rio Hondo, an average elevation of 2,182 meters is used for the simulation. The stream gage height data taken from the USGS website is added to this average river elevation in calculations for the hydraulic gradient. Given that the aquifer head is approximately 30 meters in the simulation, the datum for the aquifer is set at 2,154 meters to create the initial conditions of a gaining stream based on studies of the area (Johnson 1998; 2009). Again, despite the obvious limitations to this simplified approach, it allows for easier translatability into STELLA® 9.1. It should be reiterated that the Rio Hondo simulation is meant to describe broad trends regarding how agricultural water use interfaces with surface and groundwater flows for the purposes of engaging the public.

Finally given that field tests by Johnson et al. have shown a 91.44 meter difference in head pressure between these two aquifers, a transbasin flow is included in the simulation to mimic the effects of this vertical flow gradient. This value was estimated at 3000 acre-feet per year, which ensured that aquifer levels in the shallow alluvial aquifer maintain a consistent level during validation and projection runs. Below is a conceptual diagram of the Rio Hondo simulation. See Figure 4.

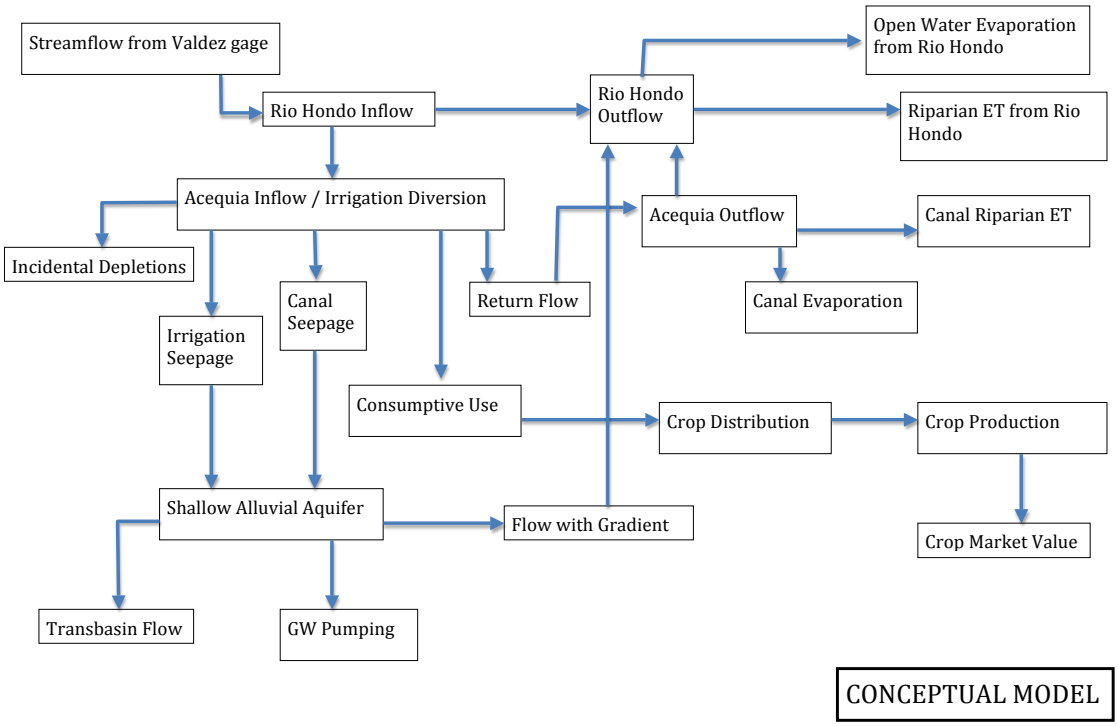

Figure 4: Conceptual Diagram of the Rio Hondo simulation

MODEL SYNTAX

The Rio Hondo simulation includes three modules. The first module, referred to as Flood, models flood irrigation. The next two modules, referred to as Drip A and Drip B, simulate two scenarios for drip irrigation. In both of the drip scenarios, there is no irrigation seepage included in the groundwater recharge component. In Drip A, the irrigation seepage returns to the Rio Hondo. In Drip B, the irrigation seepage is re-appropriated by acequia farmers allowing for increased agricultural consumptive use.

The distinguishing feature between the three modules is how agricultural consumptive use is determined. In each of the modules, the diversion for consumptive use is formulated as an IF statement. Based on evapotranspiration requirements of crops, as well as their distribution within the watershed, 3,693 acre-feet per year is the calculated agricultural consumptive use. This amounts to 33% of the total acequia allocation of 11,193. Under flood irrigation, the full suite of water use demands aside from agricultural consumption includes irrigation seepage, canal seepage, canal riparian evapotranspiration and canal surface water evaporation, and incidental depletions. In total, all of these components require 8,113 acre-feet of water per year. As long as there is at lease 8,113 acre-feet of water in the Rio Hondo, all of the agricultural consumptive use can be met for the watershed as a whole. If only 8,113 acre-feet is in the Rio Hondo inflow, then there will be no water returned to the Rio Hondo outflow. In the event that the Rio Hondo inflow has less than 8,113 acre-feet, the only component of the system where less water can be applied is in consumptive use. This is the only component of the system that is subject to voluntary increases or decreases. Therefore, in the flood scenario, the consumptive use converter is constructed to read, “If the Rio Hondo inflow

is greater than 8,113 acre-feet, then consumptive use is 3693 acre-feet, otherwise consumptive use is 3693 minus the difference between 8113 and the Rio Hondo inflow in that time step." In the Rio Hondo simulation, this syntax reads as,

Consumptive Use = IF (Rio Hondo Inflow > 8,113) THEN (3,693)
Else (3,693 – (8,113 – Rio Hondo Inflow)) (3)

This statement reads differently in both of the drip scenarios due to the fact that no groundwater recharge takes place under drip irrigation practices. In the first drip scenario, referred to as Drip A, the irrigation seepage component returns to the Rio Hondo outflow. This means less water is required for all of the components of the system to receive their full allocation. Specifically, the Rio Hondo need only have 5,762 acre-feet of water for all of the acequia components to receive their full allocation. Therefore in Drip A, consumptive use is determined by the syntax,

Consumptive Use = IF (Rio Hondo Inflow > 5,762) THEN (3,693)
ELSE (3,693 – (5,762 – (Rio Hondo Inflow)) (4)

In Drip B, the excess water from irrigation seepage is re-allocated increasing agricultural consumptive use from 3693 acre-feet to 6044 acre-feet, based on irrigation seepage of 2,351 acre-feet. In Drip B, the total amount of water required for all the components of the system to receive their full allocation of water is 8,113 acre-feet, just as in the flood scenario. The difference between Flood and Drip B is due to the fact that instead of 2,351 acre-feet seeping into the aquifer or returning to the Rio Hondo, as it does in Flood and Drip A, respectively, it is re-allocated by farmers. In Drip B, the syntax for consumptive use reads, "If the Rio Hondo inflow is greater than 8,113 acre-feet, then consumptive use is 6044 acre-feet, otherwise consumptive use is 6044 minus the difference between 8113 and the Rio Hondo inflow in that time step." The model syntax reads as,

Consumptive Use = IF (Rio Hondo Inflow > 8,113) THEN (6,044)
ELSE (6,044 – (8,113 – Rio Hondo Inflow)) (5)

Therefore, in Drip B and the Flood scenario, 8,113 acre-feet is the amount of stream flow needed for each module to receive its respective full consumptive use allocation of 6,044 and 3,693 acre-feet. In Drip A, only 5,762 acre-feet are needed for farmers to receive their full consumptive use allocation of 3,693 acre-feet. In Flood, Drip A, and Drip B, crop production follows the same formulas for determining crop yield based on crop ET requirements in semi-arid environments. In the Rio Hondo simulation, determining consumptive use according to an IF statement allows users to glean how changes in irrigation practices affect the hydrology of the watershed. The three scenarios outlined are meant simply to illustrate some possible "What if?" scenarios in order to show dynamic trends relating agricultural water use to surface and groundwater flows. These scenarios, and the Rio Hondo simulation in general, are not meant to outline the future water resources of the watershed in definite terms.

CLIMATE CHANGE INPUTS

For the Rio Hondo simulation, it was vital to find data, which downscaled General Circulation Models (GCM's) to extrapolate regional projections from these GCM's. Due to the highly aggregated nature of the Rio Hondo simulation, accounting for changes in precipitation or snowpack were not feasible. Instead, variations in stream flow inputs were used to capture the effects of climate change on agricultural water use in the watershed. Five stream flow inputs were used in the simulation. USGS gage 8267500, Rio Hondo near Valdez, continues to collect data up to the present day. For future runs, the values of 2000 to 2010 were used, and then gage data from 1935 to 2010 was recycled to represent the years 2011 to 2086. For 2087 to 2100, gage data was used from 1935 to 1948 were reused.

In addition to this baseline data set of stream flow, four projections of diminished stream flow were applied as a perturbation factor to this baseline of historic, reconstructed data. Hurd & Coonrod (2007) constructed a "river basin-scale hydro-economic (RBHE) model of the Rio Grande watershed to monetize the economic consequences as distinct from the hydrologic consequences of potential climate change." In the RBHE, three climate change scenarios are used across two future periods to represent the range of effects projected by the 18 General Circulation Models (GCMs) used by the Intergovernmental Panel on Climate Change in their Fourth Assessment Report (ibid). See Table 4.

Scenario	Conducted by
Wet	Hadley Center for Climate Prediction
Middle	Atmospheric Research from CSIRO Australia
Dry	Geophysical Fluid Dynamics Lab (NOAA)

Table 4: Climate Chance scenarios used in Hurd and Coonrood RBHE

For the Rio Hondo simulation these three climate change projections were used, as well a fourth scenario developed by the U.S. Bureau of Reclamation. In 2009, the SECURE Water Act was passed by the U.S. Congress to assess the adequacy and health of the nation's waters. The act aims at developing data focused on climate change impacts on water resources in the Western United States. The U.S. Bureau of Reclamation's report, "Reclamation, Climate Change, and Water: A Report to Congress," has projections for diminishments in stream flow for seven Western river basins including the Rio Grande.

All four scenarios yield projections of diminished stream flow for two future time periods, 2020 to 2039 and 2070 to 2089. Using a best-fit line, these two periods of projection serve as the basis for estimates of diminished stream flow to 2100. The percentages below are applied to the data set of baseline stream flow reconstructed from current and historic gage data to create four distinct stream flow regimes in addition to the baseline regime. See Table 5.

Future Time Period	Wet	Middle	Dry	US BoR
2020-2035	6.5%	3.5%	13%	1.5%
2035-2045	7.0%	7%	17%	5%
2045-2055	7.5%	11%	21%	9%
2055-2065	7.75%	14%	24%	12%
2065-2075	8%	18%	27%	18%
2075-2085	8.3%	22.8%	29%	21.7%
2085-2100	11%	26%	34%	23%

Table 5: Percentage of stream flow diminishment through four climate change projections

Note: The percentages in bold and italics are published data for two future time periods while the percentages in between these are extrapolated from best-fit trend lines.

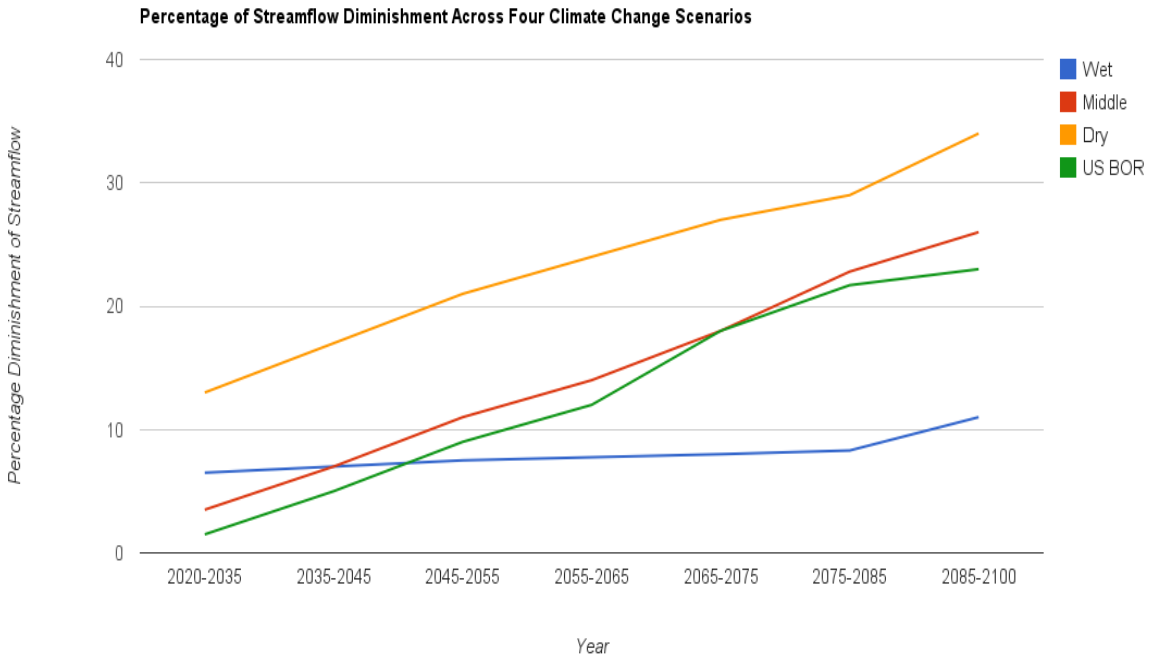

Figure 5: Percentages of Diminished Stream Flow Across Four Climate Change Scenarios

MODEL VALIDATION

The Rio Hondo simulation was validated based on historic gage data collected at USGS gage 8268500, Rio Hondo near Arroyo Hondo, which was in operation from 1935 to 1985. Once the model structure was assembled, Valdez gage from 1935 to 1985 was input into the model, and the projected outputs for Rio Hondo outflow were compared to

Arroyo Hondo gage data for the same period. In the early and later periods of the simulation runtime, projected values and Arroyo Hondo data matched or came close with small discrepancies. These early and later periods consisted of approximately the first and last 12 years of the 50-year calibration run. During the middle twenty-five years of the calibration run, the discrepancy between predicted values and Arroyo Hondo data increases. See Figure 6.

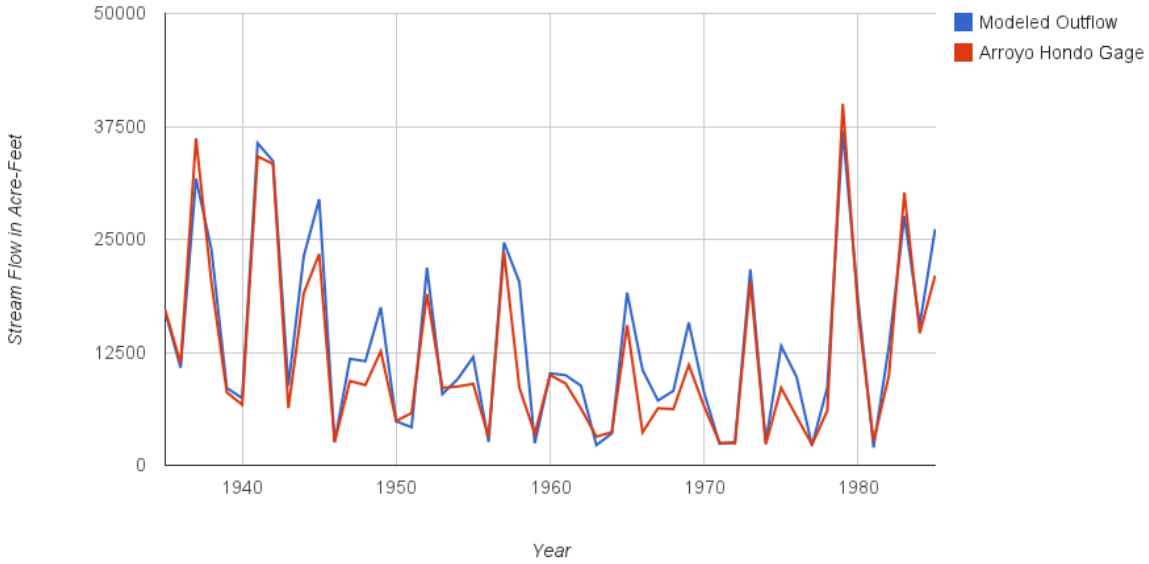

Figure 6: Validation run from 1935 to 1985

Due to the aggregated nature of the Rio Hondo simulation, there could be a number of reasons for this discrepancy. One apparent issue is that the simulation was initially constructed to create conditions a gaining stream. It seems likely that this aspect of the simulation overestimates the amount of water being contributed from the aquifer to the river in the Flood module. Also, in the simulation, there is a tributary inflow component added to groundwater recharge. This is meant to mimic water flowing from higher creeks in the higher elevations of the watershed. There is little available flow data for these creeks. In the simulation, tributary inflow is set at 1,500 acre-feet, and it flows directly into the aquifer. This is may be over-generous, and perhaps should not be entirely directed to the aquifer. If some portion of this inflow were transmitted directly to the Rio Hondo, it would be subject to evaporation and riparian ET losses. This discrepancy can be addressed in any future iterations of the Rio Hondo simulation that may be constructed. For the sake of brevity, discussion of sensitivity analysis or calibration will be left out of this article.

MODEL RESULTS AND DISCUSSION

Given the broad range of data sets incorporated into the Rio Hondo simulation, model outputs are grouped into four categories: (1) hydrologic based on climate change scenario, (2) hydrologic based on flood versus drip irrigation, (3) economic based on

Drip A and Flood versus Drip B, and (4) economic based on Alternative Crop Distribution Scenarios. The four climate change scenarios are referred to as Wet, Middle, Dry, and US BoR. As a comparison, there is a Baseline stream flow scenario with no projected diminishment of stream flow. We will leave out discussion of the economic outputs of the Rio Hondo simulation here.

Due to the way consumptive use diversions are conceptualized within the three modules, there are more years where full consumptive use requirements are not met in Flood and Drip B since they both require 8,113 acre-feet of initial stream flow whereas Drip A only requires 5,762 acre-feet. See Table 6.

Climate Change Scenario	Drip A	Drip B	Flood
Baseline	2	10	10
Wet	3	12	12
Middle	4	14	14
Dry	7	16	16
US BoR	3	12	12

Table 6: Number of years where full agricultural consumptive use is not available through four climate change scenarios and a baseline scenario

In terms of groundwater dynamics, Drip A and B follow the same pattern while the Flood module follows a separate pattern. In Drip A and B, groundwater recharge is only composed of tributary inflow and canal seepage, while in Flood groundwater recharge also includes irrigation seepage. In Flood, the aquifer stabilizes around 460,000 acre-feet, fluctuating within a range of 459,000 acre-feet and 472,000 acre-feet based on variability in stream flow through the simulation run from 2000 to 2100. Aquifer volume diminishes as input stream flow diminishes due to the fact that less water in the Rio Hondo means more instances where full consumptive use requirements are not met, which in turn means less recharge from irrigation and canals. Given the stabilizing influence of recharge to the aquifer, the groundwater flow maintains a range of 1,900 to 1,500 acre-feet per year moving from the aquifer to the Rio Hondo. Through the five climate change scenarios, final aquifer volume ranges from approximately 462,000 acre-feet to 466,000 acre-feet from the driest to the wettest scenarios. See Figure 7, 8, and Table 7.

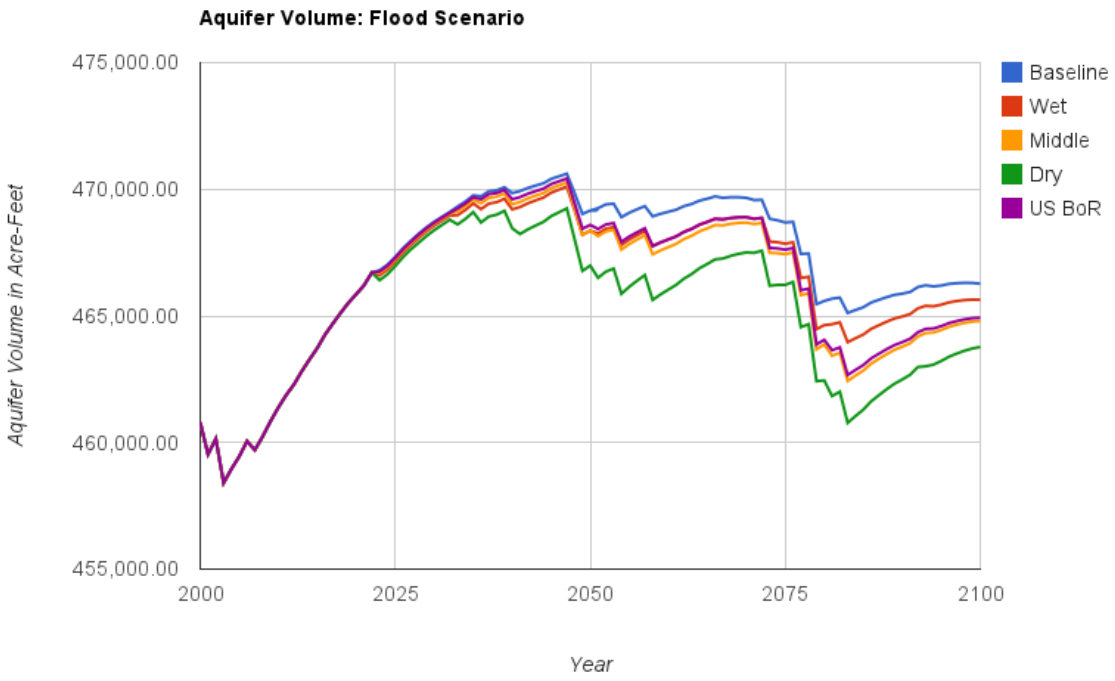

Figure 7: Aquifer volume through five climate change scenarios: Flood

Climate Change Scenario	Final Aquifer Volume
Baseline	466,270.33
Wet	465,536.49
Middle	464,798.41
Dry	463,773.06
US BoR	464,926.37

Table 7: Final aquifer volume in acre-feet through five climate change scenarios: Flood scenario

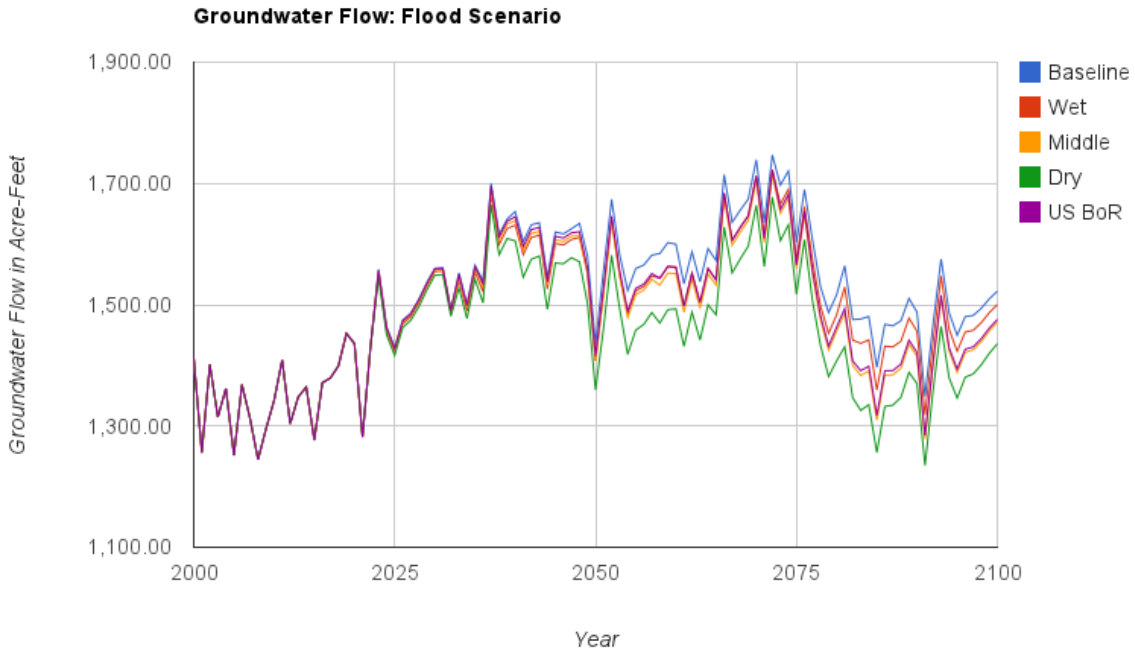

Figure 8: Groundwater flow through five climate change scenarios: Flood

In both Drip A and Drip B, the aquifer volume plummets. The absence of irrigation seepage from the groundwater recharge component creates an amplifying feedback loop where aquifer volume continues to decline precipitously. In the first time step, the aquifer volume is the same in all three modules. With the absence of irrigation seepage, the aquifer level declines to 367,000 acre-feet by the end of the simulation in both drip modules. Through the five climate change projections, aquifer volume ranges from 367,000 acre-feet to 371,000 acre-feet from the driest to the wettest scenarios. See Figure 9 and Table 8.

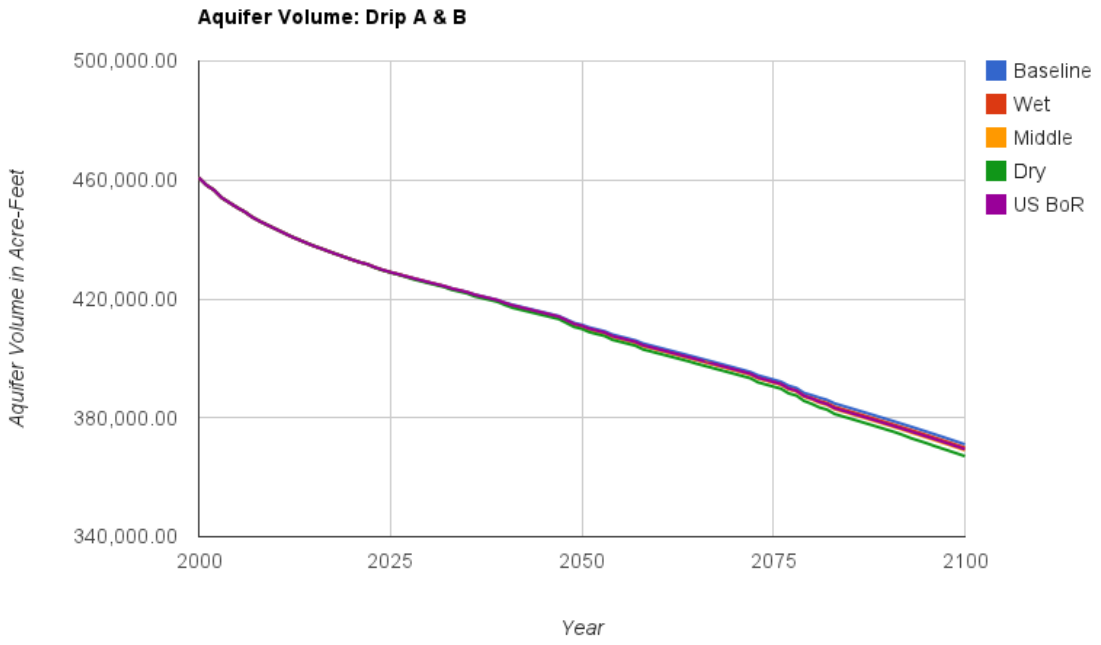

Figure 9: Aquifer volume through five climate change scenarios: Drip A & B

Climate Change Scenario	Final Aquifer Volume
Baseline	371,067.63
Wet	369,942.54
Middle	369,108.28
Dry	367,101.95
US BoR	369,434.20

Table 8: Final aquifer in acre-feet through five climate change scenarios: Drip A & B

In the drip modules, the groundwater flow component goes to zero by 2025 – 2026 in both Drip A and B. In the Baseline, Wet, Middle, and USBoR climate change scenarios, the groundwater flow becomes negative in the year 2026, while in the Dry climate change scenario, this occurs in 2025. A negative groundwater flow component means water is now moving from the Rio Hondo into the shallow alluvial aquifer creating a condition of a losing stream. As the aquifer volume diminishes and the groundwater flow component goes to zero, the aquifer essentially becomes a sink for water in the simulation. In the simulation, due to the lack of deep percolation from flood irrigation,

aquifer volume does not maintain a consistent level, which enhances the feedback loop so the discrepancy between aquifer head and river stage becomes even greater, which means larger amounts of water are moving from the river to the aquifer. See Figure 10.

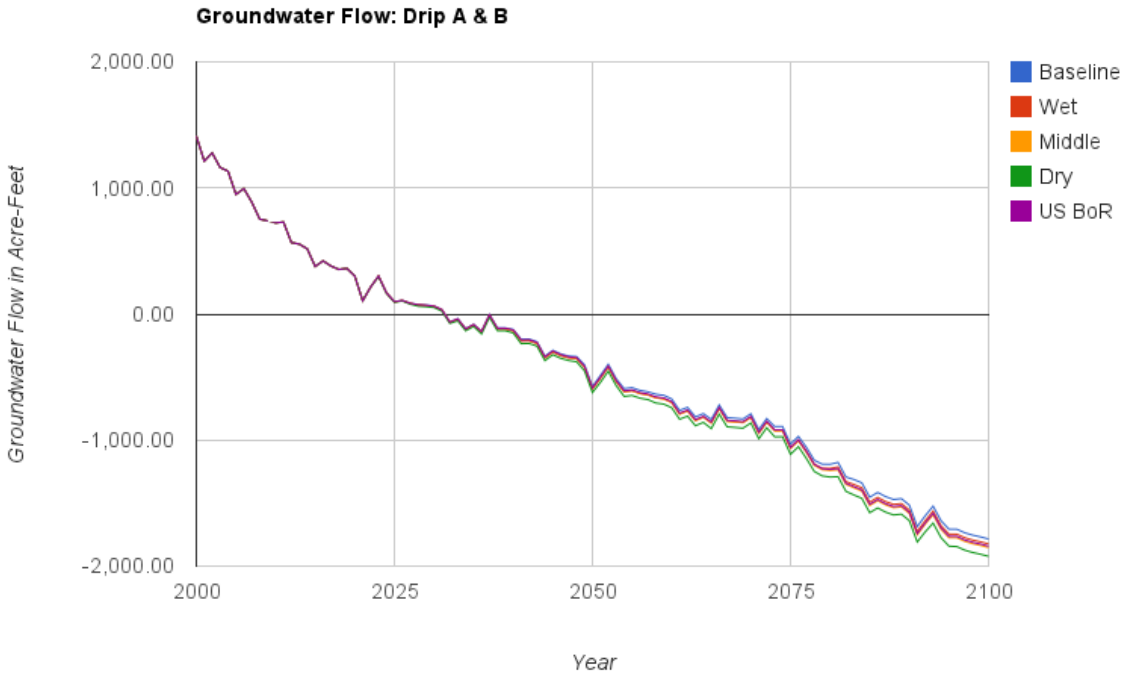

Figure 10: Groundwater flow through five climate scenarios: Drip A & B

Regarding surface water projections, the largest outputs for the Rio Hondo outflow occur in Drip A, then Flood, and last Drip B. This is due to the way the IF statement governing consumptive use is written in each of the modules as well as the difference in the groundwater flow component of the modules. In Drip B and Flood, the initial requirement for stream flow in the Rio Hondo is 8,113 acre-feet. These means that there is 2,351 acre-feet less water in the Rio Hondo in these scenarios than in Drip A which requires an initial flow of only 5,762 acre-feet for consumptive use requirements to be met. In Drip A the Rio Hondo outflow is always 2,351 acre-feet more than in Drip B. Since the initial stream flow requirements in Drip B and Flood are the same, the difference in Rio Hondo outflow lies in the different amounts of groundwater flow predicted by these two modules. Accounting for the difference in Rio Hondo outflow between the Flood module and Drip A, requires paying attention to both the difference in groundwater flow as well as the difference in the initial stream flow requirements between the modules.

Drip A always has 2,351 acre-feet more water in the Rio Hondo than the Flood scenario. However, the groundwater flow component in the Flood scenario is consistently within a range of 1,900 to 1,500 acre-feet. In the Drip A scenario, the groundwater flow becomes negative so even though there is 2,351 acre-feet more in the river, by the end of the century 1,900 to 1,700 acre-feet of water is moving from the river to the aquifer through the five climate change projections. Since groundwater flow fluctuates in the Flood and Drip scenarios based on a fluctuating stream flow, there is not

one set value that accounts for the difference in the predicted Rio Hondo outflow in the Flood and Drip A scenario. Rather, the difference in predicted outflow fluctuates based on fluctuating stream flow through the climate change scenarios as well as fluctuating groundwater flow. Therefore, the difference between Rio Hondo outflow in Drip A and Flood range from 2,500 to 600 acre-feet depending on the year. See Table 9.

	Cumulative Rio Hondo Outflow in Acre-Feet		
Climate Change Scenario	Flood	Drip A	Drip B
Baseline	1,411,817	1,495,293	1,271,742
Wet	1,265,510	1,345,851	1,126,005
Middle	1,163,587	1,240,786	1,024,236
Dry	1,003,094	1,075,946	865,049
US BoR	1,197,794	1,275,645	1,058,187

Table 9: Cumulative Rio Hondo Outflow in Acre-Feet through five climate change scenarios across Flood, Drip A, and Drip B

The differences in modeled Rio Hondo outflow between the three scenarios can be described by the following narrative formulas:

Difference between RH in Drip A and Flood = 2,351 – Difference between groundwater flow in Drip A and Flood (6)

Difference between RH in Drip A and Drip B = 2,351 (7)

Difference between RH in Flood and Drip B = Difference between groundwater flow in Flood and Drip B (8)

The time-delayed storage created by irrigation seepage into the aquifer is an important ecosystem service for the community. As population and water demand grows, this time-delayed storage of water underground could become a vital necessity for acequia communities. The Rio Hondo simulation was conceived in the hopes of encouraging community members to move towards drip irrigation; it is ironic that the modeled outputs do not support this argument entirely. This striking difference between how the groundwater and surface water interactions respond to flood versus drip irrigation create a strong argument against whole scale adoption of drip irrigation.

However, model outputs are most useful in the dynamic trends that they describe, rather than any specific values projected by the simulation. In this case, specific projected values allow us to glean an understanding of the relationship between surface water flows, groundwater flows, and aquifer volume. In terms of projected values, there is no way to state what the future might actually hold. The entire Rio Hondo simulation is based on broad assumptions and simplifications of the natural system. The simulation is aggregated at a watershed level, which makes specific projections understandably dubious. However, the primary benefit of such an exercise on a watershed level is in

showing how the overall system may function once a significant change is made to one of the variables. Also, such an exercise could be beneficial for engaging a broad number of stakeholders in envisioning possible futures of management strategies and as a tool for public education regarding how this human-natural system functions.

FUTURE WORK AND CONCLUSION

The ability to incorporate more complexity into the Rio Hondo simulation makes it a worthwhile starting point as a participatory planning tool. Socio-economic data regarding land use, income from farming versus other jobs, and production costs of drip irrigation can be incorporated into the simulation to produce more refined projections of the tradeoffs for moving towards drip. Considering mixed irrigation practices could enhance the simulation's persuasive power for drip. It should be reiterated, however, that in terms of strict values, projected outputs from the Rio Hondo simulation are limited in their applicability. Rather, the value of such an approach lies in its ability to inspire conversation among farmers and let them experiment with future water conservation measures.

While adding further levels of data to the Rio Hondo simulation enhances quantitative analysis of water use and economic value across a range of future scenarios, approaching water conservation from a qualitative approach would be crucial for achieving any real-life results within the watershed. In the course of this study, interviews were conducted to gauge whether farmers in the region would be willing to switch from flood to drip irrigation. These interviews were preliminary at best, and further qualitative research in the form of focus groups, community needs assessments, and training sessions would help farmers collectively implement any future water conservation measures.

As was shown in the Rio Hondo simulation, under drip irrigation techniques, the absence of deep percolation causes a decline in volume of the local aquifer, which creates an amplifying feedback loop with less water being delivered from the aquifer to the Rio Hondo. Therefore, of the remaining flows in the Rio Hondo, a larger proportion is required for irrigation. In the next time-step, as aquifer volume continues to diminish, there is an even greater difference between aquifer head and river stage. As head pressure in the aquifer continues to fall, it is able to transmit less and less water to the river, until finally groundwater flows are moving in the reverse direction with the river transmitting water to the aquifer. Despite the fact that less water is required under drip irrigation, the river still has less water in it due to this dynamic between the surface and groundwater flows.

The value of using a generalized modeling platform like STELLA® 9.1 as a participatory planning tool in natural resource management is not in the strict quantification of model outputs. Rather the primary value of such a tool is in its ability to explicate broader patterns within complex systems, to inform users how their actions may affect surrounding natural and manmade systems, give users some ways of imagining possible futures based on their actions, and generate discussion regarding how to plan for

the future effectively. Applications in progressive planning and community education regarding natural resource management may be one of the most useful aspects of any systems modeling exercise.

RESOURCES

Alcantar, A. 2008. A report on historical and future population dynamics in New Mexico water planning regions. New Mexico Office of the State Engineer. URL: http://www.ose.state.nm.us/PDF/Publications/TechnicalReports/BBER-WPR-Estimates-Projections-Aug2008.pdf

Blaney, H. & Hanson, E.1965. Consumptive Use and Water Requirements in New Mexico. New Mexico Office of the State Engineer. Technical Report 32.

Brown, J. and J. Rivera. 2000. Acequias de Comun: The tension between collective action and private property rights. Eigth Biennial Conference of the International Associate for the Study of Common Property. Bloomington, IN.

Daniel B. Stephens & Associates. 2008. Taos Regional Water Plan Daniel B. Stephens and Associates, Inc. Albuquerque, NM.

Drakos, P., J. Lazarus, B. White, C. Banet, M. Hodgins, J. Riesterer, and J. Sandoval. 2004. Hydrologic characteristics of basin-fill aquifers in the southern San Luis Basin, New Mexico. New Mexico Geneological Society Guidebook. 55:391-404

Fernald, A.G. and S.J. Guldan. 2006. Surface water-groundwater interactions between irrigation ditches, alluvial aquifers, and streams. Reviews in Fisheries Science 14: 79-89

Fernald, A.G., S.Y. Cevik, C.G. Ochoa, V.C. Tidwell, J.P. King, and S.J. Guldan. 2010. River hydrograph retransmission functions of irrigated valley surface water-groundwater interactions. J. Irrig. Drainage Engineering. 136(12):823-835

Fischer, R.D., 2008. "Comparing irrigation systems," URL: http://www.nm.nrcs.usda.gov/technical/handbooks/iwm/NM_IWM_Field_Manual/Section21/21k-Comparing_Irrigaiton_Systems.pdf

Holling, C.S. 2000. Theories for sustainable futures." Conservation Ecology Vol. 4(2):7. URL: http://www.consecol.org/vol4/iss2/art7/

Hurd, B. & J. Coonrod. 2007. Climate change and its implications for New Mexico's water resources and economic opportunities. NMWRRI Report 343. 59-91

Johnson, P.S. 1998. Surface Water Assessment, Taos County, NM. New Mexico Bureau of Geology & Mineral Resources. Open-File Report 440

Johnson, P., P.W. Bauer, B. Felix, 2009. Hydrogeologic Investigation of the Arroyo Hondo Area, Taos County, NM. New Mexico Bureau of Geology & Mineral Resources, Open-File Report 505

Meadows, D. 2008. Thinking in Systems. Chelsea Green Publishing. White River Junction, NH.

National Agricultural Statistics Service, USDA. 2011. Crop Values 2010 Summary.

New Mexico Office of the State Engineer, 1969. Rio Hondo Hydrographic Survey. Hydrographic Survey Bureau

New Mexico Office of the State Engineer. 2006. Impact of climate change on New Mexico's water supply and ability to manage water resources. URL: http://www.ose.state.nm.us/more_info_drought_status.html

Ochoa, C.G., A.G. Fernald, S.J. Guldan, and M.K. Shukla. 2007. Deep percolation and its effects on shallow groundwater level rise following flood irrigation. Trans. ASABE 50 (1): 73 – 81

_____, C.G., A.G. Fernald, S.J, Guldan, and M.K. Shukla. 2009. Water movement through a shallow vadose zone: A field irrigation experiment. Vadose Zone J. 8:414-425

Reclamation. 2011. SECURE Water Act Section 9503 ©. Reclamation, Climate Change, and Water. Report to Congress

Rivera, José A., 1998. Acequia Culture: Water, Land, and Community in the Southwest. Univ. New Mexico Press. Albuquerque

Tidwell, V.C., H. Passell, S. Conrad, and R. Thomas. 2004. System dynamics modeling for community-based water planning: Application to the Middle Rio Grande. J. Aquat. Sci. 66: 357-372

USGS. 2011. United States Geological Survey. Stream flow and river stage data for Gage 8267500 and 8268500. current water data for the nation [Online]: http://www.waterdata.usgs.gov/nwis/rt. last accessed October 20, 2011

Wilson, B. & Lucero, A. 2003. Water use by categories in New Mexico counties and river basins, and irrigated acreage in 2000. New Mexico Office of the State Engineer. Technical Report 51.

CORRESPONDENCE SHOULD BE ADDRESSED TO:
Sandeep Sabu
Dept. of Community and Regional Planning and Water Resources
University of New Mexico, MSC04 2530
Albuquerque, NM 87131
E-mail: sandeepsabu09@gmail.com

EVALUATING SENSITIVITY ANALYSIS AND AUTO-CALIBRATION OF A SEMI-DISTRIBUTED HYDROLOGICAL MODEL FOR TWO SEMIARID WATERSHEDS OF NEW MEXICO

Ashraf El-Sadek[1]
Manoj Shukla[1*]
Max Bleiweiss[2]
Alexander Fernald[3]
Steve Guldan[1, 4]

ABSTRACT

Semi-distributed hydrologic models can simulate water balance components but need a large amount of input data and a large number of parameters that cannot be easily optimized. Sensitivity analysis, the process of determining parameters having the most control of model functioning, is helpful for model calibration and validation because it affords the possibility of using fewer parameters. Calibration and/or auto-calibration in a hydrologic model is the process whereby model parameters are adjusted to allow the best-fit between simulated and observed data. In the present study, we applied the Soil and Water Assessment Tool (SWAT) to the Embudo Creek and the Jemez River watersheds located in northern New Mexico for the period from 2004 to 2008 for the purpose of evaluating the model performance and auto-calibration results through different sensitivity analysis procedures: 1) the auto-calibration tool in SWAT, 2) visual judgment and 3) using the parameter dataset. The effect of the three methods was evaluated through their impact on total water yield (WTRYLD), surface runoff (SURQ), evapotranspiration (ET) as well as on the shape of the hydrograph before and after the auto-calibration. A common measure of hydrologic model performance is the Nash-Sutcliffe Efficiency (NSE). NSE varies between -∞ to +1 where the +1 indicates a perfect fit between modeled and observed discharge. Using the parameter dataset that was based on visual judgment for the Embudo Creek resulted in an NSE of 0.687. The NSE was 0.567 and 0.552 when the auto-calibration and the visual inspection calibration were used for the Jemez River, respectively. These results suggested that the auto-sensitivity tool is not necessarily the best source for determining parameters for model calibration.

[1]Department of Plant and Environmental Sciences, NMSU, MSC 3Q, P.O. Box 30003, Las Cruces, NM 88003. [2] NMSU Dept. of Entomology, Plant Pathology and Weed Science; ; [3]NMSU Dept. of Animal and Range Sciences, NMSU; [4]NMSU Alcalde Sustainable Agriculture Science Center *Corresponding author: shuklamk@nmsu.edu;

Large areas of the western United States are classified as arid and semiarid. These areas have a unique hydrologic cycle with low annual precipitation consisting of short-term, high

intensity storms, snowmelt runoff and high potential evaporation. Watersheds in the domain of the Rio Grande Basin range from snowmelt dominated watersheds to monsoon storm dominated watersheds. These watersheds are characterized by high climate variability and spatial variability of land cover, soil and relief (Vivoni et al., 2009). Accurate prediction of the hydrologic processes in these watersheds using existing models is difficult because most of the hydrologic models are designed for humid regions. Our specific objectives in this study were to: (1) identify the most sensitive parameters affecting the stream flow, (2) understand the strengths and weakness of the auto-calibration by using different parameter datasets produced from different sensitivity analysis procedures and with different objective functions, and (3) compare the parameters' sensitivity before and after the auto-calibration using the Soil and Water Assessment Tool (SWAT; Arnold et al., 1998) SWAT is a physically based, semi-distributed, model and is used to simulate the hydrologic processes in a wide range of watersheds including semiarid watersheds. The details on model parameters, processes and capabilities can be referred to in Deb and Shukla (2011). Model performance for humid watersheds has been satisfactory (Van Liew et al., 2007), but it could not reproduce short-term events at the semiarid Walnut Gulch watershed because the model operates on a daily time-step. In southwestern New Mexico, Menking et al. (2003) estimated the surface runoff and groundwater flow from the closed Estancia basin using SWAT and MODFLOW within the LAK2 package. The results showed that the simulated stream flow was only within 30% of the observed flow for the gauged watersheds. More recently, in southwestern New Mexico, USA, El-Sadek et al. (2010) applied the SWAT model to the Mimbres River watershed using a homogenous gridded climate dataset and many different precipitation datasets and reported that the highest Nash-Sutcliffe Efficiency (NSE) value (0.82) was produced by using the precipitation from the Signal Peak climate station. The NSE is a measure that compares observed and modeled discharge and varies between $-\infty$ to +1 where the +1 indicates a perfect fit between modeled and observed discharge.

Modeling surface runoff in snowmelt-dominated mountainous watersheds represents a challenge for modelers. Topographic relief has a large impact on the climate components (i.e., temperature, precipitation, wind speed and relative humidity) affecting the snowpack energy budget (Dewalle and Rango, 2008). Temperature lapse rate correction is used to adjust the temperature data with changing elevation. Many successful efforts have been made to use SWAT model in snowmelt-dominated watersheds for predicting streamflow (Fontaine et al., 2002; Wang and Melesse, 2005; Wang and Melesse, 2006; Lemonds and McCray, 2007; Ahl et al., 2008; Zhang et al., 2008; Stratton et al., 2009).

Sensitivity analysis is a useful tool to improve hydrologic model performance. The auto-calibration tool in SWAT provides optimal values of parameters for multiple outputs requiring much less time than manual calibration. As a pioneer effort to compare two different approaches for the sensitivity analysis in the SWAT model, Lenhart et al. (2002) changed the mean of a parameter, one at a time, by ±10% of its initial value in the first approach and by ±25% of the entire range in the second approach. Their results showed that soil parameters displayed similar sensitivity performance for the two examined approaches, whereas, surface runoff lag time showed a highly sensitive performance by using the first approach. The sensitivity analysis integrated within SWAT was first introduced by van Griensven et al. (2006). This was followed by Green and van Griensven (2008) who evaluated the auto-sensitivity analysis that is integrated into SWAT 2005 and evaluated the performance of the model by simulating the streamflow and sediment and nutrient cycles for a small agricultural watershed located in central Texas. Using manual calibration, their results indicated that runoff curve number (CN) and soil evaporation

compensation factor (ESCO) were the most sensitive parameters followed by the surface runoff lag factor (SURLAG) and initial soil water content. The model produced a low NSE (>0.4) on a monthly and daily basis using the two calibration techniques. The combination of auto-calibration and manually adjusted parameters produced the highest NSE for the 5 year simulation period. Sensitivity analysis showed that different parameters were most sensitive for different watersheds; for example, Cibin et al. (2010) showed that for the St. Joseph River watershed, Illinois, SURLAG and CN were the most sensitive parameters with sensitivity index values of 0.51 and 0.346, respectively, and for the Illinois watershed, Arkansas, ESCO and CN were the most sensitive with sensitivity index values of 0.421 and 0.385, respectively. Their results also showed that the sensitivity of parameters was different for different years of the simulation.

Manual calibration is widely used although it is time and labor intensive and needs a full understanding of the model structure and its components. Because of this, auto-calibration procedures were developed.

Limited studies are available describing the strengths and weakness of the SWAT model's existing sensitivity and auto-calibration capability. Van Liew et al. (2005) compared the manual calibration of six parameters against auto-calibration for the same chosen parameters in the SWAT model for two USDA-ARS watersheds, the Little River Experimental Watershed in Georgia (LR), and the Little Washita River Experimental Watershed in Oklahoma (LW). Results showed that auto-calibration for 11 parameters using the Sum Squared Residuals (SSQ) objective function gave the highest monthly and daily NSE for both watersheds.

Our goal was to test and evaluate the performance of the SWAT model as well as the auto-calibration and sensitivity analysis for two snowmelt-dominated semiarid watersheds. We investigated the sensitivity of the parameters by using the sensitivity analysis tool integrated into the SWAT using the model simulated flow output as well as the daily sum of squares of residuals (SSQ) and the daily sum of squares of residual rankings (SSQR) objective functions, and compared the results from that analysis to those obtained from the visual judgment of parameter sensitivities.

MATERIALS AND METHODS

Study Watersheds

The Embudo Creek at Dixon, NM (Hydro Unit 13020101; Figure 1) covers an area of 789.59 km^2 as delineated from the USGS stream flow gauging station (N 36°12'39.08", W 105°54'49.07"). Using the ArcGIS interface for SWAT allows for watershed statistics to be determined in an efficient manner. For example, the mean elevation of the watershed is 2753 m, the land use is mainly evergreen forest (75.59 %) and the dominant soil type is loam (54.41%). The watershed receives a mean annual precipitation of 505.7 mm with an annual average Tmax and Tmin of 14.40 and -1.83 °C, respectively, as determined from our input data over the period 2004-2008 (RAWS, 2010).

The Jemez River at Jemez, NM, drains an area of 1217.3 km^2 (Hydro Unit 08324000; Figure 2) as delineated from a USGS stream flow gauging station (N 36°40'51.7", W 104°47'11.02"). The mean elevation of the watershed is 2590 m, land use types include evergreen forest, range-grasses and the soil. The watershed receives a mean annual precipitation of 485 mm with an annual average Tmax and Tmin of 13.79 and -0.74 °C, respectively, as determined from the input data over the period 2004-2008. Both watersheds are characterized by a high flow volume during spring from snowmelt runoff.

The SWAT 2005 (Olivera et al., 2006) was used in our investigation. The watersheds and subwatersheds were delineated using a 30m resolution USGS Digital Elevation Model (DEM) which was used to calculate the geomorphic parameters for each watershed. Information about the land cover was derived from the 30m Multi-Resolution Land Characteristics Consortium (MRLC) 2001 National Land Cover Dataset (NLCD). To create the hydrologic response units (HRUs), each land cover was associated with a soil type that was obtained from the State Soil Geographic (STATSGO) database.

The Remote Automated Weather Stations (RAWS) located at Truchas and Jemez were used for the climate data for the Embudo Creek and Jemez River, respectively. The Truchas station (Figure 1) is located at latitude 36° 03' 32"N and longitude 105° 46' 10" W and an elevation of 2542 m. The Jemez station (Figure 2) is located at latitude 35° 50' 28" N and longitude 106° 37' 08" W and elevation of 2,438 m. Both stations provided data on daily total precipitation (mm), maximum and minimum temperature (°C), solar radiation (MJ/m^2), wind speed (m/s) and relative humidity (%).

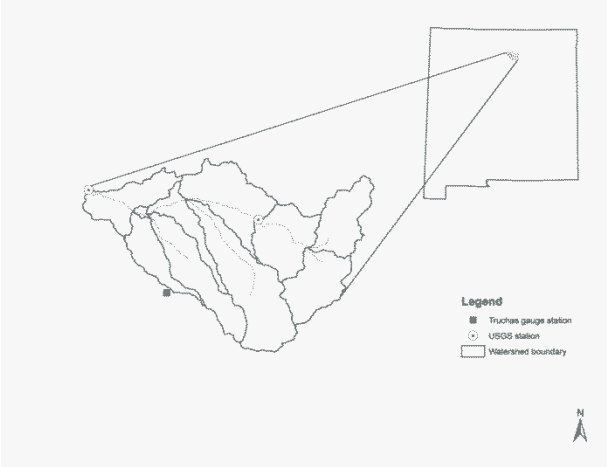

Figure 1. Location of the Embudo Creek watershed, NM

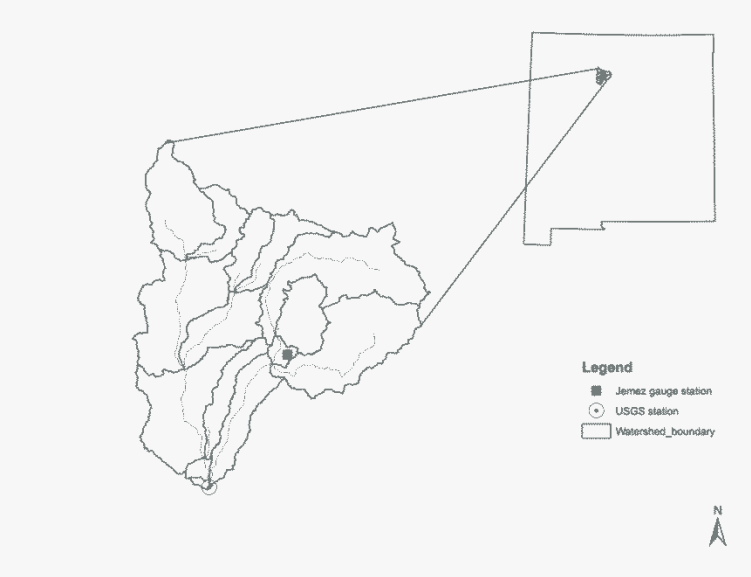

Figure 2. Location of the Jemez River watershed at Jemez, NM

Model Description

To represent spatial variability, SWAT subdivides watersheds into multiple sub-basins according to topography, which are then subdivided to create the HRUs that are based on the land cover and soil characteristics. Model outputs include surface flow, groundwater, lateral flow, sediment, and nutrient and pesticide yields. The surface runoff can be simulated by the modified Soil Conservation Service curve number (SCS-CN) method or the Green and Ampt infiltration model. The evapotranspiration can be estimated by the Hargreaves, the Priestly-Taylor and/or the Penman-Monteith method.

Snowmelt Hydrology in SWAT

The input to SWAT specific to snowmelt hydrology is the mean daily air temperature at which precipitation is classified as snowfall. Snowmelt is controlled by the snowpack temperature (a function of daily minimum and maximum air temperatures) and user specified snowmelt air temperature above which snow starts to melt. SWAT uses the temperature-index method to calculate the amount of snowmelt for a given day. The temperature-index method is based on how much heat is available for melting snow; it is a function of air temperature.

SWAT uses the climate station nearest to each sub-watershed to determine which precipitation, temperature, and other climate parameters to use. In order to account for topographic relief and orographic effects on temperature and precipitation, elevation bands and lapse rates are incorporated into the model. This option was first incorporated and presented by Fontaine et al. (2002) to handle the problem of poor performance of SWAT in mountainous regions typical of the western United States. Each band is defined by its average elevation and percent of the band in the sub-basin.

The watershed elevations range from 1,786 to 3,965 m for the Embudo Creek and from 1,718 to 3,435 m for the Jemez River. The bands were set to 300m increments for all of the sub-basins. The temperature lapse rate was calculated by relating the elevation and the mean annual temperature derived from the Parameter–Elevation Regressions on Independent Slopes Model (PRISM) maps (Daly et al., 1994). This relation is shown in Figures 3a and b, where the trend line has a slope of -4.8 °C/km and -4.6 °C/km for the Embudo Creek and for the Jemez River, respectively.

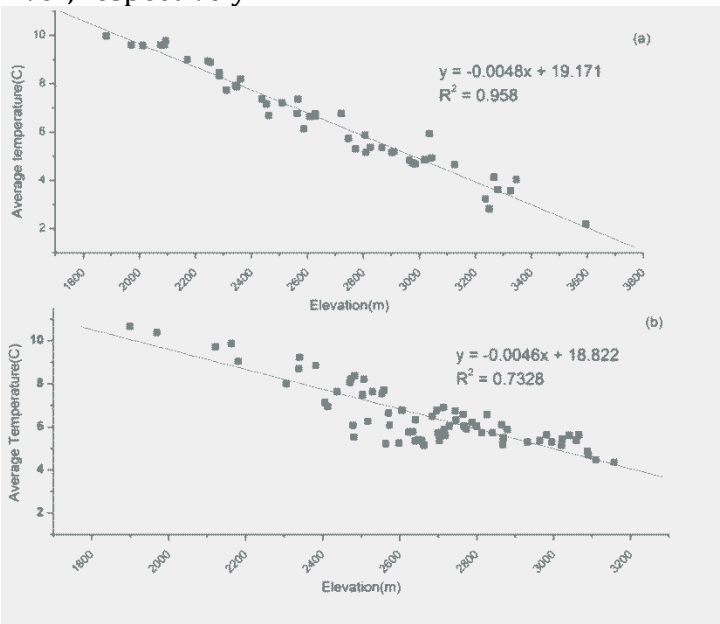

Figure 3. Embudo Creek Watershed (a) and Jemez River watershed (b). Mean Annual Temperature vs. Elevation

Base Flow Separation

More efficient calibration results can be obtained when the discharge hydrograph is separated into its component parts: baseflow and land surface runoff. Baseflow is created by ground water that enters the stream channel. Different model parameters affect the two stream flow components differently. The Base Flow Index (BFI) is used to characterize the relative importance of the two components and is expressed as a percentage. The BFI was 0.71 for the Embudo Creek and 0.71 for the Jemez River (Figure 4).

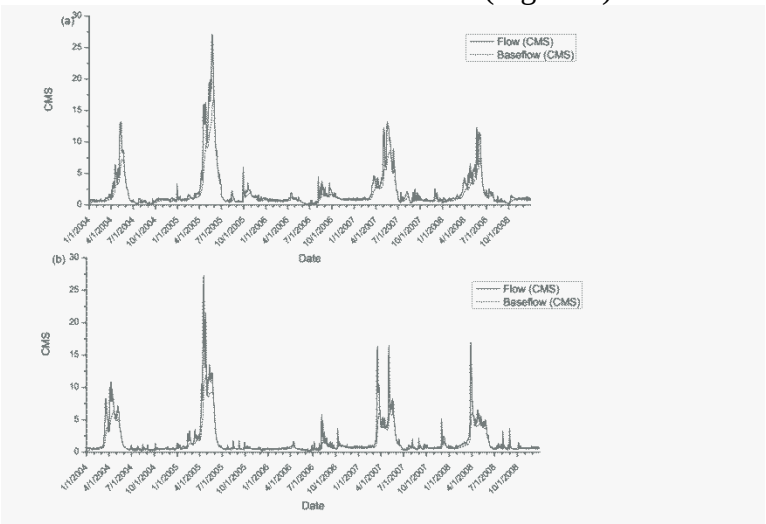

Figure 4. Base flow separation using the automated digital filter for the Embudo Creek watershed (top) and the Jemez River watershed (bottom)

Sensitivity Analysis and Auto-Calibration

Sensitivity analysis is the process whereby one determines the relative impact that a parameter has on model output. The auto-sensitivity tool in SWAT 2005 uses the Latin Hypercube Sampling (LH; McKay et al., 1979; McKay, 1988) and one-at-a-time sensitivity analysis (OAT; Morris, 1991). In this procedure, each parameter is subdivided into *m* ranges (default is 10) and then the model selects random values from each range. A dimensionless sensitivity analysis index (SI) is determined by calculating the ratio between the relative changes in the model output as a result of the change in the parameter. The user specifies a particular output to be used in the calculation, i.e., simulated flow only if no observed flow data are available, or one of the available objective functions such as SSQ and SSQR when observed flow data are available. See van Griensven et al. (2006) for a description of the auto-sensitivity analysis tool. The division of parameters into various degrees of sensitivity is subjective. For example, Lenhart et al. (2002) ranked sensitivity coefficients into four classes: small to negligible ($0.00 <| SI | < 0.05$), medium ($0.05 < | SI | < 0.20$), high ($0.20 < | SI| < 1.00$), and very high ($| SI | > 1.00$). We are using 0.2 to indicate that the parameter is sensitive.

A flow chart for the study is given in Figure 5. The sensitivity of parameters was examined using three methods as follows:

1. A manual test for evaluating the sensitivity for each of the 27 flow parameters was done while keeping all other parameters fixed to default values before the auto-calibration. For each parameter, we used the maximum, minimum and default values allowed by the model.
2. The auto-sensitivity analysis tool was used to evaluate the sensitivity of the flow parameters using the simulated flow output and using the two available objective functions:

$$SSQ = \sum_{i=1,n} \left[X_{i,measured} - X_{i,simulated} \right]^2 \quad (4)$$

Whereas, n is the number of pairs of measured ($X_{measured}$) and simulated ($X_{simulated}$) variables.

$$SSQR = \sum_{j=1,n} \left[X_{j,measured} - X_{j,simulated} \right]^2 \quad (5)$$

where, j represents the rank.

3. A manual sensitivity test for the flow parameters was done after the auto- calibration to test the difference between parameter sensitivity before and after the auto-calibration.

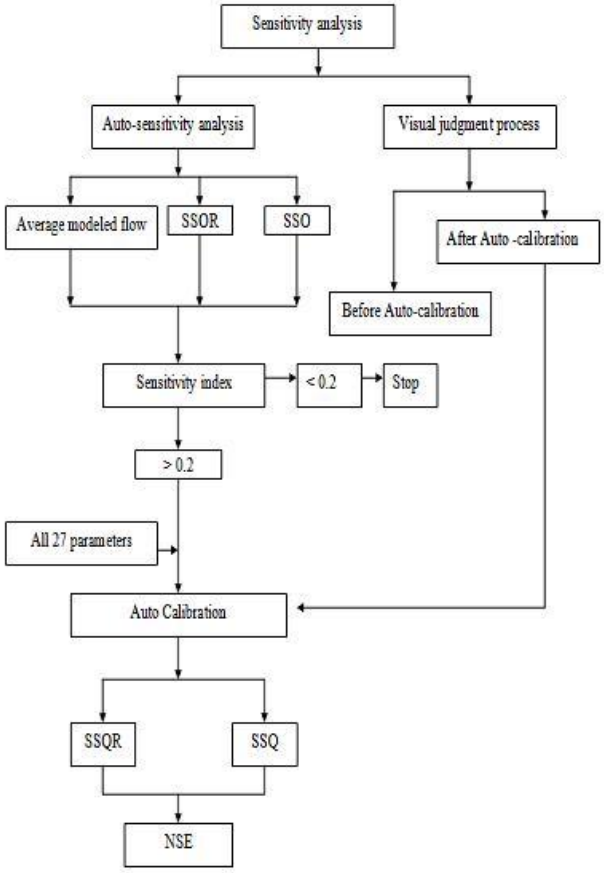

Figure 5. Flow chart of the study

Table (1) presents the 27 flow parameters and their definitions; Table (2) shows with which process each of the parameters is associated as well as the range in parameter values that were used in the auto-sensitivity analysis; and, finally, Table (3) presents all of the parameters and their ranges and the default values used for running the sensitivity analysis before the auto-calibration. Not all the sensitivity parameter results are presented for brevity.

Table 1. SWAT flow parameters considered for the sensitivity analysis.

Parameter	Description
ALPHA_BF	Base Flow alpha factor (days)
BIOMIX	Biological missing efficiency (unitless)
BLAI	Maximum Potential Leaf Area Index (unitless)
CANMX	Maximum Canopy Index (mm)
Ch_K2	Effective Channel Hydraulic Conductivity (mm/h)
Ch_N2	Manning coefficient for channel (unitless)
CN2	SCS-CN for moisture condition II (unitless)
EPCO	Plant evaporation compensation factor (unitless)
ESCO	Soil evaporation compensation factor (unitless)
GW_DELAY	Ground water delay (days)
GW_REVAP	Groundwater revaporation coefficient (unitless)
GWQMN	Threshold depth of water in the shallow aquifer required for return flow to occur (mm)
RCHRG_DP	Groundwater recharge to deep aquifer (fraction)
REVAPMN	Threshold depth of water in the shallow aquifer required for revaporation to occur (mm)
SFTMP	Snowfall temperature (°C)
SLOPE	Average slope steepness (m/m)
SLSUBBSN	Average slope length (m)
SMFMN	Maximum melt rate for snow during the year (mm/°C/day)
SMFMX	Maximum snowmelt rate (mm/°C/day)
SMTMP	Snowmelt base temperature (°C)
SOL_ALB	Soil Albedo
SOL_AWC	Available water capacity of the soil layer (mm/mm)
SOL_K	Soil conductivity (mm/h)
SOL_Z	Soil depth (mm)
SURLAG	Surface runoff lag coefficient
TIMP	Snowpack temperature lag factor
TLAPS	Temperature lapse rate (°C/km)

Table 2. Model parameters and their range.

Process	Parameter	Lower boundary	Upper boundary	Location	Type
Ground water	ALPHA_BF	0.0001	1	.gw	Sub
	GW_DELAY	0	100	.gw	Sub
	RCHRG_DP	0	1	.gw	Sub
	GW_REVAP	0.02	0.2	.gw	Sub
	GWQMN	0	300	.gw	Sub
	REVAPMN	0	500	.gw	Sub
Surface runoff	CN2	-8	+8	.mgt	Sub
	SURLAG	0.4	10	.bsn	Bas
Time of concentration	SLSUBBSN	-50%	+50%	.hru	Sub
	Ch_N2	-20%	+20%	.rte	Sub
Snow	SFTMP	-3	5	.bsn	Bas
	SMFMN	2	8	.bsn	Bas
	SMFMX	2	8	.bsn	Bas
	SMTMP	-3	5	.bsn	Bas
	TIMP	0.01	1	.bsn	Bas
	TLAPS	-50%	+50%	.sub	Sub
Evaporation	ESCO	0.001	1	bsn,.hru	Sub
	EPCO	0.001	1	bsn,.hru	Sub
	SOL_ALB	-50%	+50%	.sol	Sub
	CANMX	0	10	.hru	Sub
Channel/ Transmission loss	Ch_K2	0	150	.rte	Sub
Management/Soil	BIOMIX	0	0.6	.mgt	Sub
Soil Water	SOL_K	-50%	+50%	.sol	Sub
	SOL_Z	-50%	+50%	.sol	Sub
	SOL_AWC	-0.04	+0.04	.sol	Sub
Plant growth	BLAI	-20%	+20%	Crop.dat	Sub
Lateral Flow	SLOPE	-50%	+50%	.hru	Sub

Table 3. SWAT flow parameters, ranges and default values used for running the sensitivity analysis before the auto-calibration.

Process	Parameter	Lower boundary	Upper boundary	Default value
Ground water	ALPHA_BF	0.0001	1	0.048
	GW_DELAY	0	100	31
	RCHRG_DP	0	1	0.05
	GW_REVAP	0.02	0.2	0.02
	GWQMN	0	300	0
	REVAPMN	0	500	1
Surface runoff	CN2	-8	+8	Varies for each hru
	SURLAG	0.4	10	4
Time of concentration	SLSUBBSN	-50%	+50%	Varies for each hru
	Ch_N2	-20%	+20%	One assigned value (0.014)
Snow	SFTMP	-3	5	1
	SMFMN	2	8	4.5
	SMFMX	2	8	4.5
	SMTMP	-3	5	0.5
	TIMP	0.01	1	1
	TLAPS	-50%	+50%	-4.8
Evaporation	ESCO	0.001	1	0.95*
	EPCO	0.001	1	1*
	SOL_ALB	0.05	0.08	Varies to soil type and depth
	CANMX	0	10	0
Channel/ Transmission loss	Ch_K2	0	150	0
Management/Soil	BIOMIX	0	0.6	0.2
Soil Water	SOL_K	-50%	+50%	Varies to soil type and soil depth
	SOL_Z	-50%	+50%	
	SOL_AWC	-0.04	+0.04	
Plant growth	BLAI	-20%	+20%	Varies to crop
Lateral Flow	SLOPE	-50%	+50%	Varies for each HRU

Model calibration was conducted on a daily time scale from 2004-2008 using the auto-calibration tool for the following scenarios:

1- The auto-calibration was run, first, for all the 27 flow parameters.
2- The auto-calibration was run for the most sensitive parameters (SI>0.2) produced from the auto-sensitivity analysis using the simulated flow only, SSQ and SSQR objective functions.
3- The auto-calibration was run for the most sensitive parameters produced from the manual sensitivity analysis.
4- For the auto-calibration the sum of square residuals was used as an objective function for all the parameter datasets except for these produced from the sensitivity analysis using the SSQR as an objective function.

The Nash Sutcliffe coefficient of efficiency (NSE; Nash and Sutcliffe, 1970) was used to compare the daily measured discharge to the simulated. It is defined as:

$$\mathrm{NSE} = \frac{\sum_{i=1}^{n}(O_i - \bar{O})^2 - \sum_{i=1}^{n}(P_i - O_i)^2}{\sum_{i=1}^{n}(O_i - \bar{O})^2} \qquad (6)$$

where, P_i are the predicted values, O_i are the observed values, and $\bar{O}$ is the mean of the observed data.

RESULTS AND DISCUSSION

Sensitivity Analysis on the Embudo Creek at Dixon

Manual sensitivity analysis before the auto-calibration

To determine the influence of each parameter on total water yield (WTRYLD), surface runoff (SURQ) and evapotranspiration (ET) as well as on hydrograph shape, we manually changed the parameters according to the range of variation presented in Table 3. The results from using the lower and upper bounds were compared to the results obtained from using the default values. A description of the effect of some parameters on the WTRYLD, SURQ and ET are presented in Table 4 and on the hydrograph in Figure 6. The results can be summarized as follows:

1- For the parameters, ALPHA_BF, CANMIX, CN2, ESCO, SMFMN, REVAPMN, SOL_K and SFTMP, the higher the parameter value, the higher was the discharge (not all data shown).
2- For the parameters, CH_K2, EPCO, SFTMP, SLSUBBSN, SMTMP, SOL_AWC, SOL_Z, TLAPS, GWDELAY, GWQMN and RCHRG_DP, the lower the parameter value, the higher was the discharge.
3- For the parameters, BIOMIX, CH_N2, GW_REVAP, SLOPE, SFMX, SOL_ALP, TIMP and SURLAG, changes in values from the default results in no or only slight changes in the discharge.

Table 4. An example of the effect of some parameters on water components.

Water component	Default	Alpha_Bf		Ch_K2		Esco		Biomix	
		Min	Max	Min	Max	Min	Max	Min	Max
SURQ	29.62	29.62	29.62	29.62	29.62	22.23	30.83	29.62	29.76
ET	347.3	347.3	347.3	347.3	347.3	392.9	335.6	347.3	347.2
WTRYLD	125.52	82.7	129.29	125.52	125.52	97.23	134.44	125.52	125.44

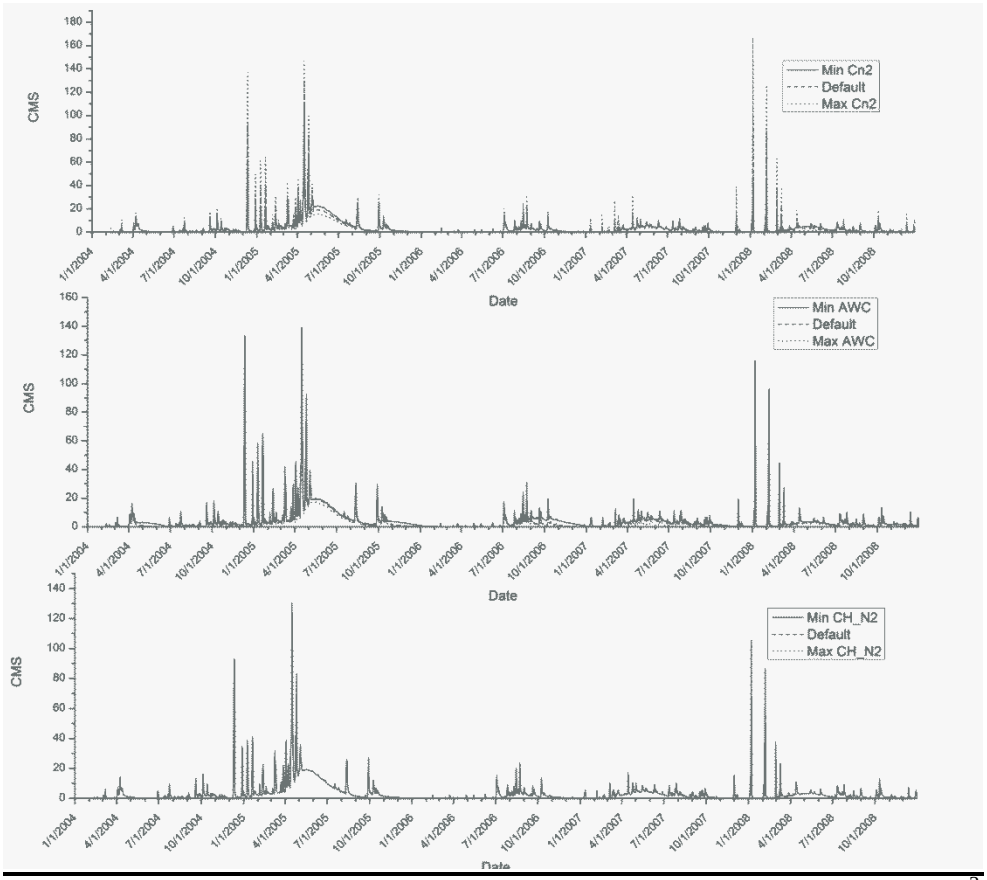

Figure 6. Example of the Embudo Creek watershed hydrograph (CMS or m^3/s) using min, max and default values for three of the parameters (Cn2, SOL_AWC and Alpha_BF).

Automatic sensitivity analysis

The automatic sensitivity analysis was performed for the 27 flow parameters using three model outputs.

1- None of the parameters received a very high sensitivity ranking (SI>1) when their impact only on streamflow was observed (as opposed to using some "objective function" such as the SSQ). However, the most sensitive parameters in this case in descending order were REVAPMIN, ESCO, SOL_AWC, GWQMN, CN2, CANMX, SLOPE, RCHRG_DP, SOL_Z and SOL_K with SI ranging from 0.69 to 0.28 (Table 5).

2- For the second case, the SSQ was used in the sensitivity index calculation and most sensitive parameters in a descending order were CN2, Timp, ALPHA_BF, CH_K2, SOL_Z, SOL_AWC, CANMX, ESCO and SURLAG with sensitivity indices ranging

from 1.50 to 0.346. Out of these, the first five parameters were obtained as highly sensitive parameters (SI>1) (not all data shown).

3- In the third case, the SSQR was used as a model output to examine the most sensitive parameters. Results showed that the same nine parameters were found to be sensitive for both SSQ and SSQR, although ranking of these parameters was different (Table 5).

Other studies showed different sensitivity ranking for different parameters using the auto-sensitivity analysis in SWAT. For example, the most sensitive parameters were CN2, ESCO and SURLAG (Green and van Griensven, 2008) in central Texas, GWQMN, SOL_Z and TIMP (Tattari et al., 2009) in Finland, and SURLAG and CN2, and ESCO and CN2 for the St. Joseph River watershed in Illinois and the Illinois watershed in Arkansas, respectively (Cibin et al., 2010).

Table 5. Sensitivity ranking and index for the flow parameters for the two watersheds.

Watershed	Embudo Creek Watershed						Jemez River					
	Flow		SSQ		SSQR		Flow		SSQ		SSQR	
Parameter	R	Si	R	Si	R	Si	R	Si	R	Si	R	Si
Alpha_Bf	13	0.028	3	1.280	6	0.954	14	0.038	1	2.240	4	1.860
Biomix	14	0.021	17	0.007	17	0.015	16	0.013	18	0.022	18	0.037
Blai	28	0.000	28	0.000	28	0.000	28	0.000	28	0.000	28	0.000
Canmx	4	0.349	7	0.427	8	0.590	5	0.450	5	0.857	6	1.300
Ch_K2	11	0.051	4	1.150	3	1.740	11	0.071	3	1.230	2	2.000
Ch_N2	20	0.000	19	0.002	20	0.004	20	0.001	19	0.004	19	0.006
Cn2	7	0.356	1	1.520	2	2.140	8	0.326	4	1.170	3	1.960
Epco	16	0.012	15	0.031	15	0.049	15	0.032	16	0.068	16	0.110
Esco	2	0.437	8	0.382	9	0.577	1	0.596	6	0.804	5	1.550
Gw_Delay	17	0.005	16	0.016	16	0.021	19	0.004	13	0.146	15	0.160
Gw_Revap	28	0.000	28	0.000	28	0.000	17	0.013	21	0.000	20	0.003
Gwqmn	5	0.357	10	0.117	13	0.072	10	0.252	15	0.106	14	0.180
Rchrg_Dp	6	0.345	13	0.049	14	0.054	9	0.261	14	0.107	13	0.215
Revapmn	1	0.692	20	0.001	19	0.008	3	0.513	17	0.023	17	0.041
Sftmp	28	0.000	28	0.000	28	0.000	28	0.000	28	0.000	28	0.000
Slope	8	0.346	12	0.059	11	0.090	4	0.452	12	0.304	12	0.523
Slsubbsn	19	0.001	18	0.006	18	0.009	21	0.001	20	0.001	21	0.002
Smfmn	28	0.000	28	0.000	28	0.000	28	0.000	28	0.000	28	0.000
Smfmx	28	0.000	28	0.000	28	0.000	28	0.000	28	0.000	28	0.000
Smtmp	28	0.000	28	0.000	28	0.000	28	0.000	28	0.000	28	0.000
Sol_Alb	15	0.018	14	0.040	12	0.085	12	0.045	10	0.353	10	0.694
Sol_Awc	3	0.433	6	0.784	5	1.130	6	0.448	8	0.418	8	0.749
Sol_K	10	0.276	11	0.090	10	0.129	7	0.412	7	0.432	9	0.719
Sol_Z	9	0.311	5	1.080	4	1.740	2	0.532	2	1.400	1	2.170
Surlag	18	0.001	9	0.346	7	0.654	18	0.004	9	0.414	7	0.841
Timp	12	0.046	2	1.370	1	2.650	13	0.043	11	0.323	11	0.563
Tlaps	28	0.000	28	0.000	28	0.000	28	0.000	28	0.000	28	0.000

Si is sensitivity index and R is the ranking; shaded cells represent the parameters that were used in the auto-calibration procedure by the three different model outputs.

Manual sensitivity analysis after the auto-calibration

Before performing the auto-calibration, using the default values of the parameters, the model overestimated the flow as compared to the measured flow. After the auto-calibration, simulated flow reduced to better match the measured flow. To determine whether the parameter sensitivity had changed after the auto-calibration, a manual sensitivity analysis was performed after the auto-calibration in a manner similar to that performed before the auto-calibration. The results for maximum and minimum values of some parameters compared to the best values chosen by the model are given in Table 6. The details of the effect of these parameter changes on the WTRYLD, SURQ and ET are presented in Table 6, on water volume and NSE values in Table 7. Similar results for the relative change in water volume and the NSE as a result of the parameter change, and on the hydrograph shape are shown in Figure 7. To summarize, 11 parameters including ALPHA_BF, CANMX, CH_K2, CN2, ESCO, GW_DELAY, GWQMN, RCHRG_DP, SOL_AWC, SOL_K and SOL_Z were sensitive to the flow.

Manual sensitivity analysis of the parameters EPCO, SMTMP, SFTMP, SLSUBBSN, SMFMN, SMFMX, SURLAG, TLAPS, after the auto-calibration showed that some of the parameters have lost their effect on either the WTRYLD, SURQ and ET or on the hydrograph shape. The loss in sensitivity is probably due to the interaction among the parameters that interactively depend on one for the other's impact. Another possible explanation could be that the model was overestimating the flow before the auto-calibration and thus allowed some parameters to appear to be more sensitive than when the flow was reduced to better match observed flow. On the other hand, some of the parameters seemed to be less sensitive before the auto-calibration; but, after the auto-calibration these parameters had a large impact on the model output (i.e., ALPHA_BF, CH_K2 and GW_DELAY).

Table 6. Comparing the effects of using minimum, maximum and best parameter values for some parameters on the WTRYLD, SURQ and ET after the auto-calibration (all units in mm).

	Calibrated	Alpha_Bf		Ch_K2		Esco		Biomix	
Water component	Optimum	Min	Max	Min	Max	Min	Max	Min	Max
SURQ	6.03	6.03	6.03	6.03	6.03	6	13.11	6.04	5.89
ET	487.6	487.6	487.6	487.6	487.6	488	383.4	487.4	492.2
WTRYLD	84.52	72.5	84.52	84.52	84.52	84.27	173.81	84.69	80.57

Table 7. Water volume and NSE values as affected by change in the flow parameter values (Embudo Creek).

	Observed	Calibrated	Alpha_Bf		Ch_K2		Esco		Biomix	
Water component		Optimum	Min	Max	Min	Max	Min	Max	Min	Max
Vol. (mm)	437.92	441.02	56.09	441.62	423.11	441.04	439.46	904.27	441.89	420.34
NSE		0.536	-0.332	-0.018	-0.323	0.532	0.536	-0.61	0.536	0.516

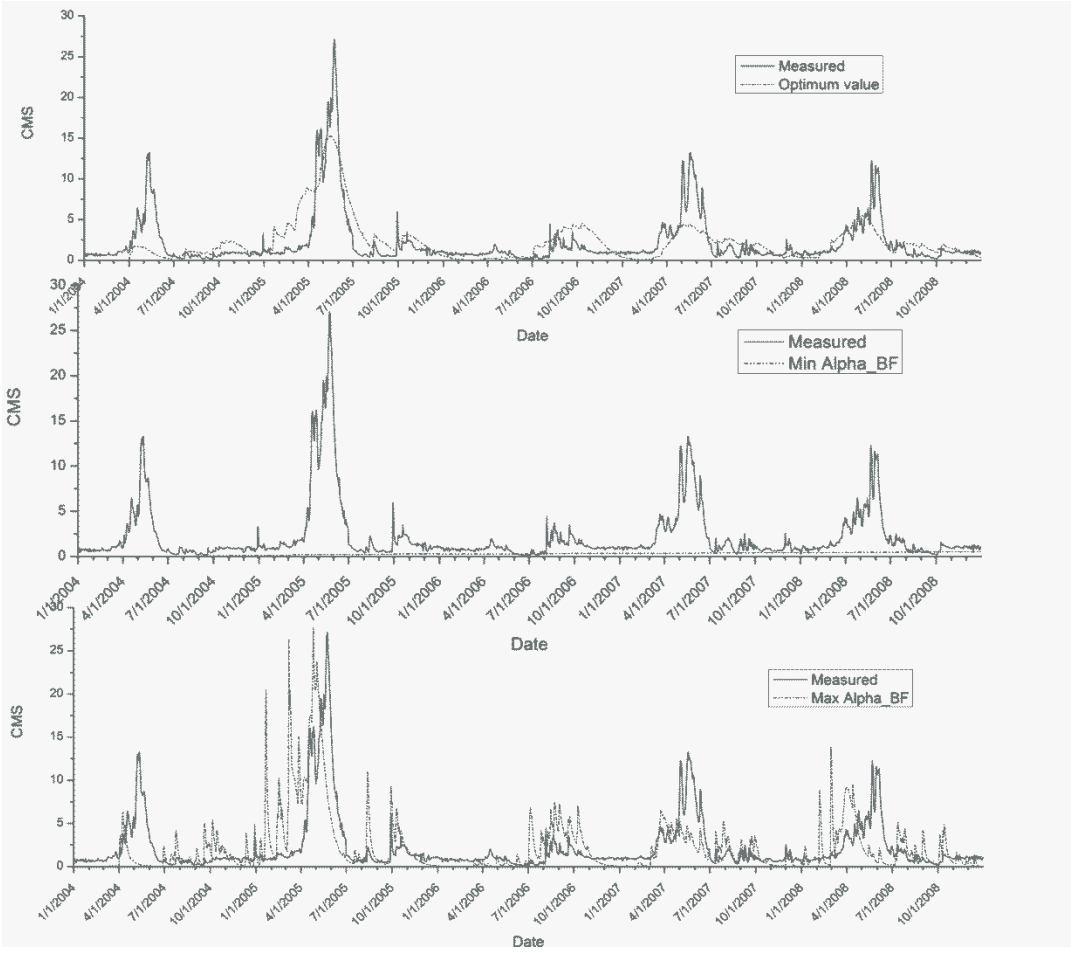

Figure 7. The effect of ALPHA_BF parameter change on the hydrograph shape.

Sensitivity Analysis on the Jemez River

Manual sensitivity analysis before the auto-calibration

The same procedure was used for manually determining the most sensitive parameters before the auto-calibration for the Jemez River watershed. The results from using the lower and upper bounds were compared to the results obtained from using the default values. The effect of parameters on the WTRYLD, SURQ and ET are presented Figure 8. The results can be summarized as follows:

1- For the parameters ALPHA_BF, CANMX, CN2, ESCO, SLOPE, REVAPMN, SOL_K and SFTMP, T-LAPS and CH_K2, the higher the parameter value, the higher was the discharge.

2- For the parameters EPCO, SLSUBBSN, SOL_AWC, SOL_Z, GWQMN, and RCHRG_DP the lower the parameter value, the higher the discharge.

3- For the parameters BIOMIX, CH_N2, GW_DELAY, GW_REVAP, SMFMN, SMFMX, SMTMP, SOL_ALP, TIMP and SURLAG, changes in values from the default results in no or only slight changes in the discharge.

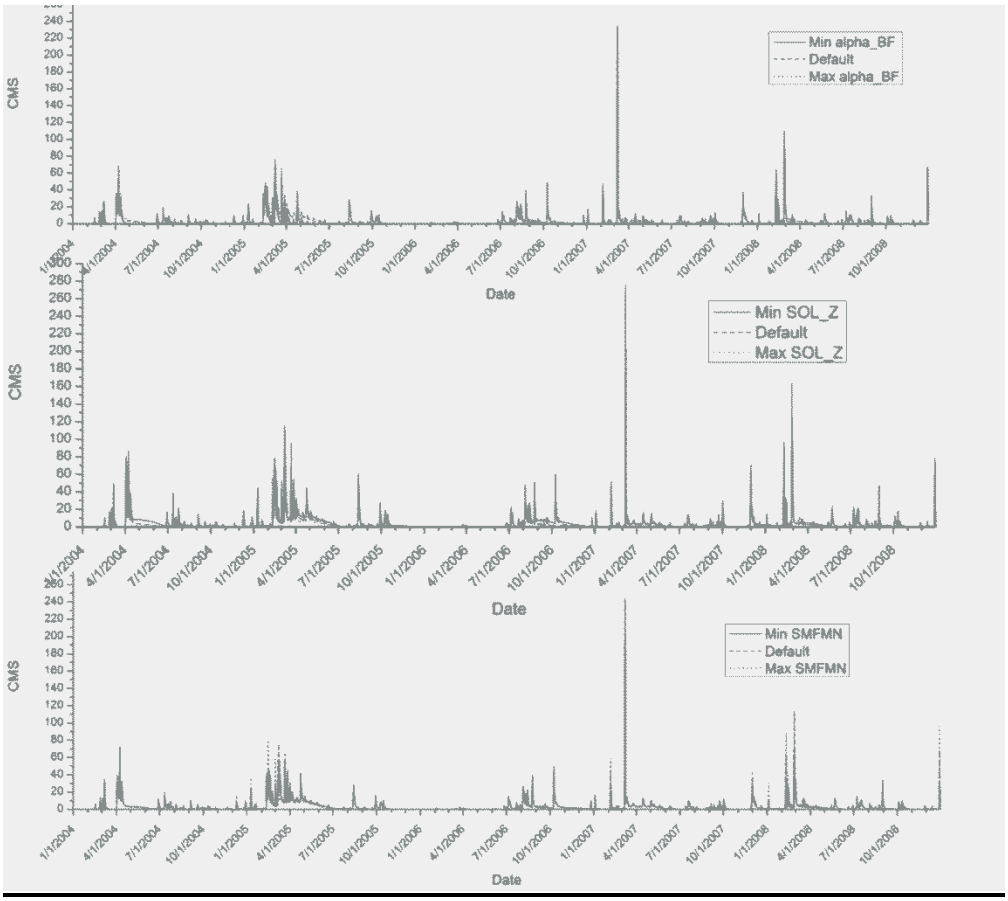

Figure 8. Jemez River hydrograph using minimum, maximum and default values for three of the parameters (Alpha_BF, SOL_Z and SMFMN).

Automatic sensitivity analysis

The automatic sensitivity analysis was performed for the 27 flow parameters using three model outputs (Table 5):

1- For simulated flow only output, none of the parameters received a high sensitivity ranking (SI>1); however, most sensitive parameters in descending order were: ESCO, SOL_Z, REVAPMIN, SLOPE, CANMX, SOL_AWC, SOL_K, CN2, RCHRG_DP, and GWQMN with SI ranging from 0.596 to 0.252.

2- When the SSQ was used in the calculation of the sensitivity index values, the most sensitive parameters in descending order were: ALPHA_BF, SOL_Z, CH_K2, CN2, CANMX, ESCO, SOL_K, Sol_AWC, SURLAG, SOL_ALB, Timp, and SLOPE with SI ranging from 2.24 to 0.304. In addition, the first four parameters were high sensitive parameters (SI>1).

3- When the SSQR was used as a model output to examine the most sensitive parameters, the results showed that most sensitive parameters in descending order were SOL_Z, CH_K2, CN2, ALPHA_BF, ESCO, CANMX, SURLAG, SOL_AWC, SOL_K, SOL_ALB, TIMP, SLOPE, and RCHRG_Dp with SI ranging from 2.17 to 0.215 and the first six parameters were classified as highly sensitive parameters.

Manual sensitivity analysis after the auto-calibration

For manual sensitivity analysis, maximum and minimum values of the parameters were compared to the best values chosen by the model. The effect on water volume and hydrograph shape are presented in Figure 9. Manual analysis revealed that nine parameters sensitive to the flow were: ALPHA_BF, CANMX, CH_K2, ESCO, SOL_AWC, SOL_K and SOL_Z, SURLAG and TIMP.

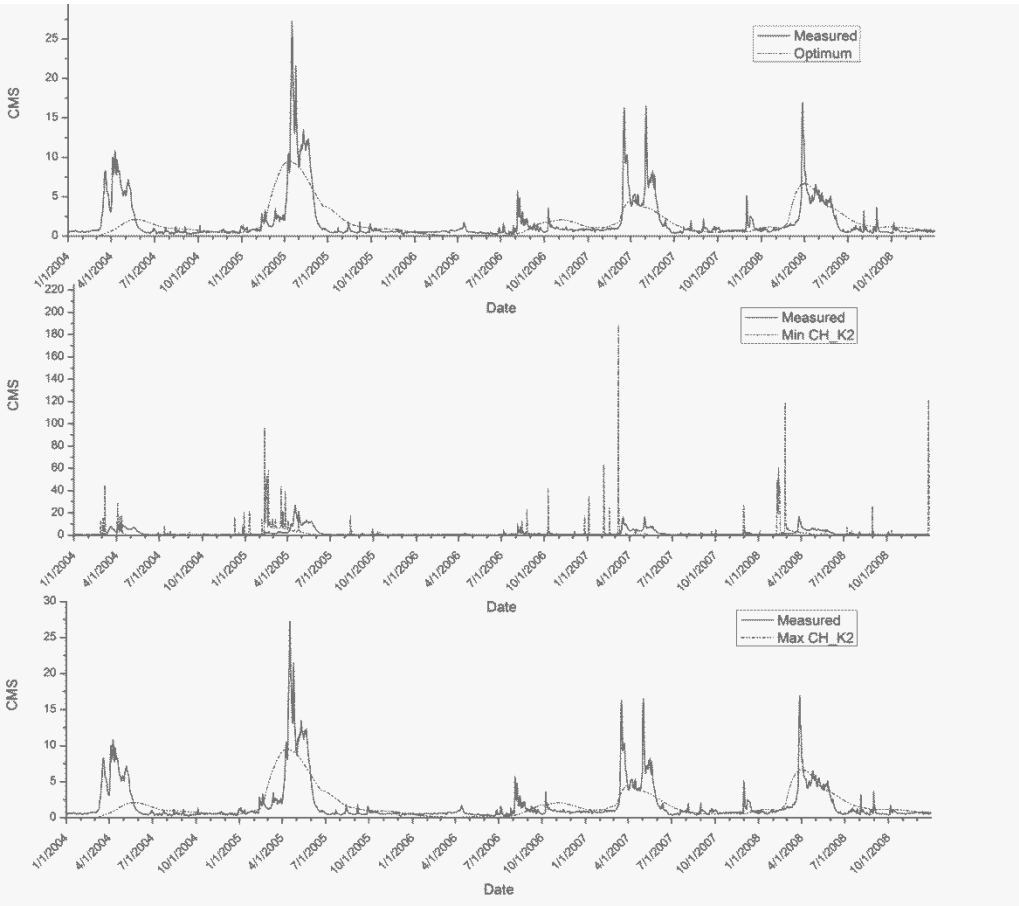

Figure 9. The Jemez River hydrograph shape affected by changing the CH_K_2 parameter.

In general, there was poor agreement between measured and simulated flow for both watersheds, especially for the Jemez river watershed simulation. This may be due to several reasons: 1) the uncertainty of input data was not explicitly taken into account, an example could be the precipitation data which has the major impact on the model simulation; 2) Another factor could be the fluctuations in the flow that vary from year to year from a high observed flow of 150.51 and 70.74 mm in 2005 to a low observed flow of 40.01 and 21.21 mm in 2006 for the Embudo Creek and the Jemez River watersheds, respectively. Moreover, the model overestimated the high flows by as much as two times of the measured flow. The simulated flows were 329.53 mm and 138.21 mm in 2005 and corresponding measured flows were 150.51 mm and 70.74 mm for the Embudo Creek and Jemez River watersheds, respectively. For these reasons we think that it was difficult for the model to best match the measured and the simulated flow during the auto-calibration process.

Calibration Performance on the Embudo Creek

The auto-calibration was conducted in two steps for the period from 2004 to 2008, first for the 27 flow parameters and second for the most sensitive parameters. According to the auto-sensitivity analysis using the simulated flow, only 10 parameters were found to be sensitive with SI>0.2, and using the SSQ and the SSQR as a model output, nine parameters were found to be sensitive. Final calibration was performed for the 11 most sensitive parameters produced by the manual sensitivity analysis. The manual calibration showed that the model produced a good NSE value when all of the 27 flow parameters were calibrated (NSE=0.536; Figure 10). However, a poor NSE value was obtained from running the model for the 10 most sensitive parameters produced by the auto-sensitivity analysis using only the simulated flow (NSE=0.184). Calibrating the model for the 11 most sensitive parameters produced from visual judgment showed the highest NSE value (0.687). The least NSE (-0.039) value was obtained using nine parameters obtained from SSQR objective function. These results were in accord with those reported by Van Liew et al. (2005).

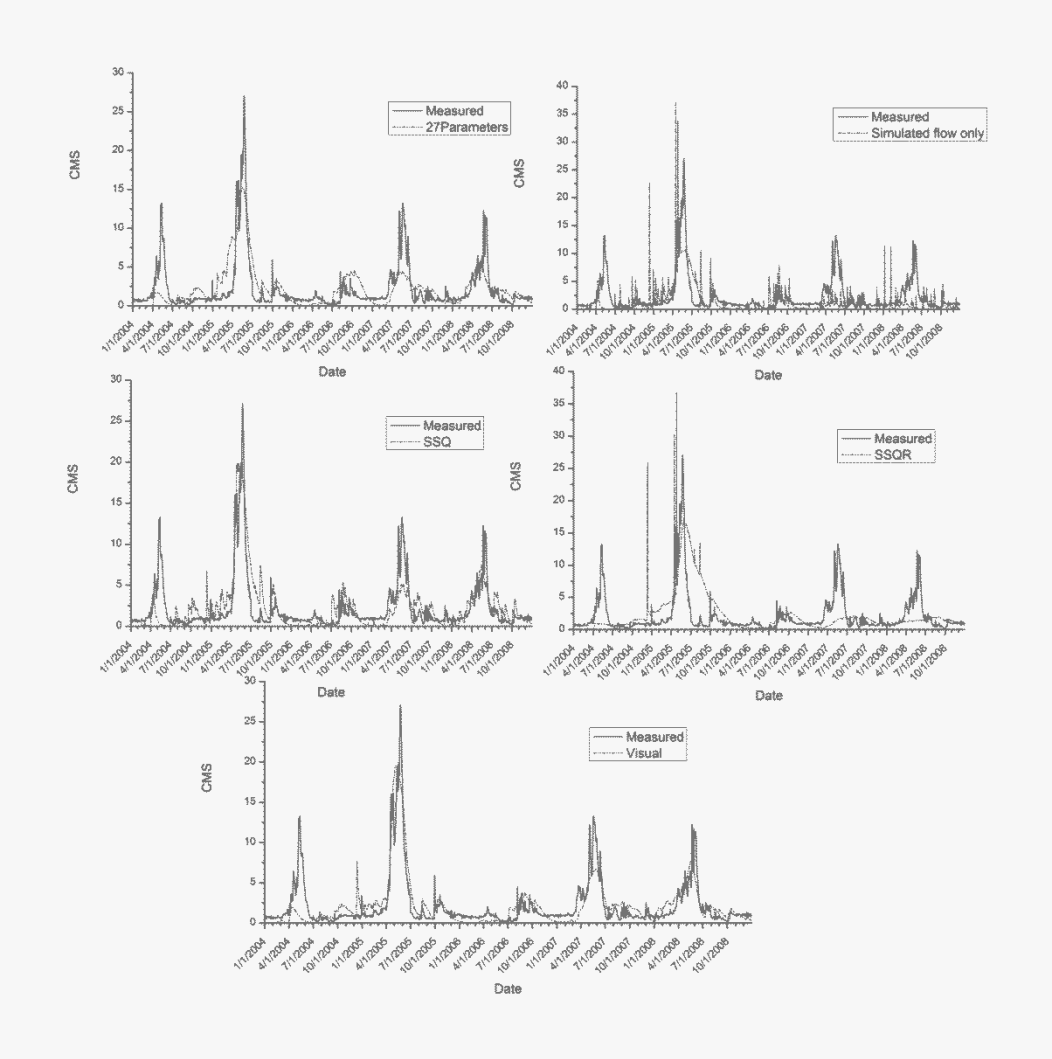

Figure 10. Measured versus simulated flow as a result of using (a) the 27 flow parameters and the most sensitive parameters produced from using (b) the simulated flow only, (c) SSQ, (d) SSQR, and (e) visual observation.

Calibration Performance on the Jemez River

The approaches used in calibrating the model for Embudo Creek watershed were used in calibrating the model for the Jemez River watershed. The highest NSE of 0.57 and 0.55 were obtained by using the SSQ as the model output and the nine parameters produced from the visual judgment, respectively. The lowest NSE (-0.55 and -0.05) values were obtained from using the parameters produced from using the simulated flow only and the SSQR as a model output. The hydrographs produced from using these different parameter datasets are shown in figure 11.

This study addressed strengths and weaknesses of the auto-sensitivity analysis and the auto-calibration. The model auto-calibration procedure was used because of the high capabilities and successes reported by some other studies using this option in the model (e.g. Van Liew et al., 2005; Kannan et al., 2008; Tattari et al., 2009).The model auto-calibration option was also used to save the time that manual calibration needs (Van Liew et al., 2005).

It was expected that calibration based on the SSQR objective function would produce the lowest NSE because SSQR aims to minimize the difference between the ranked simulated and measured flows ignoring the time of occurrence of given values; however, this was not the case. In contrast, the SSQ aims to minimize the difference between the measured and simulated flow time series on a daily basis which did improve results.

Increasing the number of parameters used could give the model a better chance and more options to match the measured flow. However, forcing the model to use all 27 flow parameters did not provide the best result. This was very clear because using the 27 flow parameters for the studied watersheds did not produce the best results or NSE values. And, there may still be another combination of parameters that can produce better results.

These results support the idea that it is not easy to find an optimum calibration solution due to the large number of parameters and the complexity of the model structure (Lin and Radcliffe, 2006).

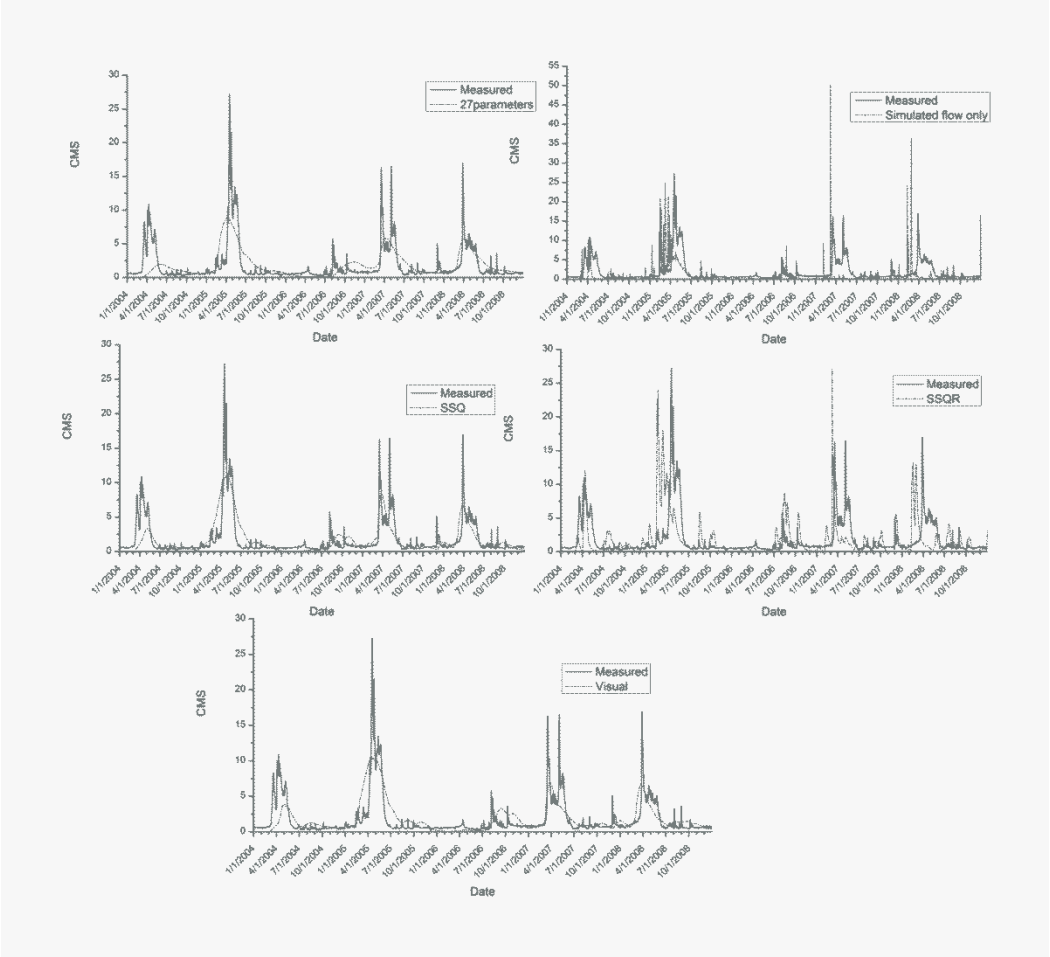

Figure 11. Measured versus simulated flow as a result of using (a) the 27 flow parameters, (b) the most sensitive parameters produced from using the simulated flow only, (c) SSQ, (d) SSQR, and (e) visual observation.

CONCLUSIONS

The ability of the SWAT model to simulate the water balance in semiarid watersheds was tested for the period from 2004 to 2008. The study was performed on the Embudo Creek and the Jemez River watersheds located in northern New Mexico. This study highlights the differences between using simulated flow only, SSQ, and SSQR outputs in the auto-sensitivity analysis as compared to the visual process to determine the most sensitive parameters and the best combination of different parameters for calibrating the model. A simple comparison has been accomplished to determine the most sensitive model parameters through the visual process before and after the auto-calibration. We examined the influence of each parameter on the WTRYLD, SURQ and ET and the hydrograph shape, by using the maximum and the minimum values as compared to the default value (before the auto-calibration) and to the best value chosen by the auto-calibration procedure (parameters sensitivity after the auto-calibration). The auto-calibration tool was evaluated by using different combinations of parameters produced from the auto-sensitivity analysis, visual judgment and finally using all the 27 flow parameters. Results showed that the highest NSE (0.69) was produced when the model was calibrated using the 11

most sensitive parameters produced from the visual judgment for the Embudo Creek watershed and it was 0.57 and 0.55 from using the SSQ and the visual judgment, respectively, for the Jemez River watershed. A poor performance from calibrating the model for stream flow was observed as a result of using the SSQR most sensitive parameters produced by the model for both watersheds. Based on the NSE values obtained from the auto-calibration, test results showed that use of the simulated flow only is not the best option to determine the most sensitive parameters. Differences between the sensitivity of some parameters before and after the auto-calibration were noticed as a result of high and low flows. It is not easy to find the optimum number and the best combination of parameters due to the complex and large number of model parameters although it is most critical for efficient model calibration.

ACKNOWLEDGEMENTS
The authors would like to acknowledge the support of the NMSU College of Agriculture, Consumer, and Environmental Sciences' Agricultural Experiment Station and New Mexico Water Resources Research Institute.

RESOURCES

Ahl, R.S., S.W. Woods, and H.R. Zuuring. 2008. Hydrologic calibration and validation of SWAT in a snow-dominated Rocky mountain watershed, Montana, USA. J. American Water Resources Assoc. 44(6):1411-1430. DOI: 10.1111/J.1752-1688.2008.00233.x.

Arnold, J.G., R. Srinivasan, R.S. Muttiah, and J.R. Williams. 1998. Large area hydrologic modeling and assessment part 1: model development. J. American Water Resources Assoc. 34(1):73-89.

Cibin, R., K.P. Sudheer, and I. Chaubey. 2010. Sensitivity and identifiability of streamflow generation parameters of the SWAT model. Hydrological Processes 24:1133-1148.

Daly, C., R.P. Neilson, and D.L. Phillips. 1994. A statistical-topographic model for mapping climatological precipitation over mountainous terrain. J. Applied Meteorology 33:140-158.

Deb, S. and M.K. Shukla. 2011. An overview of some hydrological watershed models. In: Soil Hydrology, Land Use and Agriculture: Measurement and Modeling, M.K. Shukla (Ed.), CAB International, Wallingford, UK, p75-p116.

DeWalle, D.R. and A. Rango. 2008. Principles of Snow Hydrology. Cambridge University Press, 410 pp.

El-Sadek, A., M. Bleiweiss, M.K. Shukla, S. Guldan, and A. Fernald. 2010. Alternative climate data sources for distributed hydrological modelling on a daily time step. Hydological Processes DOI: 10.1002/hyp.7917.

Fontaine, T.A., T.S. Cruickshank, J.G. Arnold, and R.H. Hotchkiss. 2002. Development of a snowfall-snowmelt routine for mountainous terrain for the soil and water assessment tool (SWAT). J. Hydrology 262:209-223.

Green, C.H. and A. van Griensven. 2008. Autocalibration in hydrologic modeling: using SWAT2005 in small-scale watersheds. Environmental Modelling & Software 23:422-434.

Kannan, N., C. Santhi, and J.G. Arnold. 2008. Development of an automated procedure for estimation of the spatial variation of runoff in large river basins. J. Hydrology 359:1-15.

Lemonds, P.J. and J.E. McCray. 2007. Modeling hydrology in a small Rocky Mountain watershed serving large urban populations. J. American Water Resources Assoc. 43(4):875-887. DOI: 10.1111/J.1752-1688.2007.00069.x.

Lenhart, T., K. Eckhardt, N. Fohrer, and H.G. Frede. 2002. Comparison of two different approaches of sensitivity analysis. Physics and Chemistry of the Earth 27:645-654.

Lin, Z. and D.E. Radcliffe. 2006. Automatic calibration and predictive uncertainty analysis of a semidistributed watershed model. Vadose Zone Journal 5:248-260.

McKay, M.D. 1988. Sensitivity and uncertainty analysis using a statistical sample of input values. In: Uncertainty Analysis, Y. Ronen (Ed.), CRC Press, Boca Raton, FL, pp. 145–186.

____, R.J. Beckman, and W.J. Conover. 1979. A comparison of three methods for selecting values of input variables in the analysis of output from a computer code. Technometrics 21(2):239–245.

Menking, K.M., K.H. Syed, R.Y. Anderson, N.G. Shafike, and J.G. Arnold. 2003. Model estimates of runoff in the closed semiarid Estancia basin central New Mexico, USA. Hydrological Sciences 48(6):953-970.

Morris, M.D. 1991. Factorial sampling plans for preliminary computational experiments. Technometrics 33(2):161-174.

Nash, J.E. and J.V. Sutcliffe. 1970. River flow forecasting through conceptual models. Part 1: discussion of principles. J. Hydrolology 10: 282-290.

Olivera, F., M. Valenzuela, R. Srinivasan, J. Choi, H. Cho, S. Koka, and A. Agrawal. 2006. Arc-GISSWAT : A geodata model and GIS interface for SWAT. Journal of American Water Resources Association. April :195-309.

RAWS, 2010. http://www.raws.dri.edu/

Stratton, B.T., V. Sridhar, M.M. Gribb, J.P. McNamara, and B. Narasimhan. 2009. Modeling the spatially varying water balance processes in a semiarid mountainous watershed of Idaho. J. American Water Resources Assoc. 45(6):1390-1408. DOI: 10.1111/J.1752-1688.2009.00371.x.

Tattari, S., J. Koskiaho, I. Barlund, and E. Jaakkola. 2009. Testing a river basin model with sensitivity analysis and autocalibration for an agricultural catchment in SW Finland. Agricultural and Food Science 18:728-439.

van Griensven, A., T. Meixner, S. Grunwald, T. Bishop, M. Diluzio, and R. Sirinivasan. 2006. A global sensitivity analysis tool for the parameters of multi-variable catchment models. J. Hydrology 324:10-23.

Van Liew, M.W., T.L. Veith, D.D. Bosch, and J.G. Arnold. 2007. Suitability of SWAT for the conservation effects assessment project: comparison on USDA Agricultural Research Service watersheds. J. Hydrologic Engineering 12(2):173-189.

____, M.W., J.G. Arnold, and D.D. Bosch. 2005. Problems and potential of autocalibrating a hydrologic model. Transactions of the ASAE 48(3):1025-1040.

Vivoni, E.R., C.A. Aragon, L. Malczynski, and V.C. Tidwell. 2009. Semiarid watershed response in central New Mexico and its sensitivity to climate variability and change. Hydrology and Earth System Sciences 13:715-733.

Wang, X. and A.M. Melesse. 2005. Evaluations of the SWAT model's snowmelt hydrology in a northwestern Minnesota watershed. Transactions of the ASAE 48(4):1359-1376.

____ and A.M. Melesse. 2006. Effects of STATSGO and SSURGO as inputs on SWAT model's snowmelt simulation. J. American Water Resources Assoc. 42(5):1217-1236.

Zhang, X., R. Srinivasan, B. Debele, and F. Hao. 2008. Runoff simulation of the headwaters of the Yellow River using the SWAT model with three snowmelt algorithms. J. American Water Resources Assoc. 44(1):48–61. doi:10.1111/j.1752-1688.2007.00137.x.

CORRESPONDENCE SHOULD BE ADDRESSED TO:
Manoj Shukla
Dept. of Plant and Environmental Sciences
New Mexico State University
PO Box 30003, MSC 3Q
Las Cruces, NM 88003
E-mail: shuklamk@nmsu.edu

DEEP PERCOLATION AND WATER TABLE FLUCTUATIONS IN RESPONSE TO IRRIGATION INPUTS: FIELD OBSERVATIONS

Carlos G. Ochoa*
Alexander G. Fernald
Steven J. Guldan
Manoj K. Shukla
Vincent C. Tidwell

ABSTRACT

Deep percolation (DP) is important for groundwater recharge in agricultural areas, yet few studies have investigated the connections between surface water and shallow groundwater in floodplain agriculture valleys. In this study, field observations were used to assess soil water transport through and below the root zone in a floodplain irrigated valley. Study objectives were to: 1) determine deep percolation following irrigation, and 2) characterize the shallow aquifer response to deep percolation. Two oat-wheatgrass fields (fields 1 and 2) near Española in north-central New Mexico were established in two predominant local soil types (Werlog clay loam and Fruitland sandy loam). A water balance method was used to calculate irrigation-deep percolation that ranged from 0 to 157 mm in field 1, and from 0 to 113 mm in field 2. Deep percolation resulted in a transient water table rise during most irrigation events that ranged from 1 to 244 mm in field 1, and from 1 to 97 mm in field 2. Study results add to the understanding of the relationships between irrigation, soil water dynamics, and water table fluctuations in a floodplain agriculture valley.

C.G. Ochoa and A.G. Fernald, Dep. of Animal and Range Sciences, New Mexico State Univ. PO Box 30003, MSC 3I, Las Cruces, NM 88003; S.J. Guldan, Alcalde Sustainable Agriculture Science Center, PO Box 159, Alcalde, NM 87511; M.K. Shukla, Dep. of Plant and Environmental Sciences, New Mexico State Univ. PO Box 30001, Las Cruces, NM, 88003; V.C. Tidwell, Geohydrology Dep., Sandia National Laboratories, PO Box 5800, Albuquerque, NM, 87185. *Corresponding author: carochoa@nmsu.edu

---

Soil water content and deep percolation play an important role in the hydrological processes that take place in the vadose zone. Water that percolates below the root zone is transported through the intermediate vadose zone and commonly adds to soil and aquifer recharge. Several studies have documented the importance of deep percolation from irrigation as a significant source of aquifer recharge. For instance, a study conducted by Willis and Black (1996) in the Macquarie Valley in Australia showed that irrigation on highly permeable soils is associated with excessive deep percolation and shallow water table formations. Fisher and Healy (2008) showed that all aquifer recharge observed at their study sites in California and Washington occurred during the growing season in response to irrigation inputs. Fernald and Guldan (2006) concluded that infiltration from surface irrigation is a significant source of shallow aquifer recharge in an agricultural valley of northern New Mexico. Recharge from surface water irrigation in the Eastern Snake River plain in Idaho provides about 60% of total aquifer recharge (Contor, 2004).

Direct observations of deep percolation are hard to obtain, therefore deep percolation is often calculated as a residual of the water balance (Bethune et al., 2008). Several studies (Sammis et al., 1982; Jaber et al., 2006; Ochoa et al., 2007) have reported the successful use of the water balance method for calculating deep percolation below the root zone. In the water balance method, deep percolation is the unknown variable, and water applied, change in soil water storage, and evapotranspiration are the known variables (Ben-Asher and Ayars, 1990). When reliable field measurements of the different components of the water budget are available, the water balance method can yield reliable rates of deep percolation. In turn, reliable measurements of deep percolation can provide important information for assessing groundwater recharge and transport of contaminants through the vadose zone (Rimon et al., 2007).

Soil textural properties play an important role in regulating different hydrological processes. For instance, field capacity is normally higher in fine-textured soils, because clayey soils can hold more water than coarser soils (Lal and Shukla, 2004; Kirkham, 2005). Also, high clay content can greatly reduce the rates of infiltration and deep percolation in irrigated soils (Willis and Black, 1996; Ochoa et al., 2009).

There is an ongoing need for measurements of soil properties, soil water content, and infiltration processes at multiple scales. In particular, proper characterization of spatial and temporal soil water dynamics becomes of great importance in agriculture areas of arid and semi-arid landscapes (Vereecken et al., 2008).

Surface water and groundwater interactions occur at different levels in different physiographic settings and these two terms cannot be seen as isolated components (Sophocleous, 2002). The development of either water component could affect the other. This is commonly observed in alluvial aquifers of irrigated valleys in arid regions (Winter et al., 1998). In these irrigated valleys water that percolates below the root zone can contribute to the recharge of the shallow aquifer. This is particularly true in alluvial irrigated valleys of northern New Mexico where highly permeable soils and excess irrigation applications are associated with rapid surface water and shallow groundwater exchanges (Ochoa et al., 2009; Fernald et al., 2010).

Deep percolation below the root zone has been investigated in different crop studies (Willis et al., 1997; O'Connell et al., 2003; Ochoa et al., 2007). Yet, the connections between surface water and shallow groundwater are not fully understood, especially those that relate to the entire process of downward vertical transport of water through and below the root zone and its effects on water table fluctuations. In this study, a combination of soil water content and other soil measurements were used to assess water movement through and deep percolation below the upper 1-m soil zone in two experimental fields with different soil types. In addition, groundwater level measurements were used to characterize the effects of deep percolation from irrigation on the shallow aquifer. Objectives of this study were to: 1) determine deep percolation following irrigation, and 2) characterize the shallow aquifer response to deep percolation from irrigation.

MATERIALS AND METHODS

Study Site and Experimental Design

This research was conducted at New Mexico State University's Sustainable Agriculture Science Center (Alcalde Science Center) in Alcalde, New Mexico. The Alcalde Science Center is at an elevation of 1733 m (above mean sea level) and it is located in the agriculture valley between the Alcalde main irrigation ditch and the Rio Grande and encompasses an area of 24 ha of irrigated land. The Alcalde Science Center, located in the Velarde sub-basin in the northern part of the Española basin overlies a shallow aquifer with depth to water table ranging from 1.5 to 10 m, depending on proximity to the river. Regional groundwater flow is mostly influenced by the Rio Grande and two of its tributaries, Rio de Truchas and Cañada de las Entrañas, coming from the Sangre de Cristo Range on the eastern side of the basin (Daniel B. Stephens, 2003). At the local level, shallow groundwater flow is mostly influenced by seepage from the Alcalde ditch and by deep percolation from irrigation (Fernald et al., 2007; Ochoa et al., 2007). Also, local groundwater flow is influenced by limited pumping by household and mutual domestic wells. Average annual precipitation in the study area is 251 mm, of which 40% occurs during the summer season. For the period of record 1953 to 2006, the average monthly temperature was 10.6°C, with the lowest average monthly temperature of -0.8°C occurring during the month of January and the highest average monthly temperature of 22.3°C occurring during the month of July (WRCC, 2006).

This research project at the Alcalde Science Center was conducted in a 2.4 ha crop field within which were delineated two experimental fields (Fig. 1). The two fields were established on two predominant soil types. Field 1 covered an area of 11,500 m^2 with soil classified as a Werlog clay loam soil, typified as fine-loamy, mixed, active, calcareous, mesic Aquic Ustifluvents. Field 2 covered an area of 11,200 m^2 with soil classified as a Fruitland sandy loam soil, typified as coarse-loamy, mixed, superactive, calcareous, mesic Typic Torriorthents (Soil Survey Staff, 2008). Soil types present in these experimental fields are commonly found in the Alcalde agricultural valley.

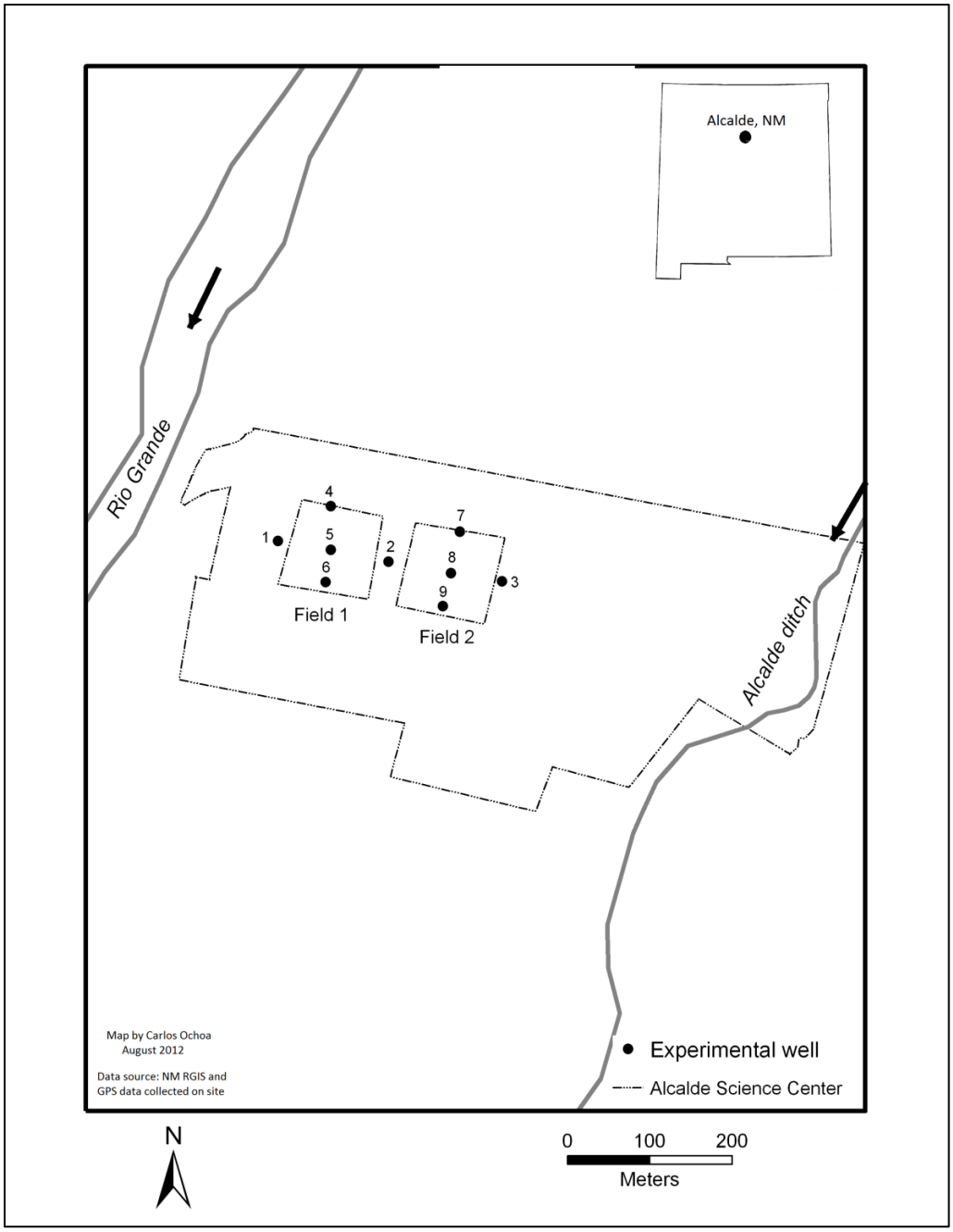

Figure 1. Experimental fields showing monitoring wells at the study site in Alcalde, NM.

Both fields were instrumented to record total irrigation water applied, soil water content, irrigation water runoff, and shallow groundwater level. Figure 2 shows a schematic of field instrumentation in field 1, both fields were instrumented similarly. Irrigation valves located near the northern side of each field and aluminum irrigation pipe were used to irrigate each field from east to west. Three soil water content stations and three experimental wells were installed in each field. Flow meters were installed on the water feeding pipes and at the southern end of each field for measuring total irrigation applied and tail water running off the field, respectively (Fig. 2).

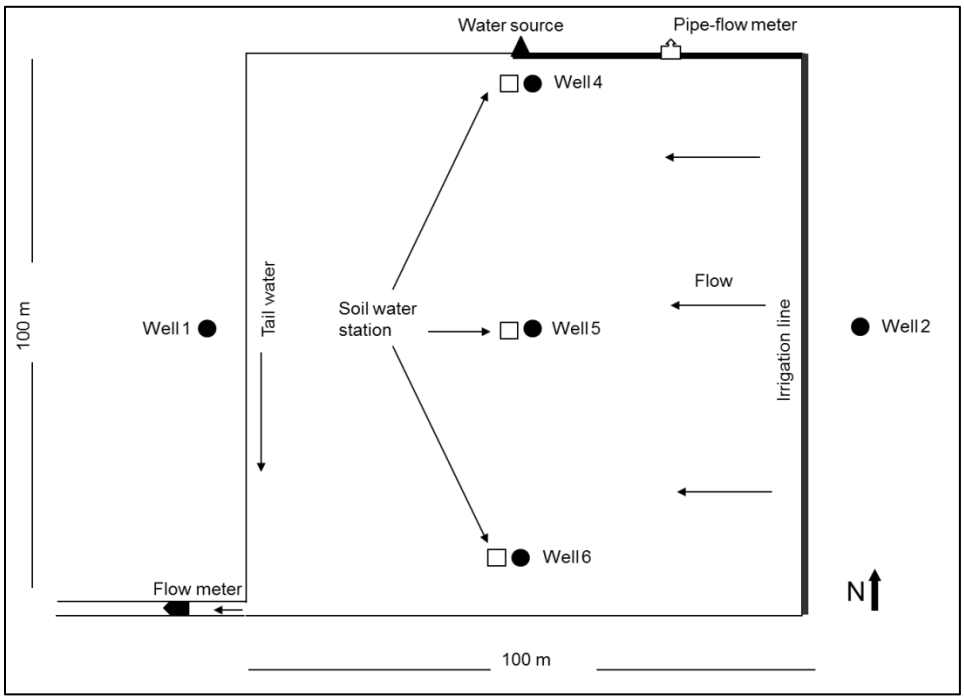

Figure 2. Schematic of field instrumentation in experimental field 1.

Elevation measurements taken with a total station (Model 226,Topcon positioning systems; Pleasanton, California) were used for determining slope in each field. Slope was calculated over the length of each field in the direction of irrigation flow, from east to west. A 1% slope was obtained for field 1 and a 0.8% slope was obtained for field 2. A mixture of wheatgrass (*Thinopyrum intermedium*) and oats (*Avena sativa* L.) were planted in each of the two fields in the summer of 2008.

Soil Physical Properties

Soil samples for determining soil physical properties in horizontal and in vertical planes were collected. For determining soil properties in the horizontal plane, soil samples were collected in the top 0.3 m and were used to characterize topsoil texture variability. A total of 103 soil samples were collected from different locations in the study area at the Alcalde Science Center after it was partitioned into two experimental fields. These 103 soil samples were collected from 49 different locations in each field, at approximately 14 m from each other, and from five locations in between fields. One soil sample of 300-mm length was collected at each location using a 0.813 mm I.D. by 300 mm soil sampler (model LS, Oakfield Apparatus, Inc.; Oakfield, Wisconsin). Soil samples were air-dried for several weeks prior to soil texture analysis using the Hydrometer method (Gee and Bauder, 1986). Soil sampling locations were positioned using a GPS unit (Model 76Cx, Garmin International, Inc.; Olathe, KS) and were geo-referenced in the Universal Transverse Mercator (UTM) projected coordinate system. For determining soil properties in the vertical plane, soil samples were collected at different depths. These soil samples were collected during soil water content sensor installation in each field and were used for determining bulk density and soil texture at different soil depths. Three soil samples (50-mm

diameter by 30-mm length) for determining soil bulk density (ρ_b) were collected using a soil core sampler at 0.1, 0.6, and 1.1 m depths in the midfield sensor locations in each field (Fig. 3). The ρ_b was determined following the method in Blake and Hartge (1986). Also, 50-g soil samples for soil texture analysis were collected at the same depth as the bulk density soil samples. Soil texture of these samples was determined using the Hydrometer method (Gee and Bauder, 1986). Soil texture and bulk density data obtained from a previous experiment that aimed to characterize water transport through the vadose zone in small-sized experimental plots (Ochoa et al., 2009) were used to characterize soil properties at the north and south sensor locations in each experimental field.

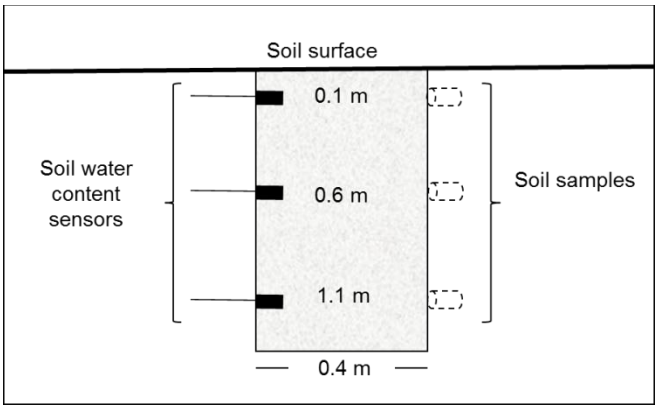

Figure 3. Schematic of bulk density soil sample collection and soil water content sensor installation.

Soil Texture Spatial Analysis

Soil texture data and UTM coordinates of the soil sampling locations were used to determine the spatial variability of the top soil. Variogram and contour map techniques were used to characterize the spatial variability of soil texture, specifically clay content, in the entire 2.4 ha crop field. We used the computer program Surfer (version 9, Golden software, Inc.; Golden, CO) to generate a spherical variogram for percent clay content. The variogram generated was in turn used to create a contour map to illustrate the spatial variability of clay content in the field. While soil properties below 0.3 m may be different in the two experimental fields, physical properties above 0.3 m can provide valuable information of infiltration and runoff processes occurring in these two fields.

Soil Water Instrumentation

A vertical nest of three soil water sensors (model CS616, Campbell Scientific Inc.; Logan, Utah) was installed in the midfield of each of the two experimental fields, covering the upper 1.1 m soil depth. Sensors were installed horizontally at 0.1, 0.6, and 1.1 m depth (see Fig. 3). Nests of soil water content sensors installed during the plot experiment (Ochoa et al., 2009) were used in this field scale experiment. After the plot experiment, plot borders were removed but the nests of sensors remained inside the experimental fields, at the northern and southern ends, used in this study. The sensors were attached to dataloggers, which were programmed to collect soil volumetric water content (θ) data every 1 h during all irrigation events in 2008.

Irrigation Applied and Field Runoff

Across two irrigation seasons (2008 and 2009), twelve surface (furrow) irrigations were applied to each field. The volume of water applied (*V*) for each irrigation event was measured using a propeller flow meter with totalizer (McCrometer, Inc.; Hemet, California) mounted in a 250-mm diameter PVC pipe. Irrigation depth (*IRR*) was calculated based on the volume of water applied divided by the total area (*A*) of each field.

Total field runoff (*RO*) for each irrigation event was determined based on the amount of irrigation water flowing out of each field during and after irrigation. An S-M open channel flow-measurement device was built based on the work published by Samani and Magallanez (2000). This flow-measurement device was installed in a relief ditch constructed at the southern end of each field, where excess water was routed out to a nearby ditch that carries tail-water. The S-M flume was installed and equipped with a submersible pressure transducer (Model CS420, Campbell Scientific, Inc.; Logan, Utah) for measuring ditch water stage every 5 min. Measured ditch water stage was used to calculate runoff flow rate (*Q*) using the following equation by Samani and Magallanez (2000):

$$Q = 0.701 * \left(\sqrt{g}\right) * (Bc)^{0.91} * (H)^{1.59} \quad (1)$$

Where, Q = Flow rate ($m^3 s^{-1}$); g = Gravity acceleration (9.81 m s^2); Bc = Flume throat width (m); and H = Measured water stage (m).

Water Balance Method (Wbm) To Calculate Deep Percolation

A water balance approach was used for determining *DP* below the upper 1-meter soil depth after each irrigation event. We calculated *DP* on a daily basis using the following water balance equation:

$$DP = IRR + R - \Delta S - RO - ET \quad (2)$$

Where, DP = Deep percolation (mm); IRR = Irrigation depth (mm); R = Rainfall (mm); ΔS = Soil water content 24 h after the end of irrigation minus soil water content at the onset of irrigation (mm); RO = Field runoff (mm); and ET = Evapotranspiration (mm).

DP was determined as the total amount of water passing below the upper 1-m soil depth after each irrigation event. It was assumed that water passing below the upper 1-m soil depth was no longer subject to significant plant root uptake. Soil volumetric water content (θ) data collected at each soil water-measuring station was used to determine the change in soil water content (ΔS). The ΔS in the upper 1-m soil profile was determined by subtracting soil water content measured at the onset of irrigation from soil water content measured 24 h after peak θ measured at each soil depth.

Some assumptions were made to characterize soil water content in the upper 1-m soil profile at the field scale: 1) soil volumetric water content measured at the 0.1 m soil depth was assumed to be the same for the entire 0 to 0.1 m soil layer, and 2) three station-averaged θ data were assumed to be representative of soil water content conditions at the entire field scale.

Linear interpolation was used to determine soil water content every 10 mm in the 0.1 to 1.1 m soil layer using θ collected at the 0.1, 0.6, and 1.1 m soil depths. These data were used to calculate the average soil water content for the 0 to 1 m soil profile at each measuring station. Total field RO after irrigation in each field was determined from data collected with the S-M flume. Daily actual evapotranspiration (*ET*) values were obtained from the New Mexico Climate Center website, which uses data collected from a weather station located 500 m east of the center of the farthest experimental field (field 1) at the Alcalde Science Center (NMCC, 2010).

Shallow Aquifer Water Level Response

A total of 9 driven-point wells with 50-mm diameter galvanized pipe and a bottom screen of 1.2-m length were installed in each plot (see Fig. 1). Three wells were installed inside field 1 (wells 4, 5, and 6) and three more were installed in field 2 (wells 7, 8, and 9). These wells were located next to the soil water content stations and were installed at the same time as the soil water sensors (see Fig. 2). Three more wells were installed at between and outside of the fields, the first well (1) was installed approximately 20 m west of field 1, the second well (2) was installed in between the 2 fields, and a third well (3) was installed 20 m east of field 2 (see Fig. 1). At installation, all wells were submerged at least 0.3 m below the water table. All wells were equipped with water level loggers (model U20-001-01, Onset Computer, Corp.; Bourne, Massachusetts). All water level loggers were programmed to record water level data every 10 min. On-site water level data for calibrating and validating data obtained with the automated water level loggers were collected using a water level indicator (Model 16036, Durham Geo Slope Indicator.; Mukilteo, Washington) one day after well installation and three other times during the time of the experiment. Water level data recorded were used to characterize water level fluctuations during specific irrigations and throughout the duration of the experiment.

RESULTS AND DISCUSSION

Soil Properties

Soil physical properties obtained from samples collected in the upper 1.1-m soil profile during sensor installation were different across fields and soil depths (Table 1). As expected, higher clay contents were observed in field 1(Werlog clay loam soil) than in field 2 (Fruitland sandy loam soil). The highest sand content values were observed at the 1.1 m sensor location in field 1 and at the 0.6 m sensor location in field 2. Clay content was slightly different at all depths in field 1 but it was quite variable in field 2.

Table 1. Soil physical properties in the two experimental fields.

Location	Soil depth	Bulk density	Sand	Silt	Clay
	(m)	($Mg\ m^{-3}$)	---------- ($g\ kg^{-1}$) ----------		
Field 1 - Werlog clay loam soil					
South	0.1	1.60±0.02‡	588	108	304
South	0.6	1.39±0.02	528	148	324
South	1.1	1.27±0.02	628	68	304
Midfield	0.1	1.57±0.02	579	114	307
Midfield	0.6	1.43±0.03	512	153	335
Midfield	1.1	1.32±0.02	631	71	298
North	0.1	1.60±0.02	571	151	278
North	0.6	1.44±0.04	270	390	340
North	1.1	1.34±0.02	670	70	260
Field 2 - Fruitland sandy loam soil					
South	0.1	1.53±0.06	568	28	404
South	0.6	1.52±0.05	688	148	164
South	1.1	1.63±0.02	548	188	264
Midfield	0.1	1.52±0.05	628	227	145
Midfield	0.6	1.50±0.02	703	154	143
Midfield	1.1	1.47±0.04	596	186	218
North	0.1	1.54±0.06	633	222	145
North	0.6	1.51±0.03	713	152	135
North	1.1	1.45±0.05	612	192	196

‡ Mean ± standard deviation

Observations of higher clay content in field 1 when compared to field 2 are similar to those results obtained by the soil spatial variability analysis performed. The contour map derived from the variogram calculated from soil samples collected in the upper 0.3 m depth showed that the variability of clay content ranged from 11% in the northeastern corner of field 2 to 17% in the southwestern corner of field 1 (Fig. 4).

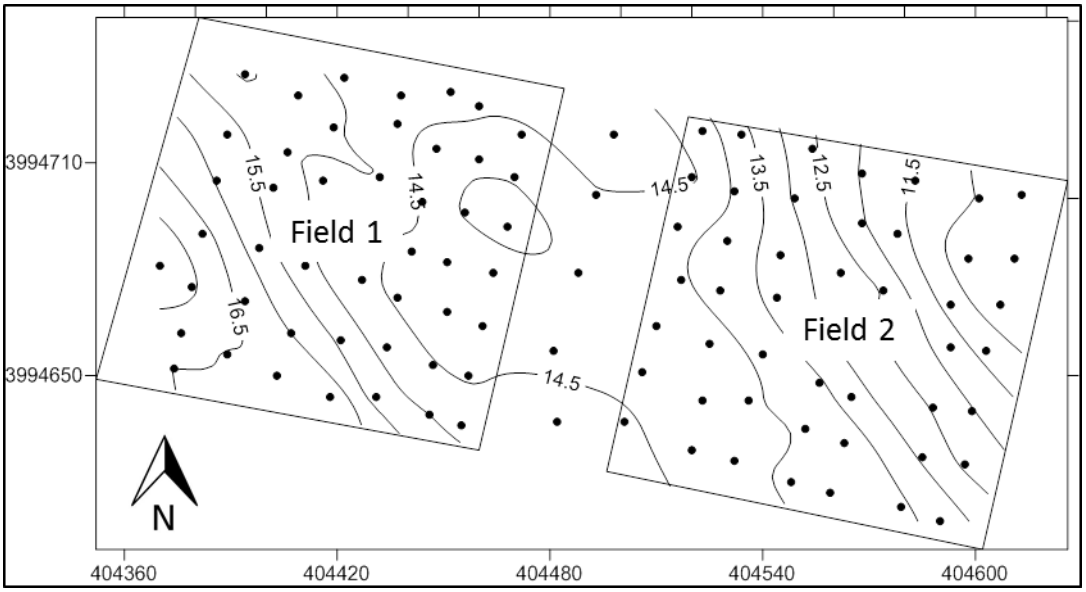

Figure 4. Variability of soil clay content, expressed as percentage, at the study site showing soil sampling locations and experimental field boundaries.

Deep Percolation – Daily Water Balance Method

Deep percolation below the upper 1-m soil depth varied across fields. In general, higher *DP* values were obtained in field 1 (Table 2) when compared to *DP* results obtained in field 2 (Table 3).

Table 2. Deep percolation (*DP*) results by the water balance method in field 1 (Werlog clay loam soil), showing total number of hours of irrigation (*T*), total irrigation amount (*IRR*), rainfall (*R*), change in soil water storage (*ΔS*), runoff (*RO*), and actual evapotranspiration (*ET*).

Date	*T*	*IRR*	*R*	*ΔS*	*RO*	*ET*	*DP*
	(h)	mm					
10-Jun-08	26.5	211	0	31	14	9	157
24-Jun-08	23.0	187	0	34	17	7	129
7-Jul-08	11.5	85	0	24	9	4	48
12-Aug-08	7.0	59	0	44	0	4	10
9-Sep-08	7.6	81	0	94	11	5	0
28-Oct-08	7.6	42	0	50	0	4	0
29-Apr-09	9.4	122	0	34	2	8	79
21-May-09	8.0	97	0	63	5	4	26
15-Jun-09	7.7	93	0	62	7	8	17
13-Jul-09	7.2	88	0	111	1	1	0
27-Jul-09	7.0	85	0	109	16	9	0
2-Sep-09	7.3	103	0	140	6	4	0
Total		1253	0	796	88	67	466

Table 3. Deep percolation (*DP*) results by the water balance method in field 2 (Fruitland sandy loam soil), showing total number of hours of irrigation (*T*), total irrigation amount (*IRR*), rainfall (*R*), change in soil water storage (*ΔS*), runoff (*RO*), and actual evapotranspiration (*ET*).

Date	*T*	*IRR*	*R*	*ΔS*	*RO*	*ET*	*DP*
	(h)	mm					
16-Jun-08	27.0	267	0	104	42	9	113
1-Jul-08	8.8	96	0	60	22	5	8
14-Jul-08	11.5	125	0	41	40	4	40
7-Aug-08	8.0	87	0	95	39	4	0
11-Sep-08	7.5	74	0	52	16	4	2
20-Oct-08	7.5	41	2	84	0	3	0
6-May-09	7.1	84	0	69	8	9	0
4-Jun-09	8.8	117	4	173	24	8	0
25-Jun-09	7.2	85	0	86	8	7	0
20-Jul-09	6.8	85	0	73	2	8	2
10-Aug-09	7.0	85	0	67	9	9	0
1-Sep-09	6.7	101	0	149	35	4	0
Total		1247	6	1053	245	74	165

In field 1, *DP* occurred during seven out of the total twelve irrigations applied to this field. Values of *DP* ranged from 0 to 157 mm depending on the amount of irrigation water applied (*IRR*) and antecedent soil water content. The highest *DP* value of 157 mm corresponded to the highest amount of irrigation applied (211 mm) during 10 June 2008. When greater than zero, the lowest *DP* value of 10 mm corresponded to the 59 mm *IRR* applied on 12 August 2008. Time of irrigation (*t)* ranged from 7.0 to 26.5 h, with the higher *t* values observed during the first irrigation events for establishing the crop. There was no rainfall noted during any of the irrigation events. During those irrigation events where *DP* was observed, soil water content difference between initial and 24 h after the end of irrigation ranged from 24 to 63 mm and it ranged from 50 to 140 mm when *DP* was not obtained. For all irrigation events, *RO* ranged from 0 to 17 mm and estimated values of *ET* ranged from 1 to 9 mm (see Table 2).

In field 2, *DP* occurred during five out of the twelve irrigations and ranged from 0 to 113 mm. The highest *DP* value of 113 mm corresponded to the highest amount of irrigation applied (267 mm) on 16 June 2008. The lowest *DP* values of 2 mm corresponded to the 74 mm *IRR* applied on 11 Sep 2008 and to the 85 mm *IRR* applied on 20 July 2009. Time of irrigation (*t)* ranged from 6.7 to 27 h, with the higher *t* value observed during the first irrigation event. Total amount of water applied ranged from 41 to 267 mm. During those irrigation events where *DP* was observed, soil water content difference between initial and 24 h after the end of irrigation ranged from 41 to 104 mm and it ranged from 67 to 173 mm when *DP* was not obtained. For all irrigation events, *RO* ranged from 0 to 42 mm and estimated values of *ET* ranged from 3 to 9 mm (see Table 3). Lower runoff observed in field 1 as compared to field 2 was attributed to slight differences in pipe-gate opening during irrigation that created more rapid flow in some rows of field 2. Hence, irrigation water in those rows reached the end of the field more rapidly and that translated into more water running off from field 2.

Similar amounts of total irrigation (~ 1250 mm) were applied in each field during the two-year experiment. However, total *DP* as a percentage of total water applied was much higher in field 1 (37%) when compared to total *DP* in field 2 (13%). Lower *DP* observed in field 2 was partially attributed to more runoff observed in that field, which may have reduced the time of standing irrigation water (intake opportunity time). Also, the change in water storage was less in field 1 than in field 2 (see Tables 2 and 3), this may be due to the higher clay content observed in field 1 that held more water in the soil, consequently antecedent soil water content was higher prior to irrigation. Field 2 has greater depth to water table and so more volume for water storage. Even though depth to water table in field 1 was about 2.9 m, 1.6 m at the top was fine textured soil with the remainder below being coarse sand and gravel (Ochoa et al., 2009).

When *DP* was obtained, a high correlation between *IRR* and *DP* was observed in field 1 (r = 0.94) and in field 2 (r = 0.98). High positive correlation between total irrigation and deep percolation has also been reported by Willis et al. (1997), Scanlon et al. (2003), and Ochoa et al. (2007 and 2009).

Water Table Rise in Response to Deep Percolation

Deep percolation below the upper 1-m soil profile resulted in a transient water table rise during most irrigation events. Water table rise was variable between fields but also it was variable among wells in each field. In general, higher water table rise values were observed in field 1 (Table 4) than in field 2 (Table 5).

Table 4. Deep percolation (*DP*) and well-water level rise following irrigation (*IRR*) in field 1.

IRR	*DP*	*Well 1*	*Well 2*	*Well 4*	*Well 5*	*Well 6*
---------- mm ----------						
211	157	1	3	NA	15	NA
187	129	111	244	242	175	135
85	48	1	12	0	0	13
59	10	0	0	0	0	0
122	79	16	32	13	40	28
97	26	12	16	7	23	24
93	17	20	30	10	30	20

NA: data not available

Table 5. Deep percolation (*DP*) and well-water level rise following irrigation (*IRR*) in field 2.

IRR	*DP*	*Well 2*	*Well 3*	*Well 7*	*Well 8*	*Well 9*
---------- mm ----------						
267	113	97	82	NA	17	NA
96	8	27	30	12	34	2
125	40	2	3	0	0	0
74	2	0	6	1	0	0
85	2	8	0	0	0	7

NA: data not available.

The transient water table rise in field 1 ranged from 1 to 244 mm. The highest water table rise values ranged from 111 mm in well 1 to 244 mm in well 2 and were observed during the 187 mm irrigation with 129 mm *DP*. Relatively low water table response was observed during the first irrigation event with the highest amount of water applied and the highest deep percolation rate calculated. We attributed this relatively low water table response to the recharge of the deeper soil layers that may have captured most of the percolation water before it reached the shallow aquifer. No water table rise was observed during the irrigation of 59 mm with the smallest *DP* value of 10 mm. Water table rise values greater than deep percolation values were observed in wells 2, 4, 5, and 6 during the 187 mm irrigation event. Similarly, greater water table rises were observed in wells 1, 2, 5, and 6 during the 93 mm irrigation (see Table 4). Figure 5 shows the water table response to deep percolation in five wells on field 1 corresponding to the 187 mm irrigation. It can be noted that the water table started rising towards the end of the irrigation event, which lasted 23 h (see Table 2), but peak water level was not reached until about 90 h after the onset of irrigation in all wells. Well number 2, which is the closest well to the irrigation line, showed the greatest water table response (see Table 2).

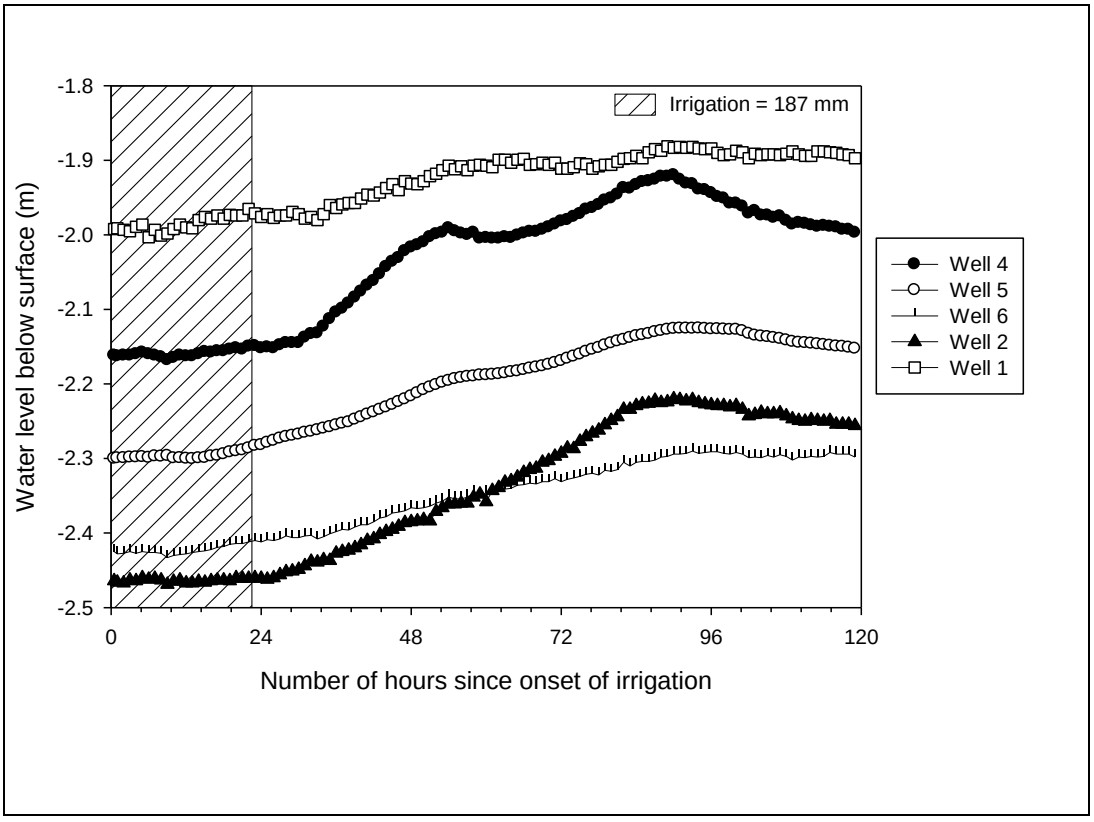

Figure 5. Groundwater level response to a 187 mm irrigation event measured in five experimental wells in field 1.

The transient water table rise in field 2 ranged from 1 to 97 mm. The highest water table rise value of 97 mm was observed in well 2 during a 267 mm irrigation event that yielded 113 mm of *DP*. Irrigations below 90 mm showed minimal *DP* that was reflected in the small water table rise values obtained in selected wells (see Table 5). However, no water level response was observed

during the 125 mm *IRR* with 40 mm of *DP*. We attributed the muted response to an observed water table mound, probably from irrigation in neighboring fields, which may have masked the possible water level rise from the 125 mm irrigation. Similar to that observed in field 1, water table rise values greater than deep percolation values were observed in wells 2, 3, 7, and 8 during the 96 mm irrigation event. Also, water table rises greater than *DP* were observed in wells 2 and 9 during the 85 mm irrigation (see Table 5).

Water table rise values (1 to 97 mm) observed in field 1 were significantly lower than those observed during a similar study conducted by Ochoa et al. (2007). This comparable study was conducted in a neighboring alfalfa-grass field with similar soil and water table depth, where water table rises that were observed during all irrigation applications ranged from 140 to 380 mm.

CONCLUSIONS

Deep percolation occurred during most irrigation events in field 1 (Werlog clay loam soil) and during almost half of the irrigation events in field 2 (Fruitland sandy loam soil). When present, deep percolation was positively related to the amount of water applied. Antecedent soil water content also played an important role in observed deep percolation. Greater total deep percolation was observed in the field with higher clay content, but with the shallowest depth to water table. More runoff, consequently less ponding time, and a greater depth to water table may have contributed to lower deep percolation observed in field 2. When irrigation water percolated below the top 1-m of soil, a transient water table rise of up to 244 mm was observed. In several occasions, the transient water table rise observed in different monitoring wells was higher than deep percolation values. We attributed this higher response to the presence of preferential flow channels that may be present in the soil profile.

Results from this study contribute towards the understanding of the relationships between irrigation, vadose zone soil water dynamics, and water table fluctuations in a floodplain irrigated valley of northern New Mexico.

Acknowledgments:
Authors gratefully acknowledge the technical assistance of the NMSU-Alcalde Science Center staff, especially David Archuleta, Val Archuleta, David Salazar, and Estevan Herrera. This material is based upon work supported by the U.S. Department of Agriculture under Agreement No. 2005-34461-15661 and 2005−45049−03209, by the National Science Foundation, Award No. 0814449 and Award No. 1010516, and by the New Mexico Agricultural Experiment Station.

LITERATURE CITED

Ben-Asher, J. and J.E. Ayars. 1990. Deep seepage under nonuniform sprinkler irrigation. II: Field data. J. Irrig. Drain. Engin. 116(3):363–373.

Bethune, M.G., B. Selle, and Q.J. Wang. 2008. Understanding and predicting deep percolation under surface irrigation. Water Resour. Res. 44: 1–16.

Blake, G.R. and K.H. Hartge. 1986. Bulk density. *In* Methods of Soil Analysis, Part I. A. Klute (ed.). Madison, WI. Monograph No. 9. ASA and SSSA.

Contor, B.A. 2004. Percolation, runoff, and deficit irrigation. Idaho WRRI Tech. Rep. 04-004.

Daniel B. Stephens and Associates. 2003. Jemez y Sangre Regional Water Plan Daniel B. Stephens and Associates, Inc. Albuquerque, NM.

Fernald, A.G. and S.J. Guldan. 2006. Surface water–groundwater interactions between irrigation ditches, alluvial aquifers, and streams. Reviews in Fisheries Science 14:79–89.

_____, T.T. Baker, and S.J. Guldan. 2007. Hydrologic, riparian, and agroecosystem functions of traditional *acequia* irrigation systems. J. Sust. Agric. 30(2):147–171.

_____, S.Y. Cevik, C.G. Ochoa, V.C. Tidwell, J.P. King, and S.J. Guldan. 2010. River hydrograph retransmission functions of irrigated valley surface water-groundwater interactions. J. Irrig. Drain. Engin. 136(12):823–835.

Fisher, L.H. and R.W. Healy. 2008. Water movement within the unsaturated zone in four agricultural areas of the United States. J. Environ. Qual. 37:1051–1063.

Gee, G.W., and J.W. Bauder. (1986). Particle-size analysis. *In* Methods of Soil Analysis. A. Klute (ed) Part I. 2nd ed. Agron. Monogr. 9 ASA and SSSA, Madison, WI. p. 383–409.

Jaber, F.H., S. Shukla, and S. Srivastava. 2006. Recharge, upflux and water table response for shallow water table conditions in southwest Florida. Hydrol. Processes 20:1895–1907.

Kirkham, M.B. 2005. Field capacity, wilting point, available water, and the non-limiting water range. *In* Principles of Soil and Plant Water Relations. Elsevier Academic Press. p. 101–110.

Lal, R. and M. Shukla. 2004. Principles of soil physics. New York, NY. M Dekker Inc.NMCC. 2010. New Mexico Climate Center. NMSU weather data at the Alcalde Science Center. Available at http://weather.nmsu.edu/cgi-shl/cns/gdd.pl. (Accessed 30 October 2010; verified 4 April 2011). New Mexico State University, Las Cruces, NM.

O'Connell, M.G., G.J. O'Leary, and D.J. Connor. 2003. Drainage and change in soil water storage below the root-zone under long fallow and continuous cropping sequences in the Victorian Malle. Aust. J. of Ag. Res. 54:663–675.

Ochoa, C.G., A.G. Fernald, S.J. Guldan, and M.K. Shukla. 2007. Deep percolation and its effects on shallow groundwater level rise following flood irrigation. Trans. ASABE 50(1):73–81.

_____, C.G., A.G. Fernald, S.J. Guldan, and M.K. Shukla. 2009. Water movement through a shallow vadose zone: A field irrigation experiment. Vadose Zone J. 8:414–425.

Rimon, Y., O. Dahan, R. Nativ, and S. Geyer. 2007. Water percolation through the deep vadose zone and groundwater recharge: Preliminary results based on a new vadose zone monitoring system. Water Resour. Res., 43, W05402, doi:10.1029/2006WR004855.

Samani, Z. and H. Magallanez. 2000. Simple Flume for Flow Measurement in Open Channel. American Society of Civil Engineers (ASCE) J. Irrig. Drain. 126(2):127–129.

Sammis, T.W., D.D. Evans, and A.W. Warrick. 1982. Comparison of methods to estimate deep percolation rates. J. Ame. Water Resour. Assoc. 18(3):465–470.

Scanlon, B.R., A. Dutton, and M.A. Sophocleous. Groundwater recharge in Texas. 2003. The University of Texas at Austin, Bureau of Economic Geology, submitted to Texas Water Development Board.

Soil Survey Staff, Natural Resources Conservation Service, United States Department of Agriculture. 2008. Soil Series Classification Database [Online]. Available at https://soilseries.sc.egov.usda.gov/osdname.asp (Accessed 4 May 2011; verified 15 May 2011). USDA-NRCS, Lincoln, NE.

Sophocleous, M.A. 1991. Combining the soil water balance and water level fluctuation methods to estimate natural groundwater recharge-practical aspects. J. Hydrol. 124:229–241.

_____, M. 2002. Interactions between groundwater and surface water: the state of the science. Hydrogeol. J. 10:52–67.

Vereecken, H., J.A. Huisman, H. Bogena, J. Vanderborght, J.A. Vrugt, and J.W. Hopmans. 2008. On the value of soil moisture measurements in vadose zone hydrology: A review. Water Resour. Res. 44:1–21.

Willis, T.M. and A.S. Black. 1996. Irrigation increases groundwater recharge in the Macquarie Valley. Aust. J. Soil Res. 34:837–847.

_____, T.M., A.S. Black, and W.S. Meyer. 1997. Estimates of deep percolation beneath cotton in the Macquarie Valley. Irrig. Sci. 17:141–150.

Winter, T.C., J.W. Harvey, O.L. Franke, and W.M. Alley. 1998. Ground water and surface water: A single resource. USGS Circular 1139. Reston, VA. U.S. Geological Survey.

WRCC. 2006. Western Regional Climate Center. Alcalde, New Mexico (290245). Period of record monthly climate summary. Period of record 04/01/1953-12/31/2005. [Online]. Available at http://www.wrcc.dri.edu/cgi-bin/cliMAIN.pl?nmalca. (Accessed 27 December 2010; verified 4 May 2011). WRCC, Reno, NV.

TREATED WASTEWATER APPLICATION IN SOUTHERN NEW MEXICO: EFFECT ON SOIL CHEMICAL PROPERTIES AND SURFACE VEGETATION COVERAGE

Pradip Adhikari[1]
Manoj K. Shukla[1]
John J. Mexal[1]

ABSTRACT

Land application of wastewater is the earliest forms of wastewater treatment technology and is experiencing resurgence in Southern New Mexico due to the dwindling natural water resources. Lagoons treated wastewater generated from the West Mesa Industrial Park, Las Cruces, NM has been applied since 2002 to a 36 ha area by fixed head sprinkler irrigation system. The study was conducted to determine the uniformity of sprinkler irrigation, temporal variability of amount and quality of applied treated wastewater, and effect of treated wastewater on soil chemical properties and surface vegetation community. Sprinkler uniformity tests were conducted during 2007-2009, soil chemical properties analysis was done during 2005, 2007, and 2009. Total amount of wastewater application and chemical properties from 2002-2009 were obtained from the City of Las Cruces. Spatial variability was analyzed during 2009 and surface vegetation coverage was determined during May and September 2012. Christiansen's sprinkler uniformity coefficient ranged between 46 to 67%. The soil SAR and chloride were 50.45 and 1270.5 mg kg^{-1}, respectively at the northwest and southwest portions of the application site. This was due to the low uniformity and temporally variable chemical composition of applied wastewater. Photographs of the surface vegetation showed substantial more surface coverage (65-100%) in the irrigated area than unirrigated (3-35 %) area. Therefore, application of the wastewater is important for the survival of native and perennial vegetation. However, high soil SAR and chloride indicates initiation of management practices for controlling soil salinity, soil sodicity, and reducing evaporation from treatment ponds for the sustainability of wastewater application.

---

[1]*New Mexico State University, Department of Plant and Environmental Sciences, P.O. Box 30003, MSC 3Q,, Las Cruces, NM, 88003-8003.*

*Corresponding author: Pradip Adhikari; e-mail: adhikari@nmsu.edu; phone # 57565022

Treatment of urban and industrial wastewater is complex, expensive, and requires energy and technology. The safe disposal of the treated wastewater is a challenge because the effect of wastewater on the soil and plant environment is dependent on the amount of harmful elements present in the wastewater. Reuse of effluent could be beneficial especially in areas where water stress is a major concern primarily due to limited water resources, high water demands and limited economic resources. Wastewater can add nutrients to the soil system stimulating plant growth, increasing plant nitrate (NO_3^-) uptake, and turnover of soil NO_3^- and denitrification. A major objective of land application systems is to allow the physical, chemical, and biological properties of the soil-plant environment to assimilate wastewater constituents without adversely affecting beneficial soil properties (Magesan, 2001). However, when wastewater is irrigated beyond the assimilation capacity of the soil-plant system, it can provide a source of readily leachable nutrient or contaminant (Magesan and Wang, 2003).

Wastewater can also affect soil physical properties, including bulk density, drainable porosity, soil moisture retention and hydraulic conductivity (K_s). Adhikari et al. (2012a) observed lower K_s and fewer macropores in areas where higher amounts of wastewater was applied. The levels of dissolved organic matter and suspended solids in effluent depend on the quality of the raw water and the degree of treatment (Mamedov et al., 2000; Abedi-Koupai et al., 2006). Suspended solids present in effluents can accumulate in soil voids and physically block water-conducting pores leading to a sharp decline in soil hydraulic properties (Rice, 1974; Mamedov et al., 2000). The reduction in K_s could be due to the retention of organic matter during infiltration and the change of pore size distribution as a result of expansion or dispersion of soil particles.

Application of high sodium (Na^+) wastewater increases sodicity, which causes swelling and dispersion of clays (Sparks, 2003), changes pore geometry, and reduces hydraulic conductivity (Halliwell et al., 2001; Adhikari et al., 2012a). In contrast, Agassi et al., (2003) found no adverse impact on the hydraulic parameters while applying standard domestic effluents to the soil in Israel.

Soils in arid regions are generally calcareous and have a high pH in the upper soil horizons favoring the precipitation of most heavy metals there by reducing the risk of groundwater pollution (Fuller, 1990; Rostango et al., 2001). The primary goal of land application of wastewater is to maximize vegetative cover, increase the capacity of soil to serve as a sink for wastewater contaminants, minimize salt accumulation in the root zone, and avoid NO_3^- leaching to the groundwater (Ruiz et al., 2006; Babcock et al., 2009). In this context application of treated wastewater in the arid and semiarid shrub could be more economical and environmentally beneficial.

Soil chemical properties are one of the most researched aspects of wastewater irrigation. Changes due to application of wastewater in the soil chemical properties and surface vegetation cover depend on the quality of the irrigation water and uniformity of the application. However, little work has been conducted on the impact of water quality, application uniformity on native surface vegetation cover in the Chihuahuan desert ecosystem (Picchioni et al., 2012). Therefore, the objectives of the study were to determine the uniformity of sprinkler irrigation, temporal variability of amount and quality of applied treated wastewater, and the effect of treated wastewater on soil chemical properties and surface vegetation coverage.

MATERIALS AND METHODS

Experimental Site

The West Mesa industrial and municipal wastewater land application facility (West Mesa) is located near Las Cruces, NM (32°15'59"N, 106°54'24"W latitude and longitude, 1298 m altitude). This includes a wastewater treatment plant and a land application system. The untreated industrial and municipal wastewater generated from West Mesa industrial park is treated in a 1,500 m^3 d^{-1} capacity treatment plant, which can discharge 200 m^3 d^{-1} of wastewater to the 36-ha study site. The wastewater effluent first enters a 4,500 m^3 synthetically-lined complete mix cell and undergoes microbial decomposition. It is then transferred to 9,000-m^3 synthetically-lined, partial mix cells for further decomposition and then to a non-mixing cell for the settling of solids. The treated wastewater is stored in a 4,600-m^3 synthetically-lined holding pond before being land applied.

Application of wastewater on this site began on February 5, 2002 to the Chihuahuan Desert adjacent to the wastewater treatment plant by 1,243 fixed-head sprinklers operated by automated pumps (Babcock et al., 2009). This area is dominated by the woody perennials creosote (*Larrea tridentata,* (DC) Cov.) and honey mesquite (*Prosopis glandulosa* Torr. var *glandulosa*) whose percent groundcover in 2002 were approximately 8.7 and 14.4%, respectively (Babcock et al., 2009). The visual observation during the spring and early summer months of 2008 revealed that approximately 80% of the irrigated area was covered with vegetation including, desert daisy (*Bebbia juncea* Benth.), snakeweed (*Gutierreiza* Lag.), pigweed (*Amaranthus* L.), spiderling (*Boerhavia* L.), sagebrush (*Artemisia* L.), and chinchweed (*Pectis* L.) (Adhikari et al. 2011a).

Coppice dunes occur under mesquite canopies and occasionally under creosote canopies over most of the experimental site. Before the development of coppice dunes the area was level and surface horizons consisted of coarse textured materials (Gile et al., 1981) that provides better conditions for infiltration and entrapment of sodium and other soluble salts. Soil texture of the coppice dunes and the intercanopy areas varies from sand to light sandy loam with little or no gravel. Soil series identified in and around the West Mesa study site are Onite (coarse-loamy, mixed, superactive, thermic Typic Calciargids), Pintura (Mixed, thermic Typic Torripsamments), Bucklebar (Typic Haplargid), Pajarito (Coarse-loamy, mixed, superactive, thermic Typic Haplocambids), and Bluepoint (Mixed, thermic Typic Torripsamments) (Gile et al., 1981). During September 2008 about 32 non recording type rain gauges were also installed to record the spatial distribution pattern of treated wastewater and natural precipitation.

Sprinkler Uniformity

Sprinkler uniformity tests were conducted during 2007, 2008 and 2009 to determine the effectiveness of sprinklers to discharge the wastewater uniformly in two plots; plot-I (north site) and plot-II (south site) in the land application site. The sprinklers in plot- I were installed on a trapezoidal grid rather than on a square grid. The spacing of sprinklers was 11 m by 12.7 m and 11.5 m by 14.2 m in plot-I and 11.9 m by 12.6 m and 12.0 m by 11.4 m in the plot-II. Uniformity of water application with sprinkler irrigation

system was calculated by Christiansen's coefficient (*Cu*; Christiansen, 1942) using the American Society of Agricultural Engineers standard #3301 (ASAE Standards, 1993). Loose soil samples were also collected immediately after the sprinkler uniformity test from uniformity test area at 1x1 m grids to analyze the soil EC.

$$Cu = 100\left(1.00 - \sum |dv| / nX\right) \quad (1)$$

where C*u*= Christiansen's coefficient, *dv* = deviations of volume of water collected in the catch funnel from the mean catch volume; *n* = number of catch funnels; *X* = mean volume collected in catch funnel

Soil and Surface Vegetation Coverage Sampling and Analysis

Soil chemical properties during 2005 was obtained from Babcock et al. (2009), 2007 from Adhikari et al. (2011b) and 2009 from Adhikari et al (2012b). During 2005, soil samples were collected from unirrigated and one of the irrigated plots, the soil order was Bluepoint loamy sand. In the following year a second irrigated area (plot-II) was included and soil order was classified as Onite-Pajarito association. During 2009, soil samples were collected at 50 m x 50 m grid samples including all the three plots inside the land application area (for details see Adhikari et al. 2012b). Bulk soil samples were collected by using a metal auger (3 cm diameter) from 0-20 cm depths. Visual observations were made to detect the signs of stress and leaf burn caused by wastewater application.

Chemical properties, EC and pH, were determined on 1:2 ratio of soil: water. Other chemical properties including Cl^-, Na^+, and SAR were analyzed in Harris Lab, Columbus, Nebraska. Chemical properties of wastewater from 2002-2009 were provided by the City of Las Cruces, Water Quality Lab. Wastewater analysis was conducted in the Continental Analytical Service Inc., Salina Kansas, following the United States Environmental Protection Agency (USEPA) guidelines. Plant samples of mesquite, creosote and perennial weeds from the land application site were also collected from irrigated and unirrigated areas during 2009. Plant samples were washed, oven dried at 60^0 C, ground and analyzed for Na^+ and NO_3^- at Harris Lab, Columbus, Nebraska.

Nine quadrants (2x2 m) were randomly selected inside the land application site, three of them in the unirrigated area where no wastewater was applied and six in the areas where wastewater was applied. Photographs of each quadrant were taken by ordinary camera (10 mega pixels) from 3 m height in May and September 2012 to monitor the surface vegetation coverage. Each quadrant was divided into smaller quadrants and percentages of vegetation coverage were calculated following the procedure described in U.S. Department of Interior, Bureau of Land Management (1996).

RESULTS AND DISCUSSION

Wastewater Quality and Application

SAR, total salinity, EC, and specific ion concentration are important criteria for irrigation water quality particularly at the West Mesa wastewater treatment facility. It is estimated that evaporation losses can range from 50 to 90% in arid regions resulting in 2 to 20 fold increase in soluble salts (Sparks, 2003). Wastewater analysis showed sodic and saline behavior from 2002 to 2009 with higher amounts of Cl^-, Na^+, EC, and SAR (Table 1). Wastewater generated from meat and dairy processing industry is reported to contain elevated concentrations of Na^+, with SAR ranging between 4 and 50 (Menner et al., 2001). The average SAR, Na^+ and Cl^- concentration of applied wastewater was 31.77 ± 2.07, 888.34 ± 62.17 and 1171±95.97mg L^{-1}respectively from 2002-2008. During 2002 the level of SAR in the wastewater was lower compared to 2003-2008, however, for the same duration NO_3^- and Cl^-concentration fluctuated but pH and EC did not show large differences. Irrigation with water having high SAR may cause an accumulation of exchangeable Na^+ on soil colloids and affect the survival of vegetation in the long run (Jalali and Merrikhpour, 2007). Visual observations during field visits also indicated sign of stress e.g., leaf burn in creosote and wilting in the mesquite possibly due to the application of sodic wastewater. The EC tolerance limit for mesquite is 9.36 dS m^{-1} (Felker et al., 1981) and for creosote is 7.51 dS m^{-1} (Al-Jibury, 1972). The highest measured wastewater EC form 2002 -2009 was 6.67 dS m^{-1}. Thus, with regard to EC of wastewater, there is no immediate danger to the sustainability of native shrubs in the area.

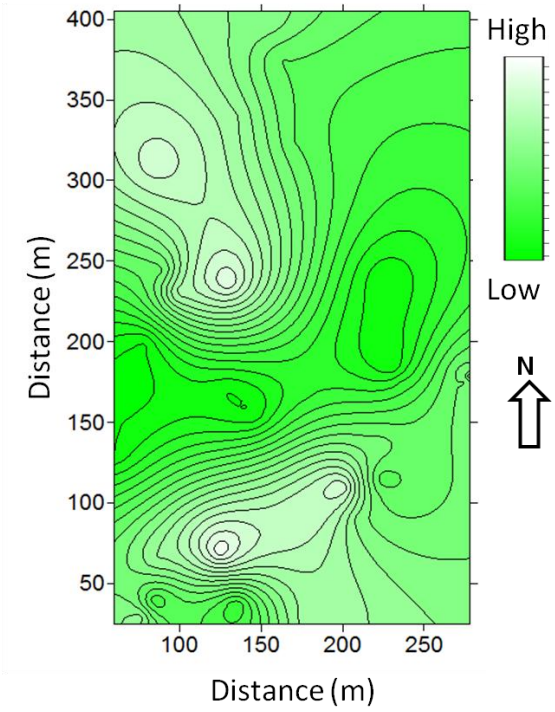

Figure: 1. Spatial distribution of wastewater application in the West Mesa land application site during 2009.

Table:1. Mean and ± standard error of total wastewater application and chemical concentration of wastewater during 2002-2009 in the West Mesa land application site.[1]

Year	pH	Cl^- (mg kg^{-1})	NO_3^- (mg kg^{-1})	Na^+ (mg kg^{-1})	EC (dS m^{-1})	SAR
2002	9.45	1133.80 ± 105.46	3.17 ±1.36	697.27 ± 38.49	4.31 ± 0.31	14.26 ± 0.67
2003	9.67	327.60 ±11.01	33.48 ±8.09	650.6 ± 39.40	3.25 ± 0.17	26.10 ±1.53
2004	9.46	244.60 ± 12.70	34.76 ±10.49	600.20 ± 25.47	2.87 ± 0.11	28.10 ± 1.42
2005	8.98	329.00± 27.29	17.87	903.25 ± 69.68	3.99 ± 0.30	42.47 ± 3.48
2006	8.90	528.00 ± 169.00	1.47 ± 0.47	1175.33 ± 149.69	4.93 ± 1.40	41.47 ± 4.33
2007	9.30	633.25 ± 67.71	1.61 ± 0.97	1094.00 ± 17.87	5.39 ± 0.45	36.89 ± 1.60
2008	9.10	855.00 ± 127.19	0.66 ± 0.22	1097.75±94.63	5.64 ± 0.72	33.14 ± 1.52
2009	9.61 ± 0.21	10121.50 ± 245.70	NA	NA	6.67 ± 1.19	NA
Average	9.30	1771.50 ± 95.75	13.28 ± 3.08	888.34 ± 62.17	4.63 ± 0.51	31.77 ± 2.07

[1] Cl^- is chloride, NO_3^- is nitrate, Na^+ is sodium, EC= electrical conductivity, SAR is sodium adsorption ratio, NA= not available

From 2002 to 2009, the entire land application site received an average of 32.94 cm/year of wastewater. During last two years (2010-2011), the amount of wastewater applied has generally increased (data not shown). From 2010 City of Las Cruces started to receive wastewater from Southern New Mexico Correctional Facility, Las Cruces as well as from some new factories in the West Mesa Industrial Park (Personal communication with City of Las Cruces, 2012). The spatial distribution map (Fig. 1) shows that more wastewater was applied in the southern and northern portion compared to the center of the land application site. The land application site received variable amounts of wastewater during different seasons of the year due to the temporal fluctuations in tenant-generated wastewater and the high evaporation losses from the wastewater holding ponds during peak summer months. During the late summer the application onto land application site increased usually due to the decreased evaporation and increased tenant's wastewater discharge.

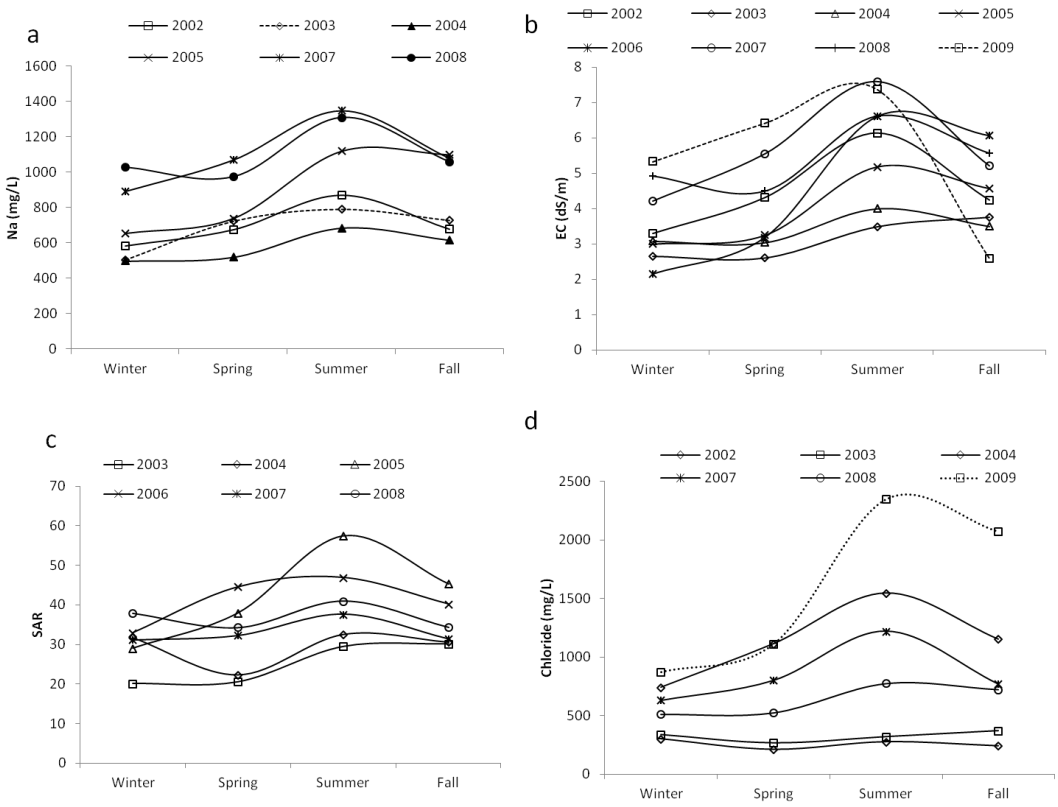

Figure: 2. Amount of chemical constituents (a) sodium (b) electrical conductivity (c) Sodium adsorption ratio (SAR), and (d) chloride observed in the treated wastewater during different seasons of the year 2002-2009 in the West Mesa land application site.

Overall, vegetation in the experimental site was water stressed specially during summer months when ET demands were high primarily because little or no wastewater was applied due to the unavailability of the wastewater. The ratio of total wastewater application and precipitation and average ET of dominant shrubs like mesquite and creosote ranged between 0.20-0.56 during 2002-2009. The non stressed ET was much

higher than the total water application indicating all the vegetation in the land application site were water stressed. However, since 2010 more wastewater was applied indicating that the natural vegetation were not moisture stressed (data not presented).

The concentration of chemical constituents of the wastewater also varied during with seasons of the years (Fig. 2a-d). During 2002- 2009, concentrations of Na^+, EC, SAR and Cl^- during summer were higher than in winter, spring and fall (Fig 2a-d).

Table 2. Total applied wastewater, precipitation average crop evapotranspiration (ET) and ratio of total water applied and ET in the West Mesa land application site during 2002 and 2009

Year	Wastewater	Precipitation	Total water applied	Average Crop ET[†]	Ratio: (Wastewater + Precipitation)/ Average ET
	----------cm----------				
2002[1]	32.50	16.85	49.35	132.47	0.37
2003[1]	20.46	12.44	32.90	142.80	0.23
2004[1]	56.28	25.53	81.81	146.77	0.56
2005[1]	33.73	23.77	57.54	123.16	0.47
2006	17.62	33.93	51.55	175.18	0.29
2007	36.79	20.45	57.24	158.53	0.36
2008	49.65	15.01	64.66	124.97	0.51
2009	16.53	11.50	28.13	134.58	0.20
Average	32.94	19.93	52.89	142.30	0.37

[1]also available in Babcock et al. (2009), [†]ET of mesquite and creosote

Sprinkler Distribution Uniformity

A Christiansen's uniformity coefficient of 90 is considered good (Zoldoske et al., 1994; Rochester, 1995). According to Solomon (1990), high winds break up the water droplets and blow the resulting droplets around areas receiving nonuniform precipitation. The *Cu* in this study was 49.34 ± 2.23 % for plot-I and 61.57± 2.11 % for plot-II in 2007 (Table 3). Average wind speed during the sprinkler uniformity test in plot-I was about 31.56 km h^{-1} and wind direction was variable. Sprinkler uniformity for plot-II was higher (61.57%), the wind speed was lower (5.6 km h^{-1}) and wind direction was less variable than during the uniformity test in plot-I. In addition, spacing of sprinklers in irrigated plot-II was more uniform than in the plot-I. Thus, variable wind speed, wind directions and sprinkler spacing were factors possibly contributing to lower sprinkler uniformity in plot-I than plot-II. Similar values of *Cu* for irrigated plot I were also reported by Babcock et al., (2009) and during 2008 and 2009 (Table 3).

The EC contour maps correlated with sprinkler distribution contour maps at some locations (Fig 3a-d). For example, in plot-I measured precipitation was 1.4 cm (or high) and within the same area EC was also high (0.95dS m^{-1}) (Fig. 3b). Similarly, in plot-II measured precipitation was 2.21 cm and measured EC was 0.90 dS m^{-1} (Fig. 3b).

Table 3: Mean Christiansen's uniformity coefficient (*Cu*) obtained from sprinkler uniformity test in plot-I and plot II during 2007, 2008 and 2009.

Plot-I	*Cu* (%)
Mean 2007 (Trial 1, Trial 2)	49.34 ± 2.23
Mean 2008 (Trial 1, Trial 2)	51.46 ± 3.47
Mean 2009 (Trial 1, Trial 2)	46.13 ± 1.48
Average	48.98 ± 2.39
Plot-II	
Mean 2007 (Trial 1, Trial 2)	61.57 ± 2.11
Mean 2008 (Trial 1, Trial 2)	67.45 ± 4.54
Mean 2009 (Trial 1, Trial 2)	57.43 ± 2.45
Average	62.15 ± 3.03

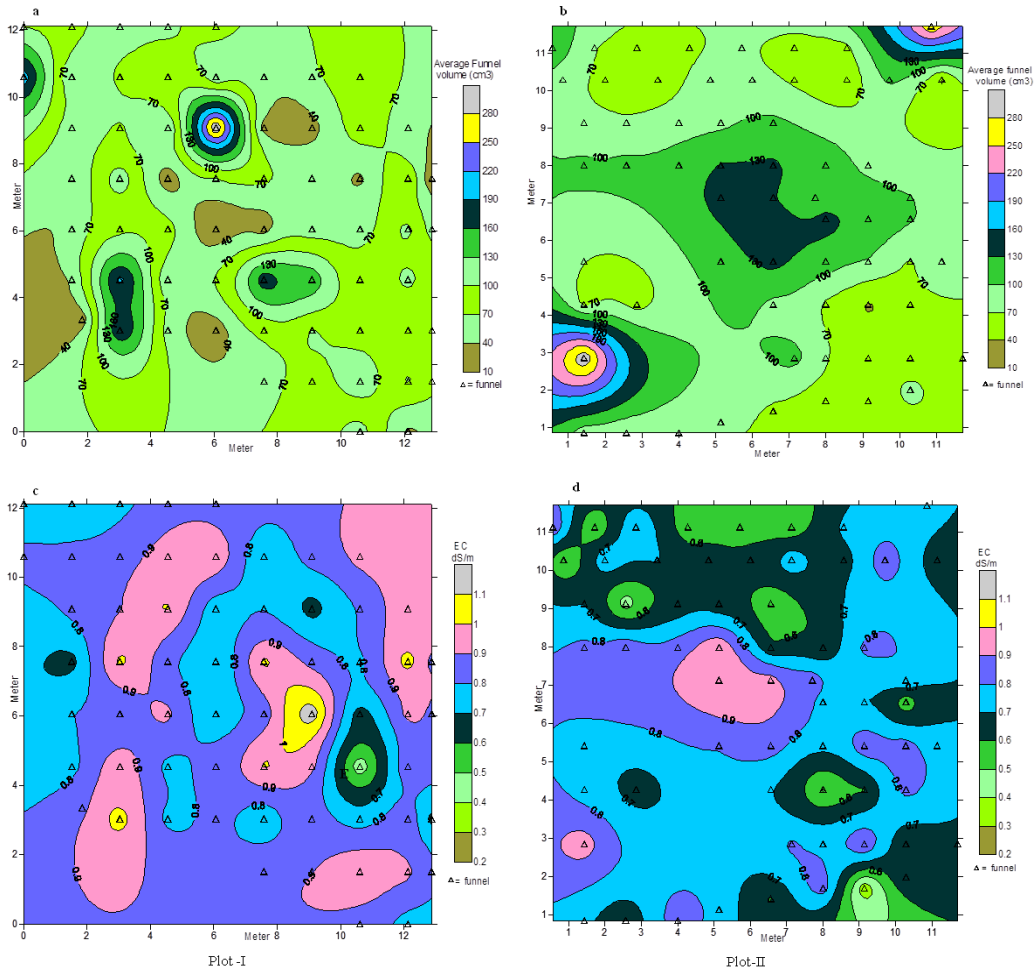

Figure: 3. Contour map showing (a-b) distribution of wastewater and, (c-d) electrical conductivity (EC) in the sprinkler uniformity test areas during 2007.

Soil Chemical Properties

Several soil chemical properties including Na^+, and Cl^- showed an increasing trend by year (Table 4) at 0-20 cm depth. This might be the result of cumulative accumulation of chemical constituents from wastewater as well as reprecipitation of these chemical constituents in the shallower depth due to higher evapotranspiration in the land application site. Costa et al**.** (1991) also reported that increased irrigation with salty water generally tended to increase soil EC because of the evaporation at the soil surface. These values were lower in 2007 than those reported in 2005 (Babcock et al., 2009), which might be due to the time of the sampling, amount of wastewater application and precipitation. Samples were collected during July 2007 and June 2009 after rainfall events and no application of wastewater was made during that period. Whereas in 2005 samples were collected during December and wastewater was continuously applied from September onwards with no precipitation recorded during the past three months.

Table: 4 Mean and ± standard errors of the soil chemical properties during 2006, 2007 and 2009 in the West Mesa land application site.

Year	EC	pH	SAR	Sodium	Nitrate	Chloride
2005	2.45±0.24	9.21 ± 0.16	35.46±3.49	664.70± 61.41	NA	121.00 ± 13.61
2007	1.31 ± 0.11	9.69 ± 0.07	39.67 ± 2.12	835.37 ±92.64	7.84 ±7.84	328.00 ± 18.76
2009	3.89 ± 0.29	9.57 ± 0.12	38.76 ± 3.42	1930.00 ± 510.00	7.96 ± 1.04	625.5 ± 19.00

The soil SAR in the land application site was >35 at 0-20 cm depth which is characterized by reduced nutrient and micronutrient availability (Brady and Weil, 2000). In some hot spots in the northern and southern portion of the field SAR and Cl^- have increased to as much as 50.45 and 1270.5 mg kg^{-1} respectively. Mesquites are deep-rooted plants which can survive with less moisture (Ansley et al., 1997). The rooting depth is about 12 m for mesquite and 3 m for creosote. However, the majority of mesquite roots are distributed within 0-100 cm depth (Heitschmidt et al., 1988) and creosote within 0-25 cm depth (Baynham, 2004). Therefore high SAR and Na^+ concentration might affect the long term survival of mesquite and creosote bushes along with other perennial vegetation.

Blocked kriged map of Cl^- and SAR showed a positional similarities with higher Cl^- and SAR content in the northern and southern portion of the field and lower in the central portion of the field (Fig. 4a-b). This correlates with the wastewater application kriged map, which also showed higher wastewater application in the southern and northern than in the central portion of the study site (Fig.1).

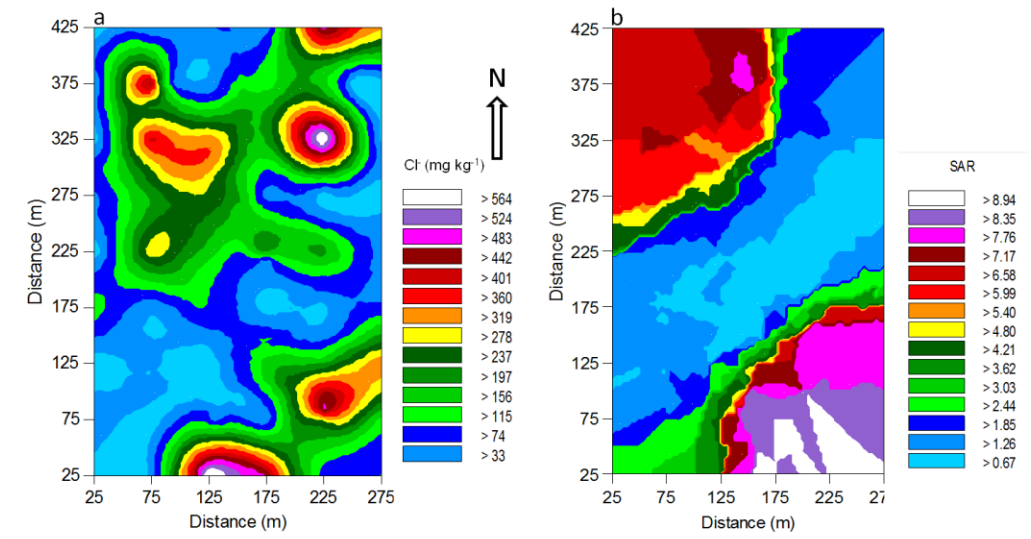

Figure: 4. Spatial distribution of (a) chloride and (b) sodium adsorption ratio in the West Mesa land application site during 2009.

Vegetation Analysis

The vegetation cover in each quadrant in the irrigated portion of the field showed a higher percentage of vegetation cover than in the unirrigated quadrants (Fig.5; Table 5). The vegetation cover in the irrigated areas was >90 % during May and >98 % during September 2012.which was much higher than those reported (7-70%) during 2002 by Babcoock et. al (2009). This could be due to the lower concentration of chemical constituents present in the wastewater during 2010-2011(data not shown).

In contrast mean surface vegetation coverage in the unirrigated plot during May and September 2012 was 6 % and 23.66 %, respectively. The higher vegetation coverage in the unirrigated plot in September might be due to the precipitation during the late summer. Vigorous growth in plant height and canopy of annual vegetation were observed in the irrigated plots during September than in May 2012. Vegetation heights during May ranged between 5-30 cm, while during September 2012, these ranged between 25 cm to 100 cm. However in the unirrigated area no such vigorous growth in plant height and canopy were observed. Only some of the annual premature weeds were seen with the plant height ranging between 2 cm to 20 cm.

The vegetation analysis of plant samples showed higher amount of Na^+ in the vegetation of irrigated areas than in the unirrigated areas. The Na^+ content of creosote was eleven times higher in irrigated areas (880 mg kg^{-1}) than in the unirrigated areas (80 mg kg^{-1}), Na^+ content of mesquite was two times higher in irrigated (1600 mg kg^{-1}) than unirrigated (800 mg kg^{-1}) and Na^+ content of perennial vegetation was three times higher in irrigated (240 mg kg^{-1}) than unirrigated (80 mg kg^{-1}) areas. The NO_3^- percentage in the irrigated perennial vegetation was three times higher (4.952) than in the unirrigated weeds. Thus, native vegetation was removing chemicals from the soil added through wastewater application.

Application of high SAR wastewater increased the SAR level in the soil and decreased infiltration rate of soil (Adhikari et al. 2012a). However, it also provided the moisture for growth and development of the annual herbs. Long term application of wastewater could further increase the SAR concentration and accumulate chemical constituents in the upper horizons due to high evapotranspiration mostly in the southern and northern portion of the land application site. The depth of treated wastewater applied per irrigation cycle during 2002-2009 ranged from 1 to 8 cm with an average application per irrigation cycle of 1.03 cm. Application of 1 cm of water penetrates up to the depth of 5 cm, whereas application of 8 cm of water penetrated up to the depth of 40 cm. Therefore, wetting front depths ranged from 5 to 40 cm. The groundwater table depth in the study area ranges from 90 to 100 m (Gile et al. 1981). Thus there is no immediate threat of groundwater contamination. However, as amount of applied wastewater during each irrigation cycle is increasing (almost three times), long term application will move the wetting fronts and chemicals in the wastewater to the deeper depths and may cause groundwater contamination. Therefore, management strategy should be initiated that lowers wastewater in the southern and northern portion and higher in the central portion of the land application site. In addition measure should be taken to reduce the higher rate of evaporation from the holding ponds especially during the summer.

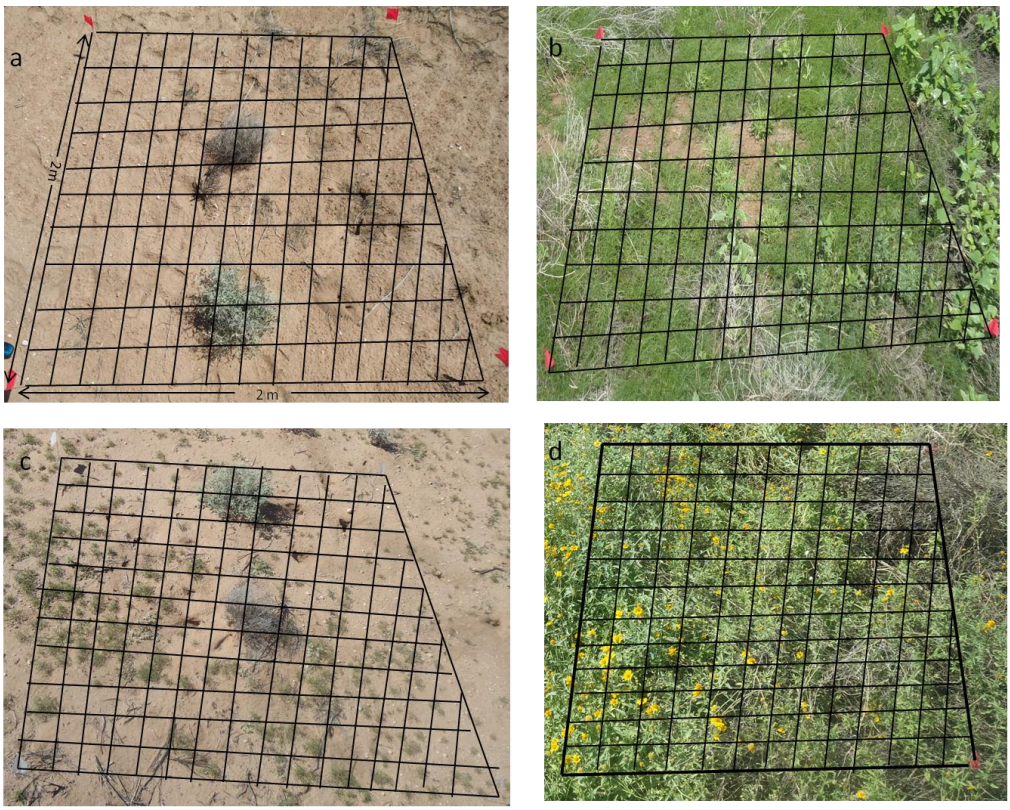

Figure: 5. Sample 2 x 2 m quadrant photographs taken by 10 mega pixels camera during May (a and b) and September (c and d) 2012 divided into smaller quadrants to calculate the surface vegetation coverage percentage (a and c) unirrigated (b and d) irrigated with wastewater in the West Mesa land application site.

Table: 5. Surface vegetation coverage in the unirrigated and treated wastewater irrigated areas during May 2012 in the West Mesa land application site.

Locations		Vegetation coverage (%)	
	Quadrant	May-2012	September-2012
Unirrigated	1	10	35
	2	3	17
	3	5	19
Average		6	23.66
Irrigated	4	100	100
	5	96	100
	6	95	99
	7	99	100
	8	95	100
	9	65	92
Average		91.67	98.50

CONCLUSIONS

Concentrations during 2002-2009 were higher in the treated wastewater during the summer months than in any other seasons of the year due to higher evaporation in the holding pond. Spatial distribution pattern showed that the variability of wastewater application resulted in the formation of hot and cold spots in the area with lower soil SAR and Cl^- patches in the center and higher in the southern and northern portion of the land application site. Application of wastewater containing high EC, SAR, and Na^+ concentration also increased the SAR of the irrigated West Mesa soil. Vegetation analysis showed 65-100 % land coverage in the irrigated areas as compared to 3-24 % in the unirrigated areas. Although application of treated wastewater is increasing the vegetation coverage still, better management practices are required. Some of them could be improving the uniformity of wastewater application, reducing the evaporation in the holding pond, and periodically monitoring of wastewater chemical properties as well as soil chemical properties in the West Mesa land application site.

ACKNOWLEDGEMENT

Authors thank New Mexico State University Agricultural Experiment Station, Water Resources Research Institute, and City of Las Cruces for help and support to this study.

REFERENCES

Adhikari, P., M. K. Shukla, and J. G. Mexal. 2011a. Spatial variability of electrical conductivity of desert soil irrigated with treated wastewater: Implications for

irrigation management. *Appl. Environ. Soil Sci.* doi: 10.1155/2011/504249.
Adhikari, P., M. K. Shukla, and J. G. Mexal, and P. Sharma. 2011b. Assessment of the soil physical and chemical properties of desert soils irrigated with treated wastewater using principal component analysis. *Soil Sci.* 176(7): 356-366.
Adhikari, P., M. K. Shukla, and J. G. Mexal. 2012a. Spatial variability of infiltration rate and soil chemical properties of desert soils: implications for management of irrigation using treated wastewater. *Transaction to ASABE* (in press).
Adhikari, P., M. K. Shukla, and J. G. Mexal. 2012b. Spatial variability of soil properties in an arid ecosystem irrigated with treated municipal and industrial wastewater. *Soil Science* 177(7):458-469, doi: 10.1097/SS.0b013e318257c331.
Abedi-Koupai., J., B. Mostafazadeh, and M.R. Bagheri. 2006. Effect of treated wastewater on soil chemical and physical properties in an arid regions. Plant Soil Environ. 52:335-344.
Agassi, M., J. Tarchitzky, R. Keren, Y. Chen, D. Goldstein, and E. Fizik. 2003. Effects of prolonged irrigation with treated municipal effluent on runoff rate. J. Environ. Qual. 32:1053-1057.
Al-Jibury, L.K. 1972. Salt tolerance of some desert shrubs in relation to their distribution in the southern desert of North America. Ph. D. diss. Arizona State Univ., Tempe.
Ansley, R.J., J.A. Huddle, and B.A. Kramp. 1997. Mesquite ecology. Texas Agricultural Experiment Station, Vernon TX 76384.
ASAE Standards, 40th ed. 1993. ASAE 330.1. Procedure for sprinkler distribution testing for research purposes. Am. Soc. of Agri. Eng. St. Joseph, Mich.
Babcook, M., M. K Shukla, G. A. Picchioni, J.G. Mexal, and D. Daniel. 2009. Chemical and physical properties of Chihuahuan desert soils irrigated with industrial effluent. Arid Land Res. Manag. 23:47-66.
Baynham, P. 2004. Sonoran originals:the unappreciated smell of rain. Master Gardener J. November/December: 22-24.
Brady, N.C., and R.R. Weil. 2002. The nature and properties of soils. Prentice Hall Upper Saddle River, NJ.
Christiansen, J.E. 1942. Irrigation by sprinkling. California Agricultural Experiment Station Bulletin 670, University of California, Berkeley, CA.
Costa, J.L., L. Prunty, B.R. Montgomery., J. L. Richardson, and R.S. Alessi. 1991. Water quality effects on soils and alfalfa: II. Soil Physical and Chemical Properties. Soil Sci. Soc. Am. J. 55:203-209.
Fuller, W. H. 1990. Organic matter applications p. 507-541.*in* C. M. Rostang ed. Biosolids Application in the Chihuahuan Desert: Effects on Runoff Water Quality. Texas Tech. Univ., Lubbock.
Felker, P., P.R. Clark, A.E. Laag, and P.F. Pratt. 1981. Salinity tolerance of the tree legumes: Mesquite (*Prosopis glandulosa* var. *Torreyana*, *P. velutina*, and *P. articulata*), algarrobo (*P. chilensis*), kiawe (*P. pallida*), and tamarugo (*P. tamarugo*) grown in sand culture on nitrogen-free media. Plant and Soil 61:311-317.
Gile, L.H., J.W. Hawley., and R.B. Grossman.1981. Soils and geomorphology in the basin and range area of southern New Mexico-Guide book to the Desert Project. New Mexico Bureau of Mines and Mineral Resources, Memoir 39.

Halliwell, D.J., M.K. Barlow., and M.D. Nash. 2001. A review of the effect of wastewater sodium on soil physical properties and their implications for irrigation systems. Aust. J Soil Res. 39:1259-1267.

Heitschmidt, R.K., R.J. Ansley, S.L. Dowhower, P.W. Jacoby, and D.L. Price.1988. Some observations from the excavation of honey mesquite root systems. J. Range Manag. 41:227-231.

Jalali, M., and H. Merrikhpour. 2008. Effects of poor quality irrigation waters on the nutrient leaching and groundwater quality from sandy soil. Environ. Geology 53:1289-1298.

Magesan, G.N. 2001. Changes in soil physical properties after irrigation of two forested soils with municipal wastewater. N.Z. J. For. Sci. 31:188-195.

Magesan, G.N., and H. Wang. 2003. Application of municipal and industrial residuals in New Zealand forests. Aust. J. Soil Res. 41:557-569.

Mamedov, A.I., I. Shainberg, and G.J. Levy. 2000. Irrigation with effluent water: effects of rainfall energy on soil infiltration. Soil Sci. Soc. Am. J. 64:732-737.

Menner, J. C., C. D.A. McLay, R. Lee. 2001. Effects of sodium contaminated wastewater on soil permeability of two New Zealand soils. Aust. J. Soil Res. 39:877-891.

Picchioni, G. A., M. K. Shukla, J. Mexal, M. Babcock, A. Ruiz, T. Sammis and D. Rodriguiz. 2012. Land application of treated industrial wastewater on a Chihuahuan desert : implications for water quality and mineral deposition. Arid Land Res. Manag. 26: 211-221.

Rochester, E.W. 1995. Landscape Irrigation Design. Am. Soc. Agri. Eng. St. Joseph, Mich. p. 217.

Rostango, C. M., and R. E. Sosebee. 2001. Biosolids application in the Chihuahuan desert: Effects on runoff water quality. J. Environ. Qual. 30: 160-170.

Ruiz, A., T.W. Sammis., G. A. Picchioni., J. G. Mexal., and A. A. Mackay. 2006. An irrigation scheduling protocol for treated industrial effluent in the Chihuahuan desert. Am. Water Works Ass. J. 98: 122-133.

Rice, R. C. 1974. Soil clogging during infiltration of secondary effluent. J. *Water Pollut.. Conro Fed.* 46: 708-716.

Solomon, K. H. 1990. Irrigation notes: Sprinkler Irrigation Uniformity. World wide web address: http://cati.csufresno.edu/cit/rese/90/900803/index.html (accessed July 23, 2009).

Sparks, D.L. 2003. Environmental soil chemistry. 2nd ed. Academic Press, San Diego, CA. p. 287.

U.S. Department of Interior, Bureau of Land Management. 1996. Sampling Vegetation Attributes. Interagency Technical Reference, BLM/RS/ST-96/002+1730.

Zoldoske, D.F., K.H. Solomon, and E.M. Norum.1994. Uniformity measurements for turfgrass: what's best ? World wide web address: http://www.wateright.org. 941102asp (accessed July 24, 2009).

CORRESPONDENCE SHOULD BE ADDRESSED TO:
Name of Corresponding Author: Pradip Adhikari
Department/Institution: Plant and Environmental Sciences, New Mexico State University
E-mail address: adhikari@nmsu.edu

EVALUATION OF LITTER HYDROLOGY IN PONDEROSA PINE AND MIXED CONIFER STANDS IN NORTHERN NEW MEXICO, USA

Alexander Fernald[1]

Joaquin Gallegos[2]

Dawn VanLeeuwen[3]

Terrell Baker[4]

ABSTRACT

Montane forests within New Mexico have increased levels of forest floor litter accumulation primarily due to fire suppression since the early 1900's and associated tree density increases. Improved understanding of forest litter hydrologic dynamics is necessary to provide land managers practical information to aid in management of forest resources. This study's goals were to determine the impacts of different amounts of forest floor litter on soil moisture, litter moisture retention, infiltration, sediment yield, and runoff from ponderosa pine and mixed conifer forest stands on gentle and steep slopes. Representative values for these parameters were determined with one-hour rainfall simulations. Results showed litter moisture retention capacity had a positive relationship with litter density. Mixed conifer litter with a density of 0.28 g cm^{-3} retained more moisture than ponderosa pine with a density of 0.21 g cm^{-3}. Deeper litter had less volumetric litter moisture content than the shallower litter depths. Litter depth was not significantly associated with sediment yield. However, steep slopes resulted in more sediment yield than gentle slopes. Data suggest that on sites previously in ponderosa forest, conversion from mixed conifer back to ponderosa forest may reduce litter moisture retention, promote increased infiltration and increased vegetative understory diversity all without increased sediment delivery. Restoration of forest stands should include analysis of litter effects on moisture retention to best manage hydrology and herbaceous vegetation.

Key Words: Forest floor litter, litter interception, ponderosa pine, mixed conifer, forest hydrology

[1]Department of Animal and Range Sciences, New Mexico State University
[2]Previously Department of Animal and Range Sciences, New Mexico State University
[3]Department of Economics, Applied Statistics, and International Business, New Mexico State University
[4]Department of Forestry, University of Kentucky

INTRODUCTION

In the southwestern United States, forested watersheds supply municipalities and rural areas with water for domestic and agricultural use (USGS, 2006). Higher elevation forested watersheds are important water sources in New Mexico where in 2000 approximately 21% of land was forested. Of this forested land, 62% (4.21 million ha or 10.4 million acres) was managed by government agencies (O'Brian, 2003). It has been demonstrated that watershed improvements can be managed to increase water yield (Stednick, 2000; MacDonald and Stednick, 2003).

Litter is defined as the dead plant material on the forest floor consisting of organic material (O horizon) of varied levels of decomposition above the mineral soil (Helvey and Patric, 1965; Sato *et al.*, 2004). Forest floor litter amounts are positively related to basal area (McClurkin *et al.*, 1987). A consequence of increased forest density is the increase in forest floor litter that often accumulates and impedes understory vegetative growth (McClurkin *et al.*, 1987; Putuhena and Cordery, 1996; Moore *et al.*, 2004). A 1-year study in a southern Loblolly pine forest thinned to a 16 m^2 basal area produced 4500 kg ha^{-1} of litter, while an un-thinned site produced 7800 kg ha^{-1} of litter (McClurkin *et al.*, 1987). An Arizona ponderosa pine forest with an annual precipitation of 47 to 57 cm produced an annual litter accumulation of 2795 kg ha^{-1} in mature stands with a basal area of 65 m^2 ha^{-1} and 460 kg ha^{-1} in clear cut strips (Klemmedson *et al.*, 1990).

The majority of litter accumulation during the year occurs in late fall (McClurkin *et al.*, 1987), for most northern hemisphere gymnosperms stands (Millar, 1974). Excessive accumulation of litter can inhibit nutrient cycling, nutrient availability, and microbial activity (Moore *et al.*, 2004). Depending on litter composition and the geographic location, the litter layer can be separated into multiple layers (Sato *et al.*, 2004): 1) an upper layer of mostly un-decomposed material from present year accumulation; and 2) a lower layer of decomposed and highly decomposed material from previous years' accumulations (Sato *et al.*, 2004). In pine forests where litter creates a mat of organic matter, there is a decrease in understory growth and production (Putuhena and Cordery, 1996; Mason et al. 2008). Recognized methods for removal of forest floor litter are natural decomposition and combustion through fire (Moore *et al.*, 2004). Fire suppression and increased forest density can enhance the tendency towards greater litter build-up.

The process of decomposition of forest floor litter provides the soil with nutrients vital to plant growth (Klemmedson *et al.*, 1985), through nutrient flux and the conversion of trapped nutrients and minerals in the litter into available nutrients and minerals in the soil (White, 1986a). Decomposition rates and nutrient flux vary according to litter in different species stands and geographical regions (White, 1986b). Decomposition rates are not the focus of this study, but they are important in general as related to accumulation of forest litter as it may affect hydrology. Decomposition rates in a mixed conifer forest were found to be significantly higher than drier ponderosa pine, with a loss of half the total mass of forest floor litter within the first three months of decomposition (Hart *et al.*, 1992).

Vitousek (1982) notes older, more established forests may result in poorer quality nutrient cycling as a result of lower decomposition rates. Decomposition and turnover rates of forest floor litter can be influenced by forest management (Klemmedson *et al.*,

1985). Fire is one method to increase nitrogen mineralization in ponderosa pine forests, an important aspect of nutrient flux in forest ecology (White, 1986b). However, over a century of fire suppression combined with and resulting in increased forest density has removed the most important mechanism for reducing litter buildup and nutrient mobilization from the forest floor. Recognizing the importance of fire within the ecosystem of a ponderosa pine forest, since the late 1960's prescribed fires have been performed to try and return forests to historical conditions (Kilgore, 1973; Agee, 1974), where fire had been previously and suppressed (Allen, 1994).

Studies performed on forest floor litter within the past fifty years, mainly focus on nutrient flux and decomposition, while litter hydrologic dynamics are often overlooked (Sato *et al.*, 2004). However, litter is an important ground cover to absorb rainfall energy to prevent soil erosion (Geddes and Dunkerley, 1999; Bussiere and Cellier, 1994). Schaap *et al.* (1997) stated that the hydrological importance of the forest floor is due to the transfer of water and energy between the sub-canopy atmosphere and the mineral soil. International research of litter hydrology focused on laboratory experiments and mathematical modeling including: analysis of moisture dynamics of litter layers on *Cryptomeria japonica* and *Lithocarpus edulis* in forests of Fukuoka, Japan (Sato *et al.*, 2004); forest floor evaporation models in a stand of Douglas Fir trees in the Netherlands (Schaap *et al.*, 1997); the development of methods and research equipment in Australia in *Eucalyptus rossii, Eucalyptus mannifera* and *Pinus radiata* stands (Putuhena and Cordery, 1996); and analysis of biomass storage and drainage rates in *Pteridium aquilinum* litter using a rainfall simulator in the United Kingdom (Pitman, 1989). Few studies have been performed *in situ*, which provide information most relatable to forest situations (Sato *et al.*, 2004; Putuhena and Cordery, 1996; Schaap *et al.*, 1997; Tobon-Marin *et al.*, 2000). Within the United States, litter hydrology research has focused on eastern hardwoods in the Appalachian Mountains and eastern U.S., while much less research has been conducted on the subject west of the 100th meridian (Blow, 1955; Helvey, 1964; Helvey and Patric, 1965). In a Douglas fir stand in the Netherlands it was reported that 25% of the evaporation from the forest floor was recharged through capillary action from the soil to the forest floor litter and that only 2.2 % of total root water uptake came from the forest floor (Schaap *et al.* 1997).

Litter interception is an important component of the hydrologic dynamics within forest floor litter. Litter interception capacity is the total amount of moisture a given amount of litter can retain. Litter interception loss is the precipitation trapped in the litter layer that does not reach the mineral soil and is evaporated into the atmosphere without adding to the moisture content of the mineral soil (Helvey and Patric, 1965). Historical literature considered 3% of the gross rainfall to be intercepted by litter (Helvey and Patric, 1965; Miller, 1977). Major research on litter interception within the United States has primarily been limited to eastern hardwoods and has demonstrated how geographical variability influences litter interception (Blow, 1955; Helvey, 1964; Helvey and Patric, 1965). Putuhena and Cordery (1996) showed that in isolated rain events, the piling of broad leaves like plates spread moisture horizontally across a larger area than found with needle litter. Needle litter allowed the moisture to drain in a more vertical pattern resulting in less potential for interception (Putuhena and Cordery 1996). Leaf litter water being evaporated in a Douglas Fir stand in the Netherlands acted as a sponge pulling

moisture up in capillary action from the mineral soil and releasing it into the atmosphere (Schaap *et al.*, 1997).

Sediment retention, hydrophobic layers, infiltration, water retention, and evaporation are all key elements to the hydrologic dynamics of litter (Schaap *et al.*, 1997; Blow, 1955; Putuhena and Cordery, 1996). Previous research found higher amounts of litter, meaning higher amounts of organic matter, resulted in increased rates of infiltration (Blow, 1955; Janeau *et al.*, 1999). The presence of fungal hyphae within the litter acts as a glue and binds litter together (Tam *et al.*, 1991), and can also act as a hydrophobic layer, resulting in increased runoff, decreased infiltration, and increased potential interception capacity. Consequently, increased litter depths provide more surface area for fungal hyphae, therefore a thicker possible hydrophobic layer. Litter accumulations because of increased forest densities and lowered decomposition of forest floor litter are part of forest floor hydrologic dynamics on a scale that previously did not exist.

Little research has been performed on the subject of forest floor litter hydrology. Better understanding of forest floor litter hydrology can impact management of forested watersheds that supply water for municipalities and agricultural lands. Objectives of this study were to determine impacts of mixed conifer and ponderosa forest litter on litter moisture retention, infiltration, sediment yield, and runoff from both gentle and steep slopes. We hypothesized that: 1) litter depth is positively associated with overstory closure; 2) litter depth is negatively associated with runoff, sediment yield and concentration, and infiltration; 3) mixed conifer stands will have greater litter mass and density, greater litter moisture retention, and less runoff than Ponderosa pine stands; and 4) steeper slopes will produce greater runoff, sediment yield and sediment concentration than gentle slopes.

METHODS AND MATERIALS

Study Site

The study was conducted from May 2004 to March 2006 on a 243-hectare area within the Walker Flats Grazing Allotment in the Pecos/Las Vegas Ranger District of the Santa Fe National Forest near Mora, NM (Latitude 32º 00.57'N, Longitude 105º 27.40' W). Field work was performed from May 2005 to August 2005. Average annual precipitation of the surrounding area ranges from 40-66 cm, the average annual air temperature ranges between 3.3-7.7°C. The average annual number of frost-free days range from 85-110 days. Elevation ranges from 2697-2879 m. Soils on the study site were predominately a silty loam and sandy loam.

The overstory vegetation stands are classified as two different types of stands. The first is a ponderosa pine (*Pinus ponderosa*) stand, where the composition of the stand is more than 60% ponderosa pine. The second stand is a mixed conifer stand, where ponderosa pine is less than 60% in composition, the other dominant tree species in these stands are White fir (*Abies concolor*), Douglas fir, and Aspen (*Populus tremuloides*). Historically this location would have been an almost purely ponderosa pine stand, and through fire suppression couple with ponderosa log removal, the fir species have invaded the stands.

As a result of high tree basal areas, dense seedling production, and high canopy cover, total live understory biomass was less than 40 kg ha^{-1}, and areal cover was less than 3%. Previous work by Madrid (unpublished) surveyed the 246-ha area using

Bitterlich plots (Grosenbaugh, 1952). Using the data from the Bitterlich plots, four 1.2 ha sites were identified to represent the dominant species stands and slope. The entire 243-hectare site was characterized by two dominant types of slopes, a steep slope that averaged 20% over the 100-m transect, and a gentle slope that averaged 5% over the 100-m transect. Four sites were identified for the current research; two on gentle slopes (average 7.1% slope) – one mixed conifer and one Ponderosa pine site and two on steep slopes (average 11.7% slope) – also containing one mixed conifer site and one Ponderosa pine site. Final sites were PP gentle, PP steep, MC gentle, and MC steep, with summary statistics given in Table 1.

Plot Selection and Plot Characteristic Measurements

Four sites were identified for the current research; two on gentle slopes (average 7.1% slope) – one mixed conifer and one Ponderosa pine site and two on steep slopes (average 11.7% slope) – also containing one mixed conifer site and one Ponderosa pine site. Final sites were PP gentle, PP steep, MC gentle, and MC steep.

Litter depths were measured across all four sites using a total of 13 equally spaced transects with litter measured every five meters. The litter was measured by pushing a metal ruler into the forest floor litter until the ruler penetrated the mineral soil. The ruler was then pulled away in a horizontal manner leaving a profile of the litter. The ruler was used to measure from the surface of exposed litter to the base, where highly decomposed litter met the mineral soil to the nearest millimeter (mm). Litter depth data were compiled and analyzed statistically using histograms and proc univariate with SAS version 9.1.3 software (SAS Institute Inc., 2006) to determine representative categories of litter depths within the study stands. Three litter depths (LDs) were created for analysis, shallow, moderate, and deep litter: LD1 with litter 0.0 to 3.5 cm deep, LD2 with litter 3.6 to 7.0 cm deep, and LD3 with litter greater than 7.0-cm deep.

At each site, four plots within each of the three litter depths were randomly selected for a total of 48 plot locations. Each plot location was verified that the litter depth at this location fell within the limits of the litter depth before the plot rings were installed.

At each plot location two plot rings were installed. The forest floor within the first plot ring was left undisturbed (littered plot ring); in the second plot ring the forest floor was removed to mineral soil (de-littered plot ring). The de-littered plot ring was installed, then a garden rake was used to collect and remove all the litter down to the mineral soil, removing all litter from the plot ring. Simulations were performed on both plot rings, including dry and wet runs. The littered and de-littered plots were placed no more than 5 m apart so that both locations had the same original litter depth.

Slope and soil collection methods were performed as described by Madrid *et al*. (2006). A soil core 0-5 cm in depth was taken according to the method of Blake and Hartage (1986). Gravimetric antecedent moisture content and bulk density were performed according the methods of Madrid *et al*. (2006). Organic matter content of the soil was analyzed according to the Walkley-Black procedure (Nelson and Sommers, 1982). A Beckman-Coulter laser diffraction particle size analyzer was used to determine particle size distribution for soil texture (Madrid *et al*. 2006). Samples were treated for removal of organic matter following the oxidation method of Anderson (1961), and analyzed with the particle size analyzer.

Using a ten factor prism, basal area was measured according to the point-sampling method of Avery and Burkhart (1994) for each plot ring location. Crown closure was also measured at each plot ring site using a spherical densitometer, facing north, south, east, and west over the ring then taking the average of the measurements (Lemmon, 1956).

Utilizing litter moisture content and litter volume data, litter volumetric water content (VWC_L = Volume of H_2O * Volume of Litter $^{-1}$) was calculated. Litter Volumetric Data differs from litter interception capacity that litter interception capacity is the maximum amount of moisture that given amount of litter can intercept.

Runoff, Infiltration, and Sediment Measurement

A portable tripod rainfall simulator design with a G10 full jet nozzle (Spray Systems Co., Illinois) was used to apply the controlled simulated precipitation (Madrid *et al*., 2006). The study used this type of simulator because of its portability and versatility (Wilcox *et al.*, 1986). The precipitation was applied by positioning the nozzle vertically downward at a height of 175 cm from the center of the simulation plot ring to simulate natural rainfall energy.

Rainfall simulations were conducted on 1 m^2 circular runoff plots. Plot rings were installed with a sledgehammer, with a collection tray placed at the lowest point on the downward slope, to ensure collection of all runoff. The area 1 cm-2.5 cm in front of the tray area that was usually disturbed during installation was tamped down to secure disturbed soil and a thin layer of litter was replaced over this area. The tray area drained into a 4.44 cm inside-diameter by 1.5 m long runoff hose clamped to the runoff tray. A runoff collection tank was placed at the end of the hose. Plastic covering was placed around the collection tank area to avoid contamination from soil and simulator overspray. The runoff was measured at two-minute intervals. The collection tank was always installed below the level of the collection tray spout to ensure accurate and complete collection of runoff.

Two one hour simulations were performed per plot ring, the first under antecedent moisture conditions (hereafter referred to as "dry run") and then the second simulation performed 14 to 18 hours later under field capacity (hereafter referred to as "wet run"). An average application rate of 18.7 cm hr^{-1} was used, with a standard deviation of 1.16 cm hr^{-1}. Plots were covered between dry and wet runs with plastic to ensure no additional moisture was added. With three litter depths, four replications, four research sites, plot ring pairs for litter treatments , and dry/wet runs, a total of 192 one-hour rainfall simulations were performed on a combination of sites and treatments. Simulated rainfall application was measured according to the methods of Madrid *et al*. (2006). Water was applied using a 5.5 horsepower Honda® engine with a Hypro® roller pump to the rainfall simulator.

Time to start of runoff was defined as the time from the beginning of the simulation to the first presence of runoff in the runoff collection tank. Time to end of runoff was defined as the time from the termination of the simulation to the time when the flow of runoff into the collection tank was slowed to five seconds between drops from the runoff hose into the collection tank. Infiltration was calculated as the difference between the application of simulated rainfall and the amount of runoff in a given two-minute interval. During one-hour rainfall simulation, a complete collection was made of

the runoff. A 1-L fully agitated sub-sample was taken to calculate sediment yield. The sub-sample was then vacuum filtered, oven dried at 105°C for 48 hours, and weighed.

Statistical Analysis

For the simulation variables, data were analyzed using a mixed model that incorporated fixed effects for species (PP, MC), slope (gentle, steep), litter depths (0.0-3.5 cm, 3.5-7.0 cm, >7.0 cm), cleared status (littered, de-littered) and all interactions among these factors. A random effect for plot location (i.e., replication within species, slope and litter depth combinations) accounted for possible correlations between cleared status pairs. Data were analyzed using SAS version 9.1.3 PROC MIXED software (SAS Institute Inc., 2006).

All data sets were checked for normality using proc univariate and histograms. There were some outliers, so the outlier strategy described by Ramsey and Schafer (2002) was applied. Because no conclusions were changed when outliers were removed, only the analysis including all data is included.
Two-tailed p-values are reported and significance was defined for two-tailed $p \leq 0.05$. In reporting results, for a given variable, the highest level interaction with $p \leq 0.05$ will supersede main effects and lower level interactions with $p \leq 0.05$.

RESULTS

Overstory and Litter

There was greater litter depth with higher basal area and crown closure. Basal area (31.1 ± 2.02 (mean ± SE) m^2 ha^{-1}) was significantly less (P = 0.0057), in stands with shallow litter depths (LD1 – 0-3.5cm) as compared to basal areas (40.1 ± 2.26 m^2 ha^{-1}) in stands with moderate litter depths (LD2 – 3.6-7.0cm) and basal areas (40.1 ± 2.13 m^2 ha^{-1}) in stands with deeper litter depths (LD3 – >7.0cm) (Table 2). A similar pattern emerged with litter depth and crown closure where crown closure in LD1 stands (83 ± 2.06 %) was less than crown closure in LD2 (90 ± 0.73 %) and LD3 (92 ± 0.94 %) stands (Fig. 1).

The variables of litter mass, litter density, organic matter and bulk density all differed according to tree species stand composition, litter depth (Table 2). Litter mass was significantly less on LD1 sties as compared to LD2 and LD3 sites but litter density was significantly greater on LD1 sites as compared to LD2 and LD3 sites. However, there was no evidence of a difference for organic matter or bulk density with in respect to litter depth (Table 2). There appeared to be greater antecedent soil moisture associated with greater litter depth, but these differences were not significant.

Runoff, Infiltration, and Sediment

More runoff was associated with less litter. For terminal runoff rate during dry runs, mixed conifer stands (5.18 ± 1.11 cm hr^{-1}) produced a higher runoff rate than ponderosa pine (3.6 ± 0.64 cm hr^{-1}) (P=0.0098). Terminal runoff rate during wet runs showed higher runoff with lower litter depths with LD1 (5.85 ± 0.26 cm hr^{-1}) greater than LD2 (3.78 ± 0.11cm hr^{-1}) and LD3 (3.49 ± 0.21 cm hr^{-1}) (P = 0.0013).

During the wet runs, terminal runoff was less in ponderosa pine (3.34 ± 0.65 cm hr^{-1}) than mixed conifer (5.40 ± 0.87 cm hr^{-1}) (P = 0.0004), less in littered plot rings (1.57

± 1.09 cm hr^{-1}) compared de-littered plot rings (7.18 ± 0.91 cm hr^{-1}) ($P < 0.0001$), but greater in shallow-litter LD1 sites (5.85 ± 1.59 cm hr^{-1}) compared to moderate-litter LD2 (3.78 ± 0.90 cm hr^{-1}) and deeper-litter LD3 sites (3.49 ± 0.46 cm hr^{-1}) ($P = 0.0013$).

Total amount of runoff during dry runs showed more runoff from plot rings without litter, where all de-littered plot rings in LD1 (74.15 ± 8.7 L), LD2 (68.47 ± 6.16 L), and LD3 (70.02 ± 5.45 L) ($P = 0.0186$) differed from littered plot rings in LD2 (11.68 ± 0.68 L) and LD3 (2.80 ± 0.315 L), and LD1 (35.93 ± 5.75 L) differed from all other litter depths and cleared status combinations (Fig. 2). Total amount of runoff during dry runs also resulted in a species by cleared status interaction ($P = 0.0147$), showing littered mixed conifer (19.02 ± 7.47 L) and ponderosa pine (14.58 ± 6.65 L) did not differ from each other while de-littered mixed conifer (83.39 L ± 8.14) and de-littered ponderosa pine (58.37 L ± 6.23) differed from all other means.

Total amount of infiltration during dry runs showed a difference between littered plot rings (179 ± 14.1 L) and de-littered plot rings (112 ± 25.0 L) ($P < 0.0001$). Similarly, terminal infiltration during dry runs also showed a difference between littered plot rings (17.41 ± 1.29 cm hr^{-1}) and de-littered plot rings (11.03 ± 2.41 cm hr^{-1}) ($P < 0.0001$). The species main effect with a during dry runs for the variable final moisture content displayed a difference between ponderosa pine (38.45 ± 6.45 %) and mixed conifer (25.91± 1.25 %) (P-value < 0.0001).

Total runoff during wet runs resulted in a difference ($P = 0.0002$) between ponderosa pine (32.81 ± 5.54 L) and mixed conifer (54.43 ± 7.03 L), cleared status ($P < 0.0001$) littered plot rings (15.3 ± 6.37 L) and de-littered plot rings (71.90 ± 7.45 L), and litter depths ($P = 0.0012$) where LD1 (57.88 ± 18.46 L) differed from LD2 (40.13 ± 12.23 L) and LD3 (32.85 ± 4.42 L).

Post simulation litter moisture was greater for gentle slopes (2.50 ± 0.28 L) than steep slopes (1.79 ± 0.150 L) ($P=0.0395$). The species main effect resulted in mixed conifer (2.99 ± 0.21 L) with higher litter moisture than ponderosa pine (1.29 ± 0.09 L) ($P<0.0001$). Post simulation litter moisture was the greatest in LD3 (2.97 ± 0.213 L) and did not differ from LD2 (2.14 ± 0.144 L). LD2 and LD1 (1.33 ± 0.088 L)(P-value = 0.0014). Utilizing post simulation litter moisture and litter volume data, litter volumetric water content (VWC_L = Volume of H_2O * Volume of $Litter^{-1}$) was calculated. The VWC_L of LD1 (0.058 ± 0.0043 VWC_L) differed from LD3 (0.038 ± 0.0026 VWC_L) ($P = 0.0054$), while LD2 (0.040 ± 0.0025 VWC_L) did not differ from either.

With sediment yield and sediment concentration showing the exact same results, we report sediment concentration only for conciseness. Sediment concentrations resulted in convincing evidence for a slope main effect difference during dry runs, where steep slopes (1.40 ± 0.62 g L^{-1}) were greater than gentle slopes (0.22 ± 0.13g L^{-1}) ($P = 0.0003$). Sediment concentrations during wet runs were very low, but were significantly greater on steep slopes (1.44 ± 0.13 g L^{-1}) than on gentle slopes (0.32 ± 0.09 g L^{-1}) ($P = 0.0002$).

DISCUSSION

Overstory

Basal area and crown closure showed positive relationships with litter depth (Fig. 1). Our results agreed with previous research that showed increased litter accumulation was associated with increased canopy closure and basal area. Increased crown closure

decreased the amount of precipitation reaching litter through canopy interception (Flanagan and Veum, 1974) and decreased the solar heat to the litter, which could slow litter decomposition (Flanagan and Veum, 1974) and facilitate litter accumulation (Klemmendson, et al. 1985).

Litter

Litter mass was greater for both steep slopes and mixed conifer sites than for gentle slopes and ponderosa pine sites. Previous studies on litter from difference species of tree (Putuhena and Cordery, 1996), comparing broadleaf and needle litter, found that different litter types have different masses. However, our data supports mass differences within needle type litter from different species. Our data confirmed a positive relationship between litter depth and litter mass, where deeper litter had greater mass.

Mixed conifer sites contained denser litter than ponderosa pine. Other research similarly found differences in species litter density (Sato et. al., 2004), but the research was performed on needle litter vs. broad leaf litter. The likely reason for higher densities of litter for mixed conifers may be associated with the smaller, more numerous needles characteristic of mixed conifer species that are more likely to pack tightly over what is observed with Ponderosa pine needles.

Litter Moisture Retention

Reviewing rainfall simulation data in relation to litter resulted in evidence that litter played a significant role in the hydrologic dynamics of the forest floor. Deeper needle litter depths decreased the amount of infiltration and increased moisture retention capacity of the litter. Moisture retention capacity may be positively related to the initial density of the litter. When identifying moisture retention capacity potential across needle bearing species, litter density can be used to provide helpful information to understand the forest floor hydrologic dynamics. As litter depths increased, litter density decreased. Data from the present study showed as litter density increased there was also an increase in VWC_L. The VWC_L data disproved part of Hypothesis 4 in regards to mixed conifer having less moisture retention capacity. Results showed the mixed conifer litter had the highest moisture retention capacity. A possible explanation was that as density increased there was an increase in surface area (potentially from the cylindrical shape of the litter) and thus, there was an increase in moisture retention capacity.

Runoff

Time to start of runoff during dry runs displayed evidence that LD1 produced the highest rate of runoff, potentially caused by LD1 having the lowest litter mass and the highest density. This resulted in less volume for the precipitation to occupy, whereas deeper depths had more volume and more material for water to adhere to. Time to end of runoff during dry and wet runs showed evidence of a negative relationship for time to end of runoff and litter depth, possibly because the lack of empty space in the shallow litter allowed saturation to occur faster and lower moisture retention capacity. The species composition resulted in a difference for time to end of runoff. Runoff stopped sooner on mixed conifer than on ponderosa pine plots that continued to drain longer which may be related to litter density. The denser mixed conifer litter was able to retain the moisture while the less dense ponderosa pine litter was allowed to drain.

Total amount of runoff during dry runs resulted in significant evidence of a litter depth by cleared status interaction (Fig. 2). There was a negative relationship between litter depth and runoff for the littered plot rings while the de-littered plot rings remained constant. Treatment plot rings resulted in a difference in runoff because different amounts of litter were driving the response. With the de-littered plot rings, the soil was driving the runoff response, and since all de-littered plot rings had basically the same soil type there was no significant difference in runoff. Counter to our second hypothesis, more runoff was produced with shallower litter. In keeping with our third hypothesis runoff was greater for steep slopes and ponderosa pine.

Infiltration

Litter facilitated increased infiltration rates for total and terminal infiltration rate as supported by Blow (1955) and Janeau *et al*. (1999). Total and terminal infiltration rate during wet runs showed significant evidence for a slope and cleared status main effect differences. The same evidence was found with the dry runs in which less infiltration was associated with steep slopes and de-littered plot rings.

Sediment

Sediment yield and concentrations resulted in a significant difference by slope. Original hypotheses speculated that ponderosa pine and shallower litter depths would result in more sediment; however there was no evidence supporting these hypotheses during the dry and wet runs. There was convincing evidence during both dry and wet runs for a positive relationship between sediment load/yield and slope. There was no evidence at the $p \leq 0.05$ level showing that deeper litter layers protected soil, or that the de-littered plot rings resulted in more sediment yield. Sediment data supported the idea that slope was one of the most important factors to sediment movement.

Litter depth and litter hydrology

Terminal runoff rate during dry runs showed no evidence of a difference between litter depth. After an hour of applied precipitation, the litter moisture retention had begun to occur and the added moisture to the litter infiltrated into the soil at a constant rate. Time to infiltration at 5 cm also showed at a gentle slope a positive relationship between litter depth and time to infiltration at 5 cm. Time to 5 cm infiltration provided more evidence of increased moisture retention capacity with greater litter depths and decreased infiltration. The deeper the litter depth, the lower runoff, the lower final soil moisture, which showed the litter did not facilitate increased infiltration but was intercepting the moisture. Runoff and soil moisture data supported the idea that the deeper litter was intercepting the precipitation in greater amounts than the lower litter depths. It was previously thought the greater amount of organic matter increased infiltration rates (Blow, 1955; Janeau *et al*., 1999), however, this may not necessarily be true for forest pine litter. The litter sat on top of the mineral soil and there was little organic matter that remained in the soil. Most of the organic matter may have been leached out which was shown by soil under the different litter depth not differing in organic matter content.

SUMMARY AND CONCLUSIONS

As water demands increase in New Mexico and the semi-arid western U.S., it will be important to consider forest stand composition effects on forest litter hydrology. This research was performed to fill a gap in the scientific literature on New Mexican montane forests, particularly to understand the forest floor hydrologic dynamics of needle litter. In low precipitation forests such as the Walker Flats site described in this study, even small amounts of precipitation are important to the watershed. Beyond supporting herbaceous vegetation on site, infiltration and subsequent runoff, the Walker Flats site provides stream flow downstream that supports beneficial uses such as irrigation water for agricultural lands and groundwater recharge for drinking water supplies. Greater basal area was associated with higher litter depth, and mixed conifer forest floor litter was shown to have a higher interception capacity than that of ponderosa pine.

Land managers should consider the manipulation of forest stands to maximize the levels of infiltration and reduce the potential for interception. Restoration of the forest to historic conditions of ponderosa pine including reduced basal area of mixed conifer would reduce the interception capacity of the litter. The change from mixed conifer to ponderosa forest would allow additional water to penetrate into the forest floor instead of being lost to the atmosphere, making that water available for soil moisture recharge, plant growth, and watershed runoff.

Table 1. Forest stand characteristics[1] for study sites in a montane forest near Mora, NM.

	Site	Minimum	25 Percentile	Median	75 Percentile	Maximum	Mean	Standard Deviation	Standard Error
Basal Area[2] (m^2 ha^{-1})	MC Gentle[a]	18.6	27.9	38.3	46.5	58.1	37.6	12.4	3.58
	MC Steep[a]	27.9	32.5	34.9	37.2	55.8	36.4	7.30	2.11
	PP Gentle[a]	25.6	27.9	37.2	45.3	48.8	36.8	8.63	2.49
	PP Steep[a]	16.3	31.4	38.3	45.3	48.8	37.6	9.74	2.81
Crown Closure[3] (%)	MC Gentle[a]	70.0	79.8	87.8	90.6	97.3	85.3	8.79	2.53
	MC Steep[a]	77.3	86.3	89.6	94.0	96.8	89.2	5.74	1.66
	PP Gentle[a]	83.5	85.6	89.9	91.9	93.8	89.0	3.52	1.01
	PP Steep[a]	65.8	89.3	90.3	92.9	98.5	89.3	7.92	2.29
Slope[4] (%)	MC Gentle[a]	2.9	4.0	6.8	8.5	12.4	6.5	2.93	0.84
	MC Steep[b]	6.8	9.1	11.5	15.5	19.3	12.2	4.25	1.23
	PP Gentle[a]	5.1	5.6	7.0	9.4	12.4	7.7	2.39	0.69
	PP Steep[b]	6.8	7.9	10.5	12.8	20.3	11.2	3.98	1.15

[1]n = 12 plots in each of the four sites
[2]Basal area was measured with various radius plots using a 10-factor prism
[3]Crown Closure was measured in north, south, east, west directions at each plot
[4]Slope was measured with a hand level
[a,b] within a variable, site sharing the same letter do not differ significantly at the 0.05 alpha level from PROC MIXED analysis

Table 2. Physical Characteristics of litter and soil compared between species and litter depth of associated rainfall simulation plot rings in the Walker Flats Grazing Allotment.

	Litter				Soil			
	Litter Mass ($kg\ m^{-2}$)		Litter Density ($g\ cm^{-3}$)		Organic Matter (%)		Bulk Density ($g\ cm^{-3}$)	
Litter Type	Mean[1]	SE	Mean[1]	SE	Mean[1]	SE	Mean[1]	SE
Ponderosa Pine	9.64[a]	1.14	0.201[a]	0.019	3.83[a]	0.21	1.45[a]	0.04
Mixed Conifer	13.07[b]	1.48	0.278[b]	0.039	4.88[b]	0.39	1.58[b]	0.06
Litter Depth 0.0-3.5 cm	7.55[A]	1.14	0.317[A]	0.04	4.57[A]	0.44	1.46[A]	0.06
Litter Depth 3.5-7.0 cm	12.00[B]	1.06	0.224[B]	0.015	4.05[A]	0.32	1.53[A]	0.05
Litter Depth >7.0 cm	14.51[B]	1.36	0.177[B]	0.015	4.45[A]	0.54	1.54[A]	0.05

[1] Within litter type means sharing the same letter are not significantly different (P>0.05).

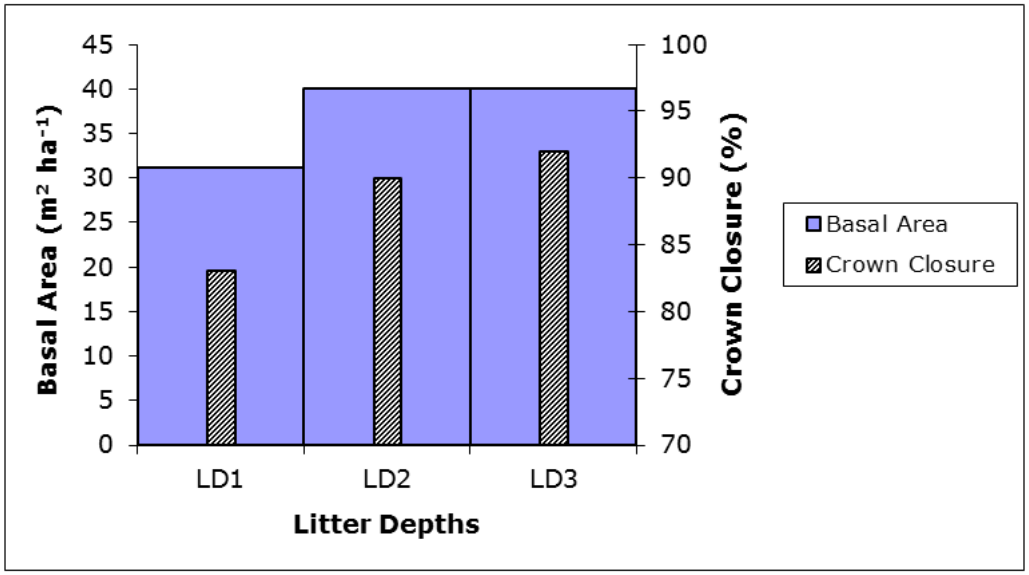

Figure. 1. Litter depth on all study plots showing significantly greater litter depth associated with higher tree basal area and crown closure. Litter depths are LD1 0.0-3.5 cm, LD2 3.6-7.0 cm, and LD3 > 7.0-cm.

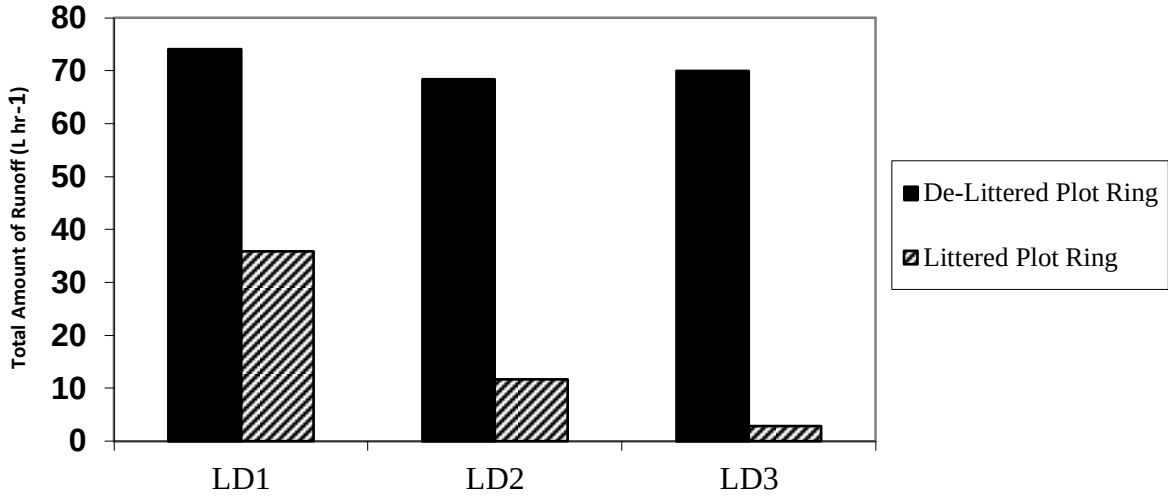

Fig. 2 Total amount of runoff during dry rainfall simulation runs showing significantly greater runoff on plot rings that have been cleared of litter. Litter depths are LD1 0.0-3.5 cm, LD2 3.6-7.0 cm, and LD3 > 7.0-cm.

REFERENCES

Agee, J.K. 1974. Fire management in the nation parks. West. Wildlands. 13:27-33.

Anderson, J.U. 1961. An improved pretreatment for mineralogical analysis of samples containing organic matter. Clays and Clay Minerals. 10:380-388.

Avery, T.E. and H. E. Burkhart. 1994. Forest measurements. McGraw-Hill Company: New York.

Blake, G.R. and K.H. Hartage. 1986. Bulk density, *In*: A. Klute (ed.), Methods of soil analysis part 1-physical and mineralogical methods, second edition. American Society of Agronomy, Inc., and Soil Science Society of America, Inc., Madison, Wis. p.363-375.

Blow, F.E. 1955. Quantity and hydrologic characteristics of litter under upland oak forest in Eastern Tennessee. Journal of Forestry. 53:190-195.

Bussiere, F. and Cellier, P. 1994. Modification of the soil temperature and water content regimes by a crop residue mulch: experiment and modeling. Agricultural and Forest Meteorology. 68:1-28.

Flanagan, P.W., and A.K. Veum. 1974. Relationships between respiration, weight loss, temperature and moisture in organic residues on tundra. (Ed. A.J. Holding et al.) *In*: Soil organisms and decomposition in tundra. Tundra Biome Steering Comm. Stockholm. pp. 249-279.

Grosenbaugh, L.R. 1952. Plotless timber estimates… new, fast, and easy. Journal of Forestry. 50:32-37.

Geddes, N. and Dunkerley, D. 1999. The influence of organic litter on the erosive effects of raindrops and gravity drops released from desert shrubs. Catena. 36:303-313.

Hart, S.C., M.K. Firestone, and E.A. Paul. 1992. Decomposition and nutrient dynamics of ponderosa pine needles in a Mediterranean-type climate. Canadian Journal of Forest Research 22:306-314.

Helvey, J.D. 1964. Rainfall interception by hardwood forest litter in the southern Appalachians, U.S. Forest Serv., Southeast Forest Expt. Sta. Res. Paper 8, 8:1964.

Helvey, J.D. and Patric, J.H. 1965. Canopy and litter interception of rainfall by hardwoods of Eastern United States. Water Resource Research. 1:193-206.

Janeau J.L., A. Mauchamp, and G. Tarin. 1999. The soil surface characteristics of vegetation strips in Northern Mexico and their influence on the system hydrodynamics an experimental approach. Catena 37:165-173.

Kilgore B.M. 1973. The Ecological Role of Fire in Sierran Conifer Forests Its Application to National Park Management. Journal Quaternary Research. 3:3.

Klemmedson J.O., C.E. Meier, and R.E. Cambell. 1985. Needle decomposition and nutrient release in ponderosa pine ecosystem. Forest Science. 31:647-660.

Klemmedson J.O., C.E. Meier, and R.E. Cambell. 1990. Litter fall transfer of dry matter and nutrients in ponderosa pine stands. Canadian Journal of Forest Research. 20:1105-1115.

Lemmon, P.E. 1956. A spherical densiometer for estimating forest overstory density. Forest Science. 2:314-320.

MacDonald, L.H. and J.D. Stednick. 2003. Forests and Water: a state-of-the-art review for Colorado. CWRRI Complete Report No. 196. Colorado Water Resource Research Institute. Fort Collins, CO. 65 pp.

Madrid, A., A.G. Fernald, T.T. Baker, and D.M. VanLeeuwen. 2006. Evaluation of silvicultrual treatment effects on infiltration, runoff, sediment yield, and soil moisture in a mixed conifer New Mexico forest. Journal of Soil and Water Conservation. 61:159-168.

McClurkin, D.C., P.D. Duffy, and N.S. Nelson. 1987. Changes in forest floor and water quality following thinning and clearcutting of 20-year-old pine. Journal of Environmental Quality. 16:237-241.

Millar, C.S. 1974. Decomposition of coniferous leaf litter. *In* Biology of plant litter decomposition. Vol.1. Edited by C.H. Dickerson and G.L.F. Pugh. Academic Press, London, p.105-128.

Nelson, D.W. and L.E. Sommers. 1982. Total carbon, organic carbon, and organic matter, p. 539-580. *In*: , Methods of soil analysis, part 2-chemical and microbiological properties, second edition. Edited by A.L. Page, R.H. Miller, and D.R. Keeney. Amer. Soc. Agron., Inc., and Soil Sci. Soc. Amer., Inc., Madison, Wis.

O'Brian, R.A. 2003. New Mexico's forests, 2000, Resource Bulletin RMRS-RB-3 Dec 2003. USDA-Forest Service Rocky Mountain Research Station.

Pitman, I.P. 1989. Rainfall interception by bracken litter- relationship between biomass, storage, and drainage rate. Journal of Hydrology. 111:281-291.

Putuhena, W.M. and Cordery, I. 1996. Estimation of interception capacity of the forest floor. Journal of Hydrology. 180:283-299.

Ramsey, F.L. and Schafer D.W. 2002. The statistical sleuth: a course in methods of data analysis. Second Edition. Duxbury Press: Pacific Groove CA. 742 pp.

Sato, Y., T. Kumagai, A. Kume, K. Otsuki, and S. Ogawa. 2004. Experimental analysis of moisture dynamics of litter layers- the effects of rainfall conditions and leaf shapes. Hydrological Processes. 18:3007-3018.

SAS Institute Inc. 2006. SAS Online® 9.1. Cary, N.C. SAS Institute Inc.

Schaap M.G., W. Bouten, and J.M. Verstraten. 1997. Forest floor water content dynamics in a Douglas fir stand. Journal of Hydrology. 201:367-383.

Stednick J.D., 2000. Timber management. *In*: drinking water from forest and grasslands; a synthesis of the scientific literature. USDA Forest Service, Southern Research Station, GTR-39, p. 103-109.

Tam S., G. Sposito, and N. Senesi. 1991. Spectroscopic and chemical evidence of variability across a pine litter layer. Soil Science Society of America Journal. 55:1320-1325.

USGS. 2006. USGS water data for the nation. [online] available from: http://waterdata.usgs.gov/nwis/ Accessed 11 June. 2006.

Vitousek, P. 1982. Nutrient cycling and nutrient use efficiency. American Naturalist. 119:553-572.

Wilcox, B.P., M.K. Wood, J.T. Tromble, and T.J. Ward. 1986. A hand-portable single nozzle rainfall simulator designed for use on steep slopes. Journal of Range Management. 39:375-377.

White, C.S. 1986a. Volatile and water-soluble inhibitors of nitrogen mineralization and nitrification in a ponderosa pine ecosystem. Biology of Fertile Soils. 2:97-104.

White, C.S. 1986b. Effects of prescribed fire on rates of decomposition and nitrogen mineralization in a ponderosa pine ecosystem. Biology of Fertile Soils. 2:87-95.

WASTEWATER EFFLUENT EFFECTS ON ARSENIC SORPTION IN ARID NEW MEXICO SOILS

Sylvia J. Nemmers[1], April L. Ulery[2*], and Manoj K. Shukla[2]

ABSTRACT

Chronic low-level exposure to arsenic has been found to increase health risks. In 2006, the Environmental Protection Agency (EPA) lowered the maximum contaminant level for arsenic in drinking water to 10 parts per billion (ppb). This affected many communities and forced them to develop procedures for lowering arsenic in drinking water. Disposal of arsenic residuals is a problem that must be considered when developing such procedures. A simple and low cost solution is to land apply the arsenic concentrates with the municipal wastewater effluent. As a first step towards investigating the efficacy of this disposal method, experiments were performed to assess arsenic sorption parameters when arsenic is added to soil as part of the wastewater stream. The sorption of arsenate [As(V)] on three NM soils was measured in the presence and absence of wastewater effluent. Kinetic batch experiments were carried out on three texturally diverse soils (sandy loam, sandy clay loam and clay) collected from a land application facility in southern New Mexico. Arsenate solutions were equilibrated with the soils for 12 to 504 h. The presence of wastewater effluent decreased the sorption of As(V), as indicated by Freundlich K_f values for all soils at all reaction times, suggesting that the arsenic could be more mobile than expected based on literature values. Furthermore, wastewater effluent caused the percent As(V) sorbed or retained over time to remain low, for all three soils, regardless of the initial As(V) concentration. Thus, it appears that while soil is an effective sorbent for As(V) in single salt solutions, when the contaminant is added with wastewater effluent, a more complex ionic mixture, the sorption capacity of the soil is decreased. This indicates that only small proportions of arsenic and potentially other metals or compounds may be tied up by the soil in land application areas receiving desalination concentrates.

ACKNOWLEDGEMENTS

The authors would like to acknowledge the support of the New Mexico Water Resources Research Institute and the New Mexico Agricultural Experiment Station who provided financial support for this research through state and federal funding of salaries and supplies. We thank Barbara Hunter and Yanhua Feng for their assistance in the lab.

[1] Colorado Technical University; [2] New Mexico State University, Department of Plant and Environmental Sciences, Box 30003 MSC 3Q Las Cruces, NM, 88003-8003, United States

*corresponding author: aulery@nmsu.edu

Arsenic (As) is found in the environment in ever increasing amounts, in both soils and groundwater, due to both natural and anthropogenic causes (Smith *et al*., 1998). According to the World Health Organization (WHO, 2004) contamination of ground and surface water by As from soils and aquifers poses a significant threat to human health. In 2001 the U.S. Environmental Protection Agency (USEPA) lowered the maximum contaminant level for As in drinking water to 10 parts per billion (ppb) with compliance required by 2006 (USEPA, 2001). This standard prompted communities across the United States to develop As removal procedures including reverse osmosis and desalination. All such procedures, except dilution by mixing, produce As-rich concentrates. A convenient and inexpensive method for disposing of these concentrates, in places where land is abundant, is the land application of desalination concentrates with treated municipal wastewater.

It has been well established in the literature that As tends to sorb to soils, to a greater or lesser extent, depending on soil properties such as texture, Fe and Al oxides (Anderson *et al*., 1975; Carbonell-Barrachina *et al*., 1996; Goldberg, 1986; Goldberg and Glaubig, 1988; Goldberg, 2002; Livesey and Huang, 1981; Manning and Goldberg, 1997; Rubinos *et al*., 2003; Smith *et al*., 1999; Williams, 2003; Zhang and Selim, 2005). However, many factors such as alkali pH, competing ions, and suspended solids have been shown to reduce As sorption and increase its mobility through the soil profile (Darland and Inskeep, 1997; Frost and Griffin, 1977; Melamed *et al*., 1995; Oscarson *et al*., 1983a; Peryea, 1991; Quaghebeur *et al*., 2005; Xu *et al*., 1991). Wastewater effluent certainly has an abundance of competing ions and suspended solids and thus presents a complex environment for As sorption. To date there have been no reported investigations of As(V) sorption in the presence of wastewater effluent.

Much research has focused on the sorption of both arsenate [As(V)] and arsenite [As(III)] species by soils and individual soil constituents. Under laboratory conditions, As sorption increases with increased additions to the soil, the sorption increasing steeply at low solution concentrations and leveling off at higher concentrations (Livesey and Huang, 1981). The magnitude of As sorption, however, varies greatly between different soils, with highly oxidic soils retaining three times more As(V) than soils containing small amounts of Fe and Al oxide minerals (Smith *et al*., 1999). For example, As sorption by soil has been positively correlated with free Fe oxide content in several studies (Wauchope, 1975; Elkhatib *et al*., 1984), and it is believed to form an inner-sphere surface complex via ligand exchange (Waychunas *et al*., 1993). Although Fe oxides appear to dominate As sorption by soils, several other soil constituents are also capable of retaining or complexing As species. These include phyllosilicate clay minerals, such as kaolinite and montmorillonite (Sieling, 1946; Frost and Griffin, 1977; Goldberg and Glaubig, 1988), Al oxides and hydroxides (Anderson *et al*., 1975; Goldberg, 1986; Xu *et al*., 1991), Mn oxides (Oscarson *et al*., 1983a, 1983b) and Ca carbonate (Goldberg and Glaubig, 1988). Sorption of As species by organic matter and humic acid is also possible. Goldberg (2002) investigated the adsorption of As(V) on Fe and Al oxides, kaolinite, illite and montmorillonite as a function of pH. Arsenic adsorption on oxides and clays was consistently higher at low pH values, and decreased above pH 9 for Al oxide, pH 7 for Fe oxide and pH 5 for phyllosilicate clay minerals.

Desorption of substantial amounts of sorbed As(V) has been observed when phosphate was used as the displacing ion (Woolson *et al*., 1973; Peryea, 1991). Melamed *et al*. (1995) performed column experiments using an Oxisol at three pH values. They found that more As was desorbed by the soil at pH 8.0 or when phosphate was added. Much less As desorption occurs in the presence of water alone (Johnston and Barnard, 1979). In aquatic systems, As concentration in suspended solids and sediments is many times higher than in water, indicating that the suspended solids are good scavenging agents and sediments are a sink for As (Mahimairaja *et al*., 2005). Arsenic sorption has also been shown to be time-dependent having rapid initial sorption rates that decrease with time (Elkhatib *et al*., 1984; Pierce and Moore, 1980).

Since land application of As residuals with municipal wastewater effluent is an inexpensive and convenient disposal method, it is important to understand the ability of soils to sequester As under these conditions. How does the application of As to desert soils, in combination with municipal wastewater effluent, affect its sorption or retention by the soil? To answer this question we set forth the following objectives: perform batch sorption experiments on three New Mexico soils using As(V) in either a simple ionic buffer or municipal wastewater effluent; fit Freundlich isotherms to obtain K_f values; and use kinetic sorption data to determine the time dependence of As sorption in the two different solutions.

MATERIALS AND METHODS

Sample Collection and Properties

The study site is located in southern New Mexico (Latitude: 31°49'39"N, Longitude: 107°38'24"W) on approximately 25 hectares of generally flat desert, and consists of three major soil units. To the west is the Soniota soil series, which is a Coarse-loamy, mixed, superactive, thermic Typic Haplargid. The eastern side of the site is primarily covered by the Hondale soil which is a Fine, mixed, superactive, thermic Typic Natrargid. The south-east corner consists of the Verhalen series which is a Fine, smectitic, thermic Typic Haplotorrert. The Soniota and Hondale soils were collected and composited from the surface (0–10 cm) of the land application site in summer 2007, after grading and just prior to the site becoming operational. The Verhalen soil was collected from the B_t horizon (30-50 cm) located in a field just east of the land application site. The soils were air-dried and passed through a 2-mm sieve. These samples were analyzed for various properties (Table 1) including: percent sand, silt and clay using the hydrometer method (Gee and Bauder, 1986), pH of saturated paste (USSL Staff, 1954), organic matter using the Walkley-Black Method (Nelson and Sommers, 1982), cation exchange capacity (CEC) using Na-saturation at pH 7 followed by ammonium acetate extraction (Chapman, 1965), carbonate using the manometer method (Soil Survey Lab, 2004), total Al and total As from microwave-assisted acid digest using USEPA method 3051 (USEPA, 1997) and analyzed using USEPA method 200.7 (USEPA, 1994). Iron oxides were measured on the composite soil samples using citrate-bicarbonate-dithionite extraction (Jackson *et al*., 1986) followed by analysis with inductively coupled plasma-optical emission spectroscopy (ICP-OES).

Wastewater effluent samples were collected from the aerated polishing pond at the municipal wastewater treatment facility. Effluent was collected via the pump used for land application into clean 10 L plastic jugs which were transported to the laboratory in Las Cruces,

NM and stored at 4 °C for up to 6 months. The wastewater effluent was analyzed for pH, electrical conductivity (EC) to calculate total dissolved solids (TDS), and elemental composition using ICP-OES and ion chromatography.

Batch Sorption Isotherms

Time dependence of As(V) sorption was studied using a modified version of the batch method described by Selim *et al*. (1992). Triplicate 1-g samples of the three soils were placed in polypropylene tubes and mixed with 10-mL of either 0.01 *M* KNO_3 or wastewater effluent equilibrating solutions containing known As(V) concentrations. Arsenic solutions were prepared using As in the form of As(V) as sodium arsenate ($Na_2HAsO_4 \bullet 7H_2O$). Six initial As(V) concentrations (C_o) were used: 5, 10, 20, 40, 80 and 100 mg L^{-1}. Six experimental reaction times were selected: 12, 24, 72, 168, 336 and 504 h. The samples were shaken at 150 rpm for 1 h out of each 24 h period, on a reciprocal shaker, and subsequently centrifuged for 10 min at 4000 rpm (maximum relative centrifugal force of about 4550 x *g*). A 2-mL aliquot was sampled from the supernatant. The collected samples were analyzed for total As concentration using ICP–OES. The amount of arsenic sorbed by each soil was calculated from the difference between concentrations of the supernatant and that of the initial solutions. Sorption isotherms were plotted for each of the soils to determine differences due to solution composition and soil properties. The experimental data were fit to the Freundlich equation:

$$S = K_f C^n \tag{1}$$

where S is the As sorbed (mg Kg^{-1}), C is the equilibrium concentration of As (mg L^{-1}), K_f is the Freundlich coefficient, and n is a fitting parameter. This fitting was performed using the Solver add-on in Microsoft Excel. To assess the goodness-of-fit of the Freundlich Isotherm for each experiment the r^2 statistic was calculated as follows:

$$r^2 = COV_{(\exp,fit)} / (\sigma_{\exp})(\sigma_{fit}) \tag{2}$$

where $COV_{(exp, fit)}$ is the covariance of the experimental and fitted values, σ_{exp} is the standard deviation of the experimental values, and σ_{fit} is the standard deviation of the fitted values. For the kinetic studies, the %As sorbed from solution was obtained as follows:

$$\%As_{sorbed} = (1 - As_f / As_i)100 \tag{3}$$

where As_i is the initial As concentration in solution at the beginning of the reaction time, and As_f is the final concentration of As in solution at the end of the reaction time.

RESULTS AND DISCUSSION

Soil and Effluent Properties

The three soils found at this land application site were texturally diverse, ranging from clay to sandy loam and they provide an interesting case study for arsenic sorption. All three soils had alkaline pH values ranging from 8.2 to 8.7, low organic matter contents, and similar extractable Fe oxide content (Table 1). The soils contained between 3 and 4 mg kg^{-1} background As. The diversity of these three soils had some impact on As(V) sorption but not nearly the

magnitude of differences shown by Zhang and Selim (2005) in three soils at the same concentrations and equilibrium times. More differences in As(V) behavior were observed between the KNO_3 buffer and the wastewater effluent used as background solutions.

Table 1 – Selected physical and chemical properties of the Soniota, Hondale and Verhalen soils.

Soil	pH[1]	SOM[2]	CEC[3]	Sand	Silt	Clay	Fe_{ox}[4]	Al[5]	As[5]	CO_3[6]
		%	cmol Kg^{-1}		%			mg Kg^{-1}		
Soniota	8.2	0.6	10.5	66.2	18.8	15.0	4691	7490	3	3.8
Hondale	8.4	0.1	13.6	50.2	25.4	24.4	5331	7721	4	4.6
Verhalen	8.7	0.0	23.6	19.2	35.8	45.0	6455	17780	3	2.6

[1]of saturated paste; [2]Soil organic matter; [3]ammonium acetate extracted Cation Exchange Capacity at pH 7; [4]Citrate-bicarbonate-dithionite extracted iron oxides; [5]total aluminum and arsenic after microwave-assisted digest using USEPA 3051 and 200.7, [6]Manometer method.

Similar to the soils, the pH of the wastewater effluent is alkaline, having a value of 8.7 (Table 2). The effluent collected from the wastewater treatment facility was used undiluted and had a Na concentration of approximately 0.03 *M* (or an ionic strength of 0.028 *M* based on conversion from EC). The sodium adsorption ratio (34.5) and the total dissolved solids (1420 mg L^{-1}) are both high (Table 2) and suggest that the finer textured soils may suffer from a loss of structure over time, due to increased sodium applied in the effluent. The wastewater effluent also contains 140 μg L^{-1} total As, a small amount for a one-time dose, but something that could accumulate over time with multiple land applications. Sulfate and phosphate, ions known to compete with arsenate for sorption sites on the soils surface, were both present in the effluent; 790 mg L^{-1} sulfate and 5 mg L^{-1} phosphate (Table 2).

Table 2 – Selected properties of the wastewater effluent used in this study.

pH	EC[1]	SAR[2]	CO_3	TDS[3]	TSS[4]	SO_4	HPO_4-P	Na	As
	dS m^{-1}		mmol L^{-1}			mg L^{-1}			
8.7	2.2	34.5	0.2	1420	21	482	5	790	0.14

[1]Electrical conductivity; [2]Sodium adsorption ratio; [3]Total dissolved solids (calculated from EC measurement); [4]Total suspended solids.

Sorption Isotherms

Figure 1 shows results from 24 h, a common equilibration time used for batch sorption studies (Zhang and Selim, 2005). The As(V) isotherms describing the distribution between simple KNO_3 solution and the soils were nonlinear and exhibited an "L" shape but with no maximum reached (Fig. 1). The highest sorption occurred at the equilibrium concentration of 5

mg As(V) per L. In soils equilibrated with wastewater effluent, sorption was lower and the slopes of the fitted Freundlich lines were less at concentrations up to 40 mg As(V) per L (Fig. 1). The Freundlich coefficient, K_f decreased when sorption was measured in effluent as opposed to KNO_3 buffer (Table 3).

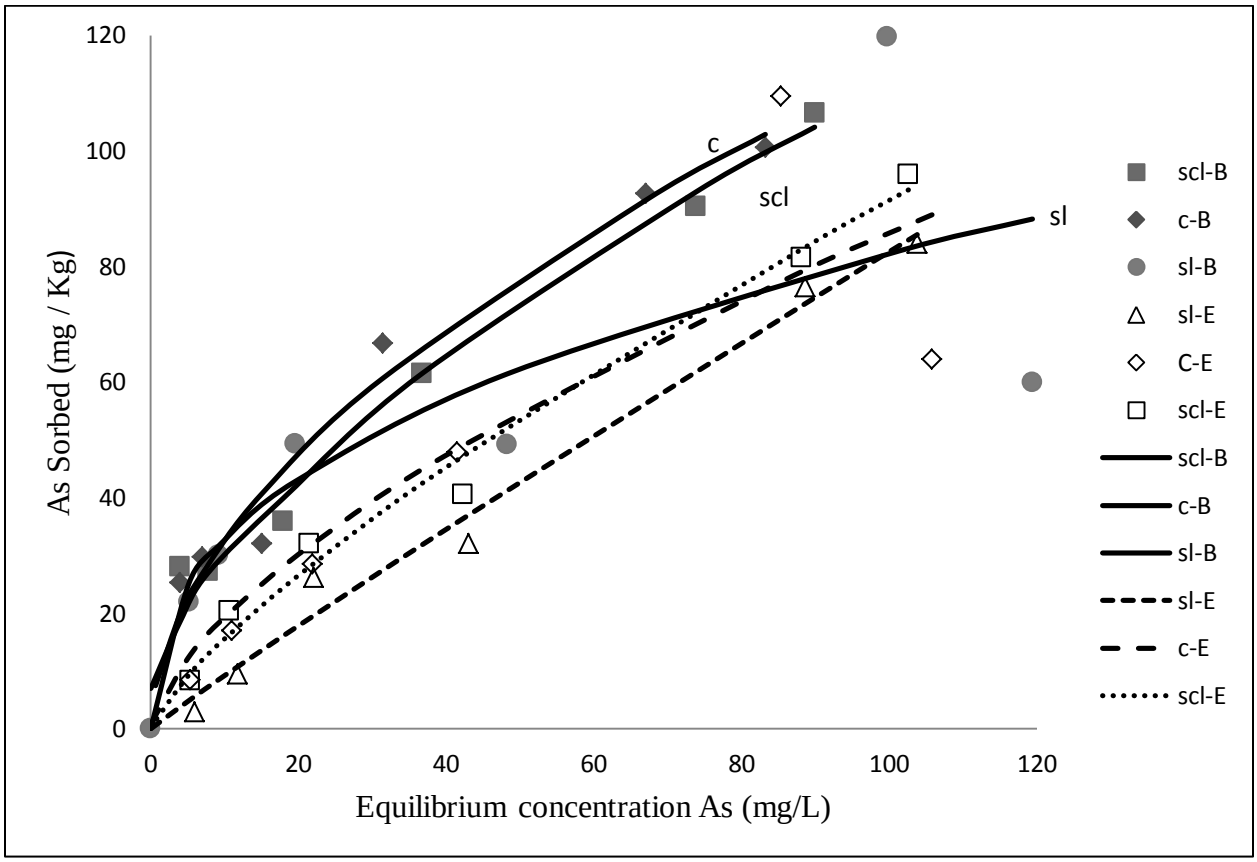

Figure 1. Arsenate sorption isotherms for the Soniota (sl), Hondale (scl), and Verhalen (c) soils in 0.01 M KNO_3 buffer (solid lines and symbols) and wastewater effluent (dashed lines and open symbols) measured at 24 h. Symbols represent mean sorption values and lines represent curve fitting with the Freundlich equation.

Soil texture also affected As(V) sorption, although not as strikingly as the equilibrating solution. The Hondale and Verhalen soils have much higher clay contents and sorbed slightly more As(V) than the sandier Soniota soil at As(V) concentrations above 20 mg L^{-1}. High clay soils have a greater surface area available for sorption which was probably also a factor. This observation agrees with results reported by Jacobs *et al*. (1970) who found higher sorption in the clay loam soils they equilibrated with 25 mg As per g of soil compared to a sand. At the NM land application site in our experiment, the finer textured soils also had slightly higher extractable Fe oxides (Table 1) which correlated to slightly higher sorption of As(V). Jacobs *et al*. (1970) and Zhang and Selim (2005) reported a positive correlation between As sorption and extractable Fe content in the soil.

Table 3 – Fitted Freundlich parameters (mean ± standard error) for sorption kinetics of As(V) on the Soniota (sandy loam, sl), Hondale (sandy clay loam, scl), and Verhalen (clay, c) soils.

Soil	Solution	Time (h)	r^2	K_f [1]	n*
Soniota	Buffer	12	0.68	14.57 ± 3.18	0.28 ± 0.08
		24	**0.70**	**11.28 ± 1.67**	**0.44 ± 0.04**
		72	0.88	15.01 ± 1.88	0.34 ± 0.03
		168	0.93	18.63 ± 4.75	0.32 ± 0.08
		336	0.82	16.29 ± 1.27	0.29 ± 0.08
		504	0.73	27.15 ± 10.27	0.17 ± 0.13
	Effluent	12	0.37	2.30 ± 0.78	0.50 ± 0.11
		24	**0.93**	**1.03 ± 0.45**	**0.95 ± 0.13**
		72	0.95	2.96 ± 1.28	0.75 ± 0.13
		168	0.69	0.44 ± 0.50	1.98 ± 1.57
		336	0.67	2.31 ± 2.10	0.76 ± 0.43
		504	0.95	0.83 ± 0.63	1.01 ± 0.32
Hondale	Buffer	12	0.86	15.68 ± 3.23	0.39 ± 0.07
		24	**0.92**	**11.21 ± 1.25**	**0.50 ± 0.5**
		72	0.93	17.77 ± 0.74	0.42 ± 0.01
		168	0.93	22.00 ± 6.25	0.40 ± 0.10
		336	0.95	19.28 ± 6.54	0.38 ± 0.11
		504	0.90	29.02 ± 4.08	0.30 ± 0.03
	Effluent	12	0.54	4.40 ± 2.25	0.42 ± 0.18
		24	**0.86**	**2.50 ± 0.15**	**0.78 ± 0.06**
		72	0.85	5.66 ± 3.25	0.69 ± 0.16
		168	0.90	0.78 ± 0.11	1.02 ± 0.04
		336	0.97	4.12 ± 1.29	0.66 ± 0.08
		504	0.86	6.16 ± 4.36	0.60 ± 0.26
Verhalen	Buffer	12	0.96	7.56 ± 1.89	0.56 ± 0.05
		24	**0.95**	**10.90 ± 1.42**	**0.50 ± 0.04**
		72	0.97	15.48 ± 1.48	0.42 ± 0.04
		168	0.99	16.21 ± 1.71	0.44 ± 0.02
		336	0.80	12.01 ± 2.95	0.45 ± 0.06
		504	0.85	23.61 ± 3.17	0.30 ± 0.03
	Effluent	12	0.79	3.81 ± 3.02	0.55 ± 0.47
		24	**0.58**	**6.98 ± 3.46**	**0.50 ± 0.15**
		72	0.99	3.00 ± 0.84	0.85 ± 0.08
		168	0.93	0.39 ± 0.36	1.26 ± 0.27
		336	0.94	3.77 ± 2.86	0.75 ± 0.31
		504	0.93	3.68 ± 0.58	0.68 ± 0.05

[1]Freundlich K value; [*]fitting parameter for the Freundlich equation. The 24 h equilibrium results are in bold because that is a common procedure and correlates to Figure 1.

Soils equilibrated in wastewater effluent had lower sorption and lower K_f values. The K_f value for each soil, when As(V) was applied in buffer, generally exceeded 15 (Table 3) and reached values greater than 20 at the longer equilibration times. In contrast, the maximum K_f values for As(V) in wastewater effluent never exceeded 7, and are generally lower than 4. The K_f values can be used as an indicator of sorption, with lower K_f values representing lower amounts of sorption (Zhang and Selim, 2005) although no mechanisms or maximum sorption amounts are indicated. Essentially the highest K_f values were obtained between 72 and 168 h for soils in KNO_3 buffer and between 24 and 72 h for soils equilibrated in effluent (Table 3).

Substantially lower sorption of As(V) equilibrated in wastewater effluent may be due to higher ionic strength, dissolved organic matter, competing ions such as sulfate and phosphate, or changes in redox that may have reduced As(V) to As(III) after 72 h (Harter and Naidu, 2001). The ionic strength of the effluent was nearly three times higher than that of the buffer solution and may have contributed to lower As(V) sorption (Harter and Naidu, 2001). However, the effect of ionic strength on sorption has been shown to be more pronounced on variable charge soils (e.g., tropical soils rich in Fe and Al oxides) and less evident on permanently charged soils such as those found in New Mexico. The electrolyte composition of the equilibrating solution may have also affected sorption. Harter and Naidu (2001) report that sorption of arsenates may decrease in the presence of Na compared to other ions such as Ca or K. Our buffer solution cation was K^+ and the major ion in the effluent was Na^+ (Table 2). Additionally, Na at high concentrations in the sample matrix may interfere with ICP-OES readings and cause lower values.

The standard error for the K_f and n values, presented in Table 3, are generally larger for the wastewater effluent isotherms, when taken in proportion to the actual values. These higher standard error values are likely due to the complex chemical composition of the wastewater effluent, and serve as a reminder of the difficulties of modeling complex systems. Notwithstanding, the large differences in the K_f values between the buffer and effluent isotherms greatly exceed the variability of the standard error values. Since the r^2 value for the Soniota effluent 12 h experiment was quite low (Table 3), the experiment was repeated with similar values of K_f and n being obtained, as well as an equally low r^2 value.

A third of all the isotherms exhibited a decrease in sorption at the highest concentration of 100 mg As per L of solution. Many studies conducted on As(V) sorption in soils use concentrations in the part per billion ($\mu g\ L^{-1}$) range where the compound is strongly attracted to and retained by many solids. In this study, being conscious of the potential for arid region soils and land application sites to accumulate large concentrations of contaminants, we used concentrations up to 100 mg L^{-1} as reported in Zhang and Selim (2005). The high values of As(V) in solution may be interfering with surface complexation, altering pH (not measured) or otherwise restricting sorption or the measurement of As in the equilibrating solution. Our results could serve as a caution against overloading the soil with arsenic in wastewater to the point where the sorbed contaminant could be mobilized and cause groundwater contamination.

Time-Dependent Sorption

To better understand the behavior of As(V) sorption over time in the two equilibration solutions, a kinetic study was conducted. In general, As(V) sorption increased rapidly between 12 and 72 h after which it did not change substantially (Fig 2). The sorption rate appears to be faster for those soils equilibrated in KNO_3 buffer with 5 mg L^{-1} As(V) added (e.g., both the slopes and the % As(V) are higher) than for soils equilibrated with effluent (Fig 2). There was little change in sorption after 24 h for the KNO_3 buffer and after 72 h for soils equilibrated in wastewater effluent. Thus, applying As(V) with wastewater effluent slows down initial sorption as well as lowers the total amount of As(V) retained by the soil (Fig. 2).

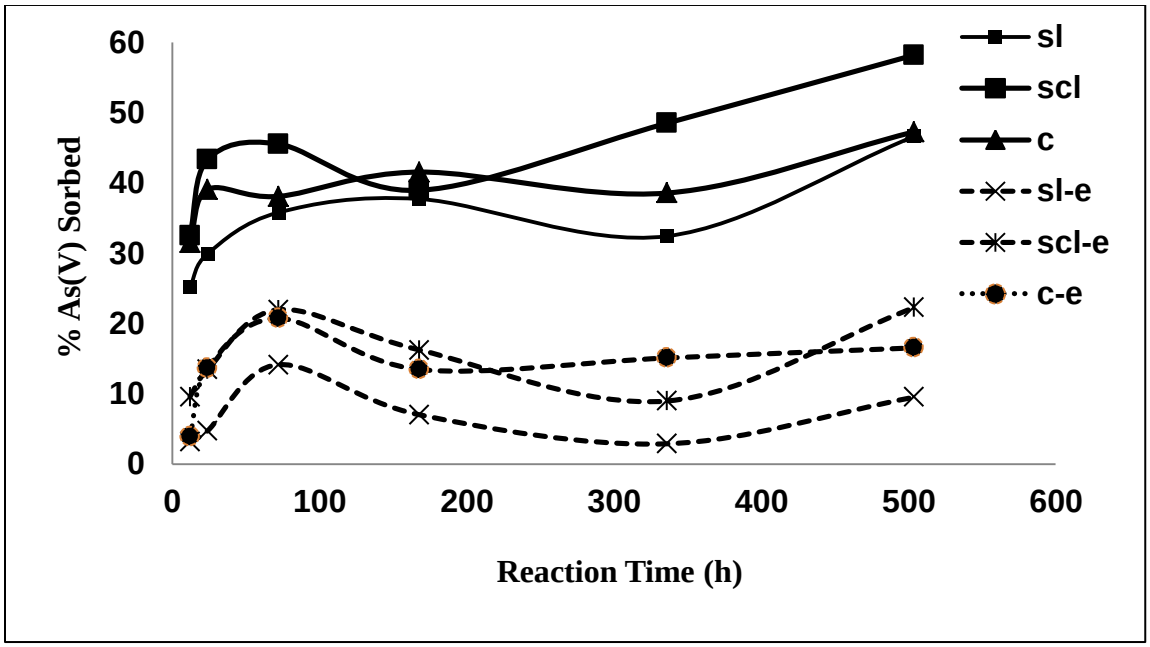

Figure 2. Percent arsenic sorbed from solution containing 5 mg As L-1 vs. time for Soniota (sl), Hondale (scl), and Verhalen (c) soils from batch (kinetic) experiments. Symbols are mean values for the three soil textures equilibrated in 0.01 *M* KNO_3 buffer (solid lines) and wastewater effluent (dashed lines).

The sorption of As has been shown to be time-dependent by several researchers (Zhang and Selim, 2005; Pierce and Moore, 1980; Smith *et al.*, 1999). Arsenic sorption rates may be rapid initially and decrease over time (Elkhatib *et al.*, 1984) or they can continue to increase steadily up to 72 h (Smith *et al.*, 1999). Zhang and Selim (2005) demonstrated that arsenate adsorption by soils was "strongly kinetic" changing rates over time and suggested that their findings support the biphasic sorption behavior observed on soils over short to long time scales.

Another factor affecting both sorption amount and kinetics is speciation. Our work did not investigate speciation of As and did not determine what percentage of the applied arsenate (V) may have converted to arsenite (III). Regardless of the oxidation state however, the total As

sorption decreased dramatically in the presence of wastewater effluent. At most land application sites in New Mexico effluent application is accomplished by flooding the fields and allowing the water to slowly percolate into the soil over a period of days. Infiltration rates are slower in fine textured soils and the increased time may provide for more surface reactions between the As and soil particles. Thermodynamic data show that under most natural surface soil conditions, oxidizing environments dominate over reducing environments (Smedley and Kinniburgh, 2002), and As(V) will be both more stable and abundant than As (III).

CONCLUSIONS

Three texturally diverse soils were collected within the space of a few kilometers at a land application area used for wastewater effluent disposal in southern NM. All three soils retained more arsenic when it was applied in KNO_3 buffer than when applied with wastewater effluent. The application of As(V) with effluent decreased the Freundlich K_f values for all soils at all equilibrium times. The maximum K_f and % As sorbed resulted from the lowest As(V) equilibrium concentration of 5 mg L^{-1} in our experiment. In buffer the isotherms for all three soils exhibit steeper slopes at lower concentrations of As(V), but sorption continues to increase, albeit more slowly, at equilibrium As(V) concentrations up to 80 mg L^{-1}. When As(V) is applied in wastewater effluent the isotherms have much lower slopes at lower solution concentrations.

The sorption isotherms showed that the finer textured Hondale and Verhalen soils held slightly more As than the Soniota sandy loam soil in both buffer and wastewater effluent. Although minor differences in As(V) sorption occurred between the three soils, the most striking influence was the equilibrating solution. This observation suggests that, when As is applied in wastewater effluent, the sorption sites are less available throughout the range of As(V) concentrations tested in this work. Thus As applied to the soil in effluent may be more mobile than previously thought. Whether due to competition from other components in the effluent, the effect of higher ionic strength, or the oxidation state of As, it is clear that wastewater effluent affects the amount of, and conditions for, As sorption and mobility in soils.

REFERENCES

Anderson M.A., J.F. Ferguson and J. Gavis. 1975. Arsenate adsorption on amorphous aluminum hydroxide. J. Coll. Int. Sci. 54: 391-399.

Carbonell-Barrachina, A.F., Burlo Carbonell, F. and J. Mataix Beneyto. 1996. Kinetics of arsenite sorption and desorption in Spanish soils. Comm. Soil Sci. Plant Anal. 27:3101-3107.

Chapman, H.D. 1965. Methods of Soil Analysis. Part 2. Chemical and Microbiological Properties. C.A. Black (ed.) Agronomy 9, Agronomy Society of America, Madison WI.

Darland, J.E. and W.P. Inskeep. 1997. Effects of pH and phosphate competition on the transport of arsenate. J. Environ. Qual. 26:1133–1139.

Elkhatib, E.A., O.L. Bennett and R.J. Wright. 1984. Arsenite sorption and desorption in soils. Soil Sci. Soc. Am. J. 48:1025-1030.

Frost R.R. and F.A. Griffin. 1977. Effect of pH on adsorption of As and selenium from landfill leachate by clay minerals. Soil Sci. Soc. Am. J. 41:53-57.

Gee, G.W. and J.W. Bauder. 1986. Particle-size analysis. p. 383–411. *In* A. Klute (ed.) Methods of soil analysis. Part 1. 2nd ed. Agron. Monogr. 9. ASA and SSSA, Madison, WI.

Goldberg S. 1986. Chemical modeling of arsenate adsorption on aluminum and iron oxide minerals. Soil Sci. Soc. Am. J. 50:1154-1157.

_____ and R.A. Glaubig. 1988. Anion sorption on calcareous montmorillonitic soil - As. Soil Sci. Soc. Am. J. 52:1297-1300.

_____. 2002. Competitive adsorption of arsenate and arsenite on oxides and clay minerals. Soil Sci. Soc. Am. J. 66:413–421.

Harter, R.D. and R. Naidu. 2001. An Assessment of Environmental and Solution Parameter Impact on Trace-Metal Sorption by Soils. Soil Sci. Soc. Am. J. 65:597–612.

Jackson, M.L., C.H. Lim, and L.W. Zelazny. 1986. Oxides, hydroxides, and aluminosilicates. p. 101-150. *In* A. Klute (ed.) Methods of soil analysis. Part 1. 2nd ed. Agron. Monogr. 9. ASA and SSSA. Madison, WI.

Jacobs, L.W., J.K. Syers, and D.R. Keeney. 1970. Arsenic Sorption by Soils. Soil Sci. Soc. Am. Proc. 34:750-754.

Johnston S.E. and W.M. Barnard. 1979. Comparative effectiveness of fourteen solutions for extracting arsenic from four western New York soils. Soil Sci. Soc. Am. Proc. 43:304-308.

Mahimairaja S, N.S. Bolan, D.C. Adriano and B. Robinson. 2005. Arsenic contamination and its risk management in complex environmental settings. Advan. Agron. 86:1-82.

Livesey, N.T. and P.M. Huang. 1981. Adsorption of arsenate by soils and its relation to selected chemical properties and anions. Soil Sci. 131:88-94.

Manning, B.A. and S. Goldberg. 1997. As(III) and As(V) adsorption on three California soils. Soil Sci. 162:886–895.

Melamed, R., J.J. Jurinak, and L.M. Dudley. 1995. Effect of adsorbed phosphate on transport of arsenate through an Oxisol. Soil Sci. Soc. Am. J. 59:1289–1294.

Nelson, D.W. and L.E. Sommers. 1982. Total carbon, organic carbon, and organic matter. *In:* Page, A.L. *et al.* (ed). Methods of Soil Analysis. Part 2. Chemical and Microbiological Properties, 2nd Ed. Agronomy 9, American Society of Agronomy, Madison WI. p 539-580.

Oscarson, D.W., P.M. Huang, U.T. Hammer and W.K. Liaw. 1983a. Oxidation and sorption of arsenite by manganese dioxide as influenced by surface coatings of iron and aluminum oxides and calcium carbonate. Water, Air Soil Poll. 20:233-244.

_____, P.M.Huang, W.K. Liaw and U.T. Hammer. 1983b. Kinetics of oxidation of arsenite by various manganese dioxides. Soil Sci. Soc. Am. J. 47:644-648.

Peryea, F.J. 1991. Phosphate-induced release of As from soils contaminated with lead arsenate. Soil Sci. Soc. Am. J. 55:1301-1306.

Pierce, M.L. and C.B. Moore. 1980. Adsorption of Arsenite on Amorphous Iron Hydroxide from Dilute Aqueous Solution. Environ. Sci. Technol. 14:214-216.

Quaghebeur, M., A. Rate, Z. Rengel, and C. Hinz. 2005. Heavy metals in the environment: Desorption kinetics of Arsenate from kaolinite as influenced by pH. J. Environ. Qual. 34:479-86.

Rubinos, D., M.T. Barral, B. Ruiz, M. Ruiz, M.E. Rial, M. Alvarez and F. Diaz-Fierros. 2003. Phosphate and arsenate retention in sediments of the Anllóns River (northwest Spain). Water Sci. Technol. 48:159-166.

Sieling, D.H. 1946. Role of kaolin in anion sorption and exchange. Soil Sci. Soc. Am. Proc. 115:161-170.

Smedley, P.L. and D.G. Kinniburgh. 2002. A review of the source, behaviour and distribution of arsenic in natural waters. Applied Geochem. 17:517-568.

Smith E, R. Naidu and A. M. Alston. 1998. Arsenic in the soil environment: a review. Advan. Agron. 64:149-195.

_____, R. Naidu and A.M. Alston. 1999. Chemistry of As in soils: sorption of arsenate and arsenite by four Australian soils. Environ. Qual. 28:1719-1726.

Soil Survey Laboratory. 2004. Calcium Carbonate HCl Treatment Manometer Method 4E1a1 from the Soil Survey Lab Methods Manual, Investigations Report No. 42, Version 4.0, November 2004.

US Environmental Protection Agency (USEPA). 1994. "Method 200.7: Determination of Metals and Trace Elements in Water and Wastes by Inductively Coupled Plasma-Atomic Emission Spectrometry," Revision 4.4. http://www.epa.gov/sam/pdfs/EPA-200.7.pdf

_____. 1997. Test Methods for Evaluating Solid Waste. USEPA Rep. SW-846, Version 2. Laboratory Manual, Physical/Chemical Methods. NTIS.

_____. 2001. EPA to implement 10 ppb standard for As in drinking water–EPA 815-F-01-010. 31 Oct. 2001. U.S. Gov. Print Office, Washington, DC.

USSL Staff. 1954. Origin and nature of saline and alkali soils. p. 4. *In* L. A. Richards (ed.) Diagnosis and improvement of saline and alkali soils. USDA Agricultural Handbook 60. U.S. Government Printing Office, Washington, D.C.

Wauchope, R.D. 1975. Fixation of arsenical herbicides, phosphate, and arsenate in alluvial soils. J. Environ. Qual. 4:355-358.

Waychunas, G.A., B.A. Rea, C.C. Fuller, and J.A. Davis. 1993. Surface chemistry of ferrihydrite: Part 1. EXAFS studies of the geometry of coprecipitated and adsorbed arsenate. Geochim. Cosmochim. Acta 57:2251–2269.

Williams, L.E., M.O. Barnett, T.A. Kramer, and J.G. Melville. 2003. Adsorption and transport of As(V) in experimental subsurface systems. J. Environ. Qual. 32:841–850.

Woolson, E.A., J.H. Axley and P.C. Kearney. 1973. The chemistry and phytotoxicity of arsenic in soils: II. Effects of time and phosphorus. Soil Sci. Soc. Am. Proc. 37:254-259.

World Health Organization (WHO). *As in drinking water.* WHO: Geneva, 2004.

Xu, H., B. Allard and A. Grimvall. 1991. Effects of acidification and natural organic materials on the mobility of As in the environment. Water Air Soil Poll. 57/58:269-278.

Zhang, H. and H.M. Selim. 2005. Kinetics of arsenate adsorption desorption in soils. Environ. Sci. Technol. 39:6101–6108.

KILLED COVER CROP RESIDUE IMPACTS ON SOIL MOISTURE IN AN IRRIGATED AGRICULTURAL SYSTEM

Mark E. Uchanski[*1]
Antonio Rios III[1]

ABSTRACT

Alternative cultural practices are one way in which the arid southwest is adjusting to its limited water resources. The use of killed winter cover crops as a pre-plant practice in irrigated agricultural systems may be one way to improve soil moisture management for summer cash crops. Four annual cover crop species were evaluated for their ability to maintain soil moisture content in a furrow irrigated field in southern New Mexico: oats (*Avena sativa* 'Monida'), annual ryegrass (*Lolium multiflorum* 'Gulf'), cereal rye (*Secale cereale*) and wheat (*Triticum aestivum* 'Promontory'). Cover crops were established in October, killed with an herbicide in January, and soil moisture was evaluated into the spring and summer months. Wheat straw was used as a fifth cover treatment in addition to a bare soil control. Determination of the moisture content was conducted with a Diviner 2000 via Frequency Domain Reflectometry (FDR). Depths of 10, 20 and 30 cm were of particular focus. Annual rye was incompletely killed and soil moisture was negatively affected as a result. In 2009, soil moisture content in the wheat and oats treatments was significantly higher than the control, particularly late in the season (June) at 20 cm. Moisture content at the 30 cm depth ranged from 50-60% in the killed cover crop treatments throughout most of the season. In comparison, the control and wheat straw ranged from 30-50% soil moisture content. In both years, at the 10 cm depth the soil moisture content in the wheat straw mulch treatment was comparable to the killed cover crop mulches and, on most dates, was significantly higher than the bare soil control. However, the presence of the wheat straw did not significantly increase the moisture content in either year at the 20 or 30 cm depth. The killed cover crop treatments maintained higher season-long soil moisture content at all depths, presumably due to slowed evaporative losses, indicating the potential of cover crops for furrow irrigated soil moisture management. Killed cover crop residues can provide the benefit of input reduction and may be included in a crop rotation schedule, but must be managed carefully.

The climate of New Mexico is semi-arid with average annual rainfall in the southern part of the state ranging from 20 cm per year in the lower elevation desert to 65 cm at high elevations (NMED, 2010). In the southwest, water is the limiting factor that affects crop growth and yield. Increasing demands on water resources throughout the southwest and western states has increased its importance in farming systems (Longworth *et al.* 2005). The dominant irrigation technique in New Mexico crop production remains furrow/flood irrigation. The efficiency of flood-irrigated systems is dependent on various on-farm factors including slope, field length, soil characteristics, and uniform application of water to reduce run-off losses and minimize deep percolation (Longworth *et al*. 2005). To minimize water loss, innovations in water management must be implemented to improve the efficiencies of available water (Costa *et al.* 2007). One such strategy is the use of killed cover crops. Killed cover crops can be defined as plant residues that

[*] Corresponding author: uchanski@nmsu.edu
[1] Department of Plant and Environmental Sciences, New Mexico State University

are allowed to persist on an untilled soil surface after death of a cover crop, and is still present when the primary crop is planted.

Killed cover crop residues can improve soil moisture retention properties as compared to bare, cultivated soils. Dabney (1998) suggests that the soil hydrologic cycle benefits from several factors when using cover crops. These components include reduced evaporation by altering net radiation, reduced surface temperature, and increased overall water infiltration rate. Soil moisture is affected by cover crops by building soil organic matter, which increases water holding capacity, and intercepting radiation to slow evaporation loss (Bristow 1988, Lu *et al.* 2000). Early studies have shown that mulched, un-tilled soils reduced surface evaporation, maintained moisture near the soil surface at a higher level, and created a favorable environment for root development at or near the mulch–soil surface interface (Triplett and Van Doren 1969). Killed cover crop residues left on the surface have the most impact on the upper 30 to 40 cm of the a soil profile (Bergamaschi and Dalmago 2006).

In semi-arid regions, surface applied straw mulch can increase soil water infiltration and accumulation (Ji and Unger 2001). Straw mulching of irrigation furrows at a rate of 900 $kg \cdot ha^{-1}$ in onions reduced soil erosion, surface water runoff, and increased onion yield by 64% in both jumbo and colossal onion (Shock *et al.* 1999). However, the lower rate of rate of 630 $kg \cdot ha^{-1}$ would have been adequate (Shock *et al.* 1999). Straw mulches have several drawbacks: Problems can arise if the main crop is not established and strong winds remove the residue. Another disadvantage of using straw mulch is the amount of manual labor needed to apply it. However, mechanical straw applicators have made straw distribution economical on a commercial scale (Shock *et al.* 1999).

Incorporating a conservation system such as killed cover crops into agricultural production could provide a moisture benefit for growers that will easily integrate into existing irrigation systems without excessive cost. The objective of this research was to evaluate soil cover treatments for their ability to maintain soil moisture in irrigated vegetable production.

MATERIALS AND METHODS

Two experiments were conducted in 2008-2009 (referred to hereafter as the 2009 season) and 2009-2010 (referred to hereafter as the 2010 season) at the New Mexico State University (NMSU) Leyendecker Plant Science Research Center (hereafter, LPSRC) located about 14 km southeast of Las Cruces, NM. Average annual precipitation is 241 mm with an altitude of 1,100 m above sea level. Plots in both years were established in a randomized complete block design (RCBD) with four replications. Land preparation in 2009 & 2010 consisted of plowing, leveling, and bedding in a north to south orientation with flood irrigation. Four cover crop species, straw mulch, and a bare ground control were evaluated in the context of conventional onion production in southern New Mexico. Onions are common in southern New Mexico and are an example of a primary cash crop. Cover crop species included oats (*Avena sativa* 'Monida'), ryegrass (*Lolium multiflorum* 'Gulf'), cereal rye (*Secale cereale*) and wheat (*Triticum aestivum* 'Promontory'). All cover crop seed was purchased from Granite Seed (Lehi, Utah). Weed free wheat straw was applied at a rate of 968 $kg \cdot ha^{-1}$ on the top of the treatment beds as a fifth cover treatment. Establishment of the cover crops in both years required an initial irrigation event for seed

germination, followed by a supplemental watering. In early March of each season onion cultivar Caballero (Seminis, Oxnard, CA) was direct seeded into a dead mulch planting bed with two seed lines per bed spaced at 34 cm using four Milton Precision Planters (Star Co. Casper, WY) that were modified on a two bar frame. This was achieved by placing two planters in parallel so the double discs could cut through the killed cover crop residues.

2009 SEASON:
Soil type for the 2009 location was a Glendale silty clay loam (mixed calcareous, thermic family of typic Torrifluvents) (NRCS, 2011). Previous crop information was unavailable prior to seeding the cover crop. Total field size was 0.413 hectares and each treatment consisted of four replications with three planting beds per replication. Beds were 1m apart from center to center. Each replication had an area of 77 m^2. The upper 70 cm of soil consisted of silty clay loam overlaying fine to medium sands (Figueroa-Viramontes, 2003). Cover crops were established in the fall and sprayed with glyphosate starting in January (Cornerstone Plus, Albaugh Inc, Ankeny, IA). Standing dead biomass was left undisturbed until spring. In the 2009 season, cover crops were seeded on Oct. 15, 2008. A hand-held broadcast grinder was used to sow the cover crop seed (Table 1). This was achieved with three walking passes to fully cover the treatment areas. Establishment of the cover crops required an initial irrigation event for seed germination (Oct. 16, 2008), followed by a supplemental watering on December 18, 2008. In late January 2009, glyphosate (Round up Power Max, Monsanto Agricultural Products, St. Louis, MO) was applied to all plots at a rate of 2.34 $L \cdot ha^{-1}$, with Urea Ammonium Nitrate solution (URAN)(32% N) 2.34 $L \cdot ha^{-1}$, and 0.219 $L \cdot ha^{-1}$ of an oil concentrate combined in a tank with 79.2 L of water. This initial application of glyphosate was insufficient to kill the cover crop completely prior to seeding the onions. An additional broadcast application of Select (Clethodim, Arysta LifeScience, Tokyo, Japan), a post emergent selective herbicide used to control grasses, was applied at rate of 1.17 $L \cdot ha^{-1}$, including a base mineral oil at 1.17 $L \cdot ha^{-1}$ that was combined in a tank 79.2 L of water. These applications were ineffective due to cool temperatures. As a result, a paint roller was attached to a 19.05 mm diameter poly vinyl chloride (PVC) tube to aid with spot applications of glyphosate (concentration 50% of total volume). The herbicide mixture was held in a 0.95 liter bottle at one end the pipe. The tool was used in a painting motion in order to concentrate the herbicide only on the cover crops. This was effective in successfully killing the cover crops. On March 3, 2009 ‘Caballero’ onion was direct seeded into the dead mulches. The crop was fertigated on May 29 with Urea Ammonium Nitrate solution (32% N) in conjunction with flood irrigation at a rate of 9.46 L/hr for 3 hrs (28.3 L total). Straw mulch was applied on June 2, 2009 or 62 days after planting (dap) to avoid losses due to wind.

2010 SEASON:
In 2010 season, the soil type consisted of Brazito very fine sandy loam (mixed, thermic family of typic Torripsamments) (NRCS, 2011). Prior to the study, the field was used for Bermuda grass (*Cynodon dactylon* L.) seed propagation. Several glyphosate (Round up Power Max, Monsanto Agricultural Products, St. Louis, MO) applications from Aug. through Sept, 2009 were sufficient to kill the Bermuda grass. Total field size was 0.507 hectares, and each treatment consisted of four replications of four planting beds with each bed 1 m from center to center. Total replication size was 112 m^2. In the 2010 season, an alternative approach was used to seed the cover crops. A 2 m landscape seeder (Sukup Manufacturing Company, Sheffield, IA) was used to drill the cover

crop seed into the tops of the beds. The seeding meter opening rates were set according to the manufacturer's recommendations for each species, which resulted in higher seeding rates than in 2009 (Table 2). This was a desirable outcome because the biomass production of the cover crops in 2009 was sparse in some areas. Establishment of the drilled cover crops required an initial irrigation event for seed germination, followed by a supplemental watering in November. Glyphosate applications did not occur until February due to excess rain in January. Glyphosate (Cornerstone Plus, Albaugh inc, Ankeny, IA) was applied at a rate of 2.34 $L \cdot ha^{-1}$, combined with a URAN (32% N) at 2.34 $L \cdot ha^{-1}$, and 0.219 $L \cdot ha^{-1}$ of an oil concentrate that were mixed in a tank volume of 79.2. Again, the initial application of the herbicide did not sufficiently kill the cover crop prior to seeding the onions. The herbicide Select (Clethodim, Arysta Life Science, Tokyo, Japan) was applied at rate of 1.17 $L \cdot ha^{-1}$, including a base mineral oil at 1.17 $L \cdot ha^{-1}$ that was combined in a tank 79.2 L of water for the 2010 season. However, this also failed to kill the cover crop. Therefore, spot treatments described in the 2009 season were used in the 2010 season. Some of the cover crop was still not completely killed when the onion was direct seeded on March 4. Weed-free wheat straw was surface applied on June 8, 2010.

Table 1. Seeding rates for broadcast cover crops in the 2009 season.

Cover Crop	$kg \cdot ha^{-1}$
Oats	95
Cereal rye	127
Wheat	127
Annual ryegrass	127

Table 2. Seeding rates for drilled cover crops in the 2010 season.

Cover Crop	$kg \cdot ha^{-1}$
Oats	151
Cereal rye	53
Wheat	63
Annual ryegrass	43

SOIL MOISTURE MONITORING:

Determination of the volumetric moisture content was conducted with a Diviner 2000 (Sentek Environmental Technologies, Kent Town, South Australia), which employs Frequency Domain Reflectometry (FDR). Beginning in October of each season, twenty-four PVC access tubes (1.5 m) were installed in the center bed of each treatment and replication at a distance of 15.3 m of the 30.5 m total treatment area for the 2009 season. For the 2010 season, access tubes were installed on the left center bed at a distance of 15.3 m of the 30.5 m total treatment area. In the 2010 season, access tubes had to be moved 1.5 m further up the rows in the cover treatments to allow for planting. The unit was calibrated using irrigation water for a water count, then factory calibration was used. Relative values were collected by hand by lowering the sensor head into

each individual access tube. Measurements were collected from 10 to 150 cm, in 10 cm increments. This project focused on the 10, 20, and 30 cm depths for the two growing seasons since these were the primary root depths for both the cover and primary crops. Data was loaded into a logger and extracted to a computer at the end of each season. Soil moisture readings in 2009 were collected every 5-6 days beginning on October 25, 2009. In 2010 season, readings were taken every 3-5 days. After an irrigation event, muddy conditions prohibited access to the field and readings could not be collected. Readings were reestablished when the soil was dry enough to walk on (~3-8 days). To make data more presentable, graphs are presented with a moving average for every two points in time for 2009. However, for the 2010 season, data is presented without a moving average due to a reduced number of data points.

STATISTICAL ANALYSIS:
Soil moisture data were evaluated for analysis of variance using SAS statistical software (SAS Institute, Cary, N.C. 2009). If the main effect was significant ($P \leq 0.05$) means were separated using Dunnett's multiple comparisons test at a probability level of 5%.

RESULTS AND DISCUSSION

2009 SEASON:
Several depths (10 cm, 20 cm, and 30 cm) are presented for season long soil moisture contents beginning on Feb 26 and ending on June 26, 2009 (Figures 1, 2, and 3). Detailed statistical analysis was conducted for a portion of the season at the 20 cm depth from April through June (Figure 4). These were the key primary crop water use months. This window was also a focus point because several key onion developmental stages occur during this time. The average maximum temperature for April was 25.4°C, 31.2°C in May, and 33.0°C in June of 2009 (NMCC, 2011).

At the 10 cm depth, throughout the growing season the control had low moisture content, ranging from 3-20% (Figure 1). The straw treatment did not fluctuate as much as the control and responded more like the cover crop treatments. The only cover crop to show a decrease in soil moisture content late in the season was the annual rye (Figure 1). Early in the season the rye appeared dead, however increased temperatures and additional irrigations caused re-growth throughout all blocks.

At the 20 cm depth the amplitude of the readings for the cover crop treatments was consistently less variable than the control and the straw (Figure 2). Late in the season (May-July), the re-growth of the annual rye depleted the soil moisture more readily at this depth. Oats, wheat, and cereal rye had an average range of moisture content from 25-45%. This is important to consider, particularly late in the season (June-July), when temperatures were the highest.

At the 30 cm depth the control and straw moisture contents ranged from 30-50% (Figure 3). The cover crop treatments, other than the annual rye, ranged from 50 to 65% soil moisture content. These differences were more pronounced late in the season. The fluctuating amplitude in moisture content over time for any given treatment was less apparent at this depth.

The remainder of this section will focus on the time period from April 27-June 26 at the 20 cm depth (Figure 4, Table 3). On May 5-6 during the first onion developmental milestone (pre-bulb), the average maximum air temperature was 32.6°C (NMCC, 2011). There were also indications that the oats and annual rye were beginning to re-grow, which introduced some variability to the experiment. Moisture content at 20 cm was 44.6% for oats, 43.8% for cereal rye, and 45.7% for wheat. These three treatments were significantly higher than the control 35.7% (Table 3).

On May 20-21 the average maximum air temperature was 27.8°C (NMCC, 2011). The moisture content was significantly higher at 45.0% in the oats in comparison to the control at 35.4% soil moisture content (Table 3). Again, some of the cover crops were beginning to re-grow. Oats, in particular, had living plants scattered throughout each treatment block, although this did not affect overall soil moisture content retention. The annual rye was also beginning to show re-growth. During the critical bulb formation period (June 4-5), the oats treatment (45.0%) and the wheat treatment (48.2%) were significantly higher than the control treatment (38.5%) (Table 3). The rest of the other cover crop treatments showed no statistical differences from the control.

About ten days later (June 15-16), the maximum average air temperature was 34.7°C (NMCC, 2011). The annual rye cover crop treatment (14.3% moisture content) was approximately 30 cm in height, and living plants were present throughout all blocks. The oats cover crop treatment was also still alive, and was beginning to set seed despite efforts to control it. None of the cover crop treatments were significantly different from the control on this date. However, soil moisture content in the cover crop treatments had a wide range from 31.2% for cereal rye and wheat, followed by oats (28.3%), and the control (17.7%) (Table 3).

On June 26-27 average maximum temperature was 35.0°C (NMCC, 2011). On this date, treatment differences remained insignificant. This likely due to the fact that many of the killed cover crop residues had been removed due to decomposition and wind. The straw also showed a decrease in the amount of surface residue remaining. The annual rye treatment was growing vigorously, causing few onions to be found in each block.

2010 SEASON:
The start of the 2010 onion growing season had many challenges. There was heavy yellow nutsedge (*Cyperus esculentus*) pressure coupled with continued difficulty properly killing the cover crop treatments. Graphs for the 2010 season (Figures 5, 6, and 7) are only presented in the last week of May through July due to calibration errors with the Diviner instrument. Statistical analysis is only presented at the 10 cm based on observed onion root depths throughout all treatments. Plants were smaller and therefore had shallower roots. The 2009 season analysis focused on developmental stages of the primary crop, while the 2010 season analysis focuses on soil moisture content after irrigation events (I).

At the 10 cm depth, the cover crop treatments increased retention of soil moisture, even on a sandy soil (Figure 5). The control showed an overall decrease in moisture content throughout most of the season, specifically late June through July when readings were <15%. The annual rye was actively growing during much of the 2010 growing season and, therefore, the moisture

content followed a similar pattern as the control. Wheat and oats had the highest numerical soil moisture contents. The straw treatment also provided water retention at this particular depth.

At the 20 cm depth, the oats and cereal rye again had the highest numerical soil moisture content, even late into the season (Figure 6). The annual rye moisture tracked directly with the control. This treatment was still alive, and the roots were likely extracting water. As the season progressed to hottest periods the killed cover crop provided a 10-12% moisture retention benefit as compared to a bare soil control. The straw treatment lost its effectiveness at this depth, however. Moisture content at the 30 cm depth was numerically highest in cover crop treatments including cereal rye, wheat, and oats (Figure 7). Late in the season (June –July), oats was the cover crop treatment with the highest moisture content (~50%).

The remainder of this section will focus on the observations made from May 28-July 21, 2010 at the 10 cm depth (Figure 8, Table 4). However, no statistical differences were detected among the treatments. An irrigation event occurred on May 22, 2010. Six to seven days later, (May 28-29) no significant differences were found among the treatments (Table 4). The average maximum temperature for this period was 34.3°C (NMCC, 2011). The oats were not completely killed and, re-growth was occurring. Although it was mown down earlier in the growing season this cover crop treatment was approximately 25-50 cm in height. Most other cover crops were showing re-growth, but were slightly shorter (15-25 cm). Moisture content was numerically lowest in the annual rye (13.2%). The straw and control moisture contents were both at 14.3% and the cereal rye was 14.4%. The wheat treatment was similar to the other treatments at 15.6%. The oats had the highest numerical moisture value at 17.7%.

Two days later (May 31- June 1), there were also no significant differences between the treatments and the control (Table 4). Maximum temperature average for the two dates was 34.5°C (NMCC, 2011). The control (11.9%) and annual rye (11.2%) were numerically lowest for soil moisture content and oats showed the same moisture content as two days prior (17.7%). The wheat treatment showed slight increase in moisture content to 17.5%. On June 17, an extra irrigation event occurred to distribute an herbicide (Dual Magnum, Syngenta) for yellow nutsedge control. Moisture readings were not recorded until six to seven days later on June 23-24. The average maximum temperature for this period was 34.3°C (NMCC, 2011). On these dates, there were no statistical differences among the treatments. The soil moisture content ranged 19.4% cereal rye to the control at 12.7% (Table 4).

No statistical differences were found on July 9-10, nine to ten days after an irrigation event that occurred on July 1. The average maximum temperature for these dates was 32.8°C (NMCC, 2011). Most cover crops were now dead due to an additional spot herbicide application. However, some treatments still had some remaining patches of living cover crop. Yellow nutsedge was still present throughout all treatments, but was observed to be less prevalent in the cover crop treatments. Soil moisture content ranged from 19.3% in the wheat treatment to the control at 9.0%, however differences were not statistically significant likely due to high variability of data (Table 4). Annual rye re-growth was extensive at this point in the season, and there appeared to be a direct impact on the soil moisture content. Six days later (July 16-17), the average maximum temperature for the two dates was 34.5°C (NMCC, 2011). On these dates no

significant differences were found between the treatments and the control (Table 4). Soil moisture content ranged from 17.9% in the annual rye treatment and 26.7% in the wheat treatment (Table 4).

Several important factors varied from 2009 to 2010 that may explain the lack of significant differences in 2010. First, the field in 2010 was significantly sandier and faster draining than 2009, which may have had an impact on overall soil moisture retention. Second, yellow nutsedge was a highly persistent and uniformly distributed weed within the plots that likely depleted any applied moisture. Finally, the cover crop seeding rate was increased in 2010 to increase biomass production observed in 2009. As described previously, some of these denser cover crop treatments re-grew in 2010, which further impacted soil moisture observations.

Figure 1: Soil moisture content (%) at 10 cm in various killed cover crop treatments; season-long trends Feb-July, 2009.

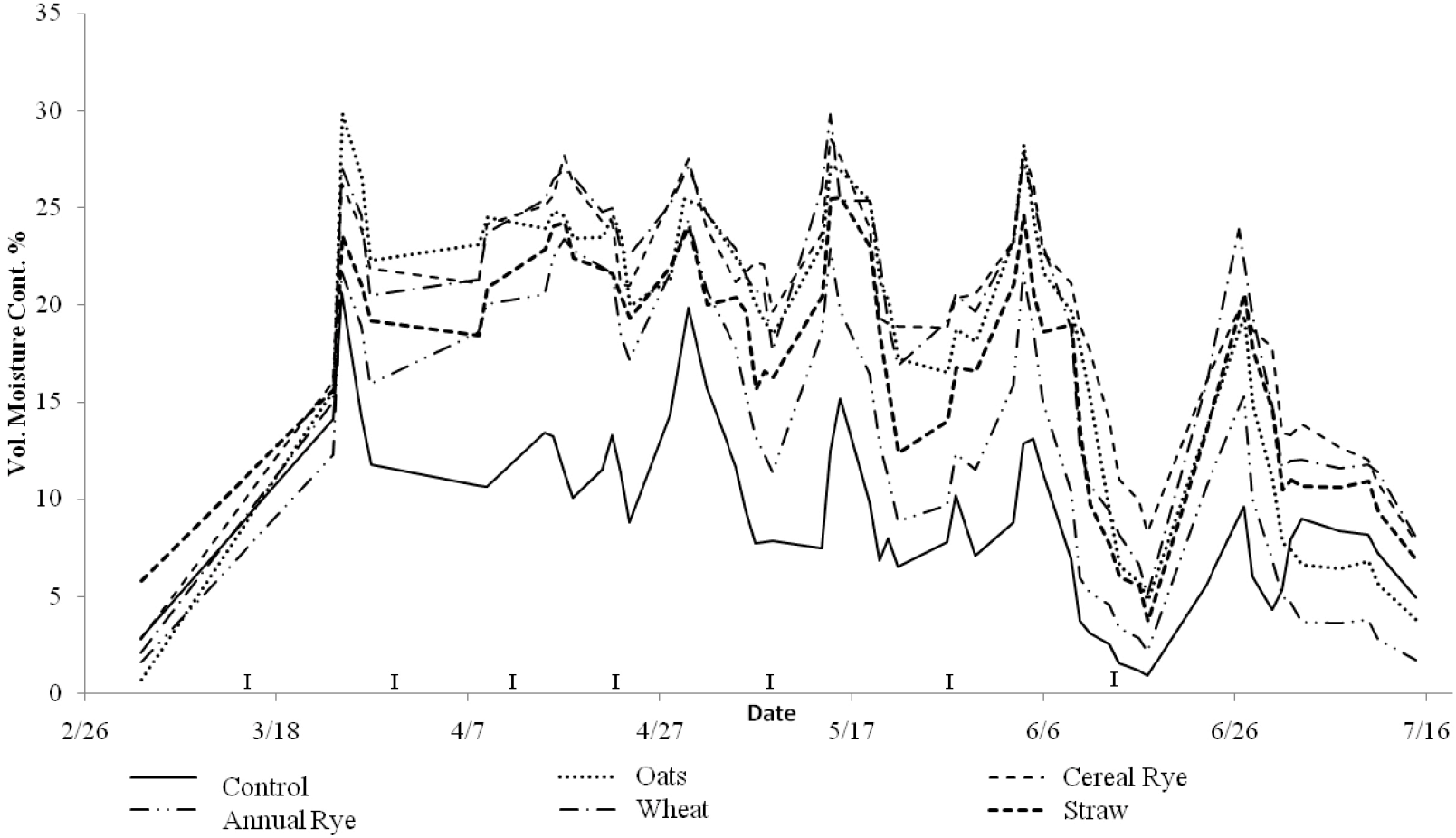

[I]Irrigation events: March 13, March 31, April 9, April 23, May 8, May 29, and June 16.
Note: Trend lines based on a two point moving average.

Figure 2: Soil moisture content (%) at 20 cm in various killed cover crop treatments; season-long trends Feb-July, 2009.

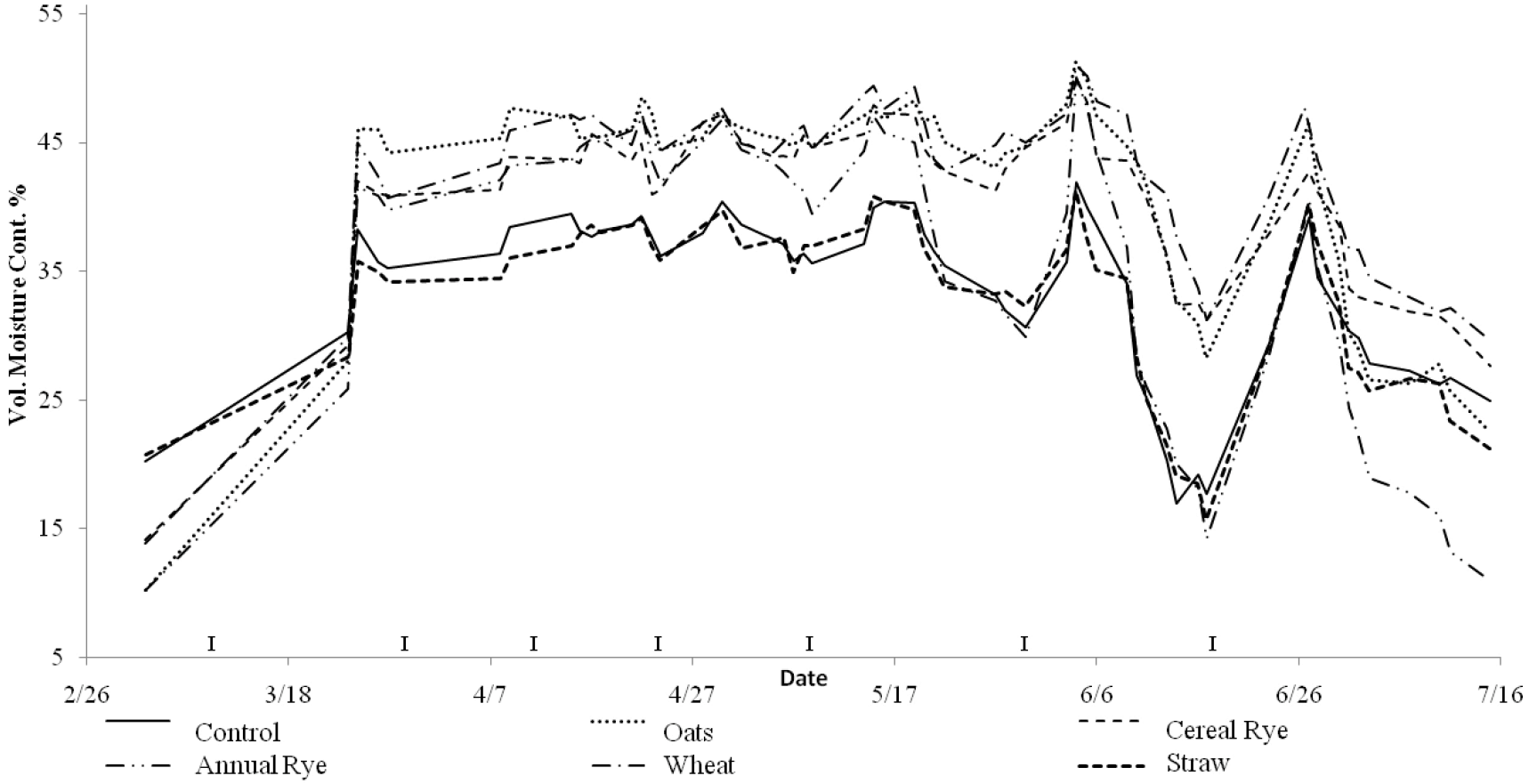

[I]Irrigation events: March 13, March 31, April 9, April 23, May 8, May 29, and June 16.
Note: Trend lines based on a two point moving average.

Figure 3: Soil moisture content (%) at 30 cm in various killed cover crop treatments; season-long trends Feb-July, 2009.

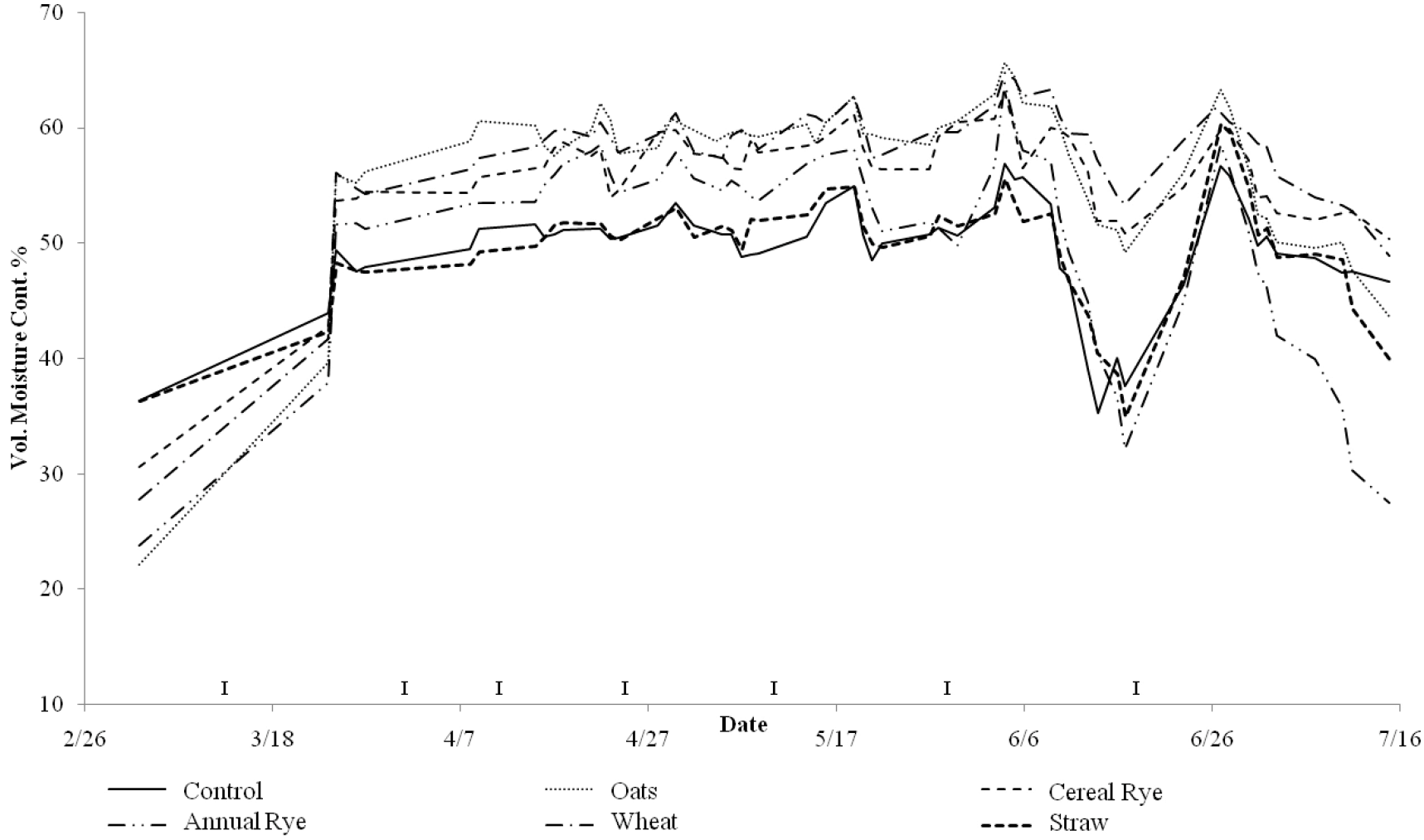

[I]Irrigation events: March 13, March 31, April 9, April 23, May 8, May 29, and June 16.
Note: Trend lines based on a two point moving average.

Figure 4. Soil moisture content (%) at 20 cm in various cover crop treatments. Detailed view of key onion growth stages (April-June) and prior to harvest, 2009.

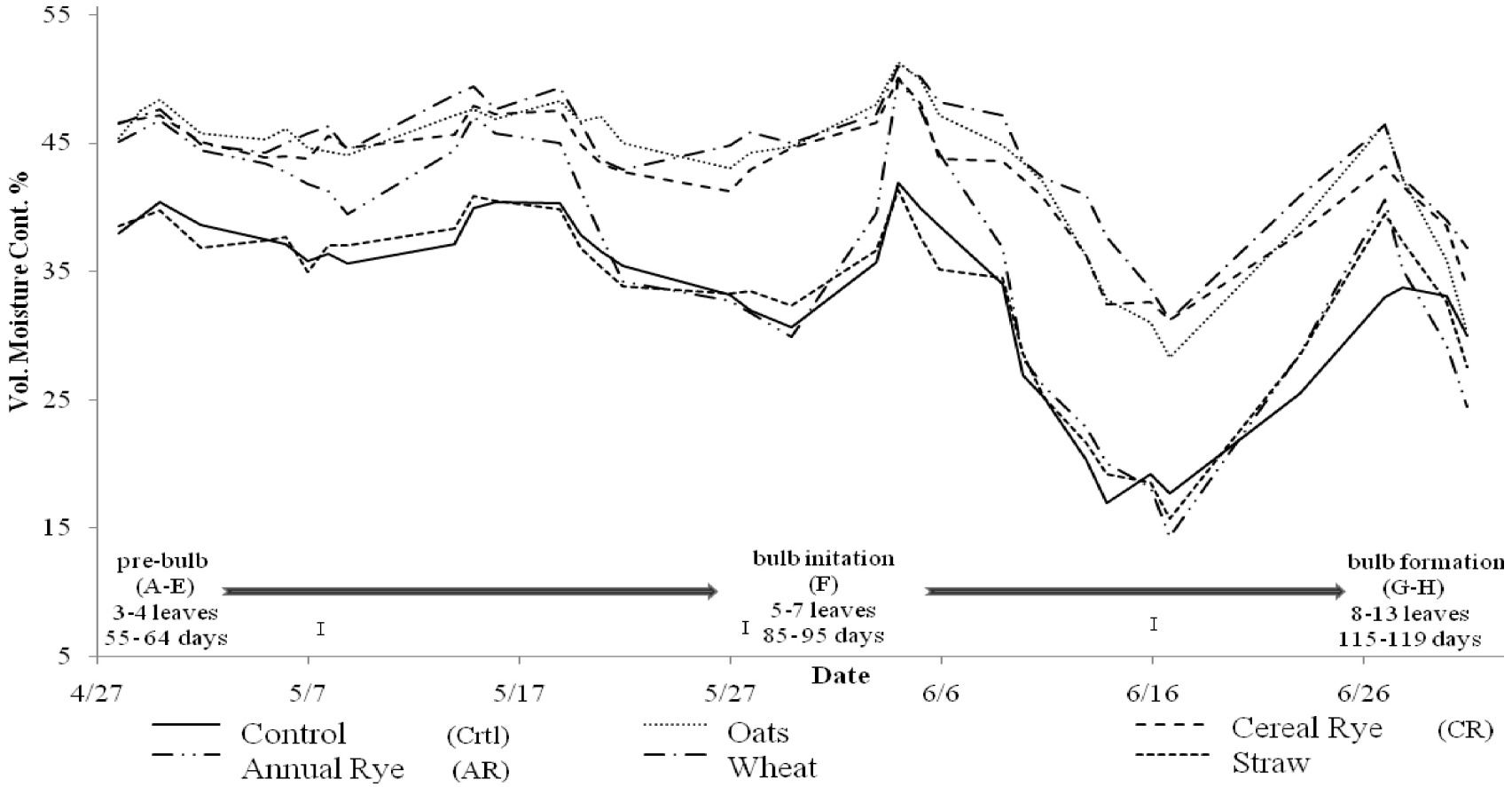

[I] Irrigation events: May 8, May 29, and June 16.

[y] Statistical analysis dates selected and data collected (within ~30 hrs) based on distinct onion developmental milestones on May 5 (A-E, pre-bulb 3-4 leaves), May 20 & June 6 (F, bulb initiation 5-7 leaves), June 16-26 (G-H, bulb formation 8-13 leaves). Based on Rey *et al.* (1974) onion development scale (Table 3).

Table 3. Soil moisture content (%) during key onion growth stages (April- June) prior to harvest, 2009.

Date [y]	May 5-6	May 20-21	June 4-5	June 15-16	June 26-27
Control	35.7	35.4	38.5	17.7	34.5
Oats	44.6*	45.0*	47.1*	28.3	42.2
Cereal Rye	43.8*	42.7	43.8	31.2	41.6
Annual Rye	41.8	34.2	44.2	14.3	35.2
Wheat	45.7*	42.9	48.2*	31.2	42.2
Straw	34.7	34.2	35.1	15.7	37.3

[y] Statistical analysis dates selected and data collected (within ~30 hrs) based on distinct onion developmental milestones on May 5 (A-E, pre-bulb 3-4 leaves), May 20 & June 5 (F, bulb initiation 5-7 leaves), June 15 & 27 (G-H, bulb formation 8-13 leaves). Based on Rey *et al.* (1974) onion development scale.

*Means were analyzed using Dunnett's multiple comparison test. Each treatment mean was compared to the control and an asterisk (*) indicates statistical significance at alpha=0.05.

Note: See corresponding data in Figure 4.

Figure 5. Soil moisture content (%) at 10 cm in various killed cover crop treatments; season-long trends May-July, 2010.

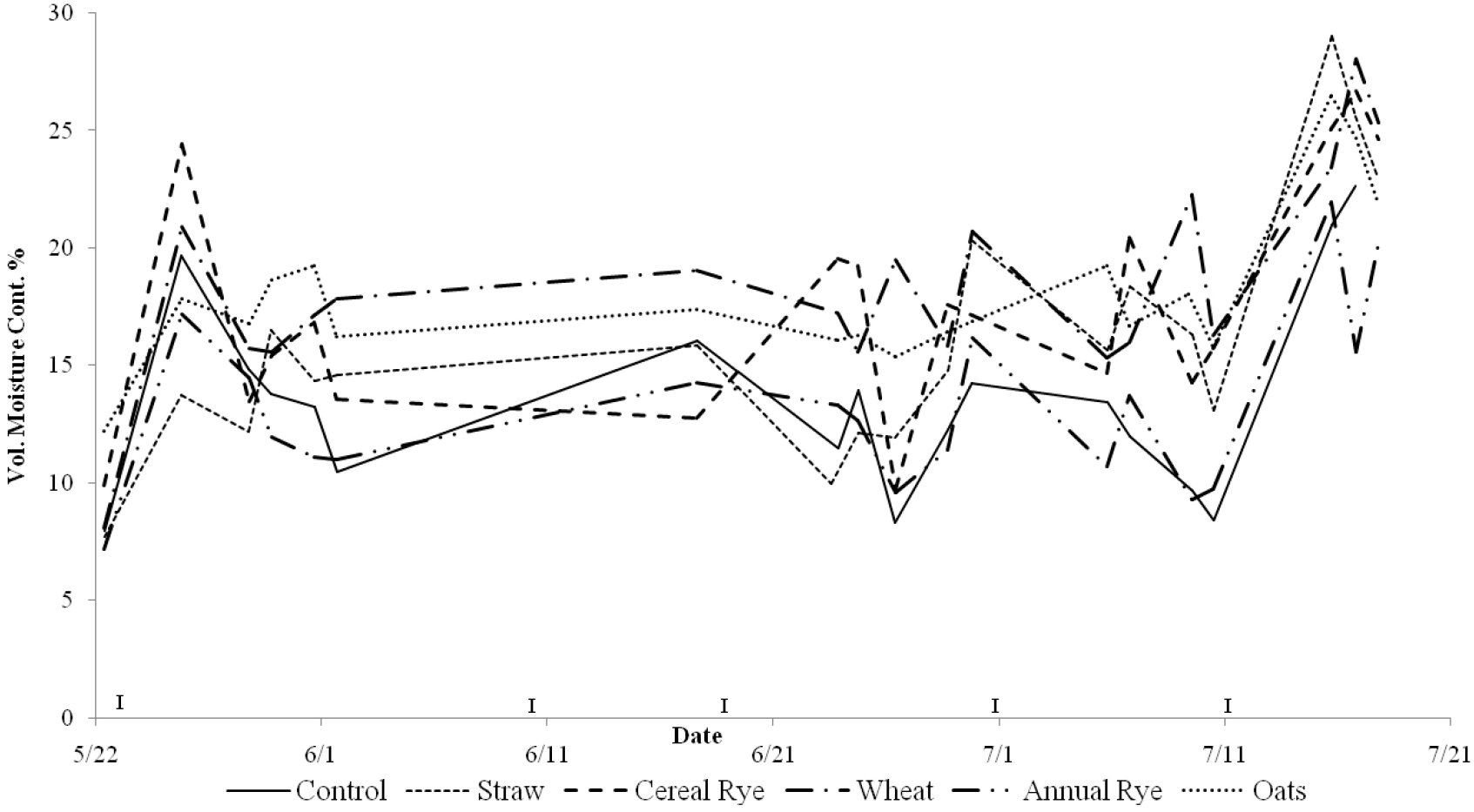

[1]Irrigation events: May 22, June 10, June 17, June 30, and July 11.
Note: Data not collected June 1-17, due to equipment malfunction.

Figure 6. Soil moisture content (%) at 20 cm in various killed cover crop treatments, season long trends (May-July), 2010.

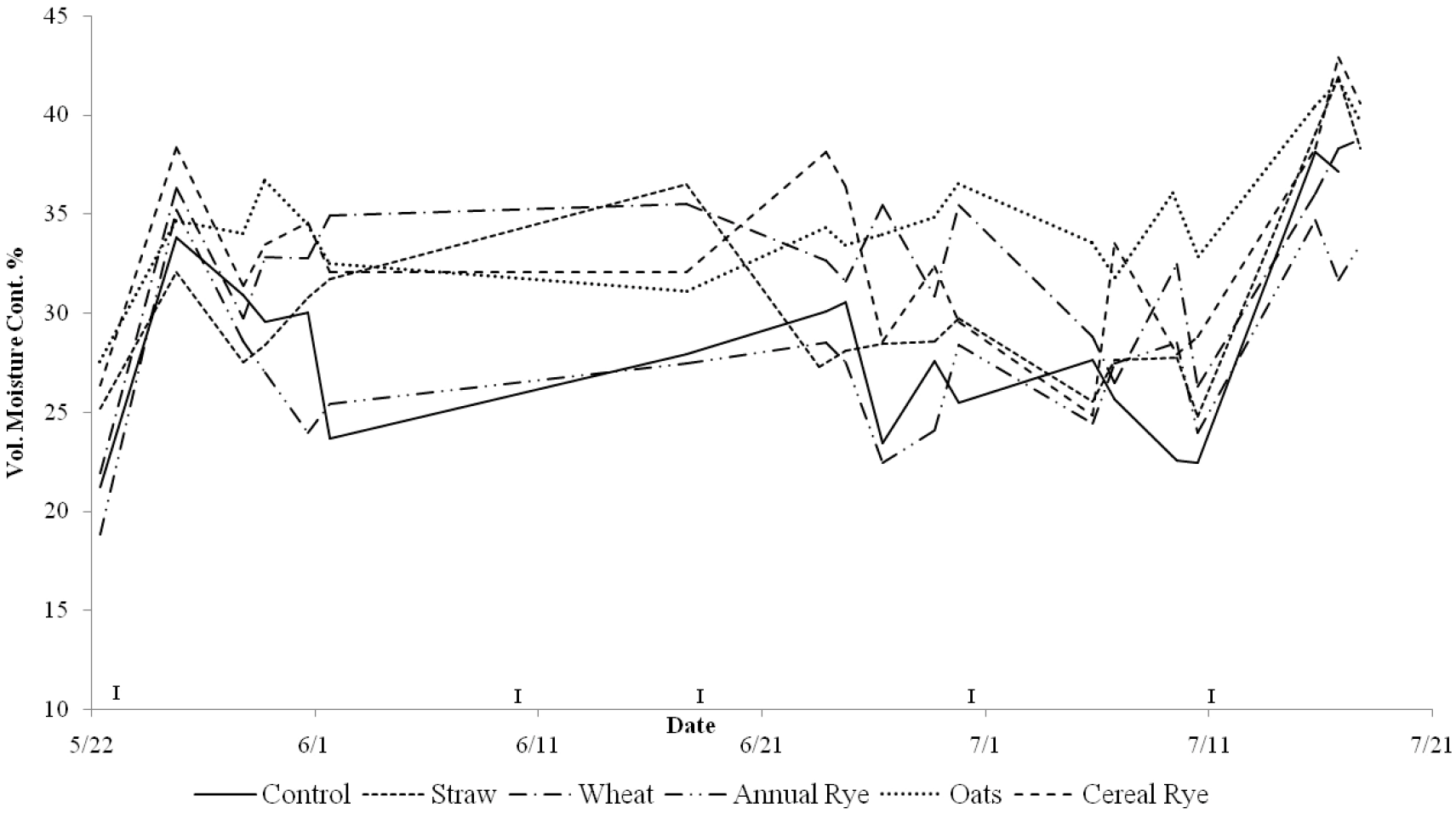

[I]Irrigation events: May 22, June 10, June 17, June30, and July 11.
Note: Data not collected June 1-17, due to equipment malfunction.

Figure 7. Soil moisture content (%) at 30 cm in various killed cover crop treatments, season long trends (May-July), 2010.

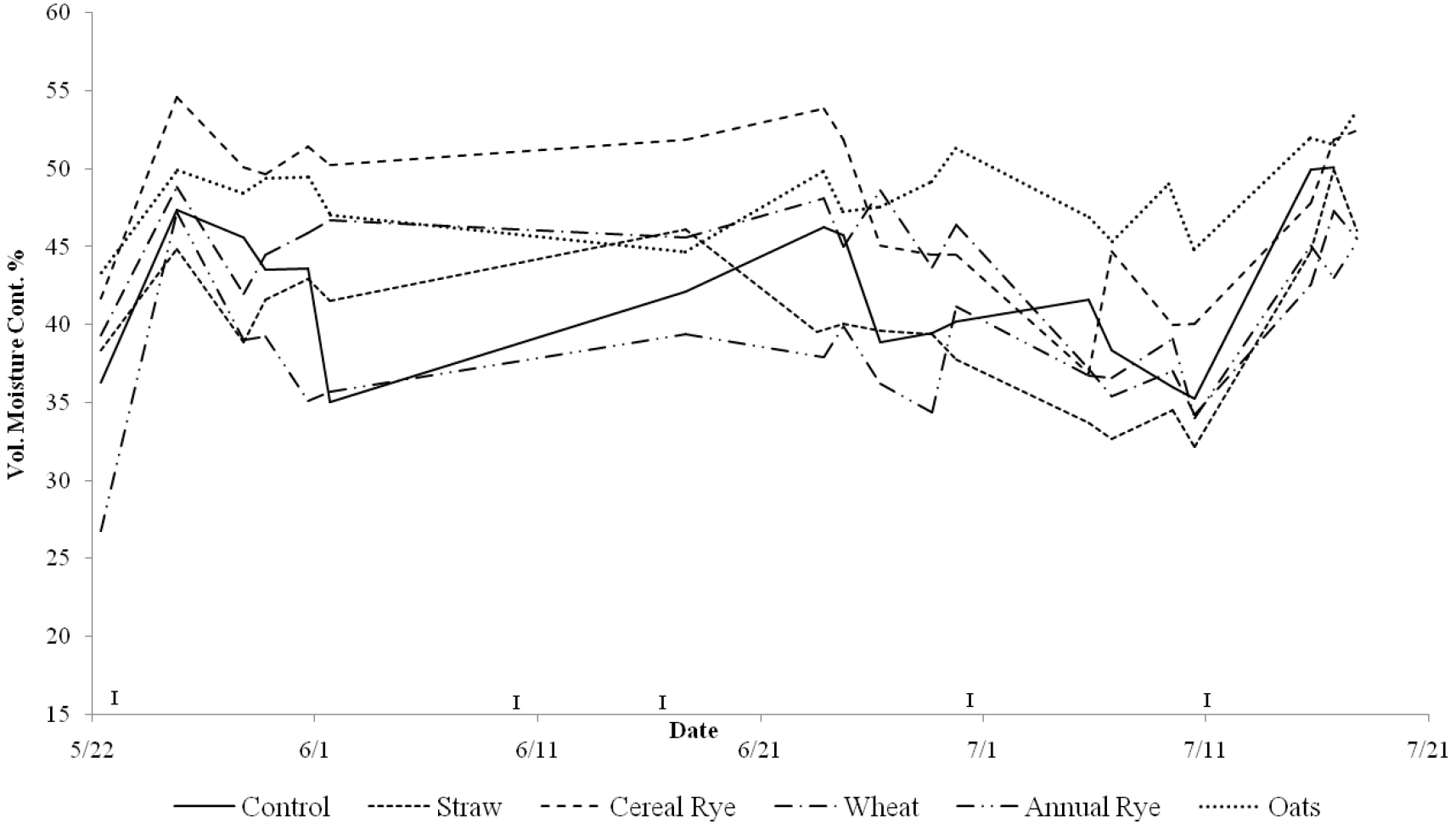

[I]Irrigation events: May 22, June 10, June 17, June30, and July 11.
Note: Data not collected June 1-17, due to equipment malfunction.

Figure 8. Soil moisture content (%) at 10 cm in cover crop treatments (May-July), 2010. Detailed view of moisture content after an irrigation event at various dates at the end of season.

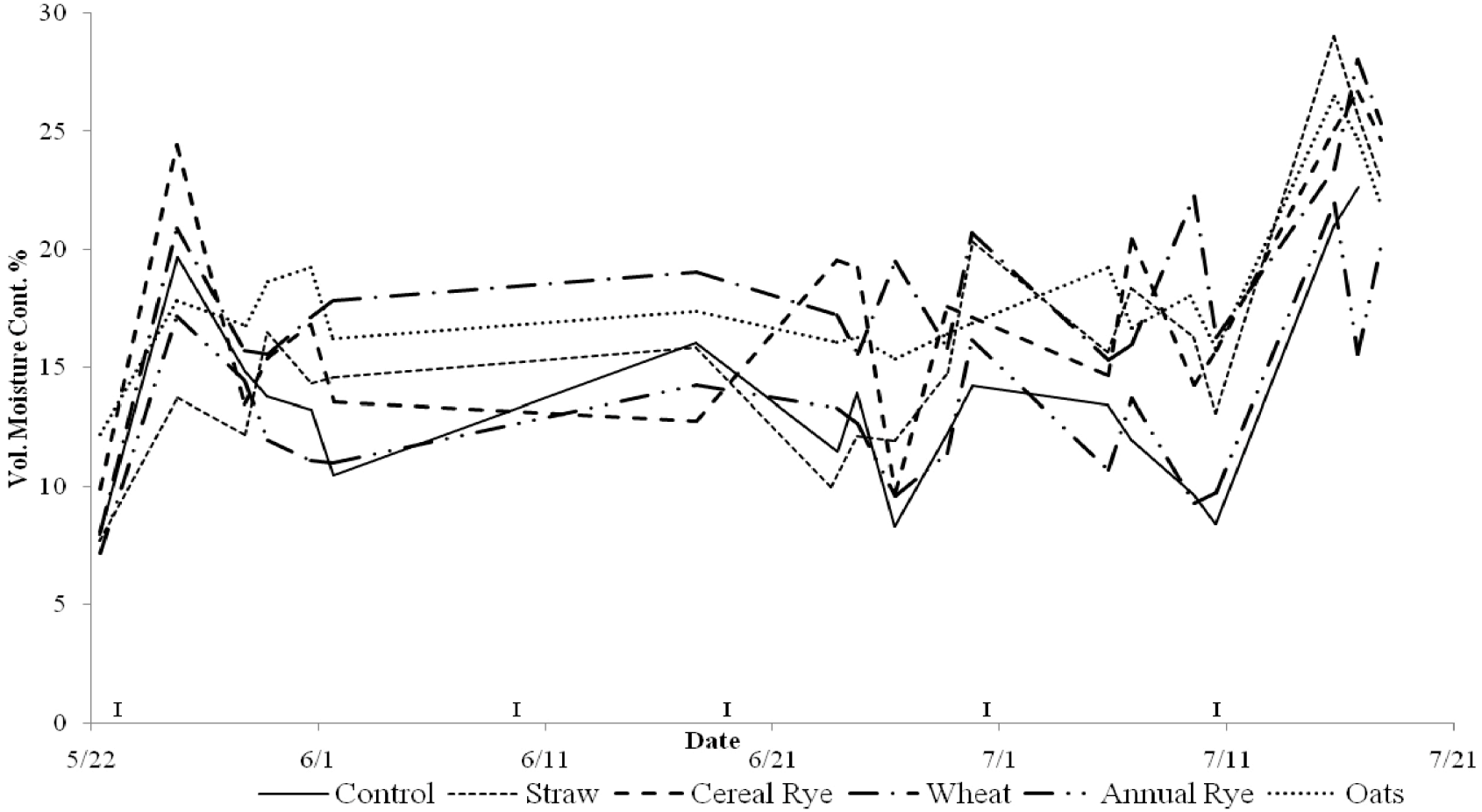

[I] Irrigation events: May 22, June 10, June 18, June 30, June 30, and July 11.

[y] Statistical analyses were conducted after an irrigation event. On May 22 irrigation event occurred, followed by an analysis on May 28-29 at (6-7 days) and May 31-June 01 (9-10 days). June 18 irrigation event, followed by the date of June 23-24 (5-6 days), June-30 irrigation event followed by the date of July 9-10 (9-10 days), and July 11 irrigation event followed by the date of July 16-17 (5-6 days) (Table 4).

Table 4. Detailed view of soil moisture content after an irrigation event at various dates at the end of season in 2010.

Date [y]	May 28 - 29	May 31 – Jun 01	June 23 - 24	July 9 - 10	July16 – 17
Control	14.3	11.9	12.7	9.0	23.0
Oats	17.7	17.7	16.2	16.9	23.3
Cereal Rye	14.4	15.2	19.4	15.0	25.6
Annual Rye	13.2	11.1	13.0	9.5	17.9
Wheat	15.6	17.5	16.4	19.3	26.7
Straw	14.3	14.5	11.1	14.7	24.3

[y] Statistical analyses were conducted after an irrigation event. On May 22 irrigation event occurred, followed by an analysis on May 28-29 at (6-7 days) and May 31-June 01 (9-10 days). June 18 irrigation event, followed by the date of June 23-24 (5-6 days), June-30 irrigation event followed by the date of July 9-10 (9-10 days) and July 11 irrigation event followed by the date of July 16-17 (5-6 days).

*Means were analyzed using Dunnett's multiple comparison test at alpha=0.05. However, no significant differences were detected among treatment means.

Note: See corresponding data in Figure 8.

CONCLUSIONS

Throughout much of the growing season in 2009, the control had lower moisture content at all depths (10, 20, and 30 cm). However, in the 2010 season, this effect was not as pronounced, possibly due to the re-growth of the cover crops, high weed populations, and soil type differences. Both factors contributed to extraction of water from all treatments, and reduced the overall measured soil moisture. Once the cover crops were killed properly, they provided the benefit of retaining soil moisture at various depths for the primary crop. A properly managed and killed cover crop is of critical importance. Earlier establishment of the cover crop would allow sufficient time for growth. Additionally, killing the cover crop while it is actively growing could facilitate a complete kill. Cover crops were sown differently in each season (broadcast vs. drill). However, both methods showed potential for soil moisture retention benefits. The annual rye treatment was not an effective cover crop in retaining moisture. The straw treatment was somewhat effective in the upper 10 cm, but its presence alone was not sufficient to retain moisture at increased depths in this study. The cover crop treatments that could provide the most potential for soil moisture retention at 10-30 cm were the oats, cereal rye, and wheat treatments.

ACKNOWLEDGEMENTS

Funding for this project was provided by the Rio Grande Basin Initiative (RGBI). Additional salaries and research support were provided by state and federal funds appropriated to the New Mexico Agricultural Experiment Station.

LITERATURE CITED

Bergamaschi, H. and G.A. Dalmago. 2006. Brazil: Can the no-tillage system affect the use of irrigation in tropical and subtropical cropping areas? Food Agriculture Organization. [Retrieved March 5, 2011] <http://www.fao.org/ag/AGP/agpc/doc/publicat/no_tillage_system/no_tillagessystem.htm#_ftn1>

Bristow, Keith. 1988. The role of mulch and its architecture in modifying soil temperature. Aust. J. Soil Res. 26:269-80.

Costa J.M., M.F. Ortuno and M.M. Chaves. 2007. Deficit irrigation as strategy to save water: physiology and potential application to horticulture. J. of Integrative Plant Biol. 49:1421-1434.

Dabney, S.M. 1998. Cover crop impacts on watershed hydrology. J. of Soil and Water Conserv. 53: 207-213.

Figueroa-Viramontes, R. 2003. Water use efficiency, growth, and fruit quality in chile (*Capsicum annuum*) under four irrigation methods and two irrigation frequencies. New Mexico State University, Las Cruces, Ph.D. Diss.

Ji, S., and P.W. Unger. 2001. Soil water accumulation under different precipitation, potential evaporation, and straw mulch conditions. Soil Sci. Soc. Am. J. 65: 442–448.

Longworth, J. W., J.M. Valdez, M. L. Magnuson, E.S. Albury, and J. Keller. 2005. New Mexico Office of the State Engineer Water Use and Conservation Bureau. Water Use by Categories for 2005.

Lu, Y.C., K.B. Watkins, J.R. Teasdale, and A.A. Abdul-Baki. 2000. Cover crops in sustainable food production. Food Rev. Intrnl. 16:121-157.

New Mexico Climate Center. 2011. Station 132: Leyendecker PSRC II 32.200261106.743. [Accessed May 24, 2011] <http://weather.nmsu.edu/cgishl/cns/uberpage.pl?selected=4>.

New Mexico Environmental Department. 2010. Air Quality Bureau. [Accessed: May 2011] <http://www.nmenv.state.nm.us/aqb/modeling/aqcr_map.html>

Natural Resource Conversation Service (NRCS). 2011. Web Soil Survey. [Accessed: June 2011] < http://websoilsurvey.nrcs.usda.gov/app/HomePage.htm>

Rey, C., J. Stahl, P. Antonin, and G. Newry. 1974. Stades repères de l'oignon de semis. Revue Suisse de Viticulture, Arboriculture et Horticulture. 6:101-104.

Shock, C.C., L.B. Jensen, J.H. Hobson, M. Seddigh, B.M. Shock, L.D. Saunders, and T.D. Stieber. 1999. Improving onion yield and market grade by mechanical straw application to irrigation furrows. Hort. Tech. 9:251-253.

Triplett Jr., G.B, and D.M. Van Doren Jr. 1969. Nitrogen, phosphorus, and potassium fertilization of non-tilled maize. Agron. J. 61:637–639.

CORRESPONDENCE SHOULD BE ADDRESSED TO:
Mark E. Uchanski
Department of Plant and Environmental Sciences
New Mexico State University
uchanski@nmsu.edu

OBSERVED TRENDS IN SNOWPACK AND SPRING SEASON SOIL MOISTURE AFFECTING NEW MEXICO

David S. Gutzler[1,*]

Sarah J. Keller[1,2]

ABSTRACT

Recent trends and interannual variability in Spring season land surface hydroclimatology in southwestern North America are described using the North American Land Data Assimilation System Phase 2 (NLDAS-2), run with the Mosaic land surface model. Spring is the dry season in central and western New Mexico, affected by snowpack variability. We define the Spring season to be the period each year between snow ablation and monsoon onset. Annual time series of Spring-average hydroclimatic variables are then calculated. The length of the Spring season, defined this way, is itself increasing over the period of record for NLDAS-2, principally due to the observed trend toward earlier snowmelt. We find a decreasing trend in spring season soil moisture. Snowpack anomalies lead to significant changes in the magnitude and timing of soil moisture in the spring season. The data suggest that persistent soil moisture anomalies can provide a source of memory in the land surface that could affect the development of the subsequent monsoon, as postulated in previous research. Monsoon onset negates this memory at the end of the spring season and resets surface hydrology. The results confirm the existence of significant trends toward surface dryness in the American Southwest.

Numerous studies have documented rising temperature and altered hydroclimatology in the western United States during the late 20th Century, continuing to the present day. These changes include the amount and timing of snowpack (Mote et al. 2005; Hamlet et al. 2005; Brown and Mote 2009), more precipitation falling as rain rather than snow (Knowles et al. 2003, Barnett et al. 2008) and earlier snowmelt runoff (Stewart et al. 2005, Barnett et al. 2008). A growing body of climate projections for the region suggests that these trends are likely to continue as climate warms, such that the western United States will become more arid with longer drought recovery times (Seager et al. 2008; Cayan 2010, Gutzler and Robbins 2011). The trend toward aridity is projected to result in lower flows on mainstem rivers (Christensen et al. 2004; Hurd and Coonrod 2008; Reclamation 2011).

On shorter time scales, year to year fluctuations in spring snowpack have been shown to have a negative correlation with subsequent summer monsoon precipitation (Gutzler and Preston

[1] Department of Earth & Planetary Sciences, University of New Mexico MSC03-2040, Albuquerque NM 87131
[2] Current affiliation: Science Communication Program, University of California at Santa Cruz
* Corresponding author: gutzler@unm.edu

1997). It was proposed that surface soil moisture anomalies modulate the surface energy budget, thus altering the land-sea temperature contrast hypothesized to drive the monsoon circulation (Gutzler 2000). The correlation seems to be nonstationary, however, and the physical mechanism underlying this relationship is not fully understood (Lo and Clark 2001; Zhu et al. 2005).

A reduction in snowpack-mediated soil moisture is also likely to change the surface energy budget of the southwestern U.S. Assuming that there is sufficient moisture for evaporation, energy at the surface will evaporate water rather than heat the surface. Since the southwestern U.S. is usually not sunlight limited, a water deficit at the surface can result in the transfer of more net surface radiation into sensible heat rather than latent heat. Through this process, a positive feedback that acts to increase local temperature may develop. By prescribing multiple levels of depleted soil moisture, and thus reducing evaporative cooling in modeling experiments, Fischer and Seneviratne (2007) found that land-atmosphere interaction played an important role increasing maximum daily temperature and European heat wave duration. In monsoonal climates such as in New Mexico, drier land surface conditions in the spring season could generate a "convective barrier" that delays monsoon onset (Seth et al. 2011).

A dearth of long-term soil moisture observations in the southwest, and the difficulties associated with modeling the large-scale evolution of soil moisture, have limited the scope of research on the impact of rising temperature and declining snowpack on regional soil moisture. Cayan et al. (2010) assessed model projections of snowpack and soil moisture, identifying possible future decreases in soil moisture and snowpack as well as prolonged drought periods. However, there are still very few studies addressing the processes by which temperature and snowpack interact to modulate interannual variability in surface soil moisture, especially at long temporal and large spatial scales.

In this study, we use newly available data from the North American Land Data Assimilation System (NLDAS-2) Phase 2 (Ek et al. 2011), implemented with the Mosaic land surface model (Koster and Suarez 1996), to describe recent trends and interannual variability in snowpack and surface soil moisture, emphasizing the Spring dry season when trends toward aridity are particularly intense in New Mexico and the Southwest. The assimilated land surface data allow us to examine soil moisture in the dry season after snow melt, thus characterizing the potential for land surface-atmosphere interactions to modify the climate as proposed in recent studies and included in 21st Century climate projections for the southwestern U.S.

We ask the following research questions to examine the direct and indirect consequences of variability and trends in snowpack on surface hydroclimatic variables in and around New Mexico:

1) What was the spatial and temporal variability of southwestern U.S. snowpack and Spring season soil moisture during 1979-2009?
2) How does interannual variability of spring snowpack affect the evolution of spring and summer season soil moisture in the southwestern U.S.?
3) Do snowpack anomalies maintain a residual effect soil moisture conditions after snow ablation through the Spring dry season?

LAND SURFACE VARIABILITY IN NLDAS-2

Studies of trends and variability in land surface hydrology, especially in mountainous regions, are difficult in part because there are few multi-decadal data sets available and spatial coverage of in situ data is sparse. This study uses derived quantities of soil moisture and surface fluxes, specifically in the form of output from a land surface model (LSM), which describes heat and water fluxes at and below the land surface. NASA's North American Land Data Assimilation System Phase 2 (NLDAS-2) is a relatively high resolution (0.125˚, 3-hourly) data product derived from the assimilation of atmospheric observation into a LSM (Ek et al. 2011). NLDAS-2 was run uncoupled from an atmospheric model, starting near the beginning of the satellite data era in January 1979. This study uses NLDAS-2 data from January 1979 – December 2009. Parallel versions of NLDAS-2 are based on four different LSMs (Ek et al. 2011); we use output from one of these, the Mosaic LSM (Koster and Suarez 1996). Ground, satellite and radar based observations of temperature and precipitation, plus atmospheric model reanalysis data, are used to initialize NLDAS-2 (Mitchell et al. 2004).

NLDAS-2 is a data product in the sense that it ingests a set of observations for each time step and interpolates the observations over the model domain using the physical equations that make up the LSM. The interpolation of temperature and precipitation observations in NLDAS-2 should provide better spatial representations of those fields than univariate interpolation of sparse surface observations. NLDAS-2 is a simulation in the sense that ingested observations are used to force an LSM that generates fields that were not ingested as observations, such as soil moisture. However, rather than being generated from simulated precipitation and temperature, modeled fields are generated from observations at each time step, theoretically improving the estimates of variables from the LSM.

The Mosaic LSM uses sub-grid vegetation tiles with vegetation classification derived from University of Maryland's (UMD) global, 1-km, Advanced High Resolution Radiometer (AVHRR)-based, 13-class vegetation database (Hansen et al., 2000; Mitchell et al. 2004). The snowpack module balances snowfall input, snowmelt output and snow sublimation. Heat flux through the snowpack is used to change snowpack temperature, phase composition and amount (Pan et al. 2003). Snow energy in Mosaic is coupled to the energy transfer of the entire LSM so the temperatures of soil layers, snowpack layers, and the soil surface are solved from heat balance equations for the entire soil, snowpack, vegetation and air system, along with the water balance equations (Pan et al. 2003). One simplifying assumption of Mosaic is that rain falling directly onto snowpack is routed directly to the soil surface where it infiltrates or runs off (Koster and Suarez, 1996).

Mosaic has three soil moisture layers to a depth of 200 cm. The first two are in the root zone. We use the 0-10 cm layer throughout this study. Mosaic was designed to account for subgrid scale vegetation variability, so each surface layer is divided into a maximum of ten vegetation tiles, and each tile has its own energy and water balance as well as soil moisture, soil type and temperature. The energy and water balances for each tile are simulated independently.

The NLDAS-2 model domain covers the continental United States where meteorological observations are dense relative to other geographic areas. For this study we focus on New Mexico and surrounding regions of the U.S. Southwest where snowpack variations affect the surface hydrology. We define an analysis domain bounded latitudinally by 31˚N and 39˚N, and longitudinally by 113˚W and 103˚W, as the Four Corners region (FC, Fig. 1). The figure shows climatological annual average soil moisture from NLDAS-2 for the Spring season. The specific definition of "Spring" used for this and similar calculations is discussed in the next section. Spring soil moisture displays very pronounced spatial gradients across FC, generally increasing with latitude from desert lowlands in the south to forested highlands in the north, and with sharp elevation-dependent increases associated with mountain ranges.

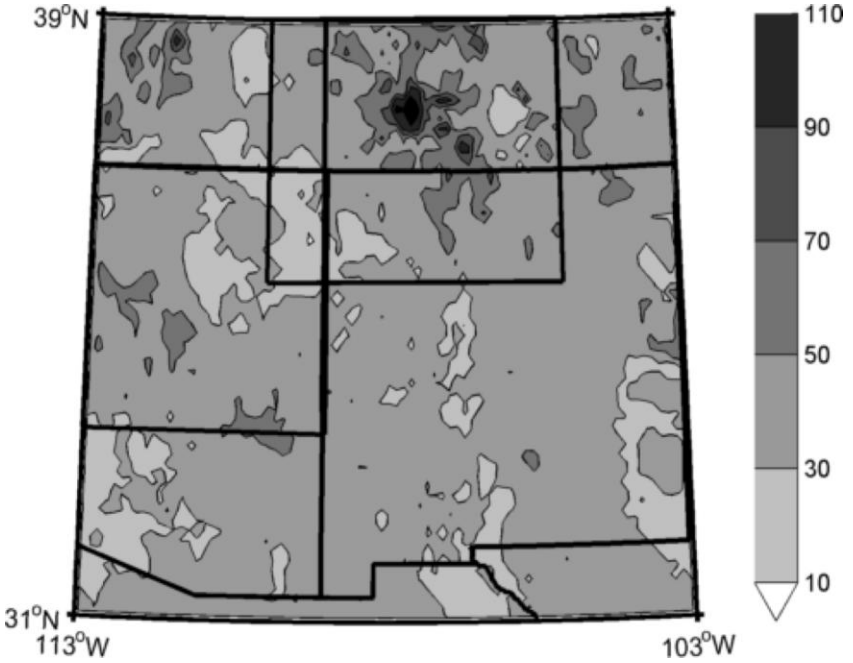

Figure 1. Climatology (1979-2009) of NLDAS-2 surface soil moisture (0-10 cm, units kg m^{-2}) during the spring season, defined as the period between the date of snow ablation and the date of monsoon onset. The Four Corners region (FC in the text) is the entire domain illustrated here. The Southern Rockies (SR) region is the rectangular subdomain in the north-central part of the FC region.

On the basis of an analysis of snowpack variability, described in the following section, a subdomain of the Four Corners region was defined that contains most of the winter snowpack in the highest elevations of the southern Rocky Mountains, and extends laterally to include the snowpack margins that exhibit the largest interannual variability and multi-decadal trends. This subdomain, denoted the Southern Rockies region (SR, Fig. 1), is used as the basis for many of the spatially averaged results in this study.

Time variations of the NLDAS-2 hydrologic fields are compared with existing indices of other hydroclimatic variables. We compared the snowpack variability in NLDAS-2 with in situ

data from 22 SNOTEL sites in the SR region. Snow water equivalent (SWE), the mass of water contained in the snowpack, is used as a common measure of snowpack in SNOTEL and NLDAS-2 data. The SNOTEL sites are predominantly located in the higher elevation portions of SR that contain relatively abundant snowpack in winter, so we expect a SNOTEL-based average of SWE to show systematically higher snow amounts than the broader SR spatial average.

To define the end of the Spring season, we use a local index of monsoon onset dates derived by Higgins (2007). "Monsoon onset" is defined as three consecutive days after May 15 with a mean daily dew point greater than 47˚F and measurable precipitation at the National Weather Service Forecast office in Albuquerque NM. The onset date thus defined is very highly correlated with a regional monsoon onset time series for the southwestern U.S. developed by Ellis and Hawkins (2004) using a similar dew point threshold from multiple stations (including Albuquerque) in Arizona and New Mexico. We therefore interpret the Albuquerque onset date as a reasonable representation of regional conditions.

VARIABILITY AND TRENDS IN SNOWPACK AND SPRING SEASON SOIL MOISTURE

The first step in the analysis is the definition of annual values of maximum daily SWE (the greatest daily SWE value found each year, denoted SWEmax) and specification of the spring season melt day (denoted SWEmelt) from the daily time series of SWE in the NLDAS-2 dataset. These two annual values are used to characterize SWE across the FC study area.

The first empirical orthogonal function (EOF) of the interannual variability of SWEmax (not shown) is used to identify regions with coherent variability within the FC domain. The Southern Rockies (SR) region (Fig. 1) corresponds closely to the first mode yielded by the EOF analysis, wherein the largest SWEmax and Spring soil moisture values occur and the headwaters of several major rivers (including the Rio Grande and San Juan Rivers that flow into New Mexico) are located. The time series of principal components associated with this analysis is shown as the bottom curve in Fig. 2. A straightforward average of SWEmax over the SR region ('NLDAS2 SR' in Fig. 2) reproduces the variability of the principal component time series very closely.

To validate the NLDAS-2 snowpack variability, we developed a time series of SWEmax derived from the 22-site set of available long-term SNOTEL sites within the SR region. That time series is the upper curve in Fig. 2. Finally, we took a subset of grid cells within SR corresponding to the higher elevation areas where the SNOTEL sites are located and recalculated the SR average using just this subset of NLDAS-2 cells. All four curves in Fig. 2 are mutually correlated, an encouraging indication that the assimilated snowpack data are reasonably based on the relatively sparse in situ observations. The ranking of the curves in absolute terms is what one would expect given the successive restriction to high elevation, high snowpack areas from the broad SR average to an average based just on in situ SNOTEL sites. The linear trend in annual SWEmax from SR SNOTEL stations is statistically significant at the 5% level (-62.0 kg/m^2/ decade) as is SR NLDAS-2 SWEmax (-7.7 kg/m^2/decade) (Fig. 2).

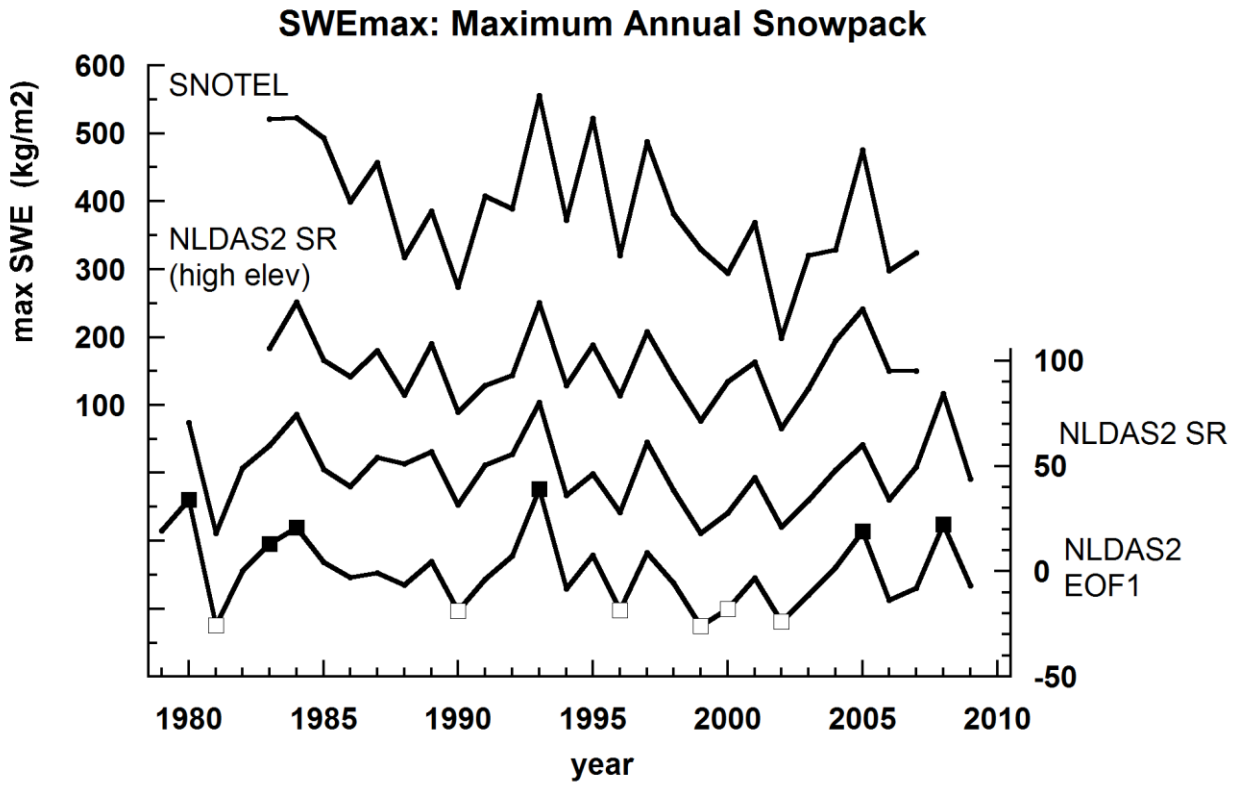

Figure 2. Time series of annual maximum SWE (kg/m^2) within the SR averaging area, derived in four different ways. From top to bottom: SNOTEL in situ data, averaged over twenty-two sites within the SR region; NLDAS-2 data, averaged over grid cells at high elevation consistent with the distribution of SNOTEL sites; NLDAS-2 data, averaged over the entire SR domain; the first EOF of NLDAS-2 annual maximum SWE of the entire FC study region shown in Fig. 1.

Black boxes on the EOF1 time series represent the six heaviest SWEmax years and white boxes represent the six lightest SWEmax years used for composite analysis.

Corresponding time series of the other snowpack metric, SWEmelt, are shown in Fig. 3. Each year's SWEmelt date is defined as the number of days into the water year (WY, starting on Oct 1) at which SWE is zero in any specific grid cell or observation site, and remains absent for seven days, after February 1 (which is day 123 in the WY). The SWEmelt value for an entire region is defined as the spatial average of the SWEmelt date at each individual grid cell in the region. There is a statistically significant (downward) linear trend in SR-averaged SWEmelt in the NLDAS-2 data (-5.8 days/decade) but not in SR SWEmelt from SNOTEL sites (-3.4 kg/m^2/ decade). NLDAS-2 and SNOTEL SWEmelt dates are poorly correlated (r = 0.42) compared to NLDAS-2 and SNOTEL SWEmax. Thus the spatial correlation of snowmelt dates is much smaller than the correlation of high and low snowpack years reflected in the SWEmax time series. The variation in trends shown in Fig. 3 indicates that the ongoing shift toward earlier

melt date is occurring first at lower elevations, which are better represented in the SR average compared to the network of exising SNOTEL sites.

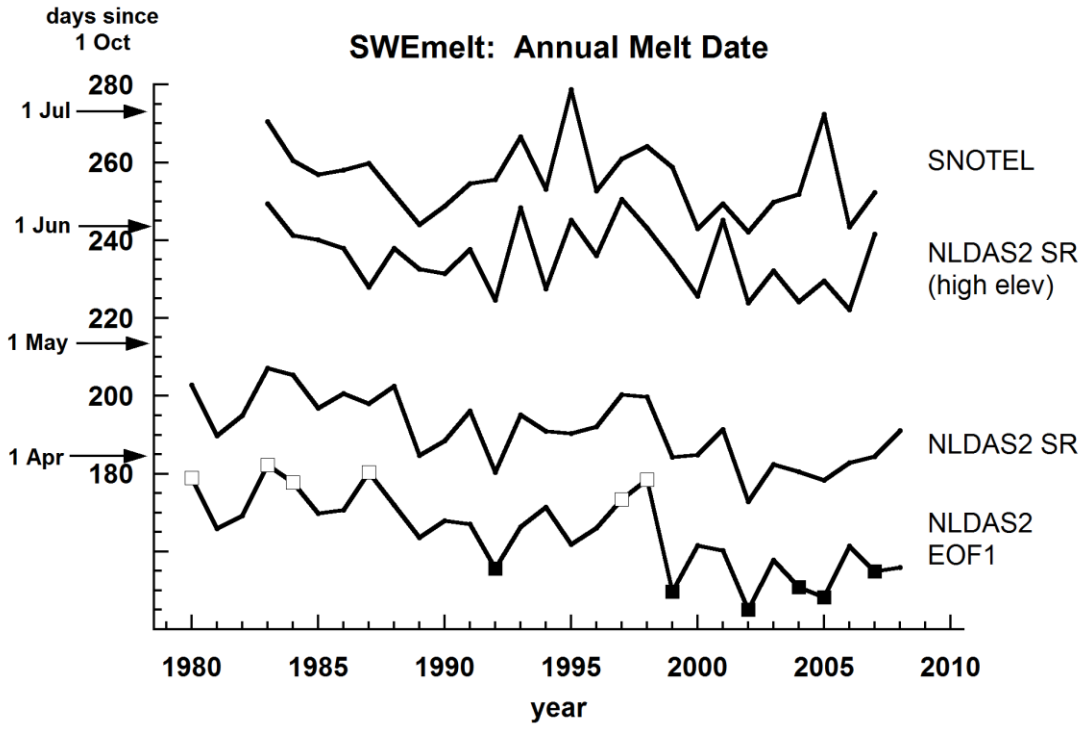

Figure 3. Time series of annual snow melt date (days since 1 October) within the southern Rockies averaging area, derived in four different ways. From top to bottom: SNOTEL in situ data, averaged over the twenty-two sites within the SR region; NLDAS-2 data, averaged over grid cells at high elevations corresponding to the SNOTEL sites; NLDAS-2 data, averaged over the entire SR domain; the first EOF of NLDAS-2 annual snow melt date of the entire study region shown in Fig. 1.

Black boxes on EOF1 represent the six latest years of SWEmelt and white boxes on EOF1 represent the six earliest years of SWEmelt, used for composite analysis of soil moisture anomalies.

The monsoon onset time series (Higgins 2007) exhibits considerable interannual variability with a modest tendency toward earlier onset (Fig. 4a). Detailed discussion of the dynamics of monsoon onset is beyond the scope of this paper; other studies (e.g. Ellis and Hawkins 2004) discuss summer monsoon dynamics associated with onset conditions in more detail. Current global models exhibit only modest skill in simulating onset conditions (Gutzler et al. 2009) and climate projections do not consistently show changes of one sign or another in onset date or total summer precipitation in New Mexico and the American Southwest (IPCC 2007). Model-based climate projections suggest that monsoon onset dates may get later as climate warms (Seth et al. 2011). However over the past two decades a weak trend toward earlier onset, about -2.45 days/ decade, is observed (Fig. 4a). This regression coefficient is not significantly different from zero.

The Spring season was calculated for each year starting with the regionally averaged snow ablation date, and ending with the regional monsoon onset date for that year (Fig 4b). For this

purpose we define the snowmelt date averaged over the entire Four Corners region; it includes considerably more low elevation area than the SR region so the melt date is somewhat earlier, however the variability and trend in the melt date are very similar averaged over SR or FC (Keller 2011). The trend toward earlier SWEmelt tends to lengthen the Spring dry season, while the trend toward earlier monsoon onset tends to shorten the Spring season. The SWEmelt trend is more pronounced so the overall trend in the NLDAS-2 data is for a lengthening of the Spring season. The magnitude of the trend in Spring season length is modest, about 2.25 days/decade, and is not statistically different from zero (Fig. 4b).

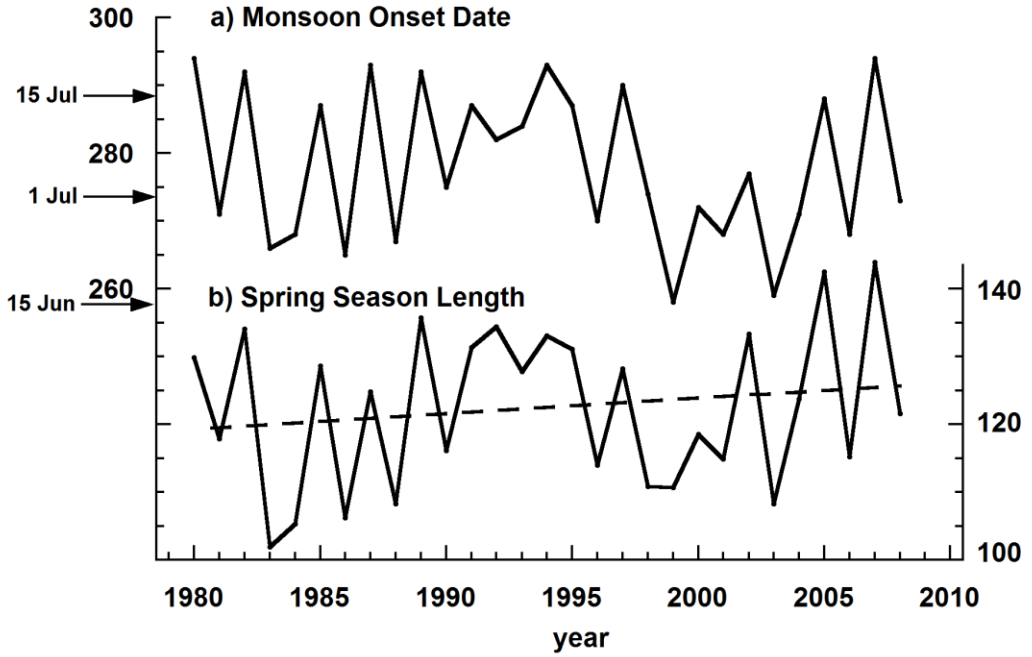

Figure 4. a) Time series of monsoon onset date at Albuquerque, NM (Higgins, 2007). Left and right ordinate labels denote the number of days since 1 October, with several calendar days relevant to monsoon onset date identified.

b) Difference between time series of SWEmelt averaged over the entire FC region, and monsoon onset at Albuquerque (Fig 4a). This difference is defined to be the duration (in days) of the spring season each year. Spring defined this way starts with snow melt and ends with monsoon onset. The dashed line indicates a best-fit linear trend of 2.25 days/decade toward a longer Spring season (not significantly different from zero).

Soil moisture averaged spatially over the entire FC region, and temporally over the Spring season, exhibits a statistically significant negative linear trend (-1.3 kg m^{-2}/decade, Fig. 5). The downward trend is not limited to the Spring season; we calculated linear trends separately for each calendar month (not shown; Keller 2011) and found decreasing soil moisture trends in every month. The Spring months of March, April and May are the months in which the linear trend is most pronounced in terms of the fraction of total interannual variance of soil moisture.

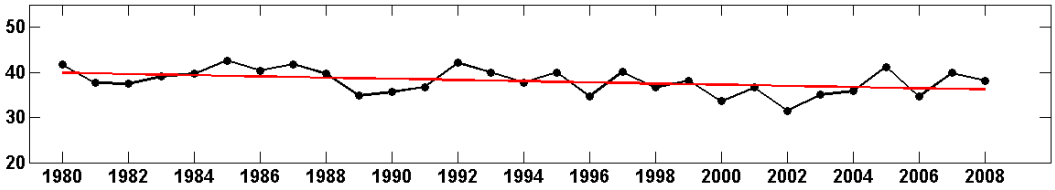

Figure 5. Time series of Spring season (post snow ablation and pre monsoon onset) mean surface soil moisture (kg/m^2) averaged over the Four Corners area. The red linear trend line fit to the area-averaged time series has a slope of -1.3 (kg m^{-2})/decade, which is statistically significant at the p=0.05 level.

Six years each of anomalously extreme low or high SWEmax or SWEmelt are defined from the first principal component of NLDAS-2 SWEmax or SWEmelt. These years, shown as open or filled squares in Figs. 2 and 3, are used to examine the persistence of soil moisture anomalies following high or low snowpack years.

We used composite analysis of pentad (5 day averaged) NLDAS-2 soil moisture in the upper layer (0-10 cm) to compare differences in soil moisture amount and timing between high and low SWEmax years (Fig. 6). Snowpack anomalies in the SR region are associated with pronounced soil moisture anomalies in the late winter; upper layer soil moisture is nearly one-third higher in the high SWEmax composite.

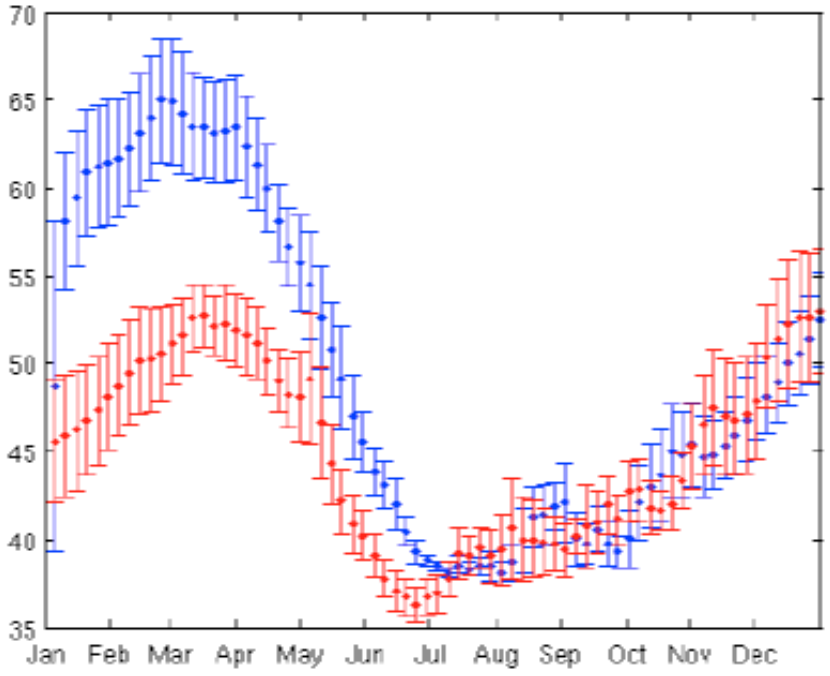

Figure 6. Pentad-average soil moisture (kg/m^2) in the southern Rockies averaged over the six years of highest (blue) and lowest (red) years of SWEmax. Error bars denote one standard error.

The soil moisture composite for high SWEmax years peaks in early March, about a half-month earlier than the corresponding peak in the low SWEmax composite. By April soil moisture in both composites is decreasing as snow melts throughout the region, snow extent decreases, and temperatures increase. After snow melt, the difference in soil moisture between high and low-SWEmax years persists as the surface dries out through the following Spring season, until soil moisture reaches its annual minimum value in early July.

The soil moisture minimum occurs about 15 days earlier in the low SWEmax composite (late June vs early July for high SWEmax composite). This difference is consistent with the known tendency for low snowpack anomalies to be followed several months later by early onset and above-average monsoon rainfall, and vice versa, during these decades (Gutzler 2000).

The effects of maximum SWE on soil moisture cease to exist by mid-July (Fig. 6). Monsoon onset effectively resets soil moisture in the Southern Rockies, so that the memory of the previous snow season (at least as captured in the upper layer of soil) is lost, and there is effectively no difference between the composites through the summer and autumn months. Soil moisture composited around high SWEmax in the SR region has an annual mean of 49±6 kg m^{-2}; the corresponding low SWEmax composite has an annual mean of 45±7 kg m^{-2}. But this relatively modest difference in annual means is entirely accounted for by soil moisture differences in the first half of the year.

Figure 6 indicates that snowpack anomalies appear to have a strong modulating influence on soil moisture that persists for several months after melt, throughout the Spring season. Thus these results provide some support for the concept that land surface anomalies associated with snowpack can persist through the Spring season and influence the development of the summer hydroclimatic regime in late June/early July (Gutzler 2000).

SUMMARY AND CONCLUSIONS

We have documented variability and trends in hydroclimatic variables over the 1979-2009 period of record. The NLDAS-2 assimilated data provide a basis for extending previous hydro-climatic studies to include land surface hydrologic variables, a critical component of observed and projected "drying" trends. With additional quantification of how the land surface behaves under changing climate conditions, we may be better able to anticipate future land surface variability and feedbacks and assess model projections with a better foundation of results from current climate change.

The principal new result is the documentation of are significant downward trends in spatially averaged snowpack and soil moisture in the NLDAS-2 data. These variables are exceptionally difficult to characterize using sparse in situ observations. The data provide direct evidence of an ongoing multivariate drying trend in the American Southwest.

In addition, we show that the NLDAS-2 data describe the tendency for persistence of the effects of anomalous snowpack throughout the Spring dry season after snowmelt. Since

decreases in high elevation snowpack have been clearly documented, our results tie the diminution of snowpack to the season when the surface hydrologic conditions are already dry. The results also provide support for previous studies postulating a delayed feedback effect of snowpack on the subsequent summer monsoon rainfall.

The time series of monsoon onset do not exhibit a positive trend (toward a later onset date), which has been recently suggested as another possible effect of Springtime drying. In this short data record the observed trend has been toward earlier onset, although the magnitude of the trend is not statistically significant. More intensive examination of monsoon onset conditions will be required to assess the delayed onset hypothesis in more detail.

We have not explicitly assessed projected future trends in surface hydrology, which are very pronounced in simulations generated by climate models forced by plausible 21st Century increases in greenhouse gases (Seager et al. 2008; Gutzler and Robbins 2011). The trends in NLDAS-2 data over the past 30 years suggest that the model-projected trends are in fact occurring in the current Springtime climate, as documented by numerous previous studies of snowpack. Our results extend the observational documentation of the impacts of ongoing climate change in the Southwest to the critical variable of Spring season soil moisture.

Acknowledgements. This research has been supported by the New Mexico Experimental Program to Stimulate Competitive Research (NM-EPSCoR). Dr. David Mocko was especially helpful in answering questions about the NLDAS-2 data. Drs. Dennis Lettenmaier and Brian Cosgrove provided advice about the soil moisture product in NLDAS-2.

LITERATURE CITED

Barnett, T.P., et al. 2008. Human-induced changes in the hydrology of the western United States. Science 319:1080-1083.

Brown, R., and P. Mote. 2009. The response of Northern Hemisphere snow cover to a changing climate. Journal of Climate 22:2124-2145. DOI 10.1175/2008JCLI2665.1.

Cayan, D. R. 1996. Interannual climate variability and snowpack in the western United States. J. Climate 9:928–948.

-----, T. Das, D. W. Pierce, T. P. Barnett, M. Tyree, and A. Gershunov. 2010. Climate change and water in southwestern North America special feature: Future dryness in the southwest US and the hydrology of the early 21st century drought. Proc. Natl. Acad. Sci. USA 107:21271-21276.

Christensen, N.S., A. Wood, N. Voisin, D. Lettenmaier, and R. Palmer. 2004. The effects of climate change on the hydrology and water resources of the Colorado River basin. Climatic Change 62: 37-363.

Das, T., H. G. Hidalgo, M. D. Dettinger, D. R. Cayan, D. W. Pierce, C. Bonfils, T. P. Barnett, G. Bala, and A. Mirin. 2009. Structure and detectability of trends in hydrological measures over the western United States. J. Hydrometeorology. 10:871-892.

Ek, M.B., et al. 2011. North American Land Data Assimilation System Phase 2 (NLDAS-2): Development and applications. GEWEX News 21(2):6-7.

Eltahir, E. A. B., and R. L. Bras. 1996. Precipitation recycling. *Rev. Geophys.*, **34,** 367-379.

Fischer, E.M. and S.I. Seneviratne. 2007. Soil moisture–atmosphere interactions during the 2003 European summer heat wave. *J. Climate,* **20,** 5081-5099.

Gutzler, D.S. 2000. Covariability of spring snowpack and summer rainfall across the Southwest United States. J. Climate 13:4018–4027.

-----, and J.W. Preston. 1997. Evidence for a relationship between spring snow cover in North America and summer rainfall in New Mexico. *Geophys. Res. Lett.,* **24,** 2207-2010.

-----, et al. 2009. Simulations of the 2004 North American Monsoon: NAMAP2. J. Climate 22: 6716-6740.

-----, and T. O. Robbins. 2011. Climate variability and projected change in the western United States: Regional downscaling and drought statistics. Climate Dyn. 37:835-849. DOI 10.1007/s00382-010-0838-7.

Hamlet, A. F., P. W. Mote, M. P. Clark, and D. P. Lettenmaier. 2005. Effects of temperature and precipitation variability on snowpack trends in the western United States. J. Climate 18:4545-4561.

Hansen, M.C., R.S. DeFries, J.R.G. Townshend and R. Sohlberg. 2000. Global land cover classification at 1 km spatial resolution using a classification tree approach. *Int. J. Remote Sensing,* **21,** 1331-1364.

Hurd, B.H., and J. Coonrod. 2008. Climate change and its implications for New Mexico's water resources and economic opportunities. *Tech. Rep. 45*, New Mexico State Univ. Agricultural Exp. Sta., 27 pp.

Keller, S. J. 2011. Trends and interannual variability in snowpack and Spring season hydroclimatology in the Southwest United States. Unpublished M.S. Thesis. The University of New Mexico, Albuquerque. 111 pp.

Knowles, N., M. D. Dettinger, and D. R. Cayan. 2006. Trends in snowfall versus rainfall in the western United States. J. Climate 19:4545–4559.

Koster, R.D., and M.J. Suarez. 1996. Energy and water balance calculations in the Mosaic LSM. NASA Technical Memo 104606. 9. 58 pp.

-----, and M.J. Suarez. 2001. Soil moisture memory in climate models. J. Hydrometeor. 2: 558–570.

Lo, F., and M.P. Clark. 2002. Relationships between spring snow mass and summer precipitation in the southwestern United States associated with the North American Monsoon system. J. Climate 15:1378–1385.

Mitchell, K.E., et al. 2004. The multi-institution North American Land Data Assimilation System (NLDAS): Utilizing multiple GCIP products and partners in a continental distributed hydrological modeling system. J. Geophys. Res. 109:D07S90. DOI:10.1029/2003JD003832.

Mote, P. W., A. F. Hamlet, and D.P. Lettenmaier. 2005. Variability and trends in mountain snowpack in western North America. Bull. Amer. Meteor. Soc. 86:39-49.

Pal, J., and E. A. B. Eltahir. 2001. Pathways relating soil moisture conditions to future summer rainfall within a model of the land-atmosphere system. J. Climate 14:1227-1242.

Pan, M., et al. 2003. Snow process modeling in the North American Land Data Assimilation System (NLDAS): 2. Evaluation of model simulated snow water equivalent, *J. Geophys. Res.*, **108,** 8850.

Reclamation. 2011. SECURE Water Act Section 9503(c) – Reclamation Climate Change and Water. Report to Congress 2011. U.S. Bureau of Reclamation, 206 pp.

Seager, R., et al. 2008. Model projections of an imminent transition to a more arid climate in southwestern North America. Science 316:1181-1184.

Seth, A., S. A. Rauscher, M. Rojas, A. Giannini and S J. Camargo. 2011. Enhanced spring convective barrier for monsoons in a warmer world? Climatic Change 104:403-414.

Stewart, T. 2009. Changes in snowpack and snowmelt runoff for key mountain regions. Hydrological Processes 23: 78-94. doi: 10.1002/hyp.7128.

Stewart, T., D. R. Cayan and M. D. Dettinger. 2005. Changes toward earlier streamflow timing across western North America. J. Climate 18:1136–1155.

Zhu, C., D. P. Lettenmaier, and T. Cavazos. 2005. Role of antecedent land surface conditions on North American monsoon rainfall variability. J. Climate 18:3104–3121.

CORRESPONDENCE SHOULD BE ADDRESSED TO:
David S. Gutzler
Dept. of Earth & Planetary Sciences
University of New Mexico MSC03-2040
Albuquerque, NM 87107
gutzler@unm.edu

WATER QUALITY DYNAMICS OF TWO HEAD WATER STREAMS AS INDICATED BY VARIATIONS IN NUTRIENT AND OTHER SOLUTE CONCENTRATIONS, PHYSICOCHEMICAL PARAMETERS AND DISCHARGE

Sebastian Medina[1]

Julie Trujillo[2]

Daryl Williams[2]

Maura Pilotti[3]

Edward A. Martinez[2*]

ABSTRACT

High elevation areas, such as the Valles Caldera National Preserve (VCNP) located in the Jemez Mountains of Northern New Mexico, have been described as exceptionally vulnerable to changes in climate and thus offer an ideal window to monitor temperature changes and their possible implications. In the present study, we examined the effects diurnal and seasonal temperature changes and discharge have on water quality. Two water sampling regimes (diurnal and grab samples) were employed over a one-year time frame (May 2010-May 2011) at four sites along two potentially vulnerable headwater streams located within the VCNP. Concentrations of primary nutrients (nitrate, nitrite, and phosphate) and other solutes (bromide, chloride, fluoride, and sulfate), along with discharge and physicochemical parameters (conductivity, dissolved oxygen, pH, and turbidity) served as indices of water quality. The results of this study indicated that primary nutrients and other solutes were largely sensitive to seasonal temperature changes, but that their sensitivity was modulated by the unique characteristics of sample sites. It was concluded that the examination of the effects of seasonal water temperature fluctuations on primary nutrient and other solute concentrations can offer a deeper understanding ofchallenges headwater streams may face as result of anticipated climate changes.

Warming trends associated with global climate change (GCC) are anticipated to have vast implications on the health and stability of streams and other aquatic ecosystems (Mulholland et al. 2009; Rieman & Isaak 2010; Strayer & Dudgeon 2010; Woodward et al. 2010). Specifically,

[1] Department of Biology and Chemistry, New Mexico Highlands University, Las Vegas, New Mexico, USA.
[2] Department of Natural Resource Management, New Mexico Highlands University, Las Vegas, New Mexico, USA.
[3] Department of Cognitive Science, New Mexico Highlands University, Las Vegas, New Mexico, USA.
[*]Corresponding author: eamartinez@nmhu.edu

warming trends have been linked to disruptions in water quality and quantity, including increased water temperatures, changes in precipitation patterns, timing of spring runoff, and increased frequency of flooding and drought (Frederick & Major 1997; Murdoch et al. 2000; Bates et al. 2008). Moreover, warming trends and related disruptions in water quality and quantity have been found to be associated with disturbances of aquatic ecosystems, including loss of biodiversity and species richness, and initiation of unpredictable alterations along the food web (Heino et al. 2009; Strayer& Dudgeon 2010).

Researchers have demonstrated that the water quality of a stream reflects the specific properties of the surrounding environment (Pejman 2009). Furthermore, water quality is regulated by natural processes and landuse changes (Garizi et al. 2011). Not surprisingly, seasonal variability in precipitation, runoff, ground water flow, abstraction and interception can have tremendous effects on stream discharge and consequently on concentrations of chemical constituents in the water (Garizi et al. 2011).

It has been reported that high elevation stream systems are amongst the most rapidly warming regions on the planet (Hassan et al. 2005). Consequently, the effects of warming trends may be particularly severe in high elevation areas of New Mexico, where such streams are a typical component of the landscape (Enquist&Gori 2008). Lenart& Crawford (2007) reported that since 1976 the average annual temperature in New Mexico has increased by 1.8˚F. Furthermore, the New Mexico Bureau of Geology and Mineral Resources projected that temperatures in New Mexico near the end of the century could increase by more than 5˚F in the winter and 8˚F in the summer (Gutzler 2007). According to Enquist&Gori (2008a) the Jemez Mountains, home of the VCNP, has experienced the greatest decrement in precipitation and the largest increment in temperature of any area in the state since the 1970's. Warmer temperatures will reduce mountain snowpack and peak spring runoff generated from snowmelt, resulting in periods of exceptionally low flow throughout the summer (State of New Mexico, Agency Technical Work Group 2005). This pattern of effects is of particular concern in the VCNP region of New Mexico where the majority of stream systems are dependent on snowpack to sustain flow throughout the summer and fall (State of New Mexico, Agency Technical Work Group 2005; Gutzler 2007; Enquist&Gori 2008).

Effects associated with altered precipitation patterns have been observed to limit the magnitude of winter snow accumulation and the timing of spring runoff generated from snowmelt (Barnett et al. 2005; Hamlet et al. 2005; Trenberth et al. 2007; Clow 2009). Alternative studies have also shown associations between temperature and the timing of peak flow events, such as spring runoff, in snowmelt dominated regions (Stewart et al. 2004; Regonda et al. 2005; Adam et al. 2009; Hidalgo et al. 2009). Spring runoff is the dominant hydrological event of high elevation stream systems and is of vital importance not only in sustaining flow throughout dry summer months, but also as a source of solutes (Williams et al. 2009).

Solutes are of vast importance in stream systems because they sustain the basis of the food web and often limit biological activity (Dodds 2002). It has been demonstrated that climate change factors can alter runoff patterns and quantity which may subsequently affect the availability of solutes (Minshall et al. 1983).

The objective of this research was to monitor the effects of water temperature on two VCNP head water streams in an attempt to gain a better understanding of nutrient and other solute dynamics in association with discharge and physicochemical parameters. The goal of this study

was twofold: First, we wanted to determine the extent to which water temperature changes were related to alterations in solute concentrations, discharge, and physicochemical parameters. Second, we set out to determine the influence of seasonal and diurnal water temperature changes on water quality, as defined by solute concentrations, discharge, and physicochemical parameters.

METHODS

Site Description

The VCNP (106˚33′23″ W, 35˚52′19″ N) is a 35,560-ha region located within the Jemez Mountain range of north-central New Mexico (Anschuetz&Thomas 2007). Established by the Valles Caldera Preservation Act of Congress in 2000, the VCNP is managed for grazing, hunting, conservation, and recreation (Liu et al. 2008). The regional climate is defined as semi-arid continental with an annual average precipitation of 62 cm as recorded from 2003 to 2007 at the Valle Grande weather station. VCNP is predominantly comprised of forested areas separated by a few vast meadows (VCNP State of New Mexico, Valles Caldera Trust 2009.). The geology of the VCNP basin reflects its volcanic history consisting of a unique and complex distribution of Paleozoic limestone, Quaternary alluvium, and other Quaternary volcanic deposits (Water Quality Control Commission 2006).

Seven streams incorporate approximately 121 km of perennial waterways that originate and meander through the VCNP (Water Quality Control Commission 2006; State of New Mexico, Valles Caldera Trust 2009). The headwaters of the 114-km^2 East Fork Jemez and 39-km^2 Jaramillo Creek subwatersheds originate within the VCNP boundary and drain southward. The Jaramillo Creek is a tributary to the East Fork Jemez stream, which later joins the Jemez River outside of the VCNP boundary (State of New Mexico, Valles Caldera Trust 2009).

Four sampling locations along these two streams were selected to represent the potential impacts of temperature change on water quality as indicated by primary nutrient and other solute concentrations, and by discharge and physicochemical parameters: the upper and lower portions of the East Fork (EFU and EFL) and Jaramillo streams (JCU and JCL; see pointers in Fig. 1). The Jaramillo originates and flows through a mostly forested area, eventually entering the Valle Grande. In contrast, the East Fork originates and flows through the open meadow of the Valle Grande.EFU (elevation, 2633 m) is located in the headwaters of the East Fork, while EFL (elevation, 2597m) is located below the confluence of the Jaramillo and East Fork streams. JCU (elevation, 2633m) is located near the headwaters of the Jaramillo, whereas JCL (elevation, 2608m) is located just before the confluence of the two streams.

The choice of the VCNP was largely based on it being located in an area of exceptional vulnerability to implications associated with climate change. Most studies have been limited to areas where human influence is probably a contributing factor to changes in concentrations, offering researchers an initial, albeit incomplete, understanding of temperature-driven alterations of primary nutrients and other solutes. It has been suggested that the study of temperature-driven alterations of primary nutrients and other solutes in pristine, high elevation areas can be critical to the understanding of the effects and implications of climate changes (Brooks 2009). To our knowledge, not many studies of primary nutrient and other solute concentrations have been conducted in aquatic ecosystems as vulnerable to climate changes and minimally affected by human activities as those of the VCNP.

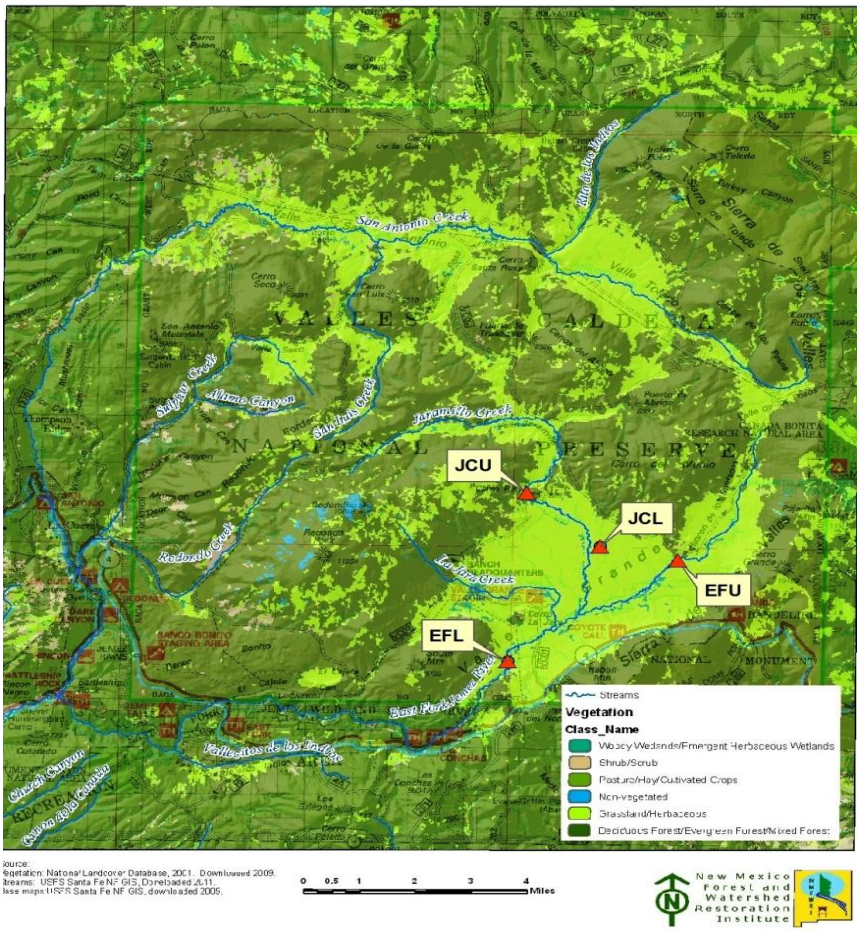

Figure 1: Valles Caldera National Preserve (106˚33′23″ W, 35˚52′19″ N) vegetation map (New Mexico Forest and Watershed Restoration Institute 2011).

Field Collection

Two sampling regimes were implemented from May 2010 to May 2011. Diurnal sampling was performed using model 3700 portable ISCO samplers (Teledyne Technologies, Lincoln, Nebraska, USA). Samplers were programmed to simultaneously collect water samples every hour, over a 24-hour period at the four sites, once a month for nine months. In addition, grab samples were taken monthly. Diurnal and grab samples collected from each site were stored on ice for transportation to the lab (~3 hrs.) and frozen (~ ≤1 week) prior to analysis. Water temperature was obtained utilizing HOBO Pendant Data loggers (Onset Computer, Cape Cod, Massachusetts, USA). A temperature logger was placed at each site on the stream bed to record temperature hourly for the entire year.Ambient temperature values for each collection date were obtained from Valles Caldera National Preserve headquarters weather station (http://www.wrcc.dri.edu/vallescaldera/).

Discharge in m^3/s for each stream was recorded at the time of grab sample collection and during diurnal sample collection utilizing a model 201D Marsh-McBirney portable water current meter (Marsh-McBirney, Gaithersburg, Maryland, USA) and a Rickly wading rod (Rickly Hydrological, Columbus, Ohio, USA), following U.S. Geological Survey methods (Olson & Norris 2007) . Additionally, physicochemical data (Dissolved Oxygen, pH, Turbidity, Specific

Conductivity, and Temperature) at each sample collection were obtained with an YSI model 6920 V2-2 sonde (YSI, Yellow Springs, Ohio, USA). Specific conductivity measurements taken from all sites were generally near the accuracy threshold of the YSI sonde (± 0.5% of measurement + 0.001 mS/cm).

Laboratory Analysis

Anion concentrations (Br^-, Cl^-, F^-, NO_3^-, NO_2^-, $PO_4^{3-}$and SO_4^{2-}) were determined by a Dionex Ion Chromatography System (ICS)-1000, AS40 automated sampler (Dionex, Sunnyvale, California, USA), utilizing an AS9-HC anion column and a ASRS self-regulating suppressor. Retention times and ionic signatures were determined according to the Dionex Quality Assurance Report serial number 18487.

All internal calibration verifications (ICV) and continuous calibration verifications (CCV) were prepared using multi element-CPI International Peak Performance standards. Both ICV's and CCV's encompassing the concentration range of samples (0.1-10 mg/L) were included in each method of analysis. The latter were performed on every 15 samples to ensure reliability of the instrument. All standards, reagents, and field blanks were prepared with 18 mega-ohm water from a Barnstead Easy Pure II UV/UF water purification system (Thermo Fisher Scientific, Waltham, Massachusetts, USA). The detection limit of the Dionex ICS-1000 was approximately 0.01 mg/L. Data were analyzed and recorded with Chromeleon 6.8 Chromatography Data System (Dionex, Sunnyvale, California, USA).

Statistical Analysis

Data were categorized according to Season (spring, summer, fall, and winter), Time of Day (day and night) and Site (EFU, EFL, JCU, and JCL). To better represent the actual seasonal patterns experienced by the VCNP region, seasons were conceptualized as follows: spring (April-May), summer (June-August), fall (September-October) and winter (November-March) (R. Parmenter, personal communication). Total solar radiation values, obtained from the Valles Caldera National Preserve headquarters weather station (http://www.wrcc.dri.edu/vallescaldera/), were used to classify data into day (>0.01 KW-hr/m^2) and night (<0.01 KW-hr/m^2). Variables were primary nutrient concentrations (nitrate, nitrite, and phosphate), other solute concentrations (bromide, chloride, fluoride, and sulfate), physicochemical parameters (conductivity, dissolved oxygen, pH, turbidity, and water temperature) and discharge.

A preliminary Factorial Analysis of Variance (ANOVA) was utilized to determine whether Season and Time of Day could be treated as reflecting water temperature changes. Post hoc Tukey's HSD comparisons were used to identify significant differences following a main effect or significant interaction.

Concentrations of primary nutrients and other solutes were at times below the detection limit (0.01 mg/L) of the ICS-1000 instrument and were not entered in the analyses.To ensure an adequate data set to conduct statistical analyses, all data for nutrients, other solutes, discharge, and physicochemical parameters, obtained from diurnal and grab sampling regimes were combined (N=515). Furthermore, to ensure the proper application of inferential statistics, non-parametric analyses were employed on all samples. Descriptive statistics for data entered into analyses are presented in Table 1. First, Spearman correlation was employed to determine the relationship between primary nutrient and other solute concentrations to changes in discharge and physicochemical parameters. Correlations were computed across sites and seasons to ensure

sufficient variability in the data spread. Second, the Kruskal Wallis test was used with Seasons as the factor to assess the effect of water temperature changes on concentrations of primary nutrients, other solutes, discharge, and physicochemical parameters at each site. The Kruskal Wallis test was also used to compare concentrations of primary nutrients, other solutes, discharge, and physicochemical parameters across sites at each of the selected seasons. Although day was warmer than night across all sites and seasons, Time of Day was excluded from the analyses described below as no significant effects on the selected dependent measures were observed. Descriptive statistics were used to show differences between/among seasons and sites as patterns of change, which are illustrated by means of graphs and tables. All analyses were considered significant at the 0.05 level.

Table 1: Descriptive statistics (sample size, mean, standard deviation and standard error of the mean) for primary nutrient and other solute concentrations entered into statistical analyses

Site		NO_2	NO_3	PO_4	S	Br	Cl	F
EFU	*n*	115	65	52	121	102	128	131
	M	0.80	0.10	0.30	1.65	0.02	2.34	0.63
	SD	0.56	0.14	0.41	0.44	0.05	3.00	0.22
	SE	0.05	0.02	0.06	0.04	0.01	0.3	0.02
EFL	*n*	79	26	51	109	61	112	115
	M	0.46	0.10	0.22	2.25	0.02	6.14	0.69
	SD	0.44	0.16	0.05	0.94	0.02	9.04	0.93
	SE	0.05	0.03	0.03	0.09	0	0.85	0.09
JCU	*n*	66	40	44	133	16	137	126
	M	0.21	0.03	0.33	2.49	0.05	0.70	0.09
	SD	0.23	0.08	0.26	0.53	0.17	0.60	0.05
	SE	0.03	0.01	0.04	0.05	0.04	0.51	0
JCL	*n*	80	54	46	113	31	112	108
	M	0.44	0.14	0.23	2.99	0.03	1.30	0.18
	SD	0.48	0.32	0.15	0.97	0.05	1.08	0.15
	SE	0.05	0.04	0.02	0.09	0	0.1	0.01

RESULTS

Preliminary Analysis: Water Temperature

As expected, for all sites water temperature was highest in the summer and lowest in the winter both during the day and at night (Fig. 2). Most sites (EFL, JCU and JCL) exhibited similar patterns of temperature across seasons. Specifically, water temperature increased from spring to summer, and decreased from summer to winter almost linearly. In contrast, EFU exhibited rather stable water temperature values across seasons for both day and night samplings (Fig., 2). From spring to fall, temperatures at EFU and EFL tended to be consistently higher in the day than at night, whereas minor or no differences were found between day and night at JCU and JCL. Water temperature results indicate that Season and Time of Day could be used to represent changes in water temperature (Table 2).

Correlations for All Sample Data

Primary nutrients did not react uniformly to changes in physicochemical parameters and discharge, both in terms of type of response (increment *vs.* decrement) and its magnitude (as illustrated by the percentage of shared variance) (Table 3). With the exception of nitrate, no primary nutrients or other solutes significantly correlated with discharge. A uniform response to increasing temperature was accompanied by declines in concentrations of primary nutrients and other solutes. Water temperature exhibited significant correlations with two primary nutrients (nitrite and phosphate), and with two other solutes (bromide and chloride).

Differences across Seasons within Sites

Descriptive statistics for concentrations of primary nutrients (nitrate, nitrite, and phosphate), other solutes (bromide, chloride, fluoride and sulfate), discharge, and physicochemical parameters (conductivity, dissolved oxygen, pH, turbidity and water temperature) across seasons at each site were computed. Patterns of seasonal change were detected for most dependent measures at each site, with several patterns showing significant changes (Fig. 3 panels a-f).

At EFU, significant seasonal fluctuations were observed for all primary nutrients and other solutes. Similarly, at EFL, significant seasonal fluctuations were observed for all nutrients and other solutes with the exception of nitrate and nitrite. At JCU, significant fluctuations were detected for all concentrations with the exception of bromide, nitrate and phosphate. At JCL, all primary nutrients and other solutes with the exception of bromide fluctuated significantly between seasons. Discharge fluctuated seasonally only at the JCU and JCL sites, whereas pH fluctuated at EFL and JCL (Table 4).

Table 2:Water temperature: main effects and interactions involving season, time of day and site

Effects	*df*	*F*	*P*-Value
Season	3	25194	<0.001
Time of Day	1	551	<0.001
Site	3	896	<0.001
Season X Time of Day	3	37	<0.001
Season X Site	9	2122	<0.001
Time of Day X Site	3	115	<0.001
Season X Time of Day X Site	9	14	<0.001

Table 3: Correlations between anion concentrations, discharge and physicochemical parameters across seasons and sites[a]

	Conductivity	Discharge	Dissolved Oxygen	pH	Turbidity	Water Temp
Nitrate	*ns*	-0.323 (10%)	-0.367 (13%)	*ns*	-0.587 (34%)	*ns*
Nitrite	*ns*	*ns*	*ns*	*ns*	+0.543 (29%)	-0.246 (6%)
Phosphate	*ns*	*ns*	*ns*	*ns*	*ns*	-0.176 (3%)
Bromide	+0.438 (19%)	*ns*	-0.431 (18%)	-0.360 (13%)	-0.495 (24%)	-0.216 (5%)
Chloride	+0.361 (13%)	*ns*	*ns*	*ns*	*ns*	-0.084 (1%)
Fluoride	+0.524 (27%)	*ns*	-0.301 (9%)	*ns*	- 0.409 (18%)	*ns*
Sulfate	-0.565 (32%)	*ns*	*ns*	*ns*	+0.661 (43%)	*ns*

[a]Percentage of shared variance is reported for each significant correlation in parenthesis

Table 4:*P*-values indicating significantly different average anion concentrations, discharge and physicochemical parameters across seasons at each site

	Nitrate	Nitrite	Phosphate	Sulfate	Bromide	Chloride	Fluoride
EFU	0.002	<0.001	0.001	<0.001	0.018	<0.001	<0.001
EFL	*ns*	*ns*	0.001	<0.001	0.004	<0.001	<0.001
JCU	*ns*	0.037	*ns*	<0.001	*ns*	<0.001	<0.001
JCL	<0.001	<0.001	0.001	0.019	*ns*	<0.001	0.042

	Conductivity	Discharge	Dissolved Oxygen	pH	Turbidity	Water Temp
EFU	*ns*	*ns*	*ns*	*ns*	*ns*	0.001
EFL	*ns*	*ns*	*ns*	0.015	*ns*	<0.001
JCU	*ns*	0.034	*ns*	*ns*	*ns*	<0.001
JCL	*ns*	0.042	*ns*	0.029	*ns*	<0.001

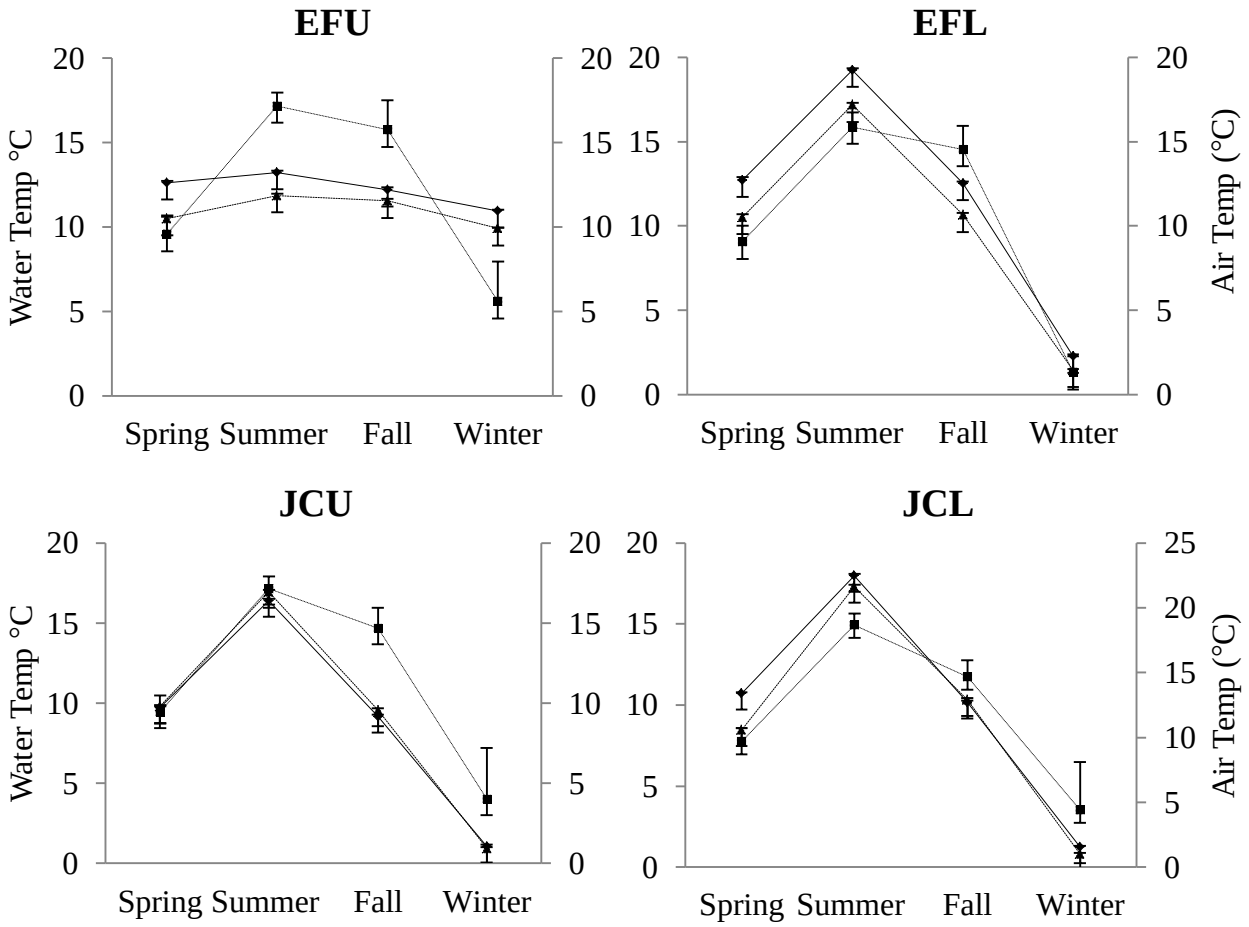

Figure 2: Means and standard errors for air and water temperature (°C) as a function of Season and Time of Day (day water: solid line, night water: dashed line and air: dotted line) at each site (EFU, EFL, JCU, and JCL) (VCNP, headquarters weather station, http://www.wrcc.dri.edu /vallescaldera/). Water temperature and air temperature share common axes.

Figure 3 (panels A-F): Primary nutrients and other solutes as a function of Season at each site (EFU, EFL, JCU, and JCL). Panels share common axes for discharge, physicochemical parameters, primary nutrients and other solutes.Nutrient and other solute concentrations are represented by the following symbols: Nitrate (*); Nitrite (x); Phosphate (●); Bromide (♦); Chloride (■); Fluoride (▲); Sulfate (+). Physicochemical parameters or discharge are displayed by the dotted line.

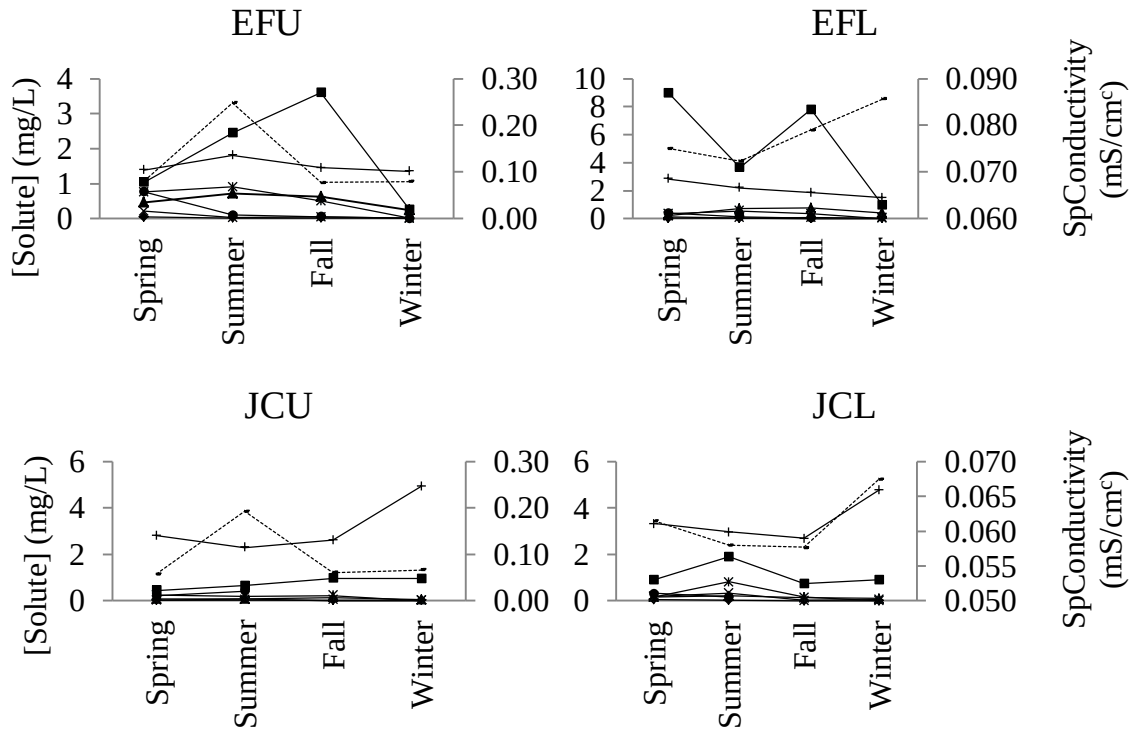

Figure 3A:Anions *versus* Conductivity

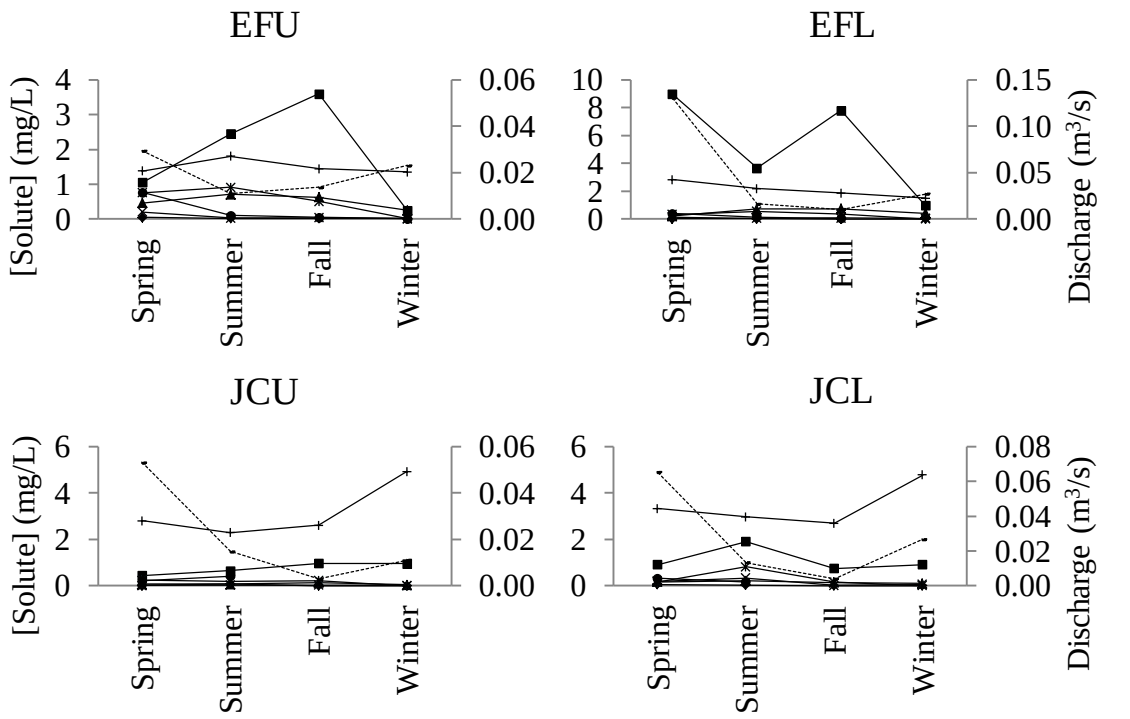

Figure 3B: Anions *versus* Discharge

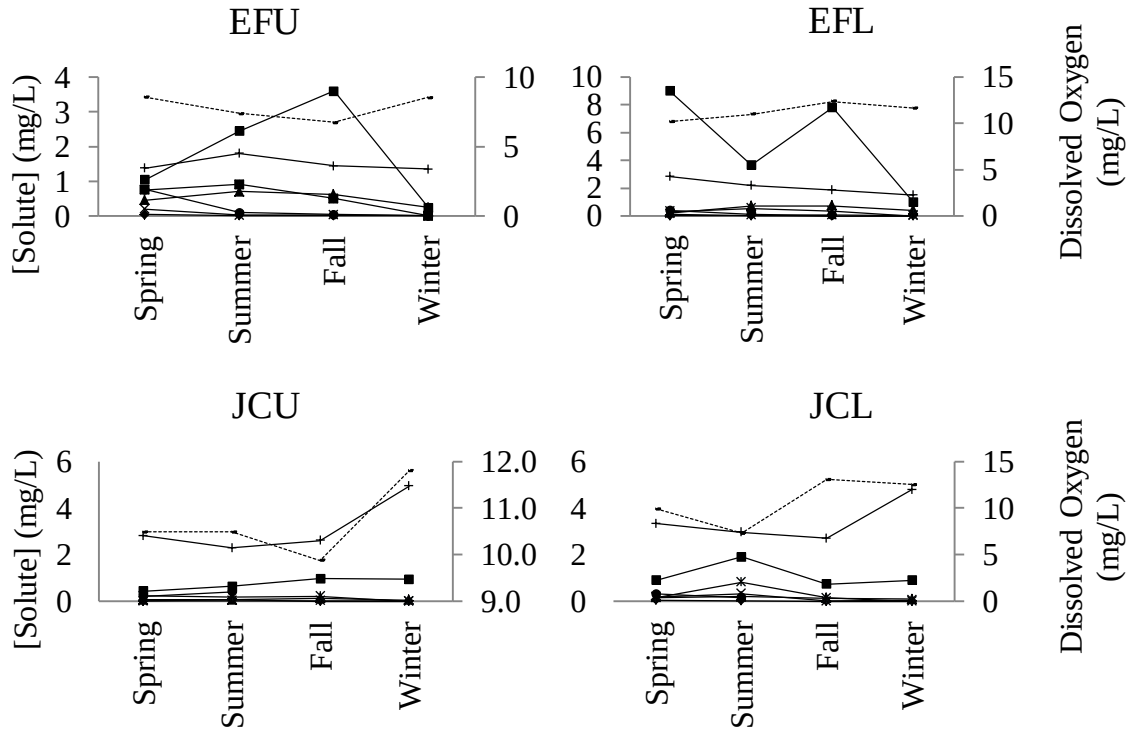

Figure 3C: Anions *versus* Dissolved Oxygen

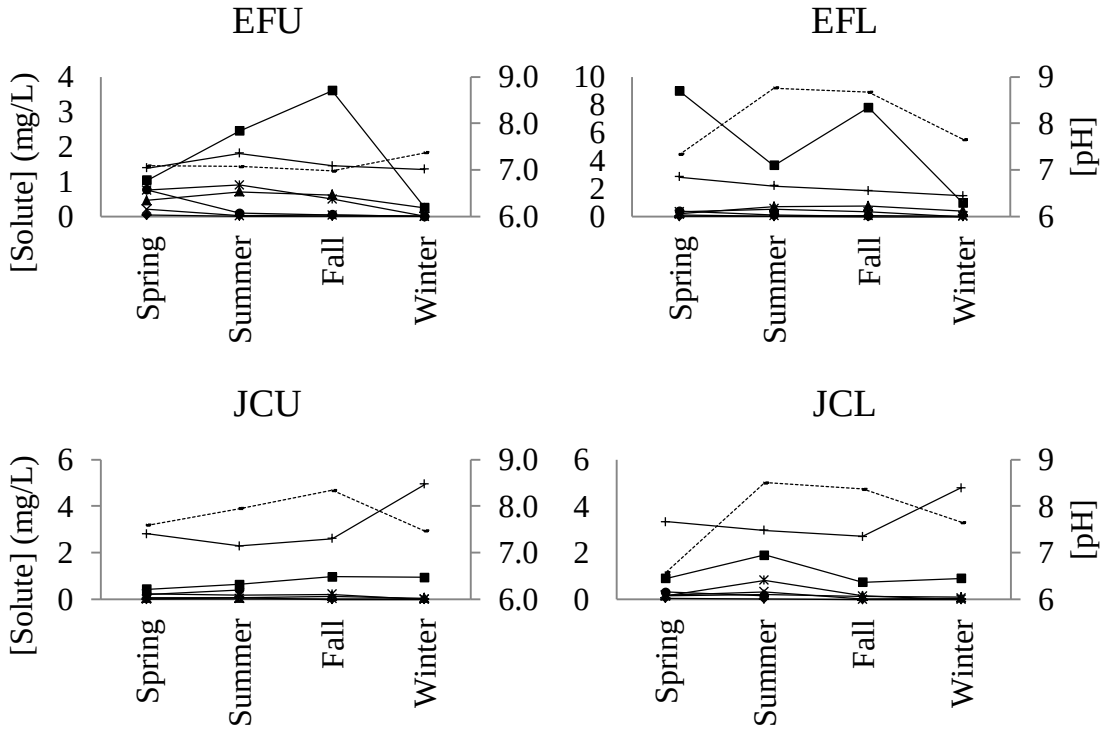

Figure 3D: Anions *versus* pH

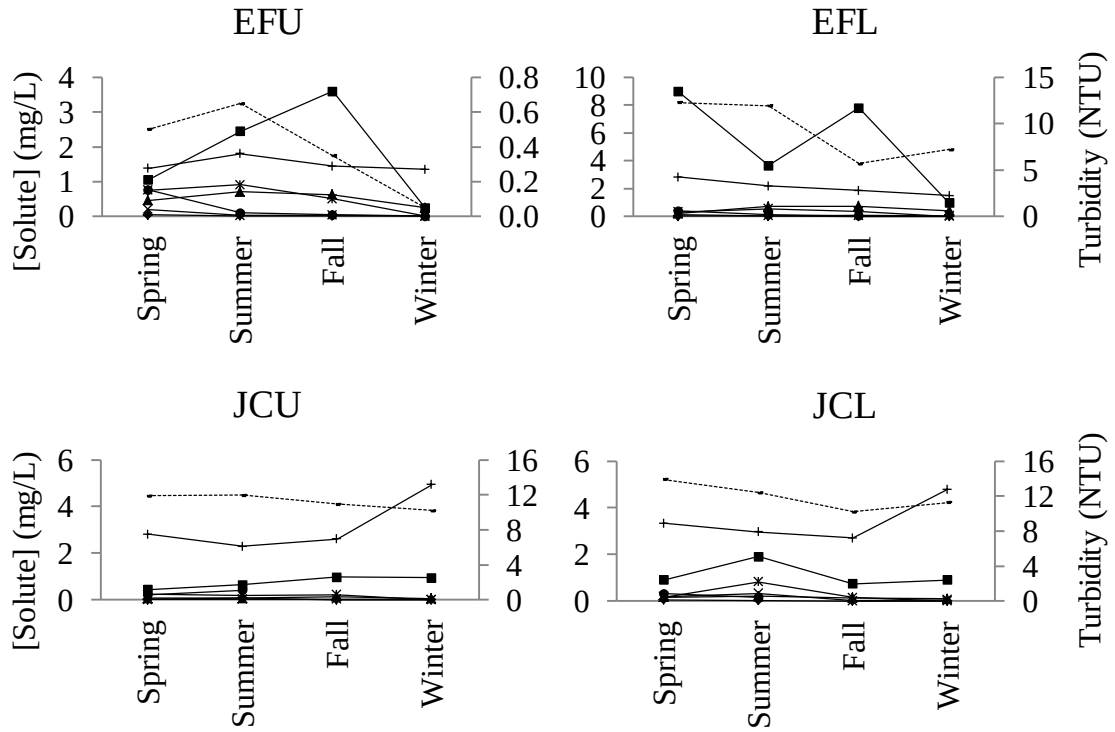

Figure 3E: Anions *versus* Turbidity

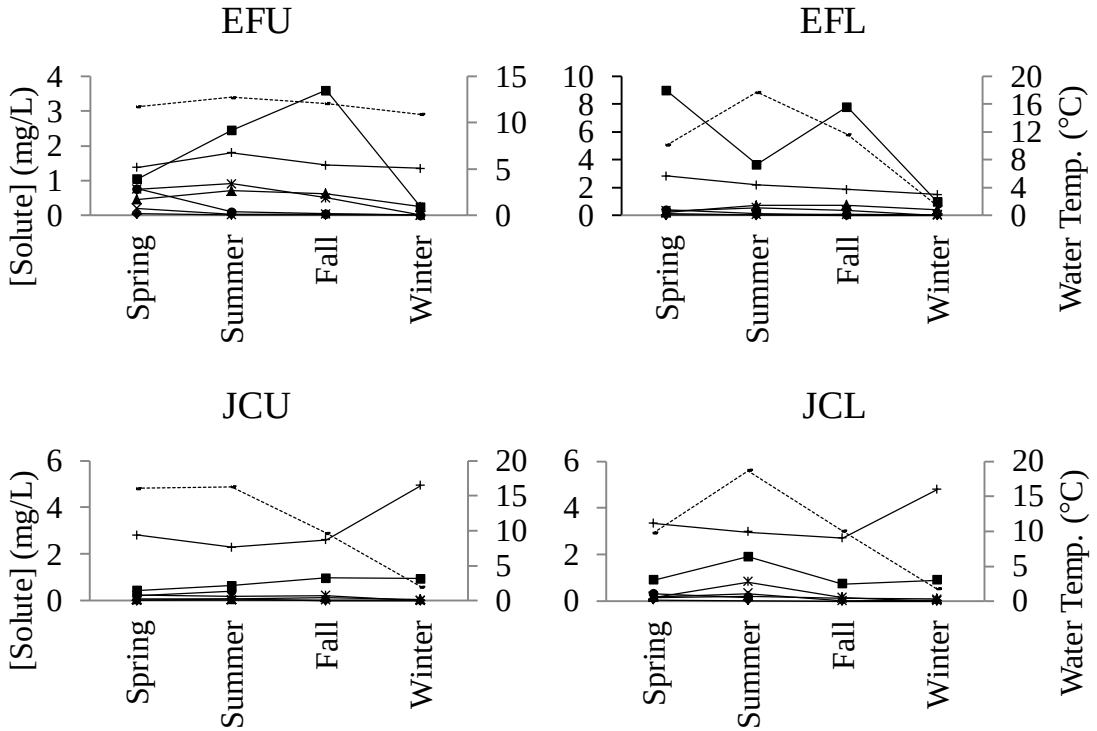

Figure 3F: Anions *versus* Water Temperature

Differences across Sites within Seasons

During the spring, there were significant changes across sites in all primary nutrients and solutes with exception of bromide. In the summer, there were significant changes in all primary nutrients and other solutes. In the fall, there were fluctuations in all primary nutrients with the exception of phosphate, and in all other solutes. In the winter, however, there were no significant changes in primary nutrients or other solutes across sites. No significant changes were observed among discharge seasonally across sites. Conductivity and dissolved oxygen changed during the fall, whereas pH changed significantly in both summer and fall (Table 5).

Table 5:*P*-values indicating significantly different average anion concentrations, discharge and Physicochemical Parameters Across Sites for Each Season

	Nitrate	Nitrite	Phosphate	Sulfate	Bromide	Chloride	Fluoride
Spring	<0.001	0.001	0.005	<0.001	*ns*	<0.001	<0.001
Summer	<0.001	0.001	0.001	<0.001	<0.001	<0.001	<0.001
Fall	0.003	<0.001	*ns*	<0.001	<0.001	<0.001	<0.001
Winter	*ns*	*ns*	*ns*	*ns*	*ns*	*ns*	*ns*

	Conductivity	Discharge	Dissolved Oxygen	pH	Turbidity	Water Temp
Spring	*ns*	*ns*	*ns*	*ns*	*ns*	<0.001
Summer	*ns*	*ns*	0.036	0.002	*ns*	<0.001
Fall	0.012	*ns*	0.033	0.035	*ns*	*ns*
Winter	*ns*	*ns*	*ns*	*ns*	*ns*	*ns*

DISCUSSION

Diurnal and Seasonal Water Temperature

Temperature changes diurnally and seasonally were as expected for all sites. Overall, day temperatures were higher than night temperatures across seasons, but such differences were not statistically significant for all sites. In addition, all sites were warmer in the spring than in the fall. Seasonal temperatures were statistically different at all sites except at EFU (Fig. 2). At the EFU site, temperature fluctuations were diminished by groundwater entering the stream. This could account for the stable temperatures found at this site diurnally and across seasons. It was also found that nutrient and other solute concentrations as well as physicochemical parameters were more stable at this site than at the other sites, highlighting the influence of temperature on nutrient concentrations and all other parameters. Consistent with this observation, Holmes (2000) reported that ground water inputs can have a moderating effect on water temperature and more subtly can contribute to changes in nutrient and solute concentrations of the surrounding stream water. These contributions could explain why EFU maintained more stable nutrient and solute concentrations across seasons whereas EFL, JCU, and JCL experienced more drastic, variable, changes as seasons progressed.

On average, the JCU site was colder diurnally and across all seasons than the EFU, EFL, and JCL sites. The location and morphology of the JCU site might account for this finding. The Jaramillo Creek originates on the north slope of the peak named *Redondito* and runs through a forested area and eventually through the Valle Jaramillo meadow which is also on the northern aspect of the *Cerro de Medio*. The JCU site is located on the northern side of the forested area and receives less sunlight than the other study sites. Additionally, the JCU site is narrow and the deepest of all study sites.

Temperature and Primary Nutrients

The finding that concentrations of primary nutrients and other solutes declined as temperature increased is not unusual (Table 3). Most water quality researchers claim that increments in water temperature promote biological activity and thus can reduce the availability of nutrients (Dodds 2002; Fellows et al. 2006; Rieman&Isaak 2010). In support of this claim, water temperature, in the present study, was negatively correlated with primary nutrients and a broad spectrum of the other solutes. Yet, the percentage of variability in nutrient and other solute concentrations accounted for by water temperature was rather limited (range: 1%-6 %), suggesting that other factors besides temperature might be responsible for fluctuations in these concentrations, including vegetation, geology, and groundwater contributions.

Primary Nutrients and Discharge

Although the finding that primary nutrient and other solute concentrations tended to fluctuate in concert is not unusual (Piatek et al. 2009), the lack of a relationship between discharge and concentrations of a variety of solutes may at first appear uncommon. Yet, the available evidence illustrates variability in the relationship between discharge and solutes, with some studies reporting relationships of different magnitude and direction, while others finding no relationship (Meyer et al. 1988; Chantal Gascuel-Odoux et al. 2010). The variability in the relationship between discharge and solutes may be attributed to site specific differences. For example, EFU is highly influenced year round by spring water entering the stream at its headwaters. Additionally the entire length of the East Fork stream flows through the Valle Grande meadow. It is highly

probable that the stream is gaining groundwater along its path as evidenced by a higher cumulative average discharge at the EFL site (0.64 m^3/s) when compared to that of the combined cumulative average discharge from EFU and JCL (0.52 m^3/s), the two main sources of discharge entering the EFL site. This fact could also explain why all variables (except turbidity) were highest at the furthest downstream site, EFL. Even though JC appears to be minimally affected by groundwater, the influence of groundwater on nutrient dynamics, for both of these streams at time of collection, may be stronger than the influence of runoff as expressed in increased discharge. Figure 3-panel B shows that discharge decreased from spring to fall and then increased from fall to winter. These findings were expected for this region, as snow melt and spring runoff diminishes into the summer, base flow remains stable until the early fall-monsoonal season. The average precipitation for our study time period, as recorded by the VCNP weather station, corroborates these findings. However, the small differences in discharge and perhaps limited measurements recorded in our study indicate that sampling did not occur immediately after a big storm event. Rather the data indicate a gradual decrease from spring to fall and a quicker increase from fall to winter.

Primary Nutrients and Seasons

Arheimer et al. (1996) and Piatek et al. (2009), reported that expected variable relationships may vary significantly in the same research between different sampling sites, as exemplified by nitrate concentrations in their studies. The present investigation found that seasonal temperature changes influenced concentrations of most primary nutrients and other solutes, but not consistently across sites. Nevertheless, seasonal changes were observed at for all primary nutrients and other solutes.

The proportion of variance explained by water temperature was rather small across sites, including EFU. The unique characteristics of the different sites may contribute to this outcome. In addition to the complex groundwater system of largely unidentified springs, differences in vegetation and geology between sites may account for the variability of nutrient concentrations across seasons. In general, primary nutrients declined from high concentrations in the cold seasons to low concentrations in the warm seasons. These findings are consistent not only with nutrient uptake by biological activity during the warmer seasons, but also with allochthonous input of organic matter. In general, nutrient concentrations were higher during the spring when runoff occurs. In addition, the JCU site had slightly overall higher primary nutrient concentrations in the fall, which could be explained by its forested origin and higher contribution of allochthonous organic matter. The absence of an increase in nutrient concentrations could possibly be due to the biological activity scavenging nutrients as they became available. For example, even though the EFL site should have expressed cumulative primary nutrient concentrations because it is the furthest downstream site, it did not. The morphology of EFL might account for this null finding. EFL was wider, shallower and warmer than the upper East Fork and Jaramillo Creek sites.

CONCLUSIONS

Findings of this investigation suggest that if temperature in the Jemez region continues to rise as projected, nutrient and other solute cycles may be considerably impacted by alterations of water temperature. Decreased snowpack and altered magnitude and timing of subsequent runoff, which provide a significant portion of solutes in aquatic ecosystems, are two of the many ways in which the abundance and distribution of solutes may be altered. These events can have severe effects on

the health and stability of aquatic ecosystems, especially those in high elevation areas such as the VCNP. Studies investigating the dynamics of solute cycling in areas vulnerable to GCC are essential to increase the predictive validity of models of the effects of GCC on water quality.

In conclusion, the present study illustrates not only the challenges of investigations of high-elevation streams, but also their usefulness for understanding the extent to which aquatic ecosystems can be modified by variations in temperature, when the effects of such variations are unlikely to have been altered by human activities. If it is assumed that the fine-grained patterns of relations between biological activity and small scale temperature fluctuations (as those associated with seasonal cycles), can be used to estimate larger scale fluctuations (as those attributable to GCC), then the results of the present investigation offer an example of how the study of seasonal temperature changes can serve as a proxy for the study of the effects of GCC.

ACKNOWLEDGEMENTS

This research was supported largely by New Mexico EPSCoR-National Science Foundation (Grant No. 0814449). We would like to recognize Dr. Abdul-Mehdi S. Ali for assistance in data processing and Leona DeSanto for assistance in data collection. We would also like to thank Robert Parmenter and the Valles Caldera National Preserve for providing valuable insight and also for allowing access to conduct field collections.

LITERATURE CITED

Adam, J.C., A.F. Hamlet, and D.P. Lettenmaier. 2009. Implications of global climate changefor snow melt hydrology in the twenty-first century. Hydrological Processes23:962-972.

Anschuetz, K. F., and M. Thomas. 2007. More than a scenic mountain landscape: Valles Caldera National Preserve land use history. Gen. Tech. Rep. RMRS-GTR-196.Fort Collins, CO, U.S. Department of Agriculture.Forest Service.Rocky Mountain Research Station.277 pp.

Arheimer, B., L. Andersson, and A. Lepistö. 1996. Variation of nitrogen concentration in streams-influences of flow, seasonality and catchment characteristics. Journal of hydrology179:281-304.

Barnett, T.P., J.C. Adam, and D.P. Lettenmaier. 2005. Potential impacts of a warming climate on water availability in snow-dominated regions. Nature 438:303-309.

Bates, B.C., Z.W. Kundzewicz, S. Wu and J.P. Palutikof (Eds.). 2008. Climate Change and Water, Technical Paper of the Intergovernmental Panel on Climate Change, IPCC Secretariat, Geneva. 210 pp.

Brooks, R.T. 2009. Potential impacts of global climate change on the hydrology and ecology of ephemeral freshwater streams of the forests of the northeastern United States. Climatic Change 95:469-483.

Clow, D.W. 2009. Changes in the timing of snowmelt and stream flow in Colorado: a response to recent warming. Journal of Climate23:2293-2306.

Dodds, W.K. 2002. Freshwater ecology: concepts and environmental applications. Academic Press. San Diego.

Enquist, C.A.F., and D.F. Gori. 2008. A Climate Change Vulnerability Assessment for Biodiversity in New Mexico, Part I: Implications of Recent Climate Change on Conservation Priorities in New Mexico. The Nature Conservancy.69 pp.

Fellows, C. S., H. M. Valett, C. N. Dahm, P. J. Mulholland, and S. A. Thomas. 2006. Coupling nutrient uptake and energy flow in headwater streams. Ecosystems9:788-804.

Frederick, K.D., and D.C. Major. 1997. Climate change and water resources. Climate Change 37:7-23.

Garizi, A.Z., V. Sheikh, and A. Sadoddin. 2011. Assessment of seasonal variations of chemical characteristics in surface water using multivariate statistical methods. International Journal of Environmental Science and Technology8:581-592.

Gascuel-Odoux, C., P. Aurousseau, P. Durand, L. Ruiz, and J. Molenat. 2010. The role of climate on inter-annual variation in stream nitrate fluxes and concentrations. Science of the Total Environment408:5657-5666.

Gutzler, D.S. 2007. New Mexico Bureau of Geology and Mineral Resources, New Mexico Tech, Climate change and water resources in New Mexico. New Mexico Earth Matters.1-6.

Hamlet, A.F., P.W. Mote, M.P. Clark, and D.P. Lettenmaier. 2005. Effects of temperature and precipitation variability on snowpack trends in the western United States. American Meteorological Society18:4545-4561.

Hassan, R, R. Scholes, and N. Ash (Eds.). 2005. Ecosystems and human well-being: current state and trends. Island Press. Washington, D.C.

Heino, J., R. Virkalla, and H. Toivonen. 2009. Climate change and freshwater biodiversity: detected patterns, future trends and adaptations in northern regions. Biological Reviews 84:39-54.

Hidalgo, H.G., T. Das, M.D. Dettinger, D.R. Cayan, D.W. Pierce, T.P.Barnett, G. Bala, A. Mirin, A.W. Wood, C. Bonfils, B.D. Santer, and T.Nozawa. 2009. Detection and attribution of streamflow timing changes to climate change in the western United States. Journal of Climate 22:3838-3855.

Holmes, R.M. 2000.The importance of ground water to stream ecosystem function, in Streams and ground waters, edited by J. Jones and P. Mulholland. pp. 137-148. Academic Press. San Diego.

Lenart, M. and B. Crawford. 2007. Global warming in the southwest: an overview, in Global warming in the Southwest: projections, observations, and impacts. Climate Assessment for the Southwest (CLIMAS), edited by M. Lenart.University of Arizona. pp. 2-5. Available at http://geo.ispe.arizona.edu/climas/publications/pdfs/GWSouthwest.pdf.

Liu, F., R. Parmenter, P.D. Brooks, M.H. Conklin, and R.C. Bales. 2008. Seasonal and interannual variation of streamflow pathways and biogeochemical implications in semi-arid, forested catchments in Valles Caldera, New Mexico. Ecohydrology1:239-252.

Meyer, J.L., W.H. McDowell, T.L. Bott, J.W. Elwood, and C. Ishizaki. 1988. Elemental dynamics in streams. Journal of the North American Benthological Society 7:410-432.

Minshall, G.W., R.C. Peterson, K.W. Cummins, T.L. Bott, and J.R. Sedell. 1983. Interbiome comparison of stream ecosystem dynamics. Ecological Monographs53:1-25.

Mulholland, P.J., B.J. Roberts, W.R. Hill, and J.G. Smith. 2009. Stream ecosystem responses to the 2007 spring freeze in the southeastern United States: unexpected effects of climate change. Global Change Biology15:1767-1776.

Murdoch, P.S., J.S. Baron, and T.L. Miller. 2000. Potential effects of climate change on surface-water quality in North America. Journal of the American Water Resources Association 36:347-366.

New Mexico Forest and Watershed Restoration Institute, cartographer. 2011. Valles Caldera Vicinity (Vegetation Map). New Mexico Forest and Watershed Restoration Institute. Las Vegas, New Mexico.

Olson, S. A., and M. Norris. 2007. U.S. Department of Interior, U.S. Geological Survey. U.S. Geological Survey streamgaging...from the national streamflow information program.Fact Sheet 2005-3131.Available at http://pubs.usgs.gov/fs/2005/3131/FS2005-3131.pdf.

Pejman, A.H., G.R. NabiBidhendi, A.R. Karbassi, N. Mehrdadi, and M. EsmaeiliBidhendi. 2009. Evaluation of spatial and seasonal variations in surface water quality using multivariate statistical techniques. International Journal of Environmental Science and Technology.6:467-476.

Piatek, K. B., S. F. Christopher, and M. J. Mitchell. 2009. Spatial and temporal dynamics of stream chemistry in a forested watershed. Hydrology and Earth System Sciences.13:423-439.

Rieman, B. E., D.J. Isaak. 2010. Climate change, aquatic ecosystems, and fishes in the Rocky Mountain West: implications and alternatives for management. Gen.Tech. Rep. RMRS-GTR-250.Fort Collins, CO. U.S. Department of Agriculture, Forest Service.Rocky Mountain Research Station.46 pp.

Regonda, S.K., B. Rajagopalan, M. Clark, and J. Pitlick. 2005. Seasonal cycle shifts in hydroclimatology over the western United States. Journal of Climate.18:372-384.

State of New Mexico, Agency Technical Work Group. 2005. Potential effects of global climate change on New Mexico. Available at http://www.nmenv.state.nm.us/aqb/cc/ Potential_ Effects_ Climate_Change_NM.pdf.

State of New Mexico, Valles Caldera Trust. 2009. Environmental assessment multiple use and sustained yield of forage resources. Available at http://www.vallescaldera.gov.

Stewart, I.T., D.R. Cayan, and M.D. Dettinger. 2004. Changes toward earlier streamflow timing across western North America. Journal of Climate18:1136-1155.

Strayer, D.L., and D. Dudgeon. 2010. Freshwater biodiversity conservation: recent progress and future challenges. Journal of the North American Benthological Society29:344-358.

Trenberth, K.E., P.D. Jones, P. Ambenje, R. Bojariu, D. Easterling, A. Klein Tank, D. Parker, F.

Rahimzadeh, J.A. Renwick, M. Rusticucci, B. Soden and P. Zhai. 2007. Observations: Surface and Atmospheric Climate Change, in Climate Change 2007: The Physical Science Basis. Contribution of Working Group I to the Fourth Assessment Report of the Intergovernmental Panel on Climate Change, edited by S. Solomon et al. Cambridge University Press. Cambridge, United Kingdom and New York, NY.

Valles Caldera National Preserve Climate Stations.Retreived September 23, 2011, from http://www.wrcc.dri.edu/vallescaldera/

Water Quality Control Commission. 2006. Total maximum daily load for the Jemez River Watershed East Fork Jemez River and Jaramillo creek. Available at http://www.nmenv.stateC.E..nm.us/swqb/VallesCaldera/.

Williams, M.W., C. Seibold, and K. Chowanski. 2009. Storage and release of solutes from a subalpine seasonal snowpack: soil and stream water response. Biogeochemistry95:77-94.

Woodward, G., D.M. Perkins, and L.E. Brown. 2010. Climate change and freshwater ecosystems: impacts across multiple levels of organization. Philosophical Transactions of the Royal Society B365:2093–2106.

CORRESPONDENCE SHOULD BE ADDRESSED TO:

Edward A. Martinez

Department of Natural Resource Management/New Mexico Highlands University

eamartinez@nmhu.edu

IMPACT OF MICRO-TEMPERATURE CHANGES ON DISSOLVED ORGANIC CARBON IN HIGH MOUNTAIN STREAMS

Julie A. Trujillo[1],
Sebastian Medina[2,]
Daryl Williams[1],
Maura Pilotti [3,]
Edward A. Martinez[1, *]

ABSTRACT

Current evidence suggests that temperatures are increasing at a rapid pace. In the Jemez Mountains of northern New Mexico, the signs of increasing temperatures are evident, resulting in reduced snowpack, longer summer seasons, and warmer annual temperatures. Many questions remain unanswered regarding the extent to which hydrological and other processes will modify streams that are dependent on winter snowpack. Dissolved organic carbon (DOC) concentrations are an essential indicator of the health of aquatic ecosystems whose homeostasis is expected to be altered by climate change. The primary aim of this study was to examine the extent to which concentrations of DOC might vary with micro-temperature changes (as indexed by seasonal and diurnal cycles) in two first-order streams at the Valles Caldera National Preserve (VCNP) within the Jemez River watershed. Based on seclusion and sub-watershed topographical differences, four sites along these streams were targeted for data collection. Analyses illustrated that DOC concentrations varied across seasons in patterns largely unique to each site. Across all sites, DOC concentrations tended to increase with temperature and turbidity, and decrease with discharge. These findings illustrate the impact of micro-temperature alterations on the homeostasis of freshwater ecosystems and can potentially be used to determine DOC dynamics induced by global warming trends.

Since the beginning of the 20th century, scientists have monitored temperature fluctuations and studied trends to determine causes and effects (Karl et al. 1995, Kullman 2001, Walther et al. 2002). The twenty hottest years for the United States have occurred mainly in the last two decades with 2010 being the hottest year on record (Gleick 2011). Temperatures continue to rise rapidly, thereby forcing the scientific community to think seriously about their effects, consequences, and means of adaptation. As temperature increases, stresses on water resources increase as well. Consequently, temperature effects on water resources have been the focal point of major ongoing investigations and conferences (NRC 1977, Donahue 1992, Stefan and Sinokrot 1993, EPSCoR 2010).

While there has been progress monitoring and understanding climate changes, many questions remain unanswered regarding the extent to which hydrological and other processes are altered by such changes. Alterations in hydrological cycles due to global warming may cause variations in the quality of streams. Hydrological and biogeochemical processes are shifting, and so too are

[1] Natural Resource Management, New Mexico Highlands University
[2] Biology and Chemistry, New Mexico Highlands University
[3] Cognitive Science, New Mexico Highlands University
*Corresponding Author: eamartinez@nmhu.edu

floral and faunal communities in freshwater ecosystems (Mohseni et al. 1999). The delicate homeostasis that characterizes freshwater ecosystems, in which the slightest alteration can influence the survival of a variety of interdependent species (Carpenter et al.1992), makes responses of these ecosystems to climate change among the hardest to predict.

Alterations of dissolved organic carbon (DOC) concentrations reflect changes to the homeostasis of freshwater ecosystems that might occur as a result of climate change (Porcal et al. 2009). DOC is the primary nutrient in the food chain and can influence many aspects of the biology and chemistry of such ecosystems (Thurman 1985). DOC is the primary portion of dissolved organic matter utilized by bacteria. Biodegradable dissolved organic carbon (BDOC) can be metabolized and assimilated by heterotrophic micro-flora (Servais et al. 1987). However, very little is known about the processes that control its production, transformation, and fate (Stedmon and Markager 2005). Understanding fluctuations in DOC and BDOC concentrations as a function of temperature variations is essential to prepare for the impact climate change has on streams.

In recent decades, researchers have maintained that climate change can substantially modify stream ecosystems including, DOC concentrations and distributions (Walther et al. 2002, Dawson et al., 2008). In temperate areas, as temperature increases, the warmest season is expected to be longer with more variable precipitation (Porcal et al. 2009). In less temperate locations, temperature increases are projected to be accompanied by a decrease in precipitation (Nandintsetseg et al. 2007, Ye 2008). Accordingly, some areas might be affected by droughts, while others could suffer from more frequent and violent storms. Ecological processes have been found to be strongly influenced by seasonal patterns of precipitation, runoff, and temperature (Carpenter et al. 1992, Poff 1996). For instance, Durance and Ormerod (2007) reported that because streams heavily depend on patterns of rainfall or melting snow, floods and droughts have major effects on the stream's ecology. Dawson et al. (2008) found a link between seasonal and catchment-specific hydrological patterns controlling DOC export. Specifically, increased DOC concentrations were found to occur between June and November with correspondingly lower DOC concentrations from December to May and indicated that DOC was unrelated to discharge and was mainly dependent on higher temperatures driving biological activity as expressed by increasing decomposition of available organic matter and solubility of DOC (Dawson et al. 2008). Although it has been suggested that DOC concentrations vary depending on whether increased temperature or change in precipitation is the dominant response to warmer weather (Schindler 2001, Pastor et al. 2003), storm event studies indicate that such events only explain a small proportion of the annual variability of DOC in streams (Hinton et al. 1997, Tranvik and Jansson 2002, Hongve et al. 2004). Evidence also exists that BDOC is influenced by seasonal changes, albeit the characteristics of the underlying landscape appear to modulate to a great extent the effects of seasonal patterns (Weigner and Seitzinger 2004, Yano et al. 2000).

Another issue that is not entirely understood is how temperature fluctuations between day and night may be altered by warming climate patterns. Evidence exists that diurnal temperature changes can impact the homeostasis of aquatic ecosystems. High temperatures with long duration and large diurnal variations in warm months have been found to be detrimental to aquatic life (Sibley and Strickland 1985, Gu et al. 1998). Surprisingly, there have been relatively few studies of diurnal variations in DOC (Kaplan and Bott 1982, Bott et al. 1984). Manny and Wetzel (1995) found little diurnal variation in DOC concentrations in a headwater stream,

whereas Harrison et al. (2005) reported higher DOC concentrations during night-time hours in a sub-tropical stream in Mexico.

Most climate studies have examined long-term temperature changes in time spans of several years. In the present study, short-range changes in DOC as a function of micro-temporal temperature alterations (as indexed by seasonal and diurnal patterns) are objects of investigation because of the essential role played by DOC in the delicate homeostasis of aquatic ecosystems. DOC, which can control bacterial productivity, influences parameters such as dissolved oxygen (DO), turbidity, pH, specific conductivity, and microbial mediated biogeochemical transformations (Meyer et al. 1998, Wetzel 2001). The overall objectives of this study were as follows: (1) develop a better understanding of the relationship between stream DOC dynamics and temperature changes and how this relationship may be modulated by hydrological changes; (2) assess the variability in DOC concentrations of different landscapes, if present; and (3) understand the relationship between stream physicochemical parameters and organic carbon (DOC and BDOC).

Two streams at the Valles Caldera National Preserve (VCNP) were selected for the investigation. To our knowledge, studies regarding the relationship between temperature changes and DOC and BDOC concentrations have yet to be conducted in areas where human influence is as limited as that of the VCNP. Furthermore, the VCNP has experienced rapid warming since the 1960s, with an overall increase of about 2°F in the colder months and 3°F in the warmer months (Gutzler 2007). According to Gutzler (2007), these trends are more than twice the annual global average of 1°F in the 20th century. Substantial climate warming in New Mexico is expected to impact aquatic ecosystems by reducing snow accumulations and water resources, and increasing stream temperatures (Covich 2003). Thus, the VCNP not only offered the opportunity to collect evidence on organic carbon largely uninfluenced by human intervention, but also could provide baseline evidence of micro temperature effects useful to the study of climate change trends.

SITE DESCRIPTION

This study was conducted on two first-order streams at the VCNP. The 89,000 acre property is located inside a collapsed crater formed about 1.15 million years ago during eruption of the upper Bandelier Tuff (Izett 1981). A total of four sampling sites, representing the major vegetation configurations in the catchment, were chosen to monitor DOC concentrations. The sites were Jaramillo Creek Upper (JCU), Jaramillo Creek Lower (JCL), East Fork Upper (EFU), and East Fork Lower (EFL) (see Fig. 1). See Medina et al. (in review) for a detailed description of the study area.

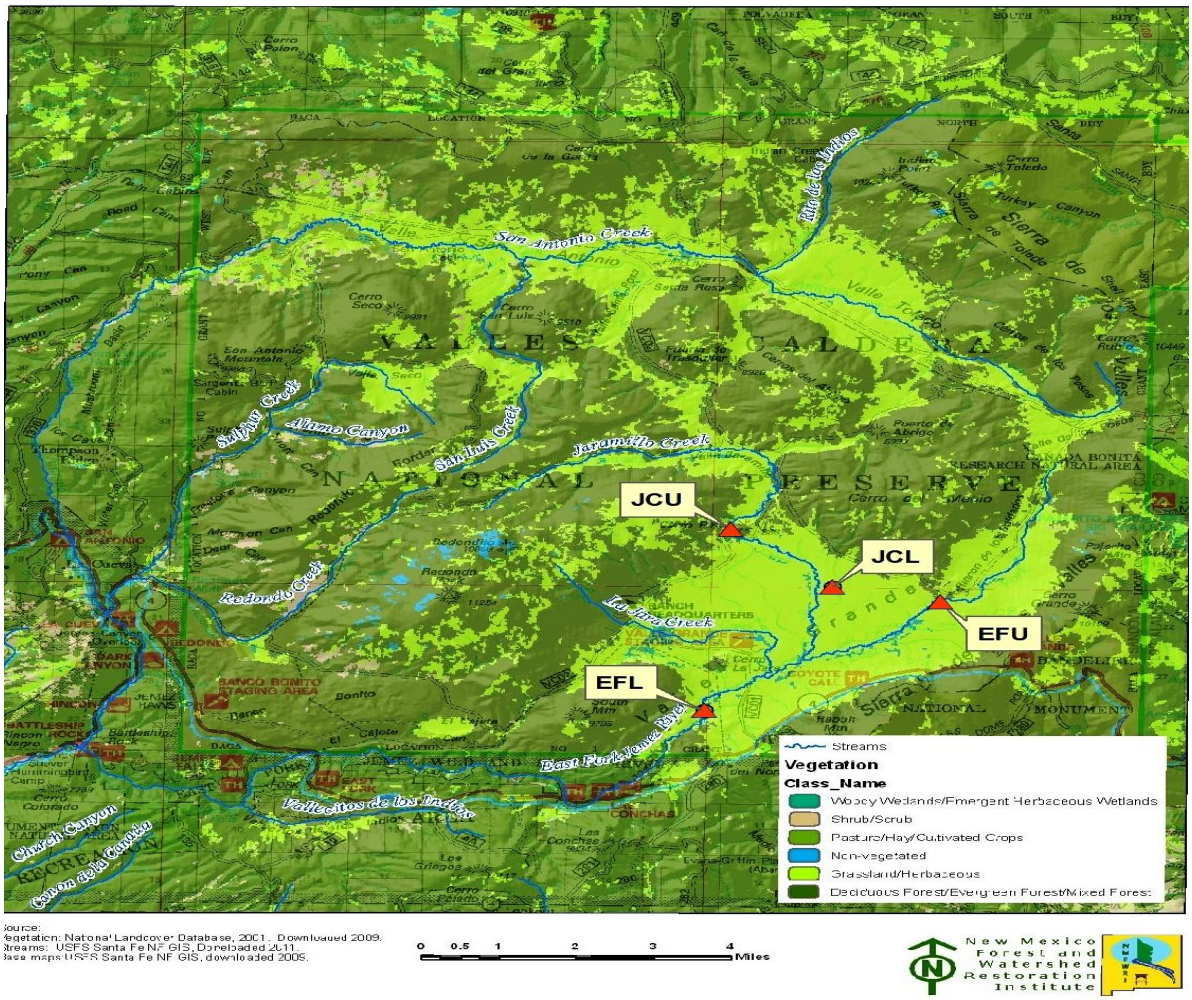

Figure 1: Site location map of Valles Caldera National Preserve

METHODS

Field/Sample Preparation

Collection of stream water samples occurred bimonthly in summer and monthly in winter over a one-year period, from May 2010 to April 2011. Limited data collection occurred during winter months due to site inaccessibility.

Prior to sampling, all glassware was pre-sterilized following Kaplan (2005b). This process included: washing glassware with detergent and rinsing it in cold water, rinsing it in 0.1N HCl followed by deionized water then wrapping glassware in aluminum and heating it in a kiln for six hrs at 500°C. The 0.45-µm pore size Whatman GF/F filters used for data collection were wrapped in foil and heated in the kiln following the same procedure used for glassware.

During grab sample collections, two 40 mL-grab water samples at each site were taken, a sample for measuring Dissolved Organic Carbon (DOC) and a sample for measuring Biodegradable Dissolved Organic Carbon (BDOC). For diurnal measurements, water samples were collected at 1hr intervals with a model 3700 portable ISCO auto-sampler programmed to collect 1000 mL each hour for 24 hours on a monthly basis. In the field, the DOC and BDOC samples were filtered into pre-sterilized borosilicate vials using Whatman GF/F filters with a 0.45-µm pore size (Kaplan 2005a). DOC samples were collected and preserved with sodium azide and stored

at 4ºC prior to analysis. The BDOC samples were immediately wrapped in aluminum foil and stored in the dark at 20±5ºC for 28 days following Kaplan (2005a).

An YSI 6920 Sonde was used to measure temperature, DO, turbidity, pH, and specific conductivity during grab sample collection. Discharge of each stream was recorded utilizing a model 201D Marsh-McBirney portable water current meter and a Rickly wading rod. HOBOware (2002) Pendant data loggers were placed at each site on the stream bed to measure real-time water temperature data at every hour throughout the sampling year.

Laboratory Analysis

Stream water DOC concentrations were determined on an OI Analytical Aurora Model 1030/Autosampler Model 1088. All calibrants, standards, reagents, and field blanks were prepared using 18Ω water from a Barnstead Easy Pure II UV/UF water purification system. Continuous calibration verifications (CCV) were utilized at 0.5, 1, 2, 5 and 10 mg/L following every 6th sample during analysis to verify accuracy of instrument measurement. Data were eliminated when CCVs were greater than ±5% of the known concentration. The analysis of samples was done in triplicate. Means of triplicates constituted DOC concentrations to be used in the statistical analyses described below. BDOC was calculated as the difference in mean DOC before and after the 28 day incubation (BDOC= Initial DOC – 28d DOC) following Kaplan (2005a).

Statistical Analyses

Statistics were considered significant at the 0.05 level and were organized into two steps. For further descriptions of data categorization (day versus night delineation and season determination) and statistical analyses of water temperature data see Medina et al. (in review).

First, a factorial ANOVA was conducted on all DOC samples to determine whether DOC changed as a function of Season (spring, summer, fall, and winter) and Site (EFU, EFL, JCU, and JCL). Initial analyses indicated that Time-of-Day did not produce any significant main effects or interactions. Therefore, the analysis described in the results section includes only Season and Site as factors followed by *Post hoc Tukey's* comparisons. Correlation analyses were conducted on DOC samples to determine the extent to which changes in DOC's related to discharge, temperature, pH, DO, turbidity, and specific conductivity. To ensure sufficient variability in the data distribution, correlations were computed across sites and seasons.

Second, a factorial ANOVA was conducted on BDOC to determine whether BDOC changed as a function of Season and Site. Correlation analyses were also conducted on BDOC to determine the extent to which changes in BDOC might correspond to variations in physicochemical parameters such as temperature, pH, DO, turbidity, specific conductivity, and discharge.

RESULTS

Physical Characteristics of Sites

Throughout the sampling period the JCU site maintained an average width of 1.10 m, an average stream depth of 0.51 m, an average discharge of 0.02 m^3/s and an elevated turbidity (11.26 NTU). The JCL site located in the Valle Grande above its confluence with the East Fork maintained a stream width of 0.93 m and was very shallow (0.17 m), with an average turbidity of 11.94 NTU and average discharge of 0.03 m^3/s. EFU was located at the East Fork headwater,

originating through the open meadow of the Valle Grande. EFL was below its confluence with the Jaramillo Creek. The East Fork stream sites were wider than the Jaramillo Creek sites. EFU had an average width of 2.44 m and depth of 0.19 m and an average discharge of 0.02 m^3/s. EFL had a width of 3.22 m and depth of 0.10 m, and average discharge of 0.05 m^3/s. EFU and EFL turbidity levels were 0.39 NTU and 9.29 NTU, respectively.

Preliminary Analysis: Diurnal and Seasonal Water Temperature

The ANOVA conducted on water temperature data (N = 36,352) indicated a significant three-way interaction between Season, Time of Day, and Site (Table 1). As expected, for all sites, water temperature was highest in the summer and lowest in the winter both during the day and at night, see Table 2 and Medina et al. (in review).

ANOVA Analysis for All Sample Data

The interaction between Season and Site suggests that seasonal changes in DOC concentrations varied across sites. Tukey's HSD revealed patterns at each site (Fig. 2) across seasons. EFU exhibited the lowest values in the spring and the highest in the fall. EFL displayed the opposite pattern for DOC collected in the spring. Spring values were the highest, whereas fall and winter values were the lowest. JCU showed the highest concentrations in the summer and lowest in the fall. In contrast, JCL had the highest values in the summer, whereas spring and fall were about the same.

Table 1: Water Temperature Data, Factorial Analysis of Variance Main Effects and Interactions Involving Season (spring, summer, fall and winter), Time of Day (day and night), and Site (EFU, EFL, JCU and JCL)

Effects	**df**	**F**	**P-Value**
Season	3	25194	<0.001
Time-of-Day	1	551	<0.001
Site	3	896	<0.001
Season X Time-of-Day	3	37	<0.001
Season X Site	9	2122	<0.001
Time-of-Day X Site	3	115	<0.001
Season X Time-of Day X Site	9	14	<0.001

Correlation Analysis for All Sample Data

DOC was positively correlated with water temperature, r = + 0.460, p = <0.001. Although higher temperatures were accompanied by greater DOC concentrations, water temperature only explained 21.16 % of the variability in DOC. DOC concentrations tended to increase with turbidity of the water, r = +0.399, p = 0.041, and decrease with discharge, r = - 0.527, p = 0.015. Selected physicochemical parameters tended to co-vary. Water temperature was negatively correlated with DO (r = - 0.367, p = 0.023) and specific conductivity (r = - 0.228, p = 0.126) explaining 13.47%, and 5.20 % of variance, respectively. Lastly, turbidity was negatively correlated with specific conductivity, suggesting that the large presence of suspended solids interfered with specific conductivity measurements.

Table 2: Water Temperature Data, Means and Standard Errors of the Mean (in parenthesis) for Season (spring, summer, fall and winter), Time-of-Day (day and night) and Site (EFU, EFL, JCU and JCL).

Site	Spring (°C)	Summer (°C)	Fall (°C)	Winter (°C)
EFU Day	12.64 (0.093)	13.24 (0.092)	12.22 (0.125)	10.95 (0.082)
Night	10.51 (0.106)	11.87 (0.107)	11.54 (0.117)	9.91 (0.073)
EFL Day	12.72 (0.158)	19.25 (0.094)	12.52 (0.086)	2.29 (0.086)
Night	10.51 (0.186)	17.17 (0.109)	10.65 (0.12)	1.46 (0.076)
JCU Day	7.87 (0.103)	16.41 (0.106)	6.79 (0.122)	0.19 (0.195)
Night	7.41 (0.113)	16.96 (0.124)	6.88 (0.112)	0.16 (0.162)
JCL Day	10.71 (0.093)	17.99 (0.092)	10.16 (0.125)	1.24 (0.094)
Night	8.47 (0.106)	17.32 (0.124)	10.33 (0.117)	0.78 (0.081)

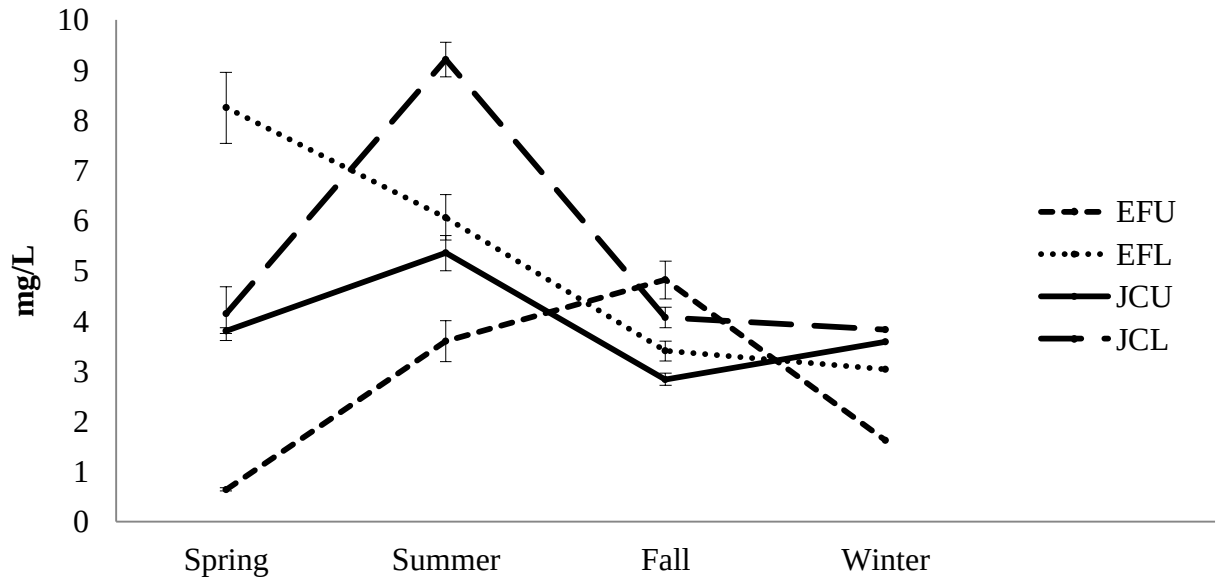

Figure 2: Mean DOC concentrations and standard error bars for each Site across Seasons.

Analyses of BDOC: Monthly Grab Samples

The ANOVA analysis for Season and Site did not produce any significant effects or interaction. However, there were trends illustrating seasonal pattern differences for East Fork sites (EFU and EFL) and Jaramillo Creek sites (JCU and JCL; Fig. 3). BDOC did not exhibit significant correlations with any of the physicochemical parameters discussed above.

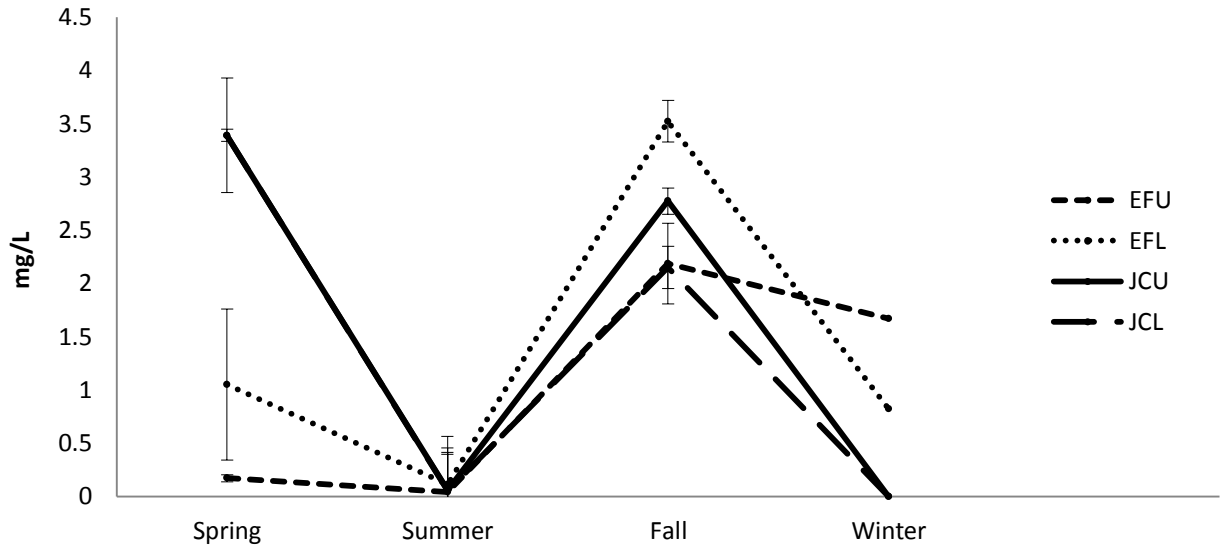

Figure 3: Mean BDOC values for each Site across Seasons

DISCUSSION

The analyses can be summarized in four main points. First, temperature was warmer during the day than at night and changed across seasons (summer > spring > fall > winter). However, there were site-specific characteristics that influenced temperature more than expected. Second, DOC, as measured in 24-hour samples, changed with seasonal patterns in ways that were unique to each site. Namely, EFU exhibited the lowest values in the spring and the highest in the fall. EFL displayed the opposite pattern. JCU showed the highest concentrations in the summer and lowest in the fall. In contrast, JCL had the highest values in the summer, whereas spring and fall were about the same. Third, DOC was positively correlated with water temperature and turbidity, but negatively correlated with discharge. Lastly, BDOC illustrated a pattern of trends similar to those of DOC, albeit none reached significance. As discussed below, the results of the present investigation uncovered significant patterns of seasonal effects and correlations for DOC and BDOC and selected physicochemical parameters.

Analysis of Diurnal and Seasonal Water Temperature

Temperature changes were as expected for all sites during diurnal and seasonal cycles, although differences were not statistically significant at all sites. A similar pattern was exhibited by temperature in the spring and fall with spring temperatures warmer than fall temperatures. EFU was the only site displaying no statistical differences between seasonal temperatures (Medinal et al. in review). This site displayed fewer fluctuations in temperatures throughout seasons as well as diurnally. The stream originates from the ground about five meters from the EFU sampling site which might account for minimal changes in temperature. According to O'Driscoll and DeWalle (2004), streams with large groundwater inputs tend to show small temperature changes. This factor explains why EFU maintained a stable temperature diurnally and throughout the seasons.

Across seasons and diurnally, JCU displayed colder average temperatures than the EFU, EFL, and JCL sites. This stream originates in a forested site located in a valley with steep slopes on its northwest and southeast aspects. The north faces tend to create more shading, which occurs until

mid morning and again early afternoon. This blockage of solar radiation probably had a large effect on the stream's heat budget. In addition, the stream's morphology at this site makes it the narrowest and deepest site, resulting in limited light and heat penetration and cooler temperatures. During runoff season, water moves quickly due to the steeper slopes and its forested watershed do not allow runoff to warm before it reaches the stream.

ANOVA Analysis for All Sample Data

Seasonal changes in DOC concentrations have been previously documented in sites with varying types of vegetation (Fraser et al., 2001, Yano et al., 2004, Fellman et al., 2008). In the present study, DOC concentrations varied both seasonally and by site. The EFU site displayed its highest DOC concentrations during the fall, suggesting that the carbon contribution from the allochthonous material (organic matter) had a larger influence on DOC concentration than the carbon contribution entering the stream via spring runoff. This finding was similar to that observed in other studies where maximum DOC export was reported in early autumn (Worrall et al., 2004, Lumsdon et al., 2005, Tipping et al., 2007, Dawson et al., 2008). EFL displayed the opposite pattern, whereby spring had the greatest DOC concentrations. Eimers and Buttle (2008) also reported a similar finding, suggesting that spring runoff had a strong influence on DOC concentrations. Both JCU and JCL sites displayed the highest DOC concentrations in the summer. The two Jaramillo Creek sites displayed a pattern similar to that of Mulholland and Hill (1997) in which DOC concentrations were the highest in the summer and the lowest in the winter.

Site differences in patterns of DOC concentrations across seasons suggest that the effects of temperature changes on DOC concentrations are likely to be modulated by site characteristics such as dominant vegetation, physicochemical parameters, and nutrient availability. For instance, EFU displayed the lowest values during the spring when runoff is expected to contribute the most DOC to the stream. However, this site is located close to where the stream originates from the ground, not allowing DOC inputs from runoff to be a contributing factor in concentration increases or decreases. In contrast, EFL had the highest values during the spring, underlying its sensitivity to spring runoff and to inputs from the Jaramillo Creek tributary.

DOC was closely related to temperature, turbidity, and discharge. The Jaramillo Creek was more turbid than the East Fork stream. Both JCU and JCL sites averaged 10.93 NTU, which explains why these sites had higher DOC concentrations compared to the East Fork sites. This effect possibly served as a positive feedback loop where the high DOC concentrations contributed to the high turbidity, and the high turbidity decreased light penetration, thereby decreasing photosynthesis. Decreased light penetration does affect aquatic productivity, and the uptake of DOC might have influenced the microbial aquatic food chains in the streams (Keller et al., 2003) and inputs of carbon to the system. It is important to note that Jaramillo Creek originates in the forested area of the watershed where allochthonous carbon might be adding to the stream DOC concentration.

The negative correlation obtained between DOC and discharge is inconsistent with findings by Hongve et al. (2004) wherein DOC was reported to increase during discharge events. One possible explanation for our findings is that our sampling did not occur immediately after spring runoff or precipitation events. The spring flood and/or precipitation events saturated and flushed old water and DOC buildup in the riparian soils into the streams prior to our sampling events. Another possible explanation is that our sampling occurred when discharge was stabilizing and

baseflow dominated, indicating that microbial activity had a stronger influence on DOC concentrations than the hydrological contribution. Nonetheless, in recent decades, there have been no consistent hydrological trends related to DOC (McCabe and Wolock 2002).

BDOC

The limited BDOC data due to instrument malfunction and the lack of sample collection during freezing periods made it difficult to evaluate trends related to water temperature. There were no significant effects or correlations involving BDOC.

Because of BDOC's importance to ecosystems, it is vital to understand how it functions with temperature changes. This energy source for aquatic life is a necessary component for a properly functioning ecosystem. For EFU, concentrations of both DOC and BDOC were the lowest in the winter. In the fall, both values were the highest. In the summer, most of the BDOC was expected to be taken up by aquatic organisms, leaving little BDOC after the 28-day incubation period. In the spring season, very little BDOC was available. For EFL, its highest value was in the spring, but most of the BDOC was consumed during the season. This pattern was similar in the summer. For the fall and winter seasons, EFL values were similar for BDOC and DOC and little was used by microorganisms. The JCU and JCL sites had similar patterns, where most of the DOC was utilized. Not surprisingly, seasonal BDOC activities have been difficult to define and explain in other BDOC studies (Findlay et al., 2001, Weigner and Seitzinger 2004).

CONCLUSIONS

It is obvious that the effects of temperature changes on the hydrology of high mountain streams are of great concern due to the impact that a progressively changing temperature is likely to have on the health and stability of aquatic ecosystems. Surprisingly, as indicated by several researchers (Butturini and Sabater 2000, Webster and Meyer 1997), the dynamics of DOC in streams have received little attention. The evidence presented in this study supports the notion that DOC, BDOC, as well as other aquatic parameters, are influenced by altered water temperatures. If temperatures in NM continue to rise as predicted, studies such as the present one will be necessary to better understand how micro-temperature increases may affect high mountain streams when baseline temperature levels are overall higher.

Associated with increasing temperatures is the uncertainty of predicting precipitation intensity and frequency. Therefore, the emerging picture of climate-related changes in hydrology is complex and undoubtedly difficult to capture entirely in the time capsule of a single study. Nevertheless, the present study highlights the usefulness of examining largely pristine areas to better understand how the health of aquatic ecosystems fluctuates with variations in DOC concentrations and physicochemical parameters in a context where human contribution is negligible. Although this study is a time capsule for its limited temporal range, it can serve as a baseline for predicting the effects of large-scale fluctuations associated with global climate change. Indeed, evidence from this study supports the notion that temperature increases result in DOC concentration increases which lead to changes in physicochemical parameters. In addition, it appears that DOC concentrations can be influenced more by site characteristics than hydrology (runoff), a finding that surely has implications for the study of the effects of climate change on water resources.

ACKNOWLEDGEMENTS

We would like to thank the National Science Foundation New Mexico EPSCoR Award number EPS 0814449. In addition, special thanks to the personnel at the Valles Caldera National Preserve and to Leona DeSanto for the field assistance they provided.

LITERATURE CITED

Butturini A. and F. Sabater. 2000. Seasonal variability of dissolved organic carbon in Mediterranean Stream. biogeochemistry 52: 303-332

Bott T.L., L.A. Kaplan, and F.T. Kuserk. 1984. Benthicbacterial biomass supported by streamwater dissolved organic matter. Microbial Ecology 10: 335-354

Carpenter S.R., S.G. Fisher, N.B. Grimm, and J.F. Kitchell. 1992. Global change and freshwater ecosystems. Annual Review of Ecology, Evolution, and Systematics 23:119-139

Chipera S.J., F. Goff, and M. Fittipaldo. 2008. Ziolitization of intercaldera sediments and rhyolitic rocks in the 1.25 Ma lake of Valles Caldera, New Mexico, USA. Journal of Volcanology and Geothermal Research 178:317-330

Covich A 2003. Chapter 8: Natural Ecosystems II. Aquatic Systems , in Wagner, F.H. (ed). Preparing for a Changing Climate. The potential consequences of climate variability and change. Rocky Mountain/Great Basin Regional Climate-Change Assessment. A report of the Rocky Mountain/Great Basin Regional Assessment Team for the U.S. Global Change Research Program

Dawson, J., C. Soulsby, D. Tetzlaff, M. Hrachowitz, S. Dunn, and I. Malcolm. 2008. Influence of hydrology and seasonality on DOC exports from three contrasting upland catchments.Biogeochemistry 90:93-113

Donahue, M. 1992. Climate and Global Change: 'The Response and Policy Issues Related to Climate Change in the Great Lakes Basin', Great Lakes Comm., Ann Arbor, MI.

Durance, S., and J. Ormerod. 2007. Climate change effects on upland stream invertebrates over a 25 year period. Global Change Biology, 13:942-957.

Eimers, M., and J. Buttle. 2008. Influence of seasonal changes in runoff and extreme events on dissolved organic carbon trends in wetland- and upland-draining streams. Fish Aquatic Science: 65: 796-808

EPSCoR. 2010. Collaborative and Interdisciplinary Climate Change Science. Lake Tahoe, NV.

Fellman, J., D. D'Amore, E. Hood, and R. Boone. 2008. Fluorescence characteristics and biodegradability of dissolved organic matter in forest and wetland soils from coastal temperate watersheds in southeast Alaska. Biogeochemistry 88: 169-184

Fraser, C.J.D., N.T. Roulet, and T.R. Moore. 2001. Hydrology and dissolved organic carbon biogeochemistry in an ombrotrophic bog. Hydrological Processes 15:3151-3166

Findlay, S., J.M. Quinn, C.W. Hickey, G. Burrell, and M. Downes. 2001. Effects of land use and riparian flowpath on delivery of dissolved organic carbon to streams. Limnology and Oceanography 46: 344-355

Gleick, P.H. 2011. 2010 The hottest year on record: The graph that should be on the front page of every newspaper. The Huff Post. Retrieved June 8, 2012, from http://www.huffingtonpost.com/peter-h-gleick/the-graph-that-should-be-_b_808747.html

Gu, R., S. Montgomery, and T. Austin. 1998. Quantifying the effects of stream discharge on summer river temperature. Hydrological Sciences 43: 885-904

Gutzler, D. 2007. Climate change and water resources in New Mexico. Earth Matters. 7:1-6

Harrison, J.A., P.A. Matson, and S.E. Fendorf. 2005. Effects of diel oxygen cycle on nitrogen transformations and greenhouse gas emissions in a eutrophied subtropical stream. Aquatic Sciences 67:308-315

Hinton, M.J., S.L. Schiff, and M.C. English. 1997. The significance of storms for the concentration and export of dissolved organic carbon from two Precambrian Shield catchments. Biogeochemistry 36:67-88.

HOBOware [Lite Apparatus and software]. 2002 Bourne, Massachussetts: Onset Computer Corporation.

Hongve, D., G. Riise, and J. Kristiansen. 2004. Increased colour and organic acid concentrations in Norwegian forest lakes and drinking water-a result of increased precipitation? Aquatic Sciences 66:231-238.

Izett G. A. 1981. Volcanic Ash Beds: Recorders of Upper Cenozoic Silicic Pyroclastic Volcanism in the Western United States, J. Geophysical Research 86: 10, 200-210, 222

Kaplan, L.A., and T.L. Bott. 1982. Diel fluctuations of DOC generated by algae in a piedmont stream. Limnology and Oceanography 27: 1091-1100

Kaplan, L. 2005a. Biodegradable dissolved organic carbon (BDOC): Suspended inoculums technique (Procedure No. S-03-08.02). New York: Stroud Water Research Center.

Kaplan, L. 2005b. Preparation of organic carbon free glassware (Procedure No. S-03-16). New York: Stroud Water Research Center.

Karl, T., R. Knight, and N. Plummer. 1995. Trends in high-frquency climate variability in the twentieth century. Nature 377: 217-220

Keller, W, J.H. Heneberry, and S.S. Dixit. 2003. Decreased acid deposition and the chemical recovery of Killarney, Ontario, lakes. Ambio 32:183-189

Kullman, L,. 2001. 20th century climate warming and tree-limit rise in the southern Scandes of Sweden. Ambio 30: 72-80.

Lumsdon, D, M. Stutter, R. Cooper, and J. Manson. 2005. Model assessment of biogeochemical controls on dissolved organic carbon partitioning in an acid organic soil. Environmental Science Technology 39:8057-8063

Manny, B.A., and R.J. Wetzel. 1973. Diurnal changes in dissolved organic carbon and inorganic carbon and nitrogen in a hardwater stream. Freshwater Biology 3:31-43

McCabe, G.J., and D.M. Wolock. 2002. A step increase in streamflow in the conterminous United States. Geophysical Research Letters 29: 2185-2188

Medina, S., J. Trujillo, D. Williams, M. Pillotti, and E.A. Martinez. In Review. Water quality dynamics of two headwater streams as indicated by variations in nutrient and other solute concentrations, physicochemical parameters and discharge. New Mexico Journal of Science

Meyer, J.L., B.J. Wallace, and S.L. Eggert. 1998. Leaf litter as a source of dissolved organic carbon in streams. Ecosystems 1:240-249

Mohseni, O., T.R. Erickson, and S.G. Heinz. 1999. Sensitivity of stream temperatures in the United States to air temperatures projected under a global warming scenario. Water Resources Research 35: 3723-3733

Mulholand, P.J., and W.R. Hill. 1997. Seasonal patterns in streamwater nutrient and dissolved organic carbon concentrations: Separating catchment flow path and in-stream effects. Water Resources Research 33:1297-1306

Nandintsetseg, B., J.S. Greene, and C.E. Goulden. 2007. Trends in extreme daily precipitation and temperature near Lake Hövsgöl, Mongolia. International Journal of Climatology 27:341-347

NRC (National Research Council): 1977. Climate, Climate Change, and Water Supply, National Academy Press, Washington, D.C.

O'Driscoll, M., and D.R. DeWalle. 2004. Stream Air Temperature Relationships as Indicators of Groundwater Inputs. AWRA Hydrology & Watershed Management Technical Committee. 6:1-5

Pastor, J., S.D. Bridgham, K. Updegraff, C. Harth, P. Weishampel, and B. Dewey. 2003. Global warming and the export of dissolved organic carbon from boreal peatlands. Oikos 100:380-386

Poff, L.N. 1996. Stream hydrological and ecological responses to climate change assessed with an artificial neural network. Limnology and Oceanography 41:857-863

Porcal, P, J. Koprivnjak, L.A. Molot, and P.J. Dillon. 2009. Humic substances-part 7: the biogeochemistry of dissolved organic carbon and its interactions with climate change. Environmental Science Pollution and Research 16:714-726

Schindler, D.W. 2001. The cumulative effects of climate warming and other human stresses on Canadian freshwaters in the new millennium. Aquatic Sciences 58:18-29

Servais, P., G. Billen, and M.C. Hascoet. 1987. Determination of the biodegradable fraction of dissolved organic matter in waters. Water Research 21: 445-450.

Sibley, T.H., and R.M. Strickland. 1985. Fishers: some relationships to climate change and marine environmental factors. In: Characterization of Information Requirements for Studies of CO2 Effects: Water Resources, Agriculture, Fisheries, Forests and Human Health (ed. By M.R. White). 95-113. US Dept of Energy, Washington, D.C.

Stedmon, C., and S. Markager. 2005. Tracing the production and degradation of autochthonous fractions of dissolved organic matter by fluorescence analysis. Limnology and Oceanography 2005:1415-1426

Stefan, H.G., and B.A. Sinokrot. 1993. Projected global climate change on water temperatures in five north central U.S. streams. Climate Change 24:353-381.

Tipping, E., E. Smith, C.Bryant, and J. Adamson. 2007. The organic carbon dynamics of moorland catchment in NW England. Biogeochemistry 84:171-189

Thurman, E.M. 1985. Organic geochemistry of natural waters. Martinus Mijhoff/Dr. W Junk, Boston, Massachusetts, USA.

Tranvik, L. and M. Jansson. 2002. Climate change-terrestrial export of organic carbon. Nature 415:861-862.

Walther, G., E. Post, P. Convey, A. Menzel, C. Parmesank, T. Beebee, J. Fromentin, O. Hoegh-Guldberg, and F. Bairlein. 2002. Ecological response to recent climate change. Nature 416: 389-395

Water Quality Control Commission. 2006. Total maximum daily load for the Jemez River Watershed East Fork Jemez River and Jaramillo creek. Retreived from http://www.nmenv.state.nm.us/swqb/VallesCaldera/

Webster, J.R., and J.L. Meyer. 1997. Stream organic matter budget-introduction. In: Webster JR Meyer JL (Eds) Stream Organic Matter Budget. J.N. American Benthological Society 16: 12-161.

Weigner, T.N., and S.P. Seitzinger. 2004. Seasonal bioavailability of dissolved organic carbon and nitrogen from pristine and polluted freshwater wetlands. Limnology and Oceanography 49: 1703-1712.

Wetzel, R.G. 1995. Death, detritus, and energy flow in aquatic ecosystems. Freshwater Biology 33:83-89

Wetzel, R.G. 2001. Limnology: lake and river ecosystems. Academic, San Diego, California, USA

Worrall, F., R. Harriman, C.D. Evans, C.D. Watts, J. Adamson, and C. Neal. 2004. Trends in dissolved organic carbon in UK rivers and lakes. Biogeochemistry 70:369-402

Yano, Y., and W.H. McDowell, and J.D. Aber. 2000. Biodegradeable dissolved organic carbon in forest soils and effects of chronic nitrogen deposition. Soil Biology and biochemistry 32:1743-1751

Ye, H., D. Yang, D. Robinson. 2008. Winter rain on snow and its association with air temperature in northern Eurasia. Hydrological Processes 22: 2728-2736

Correspondence Author: Edward A. Martinez, Department of Natural Resources Management, New Mexico Highlands University, Box 9000, Las Vegas, New Mexico, 87701. Email: eamartinez@nmhu.edu, 505-454-3366 (Office), 505-454-3103 (Fax).

A SOLAR CHOICE FOR PUMPING WATER IN NEW MEXICO FOR LIVESTOCK AND AGRICULTURE

Thomas Jenkins[1]

ABSTRACT

In many parts of the world, including NM, water and energy are growing concerns. In areas where connection to an electric utility is not available, the primary technologies for water access - hauling water, surface sources, or pumping have remained fairly constant for decades. As demands for higher quantities and quality of water, lower costs, improved reliability, and environmental concerns have increased; many livestock and agricultural producers are investigating an alternative technology for remote water pumping – direct coupled solar photovoltaic (PV) powered systems. Since the process to design and implement such a system may be a challenging task, NMSU's College of Engineering initiated a project to provide the Agriculture Cooperative Extension Service (ACES) with a demonstration module, an interactive design spreadsheet, and literature related to solar water pumping to better inform NM water users about the benefits and methodology of implementing this technology. Available through the ACES web site and their statewide extension agent network, this material will serve to educate interested constituencies (primarily farmers and ranchers) in using PV to pump water.

Livestock, crops, and people often depend upon surface sources of water (streams, ponds, dugouts, etc.) or wells accessing underground aquifers[2]. For a variety of benefits, and in some states increased regulations, it is often desirable to move the water from a surface source or a remotely located well to a different location, elevation, or "drinker".

The century old multi-blade windmill

For surface sources, a well-vegetated riparian zone establishes a buffer which filters and purifies water as it moves across the zone, reduces sediment loads, supports soil stability, improves water quality, while enhancing wildlife habitat. Livestock pressure on buffer areas often result in nutrient loading, streamside vegetation damage, erosion, pollution, and decreased animal growth and health. One approach is to remove or limit access to these areas; however, when considering limiting access to surface sources, often they may be the only viable water source for producers. Fortunately, research shows that in many

[1] New Mexico State University's (NMSU) Department of Engineering Technology.
[2] An excellent source on windmills http://aces.nmsu.edu/ces/windmill

cases pumping water to a different location combined with a managed rotational grazing plan[3], optimizes animal performance, pasture use, water quality, and wildlife in these zones (Buschermohle and Burns, n.d.; Morris and Lynne, 2002).

While cows may wade out to obtain better water, calves tend to only drink water from the shore. Wading into surface sources, cattle pollute the water with their urine and feces while their wading action may disturb the water to a level that they refuse to further drink, requiring them to be moved even though local forage is still plentiful. Calves require higher quality water and they won't fight cows or mud to obtain it. Increases of 50 pounds/head in weaning weight have been reported when water in sufficient quantity and quality is provided. Studies show, when given a choice, cattle drink from a water trough 92 percent of the time rather than from a nearby stream (Bartlett, n.d.). Research also indicates that yearling steer performance increased 23 percent when supplied with an alternate water source rather than dugouts (earthen dams or reservoirs). In addition to increased livestock and resource performance, by routing the livestock away from the riparian zones, very large reductions (50-90 percent) in streptococci and coliform fecal organisms (waterborne diseases like foot rot, red nose, TB and mastitis), nitrogen, phosphorous, suspended solids, and surrounding erosion are realized. By pumping to drinkers, ranchers can better utilize pastures; get superior animal growth and health, while providing higher quality water (Pfost et al., 2007, Surber et al., n.d.).

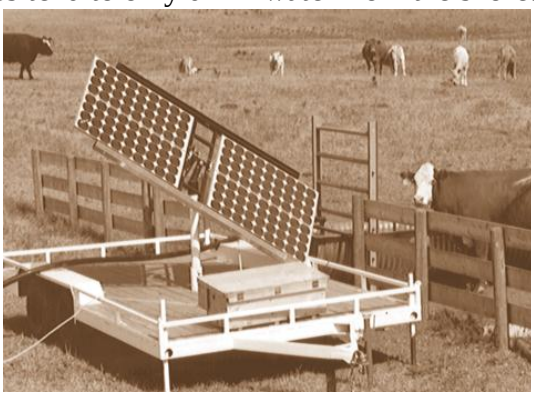

Far from utility lines, a portable PV pumping system supplies water from a fenced pond to a clean watering trough. Courtesy NREL/BR-412-21732

Costs, reliability, and environmental concerns often influence the surface water pumping system employed by producers. When producers do not have an economical access to grid electric power,[4] they generally look to options such as ram, sling, diesel, windmills, and solar powered pumps. When these choices are compared, solar pump systems are often the best choice due to the operational conditions inherent to NM which permits them to function effectively and economically (Jenkins et al., 2012).

Solar pumping systems from surface sources or wells can be portable which is appealing as more and more producers want systems that can move among varying locations. Some users are even powering broken windmill's pump jacks by PV. PV modules drive a DC electric motor to power

[3] It has been shown that livestock will only travel a limited distance to water sources with typical water source spacing of one source per 250 ha to harvest grasslands otherwise there is strong potential for overgrazing close to water supplies.

[4] It can cost $10,000 – $30,000 per mile of newly installed electrical power line through rugged terrain.

the old pump jack mechanisms. When a portable trailer with PV modules, the electric motor, and pump jack is backed into place by the well, the sucker rod from the cylinder pump is attached to the jack with a wire cable coupling. Setting up the system takes about 10 minutes. For use in different locations, the angle(s) of portable PV modules should be adjustable and often a portable stock fence is set up around the unit (NREL/BR-412-21732).

For pumping water from underground aquifers via wells, access to existing AC electric connections (closer than one-half kilometer) is again the best option. However, PV water pumping systems represents a very attractive long-term cost effective alternative in remote locations to hauling water, diesel pumps, and even traditional windmills for drinking water and selected irrigation applications (drip/trickle, hose/basin, and some channel irrigation- although typically not for very high flow rates such as might be used in flood irrigation). The plethora and variety of benefits of PV systems makes them attractive in ever more situations.

A solar pumping system involves calculations and concepts that may make it difficult to determine a design if one is unfamiliar with th**e** technology and terminologies. With this in mind, NMSU developed the following tools to aid and educate a potential user.

1. Two portable demonstration devices which illustrate the concepts and major system components for a solar pumping system. Each module is portable and therefore available for displays and presentations[5].
2. Literature and multimedia educational materials related to PV water pumping systems including comparisons between three main water pumping technologies used in NM today, contrasting two different ways to mount PV modules (fixed angle mounting vs. single axis tracking systems), as well as a simple cost analysis for each of the three technologies and mounting systems (Jenkins, et al. 2012).

Technology	Advantages	Disadvantages
Solar	• Renewable/Sustainable • No fuel costs • Can be portable and scalable • Very low operation/ maintenance • Federal and State incentives • Acceptable capital costs & low recurrent costs • Remote applications • Warranty over 20 years for panels • Relatively easy to install • System is modular & may be modified to need	▪ Variable water delivery depending on sun intensity ▪ Low flow rates ▪ Supplemental storage needed ▪ Extended time to meet storage required ▪ Higher initial costs

[5] http://www.youtube.com/watch?v=4gFbCdHle0w&list=PL89870B418A514D27&index=10&feature=plpp_video

Windmills	• Renewable/Sustainable • No fuel costs • Federal and State incentives • Remote applications • Proven technology with pool of expertise & experience • Lower initial costs	▪ Only works when wind conditions are adequate ▪ Winds are seasonal ▪ Some operating costs & higher repair/maintenance costs ▪ Labor intensive ▪ Difficult to find parts & special tools needed ▪ Low flow rates ▪ Extended time to meet storage ▪ High winds may damage windmill
Fossil fuels (Diesel)	• Higher flow rate • Often no need for storage • Proven technology with large pool of expertise • Easy to install	▪ Environmental issues ▪ Manually operated ▪ Accessibility issues ▪ Required periodic maintenance & replacement ▪ Moderate/High initial cost ▪ Fuel costs & storage/transportation

3. The formulation of a Microsoft Excel® spreadsheet to provide an easy and visual educational tool to present concepts behind PV technology and system design methodology. This tool permits a user to follow the basic step-by-step design process and offers sample components and simple economic analysis for a user-defined scenario. For the sake of organization and ease of use, the spreadsheet follows the design approach outlined below.

SOLAR WATER PUMPING SYSTEMS EXPLAINED

The design decision and a successful implementation of solar water pumping systems requires information specific to each application and an understanding of several concepts. Example information needed for project feasibility consideration is:

- Daily water requirements and usage – drinking, irrigation, etc. Requirements for high volumes or flow rates may limit applications.
- Solar resource, i.e. the amount of sunlight available - location dependent. Low levels of sun may limit application.
- Pumping/well characteristics such as water depth, draw-down levels and recharge rates, seasonal variations, discharge elevation from earth's surface to water discharge point, total feet of pipe, nominal diameter of the pipe, and valves, elbows, etc.
- Storage systems – catch tanks, storage tanks, et al. to ensure the daily water requirement is available during low-light conditions.
- Choosing/Matching PV modules and pump equipment to meet the design constraints
- Economics – capital, operation and maintenance, labor, life-cycle, … costs

In addition, these factors should be considered:

- Who will install and maintain the system.
- Security – although ideal for remote locations, this makes the system vulnerable to theft and vandalism.
- Environmental benefits (including low noise).

BASIC OPERATION

With no moving parts, the PV panels take energy from the sun and generate DC electricity where it is directed through a controller to the pump – what is termed a direct-coupled system. The pump/motor combination moves water taken from the source through a pipe to a discharge point - commonly a storage tank which feeds a trough-drinker. This direct-coupled system is intended for operation only during the day and eliminates using batteries. Batteries are complex and expensive, must be replaced every few years, and require periodic maintenance while the useful life of storage tanks may be decades. A good design of direct-coupled systems requires pumping extra water each day into a storage tank. By providing water storage, a producer can still provide his daily water requirement from the tank storage at night or on cloudy days. The amount of water pumped is predominantly dependent on the amount of sunlight hitting the PV modules, the type of pump, and a few other factors of lesser importance. The available sunlight is predictable by location, but there are always variations in weather. PV panels may produce up to 80% of their maximum output power on partly cloudy days, and even on extremely overcast days can still produce about 25% of their maximum. With the use of this simple approach, the operation and maintenance, costs, and complexity of the system is greatly reduced.

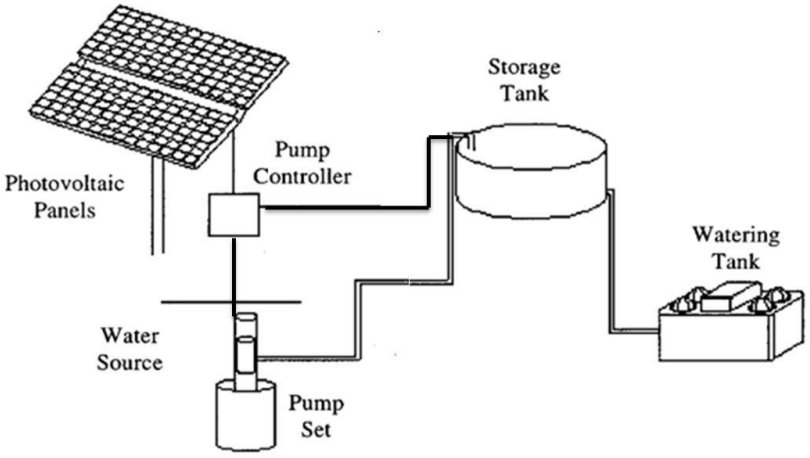

Figure 1: Direct-coupled solar pumping system.
Source: Agricultural Extension Services of the University of Tennessee

COMPONENTS

Solar water pumping systems are composed of two primary components other than the well itself - the PV panels (or modules) and the pump/motor.

Modules are installed with some type of mounting hardware that may permit orientating the

modules, adjusting the tilt of the modules to an optimum angle, elevating the modules for security, and eliminating shading and damage from animals. As a rule of thumb, PV panels are faced due south and at a tilted angle equal to the latitude location. This may be fixed or varied depending on seasonal conditions and other factors. For example, a summer tilt angle would be flatter to capture more sun with tilt angle equal to the latitude angle – 15° while a winter tilt angle might be latitude angle +15°. In Las Cruces the latitude angle would be 32° tilt, a summer tilt of 17°, and a winter tilt of 47°. It is critical to minimize shading by structures and vegetation during all watering seasons as significant loss of power can result from even partial shading of modules. Locating modules close to the water source is important to minimize power losses and costs.

PV modules are sized as to DC power (Watts) and come in all sizes from a few Watts to over 250W. Rated power is determined by the output voltage and current under standard sun intensity. A PV module rated at 50W may have an operating voltage up to 17.4V and a maximum current of 3.11A. Modules can be wired in series to increase output voltages and in parallel to increase current while also increasing total power. If sun light changes (clouds), output current will fall and thus power will fall at a relative level, i.e. if sun light is halved then current and power will be half while voltage remains about the same. PV modules are sized and configured (series/parallel combinations) to power the second major component of the system – the pump/motor.

Pumps provide a mechanism to move water from wells or surface sources. It is important to analyze the system properly in order to make it as efficient and economical as possible yet meet the watering requirements. In designing a system, one should minimize the amount of work required of the pump which minimizes the amount of energy needed to operate the pump and thus the size and cost of components. In understanding these basic concepts beforehand, the designer will be able to determine the appropriate components for a system.

In selecting a pump for the system, the following parameters should be considered:

- The required capacity – how many gallons per minute (or total per day) are needed
- The conditions on the suction side of the pump (lots of grit, sand, dissolved minerals in the water, algae growth, etc.)
- Whether the pump will be **submersible in a well**, or pump from a **surface source** such as a lake or pond

- The total head capability (how high can the pump move water)
- Space, weight, position limitations, cost of equipment and installation
- Codes and standards including the National Electrical Code (Wiles, 2001)
- The voltage(s) required for the pump and its working efficiency (average pump efficiencies are in the 25-35% range).

Once each parameter is clearly addressed, the decision to select a pump can be made. Pumps are classified as either positive-displacement or kinetic/centrifugal. The list of available pumps (and manufacturers) is very extensive and many will be capable of meeting the given application– pumping from a surface source or a well. Commonly a pump for a well application is a DC submersible pump with a range of 15V to more than 45V but may be much higher for very deep wells or high flow rates. The current is typically in the three to five amps range which equates to a rough operating power range between 1/4 to 2 HP (1HP = 746W). It has been determined that DC pumps use one-third to one-half the energy of AC pumps and are specifically designed to use PV efficiently and effectively even during low-light conditions at reduced voltages without stalling or overheating. Solar pumps are low volume, pumping an average of two to five gallons of water per minute. A majority of the pumps manufactured are positive displacement pumps (centrifugal-type pumps are used as well) which enable them to maintain their lift capacity all through the solar day at varying speeds that result from changing light conditions throughout the day[6]. A good match between the pump, PV array, and system parameters is necessary to achieve efficient operation (Morris & Lynne, 2002).

Other components that should be considered within the system are:

- PV mounting system - poles, fixed racks or some type of tracking system that follows the sun.
- Controller which allows the pump to start and operate under weak-sunlight periods (cloudy conditions, early morning - late afternoon)
- Storage water level sensor for on/off operation
- Direct-burial wire (UF), grounding, and lightning protection
- Pipe, fittings, and other balance-of-system components. A common mistake is to oversize the piping. Most PV applications will be pumping at low flow rates 1-5 gpm and these low flow rates will not have sufficient water velocity through a large pipe to keep suspended solids from settling out into the bottom of the piping. Therefore ½-inch to 2-inch piping is typically sufficient for PV without much friction losses – smaller is better, cheaper, and more efficient.

SYSTEM DESIGN METHODOLOGY

(For an example application, a livestock watering well will be assumed).

[6] See Foster, et al, 2012 for a more complete pump and PV discussion

Water-Demand: The first step is to determine the total water needed per day. Many producers are used to thinking of pumping lots of water in a short time frame with large capacity pumps. Solar pumping (like windmills) will pump a volume of water at slower flow rates (gallons per minute - gpm) over a longer time.

To determine '*Daily Water Requirement'* using the spreadsheet tool, the user enters the quantity and type - cow, horse, etc. of animal(s) they wish to service from this well. These entries and **Eqn. 1** below are used to calculate total daily water required for each animal type.

$$\boldsymbol{Gallons\ of\ Water/Day/Item} = Quantity \times required\ gallons\ of\ water\ per\ day\ per\ item$$

Livestock's daily water needs vary with air temperature, the animal's age and size, activity and distance to water, lactation, and dry matter intake (the moisture content of feed). Water needs corresponds to quantity of feed or forage intake; as intake increases, the water requirement level will increase; however, with a moisture content of 70 - 90 percent, lush forage may supply a large amount of required moisture in cooler weather. As water consumption is almost directly proportional to the level of milk production, lactating cows need much higher amounts of water. Air temperatures rising from 70 to 95° may increase water requirements by 2.5 times (Pfost et al., 2007).

Common NM values of required gallons/day per animal (or human) can be found in a spreadsheet table but the user has the option to change these default values depending on their unique situation[7]. The water demand should be estimated for the highest water demand period (typically summer) and anticipated growth during the design period (at least 10-years). In windy, hot, and dry areas the user should also take into account evaporation losses associated with open storage methods.

Table 1: Selected example amounts of water per day for various NM livestock

Item	Required amount of water per day (gallons/day)
Nursing Cow	**17.5**
Bred Dry Cows and Heifers	**14.5**
Bulls	**19.0**
Horse	**20.0**
Sheep	**2.0**
Elk	**5.0**

[7] See your NMSU extension agent for more information.

Once all the individual water-per-day-per-animal values are calculated and any extra water requirements are entered, values are summed yielding **the total daily water requirement** in gallons/day. A multiplier may be added which could provide an extra water cushion, offset evaporation losses, or to refill the storage tank. Domestic water demand for household use is variable depending on climate, usages, etc. but typically is around 75 gallons per person for drinking, cooking, and bathing.

Irrigation water-demand depends on local conditions, season, crops, delivery method, and evapotranspiration (available from agricultural agencies including NMSU ACES). Agriculture watering is usually greater in summer seasons when solar has its highest capacities.

Storage Tank Capacity: Depending on the climate and usage, storage capacity should equal three to ten days of water. For domestic use in a cloudy climate, ten days may be necessary while for sunny climates such as in NM, *three days-of-storage* for livestock watering may be sufficient. For deep irrigation such as that for trees (where the soil holds moisture for a week) three days' storage may be adequate. For irrigating a home garden, perhaps five days may be required. The storage tank size is calculated by multiplying days-of-storage by the daily water requirement.

Solar Resource: Once the daily water requirement is calculated, the '*Solar Resource*' at a specific location is determined. Sunlight will provide the energy to run the pump and is determined by the nearest latitudinal coordinate of the well location (between the values of 30 and 37 degrees). As the user inserts this value, the solar insolation is determined for winter, summer, or a yearly average automatically by the spreadsheet. It is recommended to use winter values as winter has the least amount of sunlight per day and it is best to design for the worst case scenario. Nevertheless, the user has the option to choose to design for summer if they plan to water for a summer only pasture. A good rule of thumb is that the solar resource must be greater than 3.0kWh/m^2 (3000 watt-hours per square meter of area in one day) for choosing a solar option. All areas of NMSU meet this limit with values well above 5kWh/m^2 per day. NMSU climate web site has good historical solar, wind, temperature data.

Pumping Requirements: '*Total Dynamic Head* (TDH)*'* is the total "equivalent" vertical distance that the pump must move the water; or the pressure the pump must overcome to move the water to a discharge height. Water pressure is expressed in pounds per square inch (psi) and is defined as the force caused by the weight of water in a column, also known as "head". Head is a term relating feet of water in a column which exerts a certain pressure. For example, a column of water 10 feet high would exert 10 feet of head or 4.3 psi (pressure). Knowing head, one can determine pressure and vice-versa. Head is important to determine how hard the pump must work to move water from the source to a discharge point (overcome the equivalent pressure of that water).

Static head is major part of TDH and is a term that refers to the total vertical lift (distance) from the water level in the well to the discharge level. Static head is composed of the water depth in the well at its lowest seasonal and draw-down level plus the elevation from the surface to the discharge point. Draw-down is the level of water that may drop in the well as pumping occurs – the well pipe is refilled at a recharge rate. The low flow rates of solar systems have less negative impact on draw-down. Entering these values, static head is calculated by **Eqn. 2:**

$$\textbf{Static Head (ft)} = \boldsymbol{Total\,Vertical\,Lift} = water\ level + drawdown + elevation$$

Pumps may be submersed in a well as deep as necessary to ensure reliable water supply (taking into account drawn-down levels, seasonal variations, and recharge rates). The water level variable in Eqn. 2 is measured from the SURFACE to the level of the water in the source not the depth-location of the pump. Placing the pump lower in the well (increasing its submergence) will NOT cause it to work harder or to pump less water, nor will it increase the stress or wear on the pump. However, there are reasons to NOT set the pump too near the bottom of the well:

1. A deep setting will increase cost, size (length), and weight of pipe and cable.

2. A setting near the bottom may increase the chance of sand or sediment being drawn into the pump and damaging the pump mechanism.

The pump must move the water from the well to an elevation but must also overcome friction losses in the system. These losses depend on the type of pipe (its roughness), total length of pipe including any horizontal runs, flow-rate (speed) of the water in the pipe, fittings and joints, and pipe diameter. The friction losses, which are expressed in equivalent lengths of vertical pipe distance, are added to the static head to yield an equivalent TDH – i.e. what *equivalent* height would the pump have to move water given these values.

To determine friction losses in pipe, the user is asked to enter the type of pipe (PVC, steel, etc.), total length of the pipe being used, and the nominal inside diameter of the pipe. The approximate head loss caused by friction within the pipe is calculated using the Hazen-Williams Empirical formula and it is important to note that we are assuming mediocre water temperature and the flow through the pipe is somewhat turbulent (Mott 2006). The value generated is in units of "feet of head". **Eqn. 3** below illustrates the Hazen-Williams formula.

$$\boldsymbol{H_L} = \frac{10.472}{C^{1.852}} \times \frac{Q^{1.852}}{D^{4.871}} \times L$$

The roughness coefficient variable 'C' within the equation depends on the type of pipe but is typically ~150. 'Q' is the flow rate in gpm and 'D' is the nominal diameter of the pipe in inches while 'L' is the total length of the pipe for the system in feet. Another standard "rule of thumb" is the friction losses in the pipe are typically 2-5 percent for a well-designed system.

The friction loss due to fittings must also be calculated. Friction losses for pipe fittings are converted to an equivalent length of pipe (in feet) and are a function of several variables. Losses due to fitting may be significant. To determine these losses, the spreadsheet lists many common fittings that might be utilized within the design of the system and the user is asked to input the quantity of each implemented fitting. The equivalent friction loss for each fitting is calculated using Eqn. 4. Table 2 shows a sample listing of some values used in the calculation of the friction loss due to a fitting.

Eqn. 4: $$\boldsymbol{Equivalent\ Length}\ (\boldsymbol{ft}) = pipe\ diameter\ \times quantity\ \times L/d$$

Table 2: Examples of equivalent length in pipe diameter (L/d) of specific pipe fittings

Pipe Fitting	L/d
Globe Valve, Fully Open	340
Gate Valve, Fully Open	13
90 Degree Standard Elbow	30
Swing Check Valve	135
Standard Tee, Flow Through Branch	60

Once the equivalent head pipe friction loss values are calculated for each specific fittings used within the system, they are converted to feet by dividing by 12 and then summed (Mott 2006).

TDH can now be calculated by using **Eqn. 5:**

$$\boldsymbol{Total\ Dynamic\ Head}\ (\boldsymbol{ft}) = Total\ Vertical\ Lift\ (static\ head) + \boldsymbol{H_L} + Friction\ Loss\ due\ to\ Fittings$$

Example of a TDH Calculation:

What TDH would be required to deliver 4-gpm from a well with water depth of 150-ft (no draw-down)? The well is 80-ft from the storage tank, and the delivery pipe rises 8-ft to discharge into the tank. The piping is ¾-in diameter PVC and there are three 90-degree elbows, one swing-type check value, and one gate type valve in the pipe.

Solution: the total length of pipe is 150+80+8=238-ft. From Table 2, the three "ells" add the equivalent of 3*2.0=11.25-ft of pipe; the check valve adds the equivalent of 16.875-ft; the gate valve 1.125-ft giving a total equivalent pipe length of ~**267–ft**. From calculation, 100-ft of ¾ in. pipe at 4-gpm has a pressure drop of 4.2-ft/100-ft of tube. Our friction-head requirement (H_L) is therefore 4.2*267/100=**11.2-ft** of water.

The water must be lifted 150+8=158-ft (static head) therefore TDH is 158+11.2=**169.2-ft**.

Hydraulic Workload: Often times we may work in other units than gallons and feet. There are about 0.0037854 *cubic meters* in a U.S. *gallon* of water; while 1 *foot* of distance = 0.3048 *meters.*

If we convert TDH in units of feet to meters and Daily Water Volume in gallons to cubic meters then one may calculate something called the Hydraulic Workload which is an excellent indication of the power that will be required to meet the system needs.

Eqn. 6: Hydraulic Workload (m^4) = Daily Water Volume (m^3) x TDH (m)

If the Hydraulic Workload is less that $1500m^4$, then the project is a good candidate for solar PV, if 1500-2000 it will be border-line, and greater than 2000 other options may be considered.

Pump and Flow Rate: The flow rate, or volume of water that is pumped in some time period – gallons/minute (gpm) is determined via **Eqn. 7** below:

$$\boldsymbol{Flow\ Rate}\ (\boldsymbol{Q}) = \frac{Total\ Daily\ Water\ Requirement}{Total\ Daily\ Solar\ Insolation\ \times 60\frac{min}{hr}}$$

In this first version of the spreadsheet, the user is shown the calculated Q and TDH. Using these two key values, the user must manually choose a specific pump (from an initial limited selection) that will be capable of pumping water at the necessary Q and TDH. Once a pump is selected, we determine at what voltage this pump will operate (12V, 30V, etc.) and how much power (Watts) is required to run this pump assuming standard pump efficiency (~35%). This is the power that de-rated PV modules must supply to operate the pump. De-rating takes into account temperature and soiling effects on the modules.

PV Determination: '*Array Sizing*' involves the automatic sizing of the PV array given the calculated and manually selected pump parameters. The first calculation performed is to determine the number of PV modules in series – a string. Each PV module has an operating output current and voltage. Connecting modules in series increases the total voltage to match or exceed the required pump motor voltage (determined earlier). Eqn. 8 illustrates this while Eqn. 9 describes how the PV strings may be connected in parallel to increase total current and thus total power to match or exceed the required pumps power (also determined earlier). Voltage multiplied by current determines total power provided by the PV array in Watts or converted to horsepower (HP) – (1Watt = *0.00134102209 HP)*. Note; it is possible that there will only need to be a single module or modules only in series and not in parallel.

In **Eqn. 8** below, the 17.4V value represents the operational voltage for our PV module.

$$\textbf{\textit{Modules in Series}} \text{ (rounded to higher integer)} = \frac{Pumps\ Motor\ Voltage}{17.4V}$$

In **Eqn. 9** below, the 3.11A represents the PV panel's rated current (at Standard Operating Conditions) and the 0.80 value represents the de-rating factor.

$$\textbf{\textit{Number of PV Strings in Parallel}} \text{ (integer)} = \frac{Pumps\ Peak\ Panel\ Wattage}{Modules\ in\ Series\ \times 17.4V\ \times 3.11A\ \times 0.80}$$

Because we round up the number of strings and parallel combinations to whole numbers, the total amount of energy and therefore water pumped will be greater than our required daily requirements in any full sun day. This is typically not an issue when there are float switches incorporated into storage systems which will stop the pumping when the storage tank is full.

NOTE: these values are for a pre-selected example PV module. If other size PV modules are selected, then the values must be changed to reflect this modules voltage and current.

Final Design Specs: '*Design Specification'* summarizes the design values obtained through the use of the spreadsheet and lists the key components and materials for this scenario's direct-coupled solar water pumping system. The description and quantities for specific items are obtained from calculations or specified by the user. The cost for each itemized component is calculated by multiplying the quantity of each item by a representative listing price - obviously prices will vary over time. The necessary length of UF wire is roughly determined by the length of pipe plus an extra 25 percent. The market price for the UF wire is for 250-ft rolls. Pipe is assumed to be PVC and the price is calculated by dividing the total length of needed pipe by ten and multiplying by its market price since PVC pipe is typically sold in 10-ft lengths. The grand total of the entire system (not including the well or storage) is calculated by adding up all the itemized totals. This value reflects an approximate value which the customer will need to invest into the construction of the system minus the costs of other materials, labor, sales taxes, shipping, etc. Federal and state tax incentives may lower the initial costs by up to 40 percent (as of 2012).

RESULTS

Using the spreadsheet provides options to test various key design scenarios and demonstrate the design method and terminology for a direct-coupled solar water pumping system. It is important to consider the limits of this first version as it is only able to calculate for flow rates up to 4 gpm and TDH values no greater than 230 feet due to the very limited PV and pump selection options within this version. In the case of the design values greater than these and for other pumps or PV module choices not available within the spreadsheet, the user should reference alternative pump

performance data provided by solar pump or PV manufacturers. It is envisioned that later versions of this spreadsheet will address several of this issues.

CONCLUSION

Photovoltaic powered water pumping systems are attractive for livestock and agriculture producers with remote water sources and limited access to AC power. Even though windmills have been in use for decades and will continue to provide effective solutions for water pumping, solar power has made significant steps towards becoming the system of choice for these situations. The low maintenance and simple operation, no fuel (transportation or storage) costs, environmentally benign, as well as competitive life-cycle economics of solar systems place them at the forefront of choices in supplying water to livestock or agriculture. The technology for solar water pumping is exceeding all expectations, and will continue to be a viable choice for more and more users as its capabilities, reliability, and versatility increases while costs decrease.

The spreadsheet, documentation, and demonstration modules provide NMSU constituencies with terminologies, knowledge, and skill sets which can be the foundation for informed choices relating to alternative water pumping systems. For additional information, contact your local state agricultural extension agent or NMSU.

LITERATURE CITED

Bartlett, B. (n.d.). *Watering Systems for Grazing Livestock.* Great Lakes Basin Grazing Network and Michigan State University Extension.

Buschermohle, M. J., & Burns, R. T. (n.d.). *Solar-Powered Livestock Watering Systems.* University of Tennessee, Agricultural Extension Service.

Surber, G. et al., (n.d.), Montana State University Animal and Range Sciences Extension Services, *"Drinking Water Quality for Beef Cattle; An Environment Friendly & Production Management Enhancement Technique"*

National Renewable Energy Labs, (n.d.).; *"ELECTRICITY WHEN AND WHERE YOU NEED IT FROM THE SUN, PHOTOVOLTAICS FOR FARMS AND RANCHES",* NREL/BR-412-21732

Pfost, D., Gerrish, J., Davis, M., & Kennedy, M., 2007. *Pumps and Watering Systems for Managed Beef Grazing.*

Foster, R., et al, 2003, "*Renewable Energy for Water Pumping Applications in Rural Villages*" for National Renewable Energy Lab, NREL/SR-500-30361

Morris, M., & Lynne, V., 2002, *Solar-Powered Livestock Watering System.*

Wiles, J (2001) *Photovoltaic Power Systems and the National Electrical Code"* Sandia National Laboratories, SAND87-0804

New Mexico State University, College of Agriculture's Water Task Force, various publications: http://aces.nmsu.edu/ces/watertaskforce/index.html

BOOKS

Mott, R. L., 2006. Applied Fluid Mechanics (6 ed.). Upper Saddle River, New Jersey: Pearson Prentice Hall.

Boyle, G., 2004. Renewable Energy. Oxford University Press.

Masters, G. M., 2004. Renewable and Efficient Electric Power Systems. Hoboken: John Wiley & Sons, Inc.

UNPUBLISHED/PRIVATE COMMUNICATION

Foster, R., et al, 2012, "*Technical and Operational Guidelines - Photovoltaic Power Systems*"

Jenkins, T., et al, 2012, *"Analysis of Solar, Wind, and Diesel in Water Pumping in Areas of NM"*

CORRESPONDENCE SHOULD BE ADDRESSED TO:
Thomas Jenkins, ETSE, NMSU
tjenkins@nmsu.edu

ACEQUIA CULTURE BENEFITS ECOSYSTEM FUNCTION IN THE MORA VALLEY

Shannon M. Rupert[1]

ABSTRACT

Water resources in the Southwest U.S. will become more limited in the coming decades due to increased demand, shifts in land use, and climate change. While we struggle to find ways to adjust governmental water management policies to meet these challenges, in many small communities in northern New Mexico, water is still managed locally using traditions that are sometimes hundreds of years old. In the Mora Valley, acequia management practices have reduced the natural flow of the Mora River such that a 3.4 km section is dry most of the year. In contrast to what would seem an unhealthy situation, the ecology of the river below this dry stretch appears much as it does above the diversion, suggesting that the connectivity created by the acequias allows those managing them to react to natural pulse and press events as they occur. Using a social-ecological framework, a comparison of local water data and management practices to that of larger government-managed projects shows that culturally based community management systems have a greater flexibility and quicker response to both short and long term perturbations. These community practices have a greater influence on water management in the Mora Valley than governmental policies, and have the potential to ameliorate problems normally associated with reduced or intermittent stream flow.

[1]Department of Biology, University of New Mexico, Albuquerque, New Mexico 87131

New Mexico has the lowest water to land ratio in the United States. Only 0.2 percent of the state's almost 3.5 million hectares, or about 60,600 hectares, are surface water sources such as lakes and rivers (U.S.G.S. 2012). Not all the water in these surface bodies belongs to the people of New Mexico. Water sharing agreements, or compacts, with other states make it necessary for us to deliver part of our water across state lines. Demand for this limited natural resource is only expected to increase with population growth, land use shifts, and climate change. It is not hard to understand why New Mexicans take their water seriously.

Any study of water in New Mexico has a human component. This is especially true in northern New Mexico, with its long history of human occupation. There is no place in northern New Mexico where the original biodiversity of the region has not been altered (Debuys 1985). Even on the steepest mountain slopes, past grazing has affected current distribution of flora. And acequias, traditional earthen irrigation ditches, have been diverting water away from stream channels and across the landscape for sometimes hundreds of years. It is a landscape intricately linked to people, a place where ecology and culture collide. And because cultural traditions are still a strong part of everyday life in northern New Mexico, it is perhaps the best place to understand this connection between the life of the land and that of its people. The emerging discipline of social-ecology gives us a place to begin.

Most ecologists focus on systems in which the human component is discounted, minimized, or considered in the context of how it impacts an otherwise natural system. However, in the past half-century, humans have altered ecosystems more than at any other time in history (Collins *et al.* 2011). This means we can no longer ignore the impact of human behavior and the outcome of those behaviors as they affect ecosystems. This interdisciplinary way to look at systems is opening up new questions and giving us new answers. Most simply defined, social-ecology looks at the interactions between human populations and communities and their environment. Social-ecology studies should produce actionable science that can be used to shape political and environmental decisions before human impact has a devastating effect on an ecosystem.

Social-ecology as a discipline is much more established in the social sciences than in ecology. As a result, most published research leans heavily on social science methodology. Social scientists have developed complex frameworks for analyzing how social conditions affect things such as natural resource depletion and ecosystem health (Cox 2008). One recent study by Cox, for example, investigated the social-ecology of the acequias in the Taos Valley (2010). While the research is rigorous, it illustrates the need for more collaboration between social scientists and ecologists. Cox used the single dependent variable of crop production, using the Normalized Difference Vegetation Index (NSVI), to equal collective action. From an ecological perspective, there are two problems with this. First, using a remotely sensed estimate of vegetation cover to determine crop production in areas where flood irrigation is practiced will result in an overestimation of production. Second, Cox asserts that the Taos Valley is dependent on growing crops as his justification for using this variable. Data from the USDA Census of Agriculture show that contrary to this assumption, Taos County is not dependent on farming and indeed, the average farm in Taos County loses money each year (2007). This romanticism of farming in northern New Mexico persists in the face of a changing landscape. It is perpetuated for myriad reasons, the most justifiable being that it is the cultural heritage of the Native and Hispanic peoples who have shaped this land.

Social questions about acequias often focus on cultural values and how traditional management and use of the acequias create sustainability and healthy landscapes. Cultural studies suggest that acequias have a positive influence on the local ecosystem by increasing biodiversity, extending the riparian zone, and protecting the hydrology and ecology of the watershed (Rivera 1998, Rodriguez 2006). Biophysical research on acequias has been limited in the past and has mainly focused on hydrology (Fernald *et al.* 2007, 2006) and GIS mapping. Along with our study on the ecology of the acequias in the Mora Valley, two other current projects (Roybal 2012, New Mexico EPSCoR 2011) demonstrate a shift toward social-ecological thinking about acequias.

An example of a proposed framework for social-ecological studies is the Pulse-Press Dynamics (PPD) framework of Collins *et al*. (2011). This framework suggests that pulse-press events and ecosystem services can be used as links between the social domain and the biophysical domain. Pulse events are those that occur suddenly, while press events happen slowly and pervasively. Both pulse and press events can create disturbance in the two domains, and for each the resistance and resilience of the component can be studied. Ecosystem services create a linkage between the domains by their very nature. The definition of an ecosystem service is a structure or function within an ecosystem that benefits humans. The PPD framework provides a way to examine natural systems with humans in a holistic way.

A PPD framework for the acequia system in the Mora Valley demonstrates how this works (Figure 1). The social domain of the acequia has two components. Human behaviors are those management decisions made by using place-based knowledge passed down through generations. Human outcomes are the sustainability of these community-based practices and the benefits to the overall health of the landscape. Likewise, there are two components to the biophysical, or for the purpose of our study, the ecological domain. Patterns such as community structure and biodiversity make up one component, while processes like hydrologic flow and discharge make up the other. Disturbances in the form of presses and pulses create feedbacks that push these components in a given direction. The major pulses in this system are short-term drought, spring runoff, the summer monsoonal rains, and nutrient inputs, such as fertilizers from farming and ranching, domestic use, and a fish hatchery. Presses are climate change, shifts in land use, and population growth. The social components react to the presses and pulses; these in turn shape the patterns and processes of the ecosystem, which dictate the ecosystem services used by the people. In the Mora Valley, the ecosystem services are hydrologic connectivity, irrigation that results in crops, and a continuation of cultural traditions and values. While there may be other components to this proposed PPD framework, we are limiting the scope of this article to those listed here.

The overall question is: are current water management practices, both community and governmental, affecting the ecology of the acequias and streams within the Mora Valley? We suggest that the answer is yes. Each of the four hypotheses listed in Table 1 will be addressed in a sub-section below.

Table 1. List of hypotheses (H) as they relate to the overall question of how current water management practices affect the ecology of the acequias and streams within the Mora Valley.

H1	Water resources have become more limited in recent decades, but acequia management has not.
H2	Current acequia management practices have reduced the natural flow of the Mora River.
H3	Community practices have a greater influence in water management than governmental practices.
H4	These community management practices ameliorate problems normally associated with reduced streamflow.

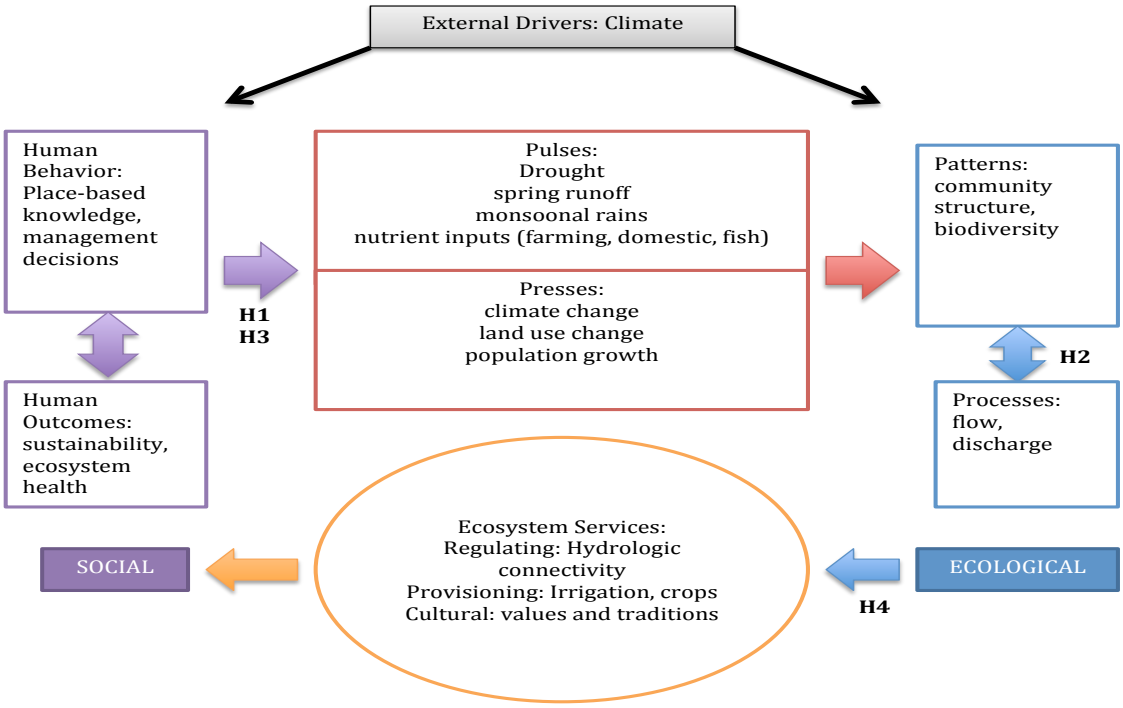

Figure 1. PPD framework for social-ecological research on the ecology of the acequias in the Mora Valley. *For clarity, only those components in our study are listed. Additional components could be added that would fit within the overall framework. Hypotheses (indicated H1-4 on the figure) are those listed in Table 1.*

STUDY SYSTEM: THE ACEQUIAS IN THE MORA VALLEY

The Mora River flows through Mora County in northern New Mexico. It begins life as a small trickle high in the Sangre de Cristo Mountains and ends its journey where it becomes a tributary of the Canadian River. To understand the hydrology of the Mora River, we first need to look at the geomorphology of the terrain through which it flows. Mora County is a max relief county, meaning that its relief is not only the greatest in New Mexico, but also ranks fifteenth of counties throughout the United States (Brekhus 2011). The difference between the county's highest point, Truchas Peak, at 3994 meters and its lowest point along the Canadian River at 1420 meters is 2573 meters. The headwaters of the Mora River are above 3660 meters and it is over 160 kilometers from headwaters to discharge into the Canadian River. The river flows from west to east and the slope is considerable, at least at first. The mountain terrain gives way to flat open plains soon after the river runs through the gage at La Cueva, a few miles downstream from the village of Mora, and about half way through the river's length. The total drainage area is 44, 806 hectares.

Along most of its length, the waters of the Mora River are diverted into acequias, or irrigation ditches. At least forty-seven major acequias have been identified on the river. The longest of these is a trans-mountain acequia that carries water for more than 16 kilometers. The shortest is 0.8-kilometer (Kammer 1992). Most are used for irrigation of pastureland and hayfields, although some support what remains of subsistence farming in the valley (Martinez 1990). Water is supplied to the watershed via snowmelt and through summer rainstorms. The Mora is a snowmelt river, meaning that highest discharge occurs in late spring/early summer, although there is another spike in discharge during the "monsoon season", generally late July through August. Groundwater and three trans-mountain acequias add a relatively small amount of water to the total water budget.

Flows on the Mora River are variable not only because of climate and weather, but also due to human influence. Each acequia is managed separate from the others, without regard to the natural flow of the river or the effects of management decisions made on other acequias. This results in the river at times going completely dry over a 3.4-kilometer stretch. At other times, flow in this area can be either greatly reduced, or near natural levels. The affected section begins just upstream of the village of Mora. Two major acequias, in close proximity to each other, divert water away from the river and over the floodplain. There are myriad smaller acequias that contribute to this connectivity between the longitudinal and lateral channels. Most of the water is not used and is redirected back into the river just downstream of the village. At the point where it returns to the river, flows are once again at natural levels, and the river appears healthy, with beaver and large fish in residence.

HYOPOTHESIS ONE: WATER RESOURCES HAVE BECOME LIMITED

Discussions about water in the Mora Valley eventually come around to stories of how much more precipitation the valley used to receive. Data from the Western Regional Climate Center's stations at Chacon do not show this to be fact. There is even a statewide trend towards greater precipitation over the past half century (Table 2). If you look at the annual averages from

the two operating stations in Chacon, between 1914 -1985 the yearly average precipitation was 50.01 centimeters and between 1985-2010 it was 56.54 centimeters. There are no data that support a sharp decline in precipitation. This may seem strange in light of the current short-term drought we are experiencing. 2011 was one of the ten driest in the state's history. When you take the current state of precipitation and combine it with increased water demand and the now accepted threat of climate change, it is easy to understand why this perception persists.

Table 2. *Thirty-year precipitation averages from the Chacon COOP stations and statewide in New Mexico. Note that these averages do not account for the current state of precipitation, nor do they show the considerable year-to year variability that is characteristic of the region. For example, the Chacon stations recorded a record low of 21.64 cm in 1956 and a record high of 89.26 cm in 1991.*

Dates for 30-yr averages	Precipitation (cm) at Chacon COOP	Precipitation (cm) for New Mexico
1931-1960		32.99
1941-1970		32.13
1951-1980		31.98
1961-1990	49.63	35.18
1971-2000	53.01	37.03
1981-2010	55.96	

There is also a strong cultural component to the perception that water resources are limited. "El agua es vida", or "Water is life", is a saying you hear often in northern New Mexico. People are taught from a very young age that it is important to protect their water, and that early training leaves a very strong impression. Traditional acequia practices go hand in hand with cultural mores. Management of the acequia stays the same decade after decade, altered only when conditions warrant. Water is not particularly scarce in Mora, and many of the acequias in the valley run most of the year.

There is one way in which water has become more limited in the Mora Valley, and that is for domestic use. Although the county's current population of just over 5600 has been greatly reduced from its high of 14,000 in the 1920's, there has been a sharp increase in water demand as new people move into the area seeking vacation and retirement homes on former large ranches (Stephens 2005). So although water resources have not been depleted in the last century, these new demands for water, combined with climate change, could forever change the embarrassment of water riches in the Mora Valley.

HYPOTHSIS TWO: ACEQUIAS HAVE REDUCED FLOW ON THE MORA RIVER

In the village of Mora, people seeking relief from the summer's heat by dipping their feet in the Mora River will often be disappointed. Current acequia management practices in the valley divert the water from the river into the acequias and leave the river mostly dry right in the center of town. The acequias extend the river's channel beyond the riparian

zone, and irrigate the valley's farmlands. At the lower end of town, water is redirected back into the river via acequia outlets, the sub-surface, or a multitude of culverts. Only several hundred meters after the first of these outflows, the river assumes the same appearance as above the diversion dam.

In the summer of 2009, we took flow measurements along a 27-kilometer stretch of the Mora River from the headwaters to below the affected stretch of the river. Using the Environmental Protection Agency's Environmental Monitoring and Assessment Program methodology (EMAP) (Peck *et al.* 2003), we recorded flow on June 9th and 10th, 2009 (Thomson and Ali 2009). At the headwaters, flow was 4.87 cubic feet per second (cfs). Within the affected stretch of the river, flow was 3.49 cfs, consistent with most of the water being diverted into the acequias, which we visually confirmed, and despite that fact that just below this stretch the flow was 38.78 cfs. This flow is about the same as we saw just upstream of the affected stretch, although we did not take measurements there. The huge difference in flow between the affected stretch and areas just upstream and downstream would not register on the gage at La Cueva, which showed a daily mean flow of 29 and 32 cfs on the dates of our study. These data are, however, consistent with our measurements, since additional water is diverted between our study sites and the gage, a distance of several kilometers, and so slightly lower values would be expected.

In our study, flows on acequias were much less than those of the river. Measurements taken from acequias that did not divert significant water from the river ranged from 0.8 to 1.6 cfs. Where most of the river water was diverted, flows were much higher, and ranged from 5.92 to 14.44 cfs. These data are consistent with USGS data for La Sierra acequia recorded during the days of our study, when flow was 10-11 cfs. The lower flow within the acequias should have significant impact on the ecology of the river and these lateral extensions.

These data are not consistent with estimates of depletion for Mora County given in the Mora-San Miguel-Guadalupe Regional Water Plan (Stephens 2005). Those data show depletions of 15,234 acre feet and a return flow of 17,437 acre feet, or a loss of roughly half of the water being diverted for irrigation. This is clearly not the case in the western half the county, perhaps because of high precipitation, increased access to snowmelt, and a higher groundwater table.

HYPOTHESIS THREE: COMMUNITY PRACTICES HAVE INFLUENCE

New Mexico water law is complex, governed by multi-state laws, tribal law and federal law in addition to state law. As a subject, it is far outside the scope of this article. However, from an acequia perspective, what is important to note are that decisions regarding water rights are based on prior appropriation and beneficial use, or who was using it first and how they are using it. Article 16 of the New Mexico Constitution gives the state sole authority over water rights. Interestingly, however, the constitution does not actually define public welfare, and determining who had the water first can be tricky. The year 1907 is used to determine priority use, and the people in a given region have, for the most part, determined public welfare. Another important concept in acequia water law is adjudication, in which a lawsuit is begun on a given stream system to determine who owns what water rights (NMAA 2008). No acequias in the Mora Valley have been adjudicated and there are no plans to do so in the near future.

The Office of the State Engineer (OSE) has been tasked with water oversight and management decisions are based on the sixteen regional water plans. The regional plan for the Mora Valley includes all of Mora, San Miguel and Guadalupe counties. The data used to create this plan are problematic. Within the region, western Mora County and parts of western San Miguel County are ecologically different than the rest of the region, mainly due to different geomorphologies. In some instances, data collected in eastern Mora County can be almost the opposite of that collected in western Mora County and when combined, they cancel each other out. So management decisions made for the region may not always be appropriate for the Mora Valley. Another problem is that any decisions to be made under the current system take a very long time to be resolved. For this reason, decisions made locally by the acequias are often more important in terms of how water resources are managed.

Another way to look at the importance of community-based management decisions made by individual acequias is to compare them to other canal systems that have no direct community influence in their decision making. Here we compare the acequia system in the Mora Valley to the Central Arizona Phoenix Canal and the Salt River Project canals in Arizona. The most important physical difference between the three systems is scale. The Mora Valley acequia system is a small rural irrigation system serving local farmers. The Salt Valley Project canal system is a much larger, mixed rural and urban system that serves the people in and around the Phoenix metropolitan area. The Central Arizona Project aqueduct is a massive water transport system delivering Colorado River water to the people of central Arizona. A short description of each system follows (Table 3).

The Central Arizona Project (CAP) was created by the Colorado River Basin Project Act of 1968 for the purpose of delivering Arizona's allocation of Colorado River water. The Central Arizona Water Conservation District, a municipal corporation, manages it. Along the length of the aqueduct are tunnels and pumping stations, as well as six recharge areas. These recharge areas divert water into shallow surface basins which drain into the ground to create "artificial groundwater". Although there are lateral extensions delivering water to end users, for the most part connectivity for the CAP is longitudinal and vertical.

The Salt River Project (SRP) canals are part of the Salt River Project, which consists of two organizations. The Salt River Project Agricultural Improvement and Power District, an Arizona state government entity, is an electrical utility created in 1936. The Salt River Valley Water User's Association, a private corporation, was created in 1903 to allow for dams to be built for the system and this corporation now delivers water to most of central Arizona. The eight main canals were built beginning in 1868, using impressions that remained of canals built by the Hohokam between 300-1450 A.D (Masse 1981; Roach *et al.* 2008). Beginning in 1947, the 131 miles of canals were lined with gunite to prevent erosion (Phillips *et al.* 2009).

The Mora Valley acequias were created for agricultural purposes by Hispanic settlers between the mid-1800's and early 1900's. The Mora Valley is about sixteen kilometers in length and the acequias run lateral to the main channel of the Mora River. Each acequia is managed by a mayordomo, or water boss, and three commissioners who are elected by the parcientes, or water users. Decisions are made collectively by the parcientes, and carried out by the mayordomo. In addition, each acequia operates independently. The acequias are physically unchanged from when they were built, with the exception of some concrete and metal replacing the traditional rock headgates. The ditches themselves are made from natural soils, mainly clay, that are re-dug and manually cleared of vegetation and debris yearly. State law declares that acequias have the right to govern and manage themselves.

Table 3. *A summary of some of the characteristics of the three canal systems.*

	Mora Acequias	Salt Valley Project	Central Arizona Project
Length of main channel (km)	~20	211	541
Length of laterals (km)	~188*	2092	N/A
Acre-feet per year	33,000*	1.0×10^6	1.5×10^6
Main purpose	Agricultural	Direct agricultural (10%) and urban multi-use (90%)	Water transfer to municipal, agricultural and Native American water districts
Hydrological Connectivity	Longitudinal, lateral	Longitudinal, lateral	Longitudinal, vertical
Construction	Soil	Gunite	Cement
Management	Mayordomos (independent)	Salt Valley Water Users Association (private)	Central Arizona Water Conservation District (public)

*These numbers represent the Mora River over its entire length.

As noted in Table 3, the Mora Valley acequias function on a much smaller spatial scale than the SRP and CAP canals. The acequias are still being maintained by the parcientes, who adjust their practices immediately to compensate for any new demand on the system. The SRV and CAP management does not have this flexibility to react and make changes on a short time scale. The SRV for example still use irrigation system field operators to open and close headgates according to schedules that may no longer be effective or even necessary. Originally, most of the canal water was directly delivered to users, now almost all of it goes through water treatment plants and then automatically out to users. In addition, some canals that are no longer used are still being maintained. Management has not kept up with operations (Gooch *et al.* 2007).

This inability to make swift changes limits the effectiveness of the SRV, CAP, and New Mexico OSE management practices. Let's examine this idea using short-term drought. Drought is a constant threat in all of these systems. In the Mora Valley, the mayordomo can see the effects of drought firsthand, and can instigate changes in operations to conserve water almost immediately. He may need to meet with other acequias to come to an agreement on how to share the water, but that can be handled quickly. The time scale for operational changes for the other three systems is so slow that by the time the changes are made in operations, it could be too late. The response of the SRV management to the long-term reduction in available water, for example, has been to purchase excess water from CAP when it is available (Phillips *et al.* 2009). What will happen if we continue to see reductions in available water due to climate change? SRV projections predict that overall runoff will be reduced by 20-50 percent in the next fifty years. There is no other plan in place in the event that CAP does not have excess water available

for purchase. The lack of response of the SRV to Phoenix becoming an urban heat island is another example. Even though there is evidence that the overall temperature in Phoenix has increased 7.5° C above that of the surrounding area and CO_2 levels are double that of the global average, management has not addressed what changes in operations should be made in response to these environmental changes (Shen *et al.* 2009). CAP and OSE management also have no plans in place to deal with climate change. Yet acequias have already been adjusting to climate shifts in some places for several hundred years.

HYPOTHESIS FOUR: COMMUNITY PRACTICES PROTECT THE ECOSYSTEM

As noted, the headwaters of the Mora River are in the Sangre de Cristo Mountains, which are the southernmost portion of the Rockies. Vegetation is mostly subalpine forest. As the river moves down into the Mora Valley, the vegetation gives way to ponderosa pine forest and non-native vegetation such as hay pastures. Gross primary production is dominated by allochthonous material throughout the length of the river, although autochthonous production increases in the main river channel down on the flat open plains. An abundance of algae in the acequias suggests they play a major role in the production of autochthonous material within the lateral extensions of the river system.

The Mora River is designated a high quality coldwater fishery in its upper reaches, and a coldwater/warm water fishery from the affected stretch until it flows into the Canadian River. Trout, native and introduced species, inhabit the upper reaches, and additional fish species also live in the river. It is not known whether fish inhabit the acequias as residents, but they are often present in the waters of even the smallest acequias, perhaps as unfortunate visitors. When there is no flow in the affected stretch of the river, pools that remain get warmer and deoxygenated as they evaporate, and many fish and other organisms die between wet flow periods and dry periods. It is unknown how this affects fish, algae and macroinvertebrate populations in the stream outside of the affected area. There also is no upstream migration, nutrient spiraling, or downstream drift of any aquatic organisms when the river is dry. The patchy nature of the acequias disrupts the simple upstream-downstream production model we should expect from the Mora River and makes assumptions based on current theoretical models about stream structure and function problematic.

We conducted macroinvertebrate sampling at three sites along the Mora River in June 2009 using a kick net and field identification. One site was above the dry stretch and two were below it. Our results showed an abundance of insect orders that are intolerant of pollution. Groups fairly to very tolerant of pollution were also present at all sampling sites, but in lower numbers (Thomson and Ali 2009). Using a Pollution Tolerance Index developed by Hoosier Riverwatch (2009), all three sites were given ratings of excellent with scores of 24, 37, and 36. Anything over 22 defines a reach as excellent, meaning the river is in good condition at our sampling sites. A more rigorous study looking at macroinvertebrate community structure between and within the river and acequias is currently underway, and based on preliminary unpublished data, there are more differences than this short study shows.

In addition, we took water samples for five sites on the Mora River and seventeen on acequias/tributaries. A total of nine of those sites were used in the results/analysis for this paper. We measured pH, temperature, dissolved oxygen, electrical conductivity, flow volume and alkalinity in the field. Analyses were conducted at the University of New Mexico's

Environmental Analysis Laboratory in the Earth and Planetary Science Department (Thomson and Ali 2009). Of these data, three river sites and three acequias were evaluated for water quality (Table 5). As expected, pH showed little variation. Temperature was within expected limits and mostly followed a predictable elevation gradient. Dissolved oxygen was always within limits, and often reached saturation. In most cases, electrical conductivity was slightly higher than the recommend level, and showed a clear increase as we moved downstream. As conductivity is often used to estimate total dissolved solids (TDS), this suggests that non-point source pollution is occurring along the river. Nutrient analyses were completed for the three river sites and four acequias (Table 4). Overall parameters were within TMDL limits established by the NMED for the Mora River, although phosphorus and total nitrogen in some cases came close or were slightly above the limits (Table 6). This was especially true in acequias. A complete analysis of all water samples can be found in Thomson and Ali (2009).

Table 4. Sampling sites from June 2009 used for this paper.

Site	Hydrology	Water Quality	Nutrient Analysis	Macro-invertebrates
Luna Creek (Headwaters)	X	X	X	X
Mora River @ Allsups	X	X	X	
Mora River @ Romero Ranch	X	X	X	X
Mora River @ Wind River Ranch				X
Acequia @ Chacon turnoff	X			
Lower Acequia-Mora Research Center	X	X	X	
Upper Acequia-Mora Research Center	X	X	X	
Acequia @ CR A002	X			
Trambley Acequia	X	X	X	
El Carmel Acequia	X			
Acequia @ Fish Hatchery	X		X	

Table 5. Summary of water quality measures on the Mora River and acequias in the Mora Valley, June 2009. *Three sites on the Mora River and three acequias were sampled. Not all data were collect for all acequias; the number in parentheses indicts how many were measured. See Table 4 for details. DO (mg/L) = dissolved oxygen in milligrams per liter, EC (µS) = electrical conductivity in microSeimens, Temp (°C) = temperature in degrees Celcius*

	pH	DO (mg/L)	EC (µS)	Temp (°C)
Mora River	7.21 - 8.95	8.5 - 11.23	247 - 490	7.8 - 15.3
Acequias	7.84 (1)	13.0 - 13.6 (2)	172 - 516 (3)	9.7 - 15.9 (3)

Table 6. Summary of nutrient analysis for the Mora River and acequias in the Mora Valley, June 2009. *The same three sites on the Mora River were sampled. Four acequias were sampled; only two were the same as in Table 5. See Table 4 for further details. Total Maximum Daily Load (TMDL) limits for the Mora Rover are 0.38 mg/L for combined nitrate and ammonium (total nitrogen) and 0.03 mg/L for phosphorus (in this case SRP phosphate).*

	Nitrate (mg/L)	**Ammonia (mg/L)**	**Total Nitrogen (mg/L)**	**Phosphate (mg/L)**
Mora River	0.09 - 0.13	0.12 - 0.25	0.21 - 0.38	0 - 0.02
Acequias	0.1 - 0.69	0.03 - 0.45	0.13 - 1.14	0 - 0.04
TMDL limits	--	--	0.38	0.03

CONCLUSIONS

While further investigation is needed to conclusively state exactly how community-based and governmental management practices are affecting the ecology of the Mora River and its acequias, we suggest that given the current situation, both are instrumental in sustaining ecological health, effective irrigation and supporting cultural traditions and place-based knowledge. Acequia management practices should be integrated into regional water plans as they can quickly compensate for both pulse and press events.

ACKNOWLEDGEMENTS

This work was supported by the American Indian College Fund's Sloan S.T.E.M. Leadership Fellowship and the Acequia Institute and would not have been possible without the guidance and support of the following people: Cliff Dahm, Becky Bixby, Scott Collins, Penny Boston, Bruce Thomson, Abdul-Mehdi Ali, Bobby James, Chad Bryant, Mitchell Nakai, and the students of UNM's WR 573 class in June 2009. This article benefitted from suggestions by an anonymous reviewer.

LITERATURE CITED

Brekhus, J. 2011. Maximum Relief Counties by State. http://www.cohp.org/records/relief/Helman_counties.html

Central Arizona Project (CAP) website. 2011. http://www.cap-az.com/

Collins, S.L., S.R. Carpenter, S.M. Swinton, D.E. Orenstein, D.L. Childers, T.L. Gragson, N.B. Grimm, J.M. Grove, S.L. Harlan, J.P. Kaye, A.K. Knapp, G.P. Kofinas, J.J.Magnuson, W.H. McDowell, J.M.Melack, L.A.Ogden, G.P. Robertson, M.D. Smith, and A.C. Whitmer. 2011. An integrated conceptual framework for long-term social ecological research. Front Ecol Environ. 9 (6): 352-357.

Cox, M., and J.M. Ross. 2010. Robustness and vulnerability of community irrigation systems: The case of the Taos valley acequias. J Environ Econ Manage. 6 (2011): 254-266.

Cox, M. 2008. Applying a social-ecological system framework to the study of the Taos valley irrigation system. Workshop in Political Theory and Policy Analysis, Indiana University, Bloomington.

DeBuys, W. 1985. Enchantment and Exploitation: The Life and Hard Times of a New Mexico Mountain Range. University of New Mexico Press, Albuquerque.

Fernald, A.G., Baker, T.T. and S.J. Guldan. 2007. Hydrologic, riparian, and argoecosystem functions of traditional acequia irrigation systems. J Sustain Agr. 30 (2): 147-171.

Fernald, A.G. and S.J. Guldan. 2006. Surface water-groundwater interactions between irrigation ditches, alluvial aquifers, and streams. Res Fish Sci. 14:79-89.

Gooch, R.S., P.A. Cherrington, and Y. Reinink. 2007. Salt River Project experience in conversion from agriculture to urban water use. Irrig Drainage Syst. 21:145–157.

Hoosier Riverwatch. 2009. http://www.in.gov/dnr/nrec/files/nc-Riverwatch_Manual.pdf

Kammer, D. 1992. Report on the Historic Acequia System of the Upper Rio Mora. New Mexico Historic Presentation Division.

Martinez, F.J. 1990. Mora- San Miguel Regional Water Study and Forty Year Plan. Office of the State Engineer, Santa Fe, New Mexico.

Masse, W.B. 1981. Prehistoric Irrigation Systems in the Salt River Valley, Arizona. Science. 214 (4519): 408-415.

New Mexico Acequia Association (NMAA). 2008. Acequia Governance Handbook. www.lasacequias.org

New Mexico EPSCoR. 2011. Acequia Reserch Impacts. http://nmepscor.org/content/acequia-research-impacts

Peck, D.V., Lazorchak, J.M., and D.J. Klemm (Eds.). 2003. Western Pilot Study: Field Operations Manual for Wadeable Streams (DRAFT). United State's Environmental Protection Agency Office of Research and Development, Washington, D.C.

Phillips, D.H., Y. Reinink, T. E. Skarupa, C. E. Ester III and J. A. Skindlov. 2009. Water resources planning and management at the Salt River Project, Arizona, USA. Irrig Drainage Syst. 23:109–124.

Rivera, J.A. 1998. Acequia Culture: Water, Land and Community in the Southwest. University of New Mexico Press, Albuquerque.

Roach, W.J., J.B. Heffernen, N.B. Grimm, J. R. Arrowsmith, C. Eisinger, and T. Rychener. 2008. Unintended Consequences of Urbanization for Aquatic Ecosystems: A Case Study from the Arizona Desert. Bioscience. 58 (8): 715-727.

Rodriguez, S. 2006. Acequia: Water Sharing, Sanctity and Place. School from Advanced Research Press, Santa Fe, New Mexico.

Roybal, M. 2012. Measuring Acequia Functionality: Developing a tool for assessing New Mexico's community based irrigation systems. Unpublished Professional Project. University of New Mexico, Albuquerque. 123 pp.

Salt River Project website (SRP) 2011. http://www.srpnet.com

Shen, W., J. Wu, N. B. Grimm, and D. Hope. 2008. Effects of Urbanization-Induced Environmental Changes on Ecosystem Functioning in the Phoenix Metropolitan Region, USA. Ecosystems. 11: 138–155.

Stephens, D.B. and Associates, Inc. 2005. Mora-San Miguel-Guadalupe Regional Water Plan. http://ose.state.nm/isc_regional_plans8.html

Thomson, B. and A-M. Ali. 2009. Water resources assessment of the Mora River. http://hdl.handle.net/1928/9704

United States Department of Agriculture (USDA). 2007. Census of Agriculture: Volume 1: Chapter 2, County Level Data / New Mexico. http://www.agcensus.usda.gov/Publications/2007/Full_Report/Volume_1,_Chapter_2_County_Level/New_Mexico/

United States Geological Survey (USGS). 2012. Water Science for Schools. http://ga.water.usgu.gov/edu/wetstates.html

United States Geological Survey (USGS). 2009. USGS Real-Time Water Data for USA. http://waterdata.usgs.gov/nwis/rt

Western Regional Climate Center (WRCC). 2012. http://www.wrcc.dri.edu

CORRESPONDENCE SHOULD BE ADDRESSED TO:
Shannon M. Rupert
Department of Biology/University of New Mexico
srupert@unm.edu

THE CANALIZATON OF THE RIO GRANDE: A BRIEF HISTORY

Christopher Vigil

ABSTRACT - The largest water-control project undertaken in New Mexico during the 1930s was the Rio Grande Canalization Project, which aimed to minimize flooding by straitening the river and constraining the extent to which the river could meander. Like other such projects undertaken in the same period, the Canalization Project had multiple, long-term goals, which included flood-control, water conservation and storage, distribution of water and irrigation, as well providing jobs and stimulating local markets by creating demand for goods and services. But the Canalization Project had two other goals that set it apart from other water-control projects of the era: helping to fulfill the United States' treaty obligations to the Republic of Mexico, and stabilizing the international border shared by the two nations. This article focuses on the political strategy that led to the conceptualization and construction of the Canalization Project as national project in service of American foreign policy.

The Mesilla Valley is home to New Mexico's largest and most productive agricultural lands. Since the construction of Elephant Butte Dam in 1916, the region has produced cotton, pistachio nuts, chili, and beans as commercial commodities. It is also the location of Las Cruces, the second largest city in New Mexico, and the state's premier agricultural business hub. The Rio Grande Canalization Project was intended, in part, to serve this region's flood-control and irrigation needs, replacing *ad hoc* water-control systems with a modern project based on scientific engineering principles. The project was also intended to fulfill the United States' treaty obligations to the Republic of Mexico in regards to the distribution of the waters of the Rio Grande. Conflicts between the two nations had plagued their relationship since the end of the Mexican-American War in 1848. The Canalization Project was aimed at providing the means to end these problems.

The Rio Grande Canalization Project consisted of Caballo Dam and Reservoir in Sierra County, a series of diversion dams, a straightening of the river channel flanked by two parallel levees, and the American Dam and Canal at El Paso, Texas. With a span of 112 miles and an approximate width of 800 feet, the Canalization Project proved a superb feat of engineering.

HISTORICAL BACKGROUND

Since the Gadsden Purchase of 1853, which reconfigured the post-Mexican-American War international border between the United States and the Mexico, the two nations have shared a common boundary of 1,952 miles (International Boundary and Water Commission 1981: Introduction). As a result, both nations have been faced with many issues related to the management and distribution of the natural resources they share. In an effort to effectively address these concerns, the two nations mutually created the International Boundary Commission (IBC) by treaty in 1889 (U.S. Dept. of State 1960).

The initial purpose of the IBC was to track and resolve all problems arising out of the changing courses of the both the Rio Grande and the Colorado Rivers. In their natural state, both rivers meandered irrespective of the fictitious political borders. What this meant to individuals living on either side of the Rio Grande was that a shift of the river could literally move them

from one nation to the other. One good hard rain could redirect the river's course and place a Mexican farm in American territory, or vice versa. Until the beginning of the twentieth century, the mission of the IBC continued to be strictly related to resolving issues arising out of boundary disputes between the United States and Mexico.

At the dawn of the twentieth century, several groups within the United States created a political movement that sought the conservation of America's natural resources and the reclamation of arid lands (Robinson 1979). This movement culminated in the passage of the Reclamation Act of 1902, which provided federal loans for the development, or "reclamation" of arid lands through irrigation projects (Ibid). As part of this shift in attitude toward natural resources, the IBC became increasingly responsible for the use, management, and distribution of waters shared by each nation. This was especially true for the Rio Grande. Unlike the Colorado River, the Rio Grande served as an international border as well as a source of water for domestic, industrial, and agricultural use. In 1906, the United States and the Republic of Mexico entered into another treaty concerned with the distribution of the waters of the Rio Grande. By this agreement, the United States guaranteed to the Republic of Mexico the annual delivery of 60,000 acre feet of water from the river (U.S. Congress 1906). A commitment to fulfilling the United States' obligation to this treaty became one of the major reasons for the building of the Elephant Butte Dam and Reservoir in New Mexico in 1916 (Hundley1966).

With the advent of the Great Depression in the 1930s, well-established reclamation policies combined with the economic crisis to put water policy issues squarely into the American public sphere. Looking to reclamation as a possible source of economic stimulus, both the United States and Mexico entered into yet-another treaty in 1933, which gave the IBC an expanded mission (U.S. Congress 1933). Reflecting the hopes of reclamation advocates in the U.S., the IBC was charged with the "control and improvement of certain sections of the boundary-rivers" (International Boundary and Water Commission 1981: Introduction). In practice, the IBC became responsible for developing and implementing "immediate and long term solutions to flood-control, equitable distribution of waters, water conservation and storage, development of hydroelectric power, relocation and stabilization of river boundaries, and the solution of all border sanitation problems" (Ibid).

Along with the economic crisis and reclamation policy, the first early-1930s saw the rise of another ideology that came to bear on the Rio Grande: the "Good Neighbor Policy." This was Franklin D. Roosevelt administration's response to the diplomatic wreckage left throughout Latin America by the five previous presidential administrations. In an attempt to repair the political damage caused by U.S.'s military and economic intervention throughout Latin America, the Roosevelt Administration hoped to create a virtual alliance with the southern hemisphere. In the words of Roosevelt himself, the Good Neighbor Policy was "the policy of the good neighbor – the neighbor who resolutely respects himself and, because he does so, respects the rights of others – the neighbor who respects his obligations and respects the sanctity of his agreements in and with a world of neighbors" (Rosenbaum 1938: 14). In reality, the Good Neighbor Policy became simply a softer use of American muscle. Instead of using the Marines as a diplomatic tool, policymakers in the United States sought to achieve American hegemony in the region through "economic penetration, political subversion, non-recognition, [and] support of dictators" (Patterson *et al* 2000: 154).

The Good Neighbor Policy provided the diplomatic framework under which the negotiations for the 1933 treaty were conducted, and it became a major ideological component of the Rio Grande Canalization Project. American negotiators and diplomats were hesitant to insult

the revolutionary nationalism of their Mexican counterparts and, at the same time, remained committed to limiting Mexico's water use to the amounts specified in the 1906 treaty. American negotiators were intent on maximizing water use for the U.S., in anticipation of urban development in the Mesilla and El Paso Valleys.

A strong supporter of Roosevelt's Good Neighbor Policy, Congressman Dennis Chávez (D-NM) saw the Canalization Project as a winning prospect for all sides. In Chávez's view, the project would economically benefit New Mexico, improve relations between the U.S. and Mexico, and strengthen his political position both locally and nationally. Working closely with N. B. Phillips, manager of the Elephant Butte Irrigation District (EBID), Chávez was instrumental in shaping the 1933 treaty. By crafting a successful political campaign that aimed to sell a canalization project in New Mexico as part of the United States' treaty obligations to Mexico, Chávez and Phillips expanded the purpose of the treaty and brought to New Mexico the Canalization project - the largest water-control project of the decade.

THE SCOPE OF THE CANALIZATION PROJECT

During the 1930s, the Rio Grande was reconsidered through the eyes of reformers. In the view of many officials concerned with water policy, the Rio Grande surged through the state as an untamed river in need of control. This was an attitude widely held throughout the United States in general and in New Mexico in particular. During the first years of the 1930s, New Mexican newspapers often humanized the Rio Grande, portraying the uncontrolled lengths of the river as destructive and deviant, running with "menacing" and "angry waters" (*Socorro Chieftain,* May 27, 1937; and *Roswell Morning Dispatch,* May 29, 1937). The Rio Grande was untamed and dangerous, and policy makers sought to civilize the river and harness its power for private profit and public service.

Canalization meant that the meandering Rio Grande would be stabilized through a series of parallel canals designed to catch floodwaters and facilitate irrigation deliveries to the state's largest agricultural communities – all located in Sierra and Doña Ana counties. The canalization would also keep the river flowing in a stable, permanent channel, thus providing maximum predictability and control of the river, especially in times of flooding. Caballo Dam and Reservoir, as the northernmost point of the project, was conceived as a way to control the overflow from Elephant Butte Dam, storing the water for use in the future development of hydroelectric power for the Lower Rio Grande Basin. At the southern end of the project, the American Dam and Canal would serve to stabilize the international border at El Paso and provide the first diversions of water for Mexican storage and use. In addition to the Caballo and American Dams, there were to be four secondary diversion dams, 130 miles of flood-control levees, and dozens of flumes and siphons, each serving to divert waters for flood-control and irrigation for nearly 250,000 acres.

ECONOMIC CRISIS IN THE MESILLA VALLEY

As a member of Congress, Dennis Chávez was perfectly placed for each phase of the Rio Grande Canalization Project. In 1931, his first term in the U.S. House of Representatives, Chávez had managed to gain a seat on the House Committee on Reclamation and Irrigation. It was during this time that the Canalization Project first passed through the various congressional committees on its way to approval. By the time the project came up for final approval in 1935, Chávez had been appointed senator, as well as a member of the Senate Foreign Relations Committee, which made the final recommendation on the project to Congress and to President Roosevelt. Chávez

not only served on committees crucial to the development and realization of the Project, he was also the key figure in the effort to place the project under the jurisdiction of the United States Department of State (Lujan 1999, Vigil 2006).

The original river-control plan developed and recommended to Congress and the Department of State by the IBC had nothing to do with New Mexico. In a report to the Department of State in 1930, the IBC had recommended that an extensive canalization project be undertaken entirely in Texas, between Ft. Quitman and the Gulf of Mexico (U. S. Congress, House of Representatives April 1930). In their report, the IBC commissioners had argued that the canalization was necessary due to the meandering nature of the Rio Grande and the problems that ensued when residents on either side of the river found that a spring flood had literally placed them in the other country, and/or completely destroyed their property.

Serious flooding along this leg of the Rio Grande occurred about every five years, resulting in millions of dollars in damage and affecting hundreds of thousands of people on both sides of the border (Vigil 2006). In addition, since the Rio Grande served as an international border, residents on either side of the river were powerless to construct effective flood-control systems. They needed some sort of international agreement. Local attempts to improvise flood-control dams, especially on the American side of the river, often served only to redirect floodwaters onto Mexican soil, causing damage and provoking a string of complaints and lawsuits against the U.S. (U. S. House of Representatives Committee on Flood-Control 1935). As recommended by the IBC, the solution to this problem was for the two nations to enter into negotiations aimed at producing a new treaty concerned with the canalization of the Rio Grande in Texas. Congress approved the plan, and in 1931 authorized $287,000 for the State Department to undertake a joint study with Mexico to develop a comprehensive plan for the project (U. S. Department of State January 3-June 27, 1931).

These events were watched very closely by New Mexico's Congressional delegation, especially Chávez, who, like all good western politicians, was interested in getting as many federal dollars for his state as possible. As a newly elected member of the House of Representatives with a seat on the House Committee on Reclamation and Irrigation, he had great leverage in deciding which projects moved forward and which died in committee. This was no small matter, because competition for federally funded water projects was fierce and involved all forty-eight states.

Large landowners and farmers in the Lower Rio Grande Valley were also deeply interested in these events. Fortunately for them, they had a brilliant and aggressive advocate in N. B. Phillips, an engineer with a taste for land speculation. Phillips saw great potential benefit for both New Mexico and private individuals from any large-scale federal water projects that the state could secure. As the manager of the irrigation district serving lands from Elephant Butte Dam to El Paso, Phillips was familiar with the problems and potentials of the Lower Rio Grade Basin. As he saw it, one of the biggest problems lay in the growing burden of tax-based assessments to the Bureau of Reclamation in repaying the construction costs for Elephant Butte Dam. Phillips and the EBID Board of Directors bore continual witness to farmers succumbing to the double burden of decreasing crop prices and an inflexible system of tax-based construction repayments (Vigil 2006).

Phillips had seen first hand the punitive aspects of the tax-based repayment system of the Bureau of Reclamation. Since the 1929 Crash, he had witnessed many farmers in the irrigation district fall in arrears on taxes, trapped in a downward spiral of decreasing crop prices and past-due construction payments. As manager of the EBID, Phillips was charged with initiating legal

proceedings against farmers in tax default, which often resulted in foreclosure. As early as the summer of 1927, the directors of the EBID had sought from the Bureau of Reclamation some sort of construction-repayment relief for the irrigators. In the view of the District, payments for these construction charges were "higher than settlers could face" (Elephant Butte Irrigation District Library, Meeting Minutes of the Directors of the Elephant Butte Irrigation District, September 6, 1927). But, the small landholders and farmers faced a real problem: while the district directors did attempt to lower tax-based construction payments, the directors themselves apparently did not have much empathy for individual water users who fell delinquent in their taxes (Vigil 2006).

By the fall of 1927, the district had decided to adopt a policy of confiscating lands in lieu of unpaid taxes – a means of increasing the district's "proper assets" (Ibid September 29, 1937). By May 1929, the District embarked on a program aimed at reducing the amount of tax-delinquent lands by confiscating the properties and offering them to adjacent landowners. This policy virtually guaranteed that impoverished landowners would be pushed aside and that their wealthy neighbors would consolidate more land into fewer hands (Ibid, May 17, 1929). Out of this situation, land speculation began to take root, with Phillips at the forefront. By the end of 1930, there was no relief from tax-based construction payments forthcoming, despite the deepening economic crisis in the region. This ensured that more cheap irrigated lands would be up for grabs by the valley's more prosperous businessmen.

By 1931 the situation had became desperate for many small farmers. Not only were they often in tax arrears and in danger of losing their land, if they wanted any additional water they would be obliged to go into debt to the EBID. This was a boon to prosperous landowners in the Mesilla Valley interested in increasing their holdings. Later in the same year, the EBID passed a resolution calling for a moratorium on collecting unpaid water fees during the resale of foreclosed land. The EBID felt that forgiving the unpaid fees would make the land "attractive" to potential buyers (Ibid, July, 1931). Interestingly, when many of these foreclosure cases were brought to court, the EBID was often found to be overestimating land holdings and overcharging water fees (Vigil 2006). In dozens of cases, the district was ordered to correct acreage information and refund water users for overcharges (Elephant Butte Irrigation District Records, 1906-1974, Box 235, Folders 1 and 2). But the lure of cheap land could not redeem the Mesilla Valley. By the end of 1931, the income from the payment of water-use fees and construction charges had dropped almost to nothing. Something else had to be done.

THE CANALIZATION PROJECT

By the 1930s, the relationship between the Bureau of Reclamation and the members of the EBID had seriously deteriorated. In the view of the Irrigation District, the Bureau had caused hundreds of thousands of dollars in flood damages through ill-conceived and poorly placed diversion dams and canals. In addition, water rushing out of the spillway from Elephant Butte Dam was filling the Rio Grande with silt, thus raising the riverbed and increasing the instances of flooding. At the end of 1929, L. G. Mayfield, then president of the EBID, met with Lawrence M. Lawson, the American commissioner of the IBC. They discussed having a delegate from the district accompany the El Paso delegation to Washington, D.C., to lobby in favor of building the Caballo Dam as a way of slowing the accumulation of silt in the river (Vigil 2006).

This attempt stalled until late 1931, when Chávez and Phillips began discussing the possibility of an even larger scale project with Commissioner Lawson. Together, Chávez and Phillips developed a strategy in which they would link their desired project with the original

recommendations of the IBC and promote the plan to the Department of State as a necessary part of the nation's obligations to Mexico under the treaty of 1906 (Ibid). Lawson, as the head of the American Section of the IBC, was supportive of the plan, and he lobbied on its behalf at both the Bureau of Reclamation and the Department of State (Ibid).

In 1932, the Elephant Butte Irrigation District, under the leadership of Phillips, financed and undertook an independent study aimed at developing a plan for the canalization of the Rio Grande from just below Elephant Butte Dam to El Paso, Texas (Ibid). The intent of the EBID study was to link its project to the larger proposal recommended by the IBC in 1930. In October 1933, the EBID submitted its proposal to United States Congress (Dennis Chávez Papers, box 193, Folder 1). In its report to Congress, the EBID argued that local, state, and federal *ad hoc* flood-control and irrigation projects had led to a cycle of increased flood damage and the need for repair (Ibid). The financial burden of these damages almost always fell on the federal government. The district argued that, in the long run, it would be more cost efficient for the U.S. to spend the one-and-three-quarters of a million dollars on canal projects along the middle length of the river rather than continue to pay for an endless stream of damage claims, many of which were illegitimate. In the view of the EBID, the Rio Grande was a menace that had be brought under human control in order to better serve human needs. If left to its natural course, the river would not only wreak havoc on the inhabitants of the Middle Rio Grande Valley, it would also cost the federal government millions of dollars in damage claims.

Much of this argument was true. For over six hundred years, the Rio Grande had periodically flooded the valley floor. But for most of this time, the valley's inhabitants had built their permanent settlements in respect to the river's characteristic behavior. With homes out of the reach of the river's floodwaters, the pre-twentieth-century inhabitants of the Middle Rio Grande Valley - Indian, Hispanic, and Anglo – had lived in relative harmony with the Rio Grande. They had good reason to do so. In addition to remaining on dry ground, they were able to take advantage of the rich alluvial soil that the floodwaters deposited on their farmlands. It is unclear whether or not they knew this was the source of the land's continual fertility. Nevertheless, by living outside of the river's flood plain, they were able to secure an adequate livelihood (Vigil 2006).

Except for the Indigenous peoples of the Middle Rio Grande Valley, the twentieth-century inhabitants did not share the worldview of their predecessors. The view of the EBID was probably representative of most non-native New Mexicans living in the Mesilla Valley. If earlier inhabitants had viewed life in the valley in terms of sustainable agriculture, their twentieth-century counterparts saw life in terms of science, technology, and prosperity. Sustainability was no longer the issue; instead, they focused on efficiency and, if at all possible, a tidy profit.

But flooding was not the only issue that concerned the EBID. In its proposal, the District emphasized the interstate and international character of the Rio Grande. With its origins in southern Colorado, the river provided the source of irrigable water for many farms in both Colorado and northern and central New Mexico. Below the Caballo Dam, the Rio Grande served the agricultural and domestic needs of southeastern New Mexico, the southwestern tip of Texas, and the northern region of the Mexican state of Chihuahua. In spite of this, the river channel largely remained in private ownership, something the district claimed was unsuitable for a river whose waters were subject to interstate and international water-sharing treaties.

Regional unemployment was another concern of the irrigation district. Now in its fourth year, the economic crisis of the 1930s was only getting worse, with no end in sight. With the creation of the Public Works Administration in June 1933, the hope of federal dollars loomed

large with the executive members of the District. (Ibid). The canalization project, they reminded Congress, would have to depend on an enormous number of manual laborers. Thus, the canalization of the Rio Grande would create a great number of jobs in a very poor section of the nation.

Their final recommendation was that the federal government purchase the entire river channel and several hundred feet of its immediate borderlands, thereby creating a federally owned strip of land a few hundred feet wide and over one hundred miles long (Ibid). Out of this purchase, the EBID also recommended that the federal government initiate a comprehensive flood-control and irrigation program that would span the entire length (Ibid). In this way, the United States could accomplish several goals. First, the canalization and dam projects would minimize flood damage while at the same time ensuring a reliable source of irrigation for farmers below the Caballo Dam. Second, by assuming ownership of the river and the land that bounded it, the federal government would ensure that its treaty obligations to Mexico could be fulfilled. Third, by funding the project with New Deal money, the United States could create employment in the region, helping to counter the consumer deficit that many New Deal technocrats blamed for the Depression.

But unlike many other reclamation projects, those who advocated for the canalization of the Rio Grande did not want the Bureau of Reclamation to fund the project. The Reclamation Act of 1902 had stipulated that any moneys used to fund projects would need to be repaid by taxes levied on the beneficiaries of the project in question. This was out of the question as far as the EBID was concerned, in light of the district's struggle with previous debts to the bureau (Ibid).

With all of this in mind, the goal of the Senator Chávez and N. B. Phillips was to sell the project to the U.S. as a fulfillment of the 1906 Treaty with Mexico. By doing this, the responsibility for the project's construction and maintenance, in perpetuity, would fall to the State Department. By placing the project under State Department jurisdiction, the irrigation district would avoid two unpleasant realities of reclamation projects. First, by identifying the canalization project as a State Department project, the irrigation district members would not be obligated to repay funds, as they would under the Reclamation Act of 1902. Second, since the canalization would be an *ongoing* foreign relations project, the State Department, not the EBID, would be obligated to pay for continued maintenance (Ibid). This was partly true. The canalization project would, in theory, help the U.S. meet its treaty obligations to Mexico, but an updated irrigation system for the EBID's own use, paid for by American taxpayers at large, was the primary motive. Plus, those EBID members who had bought foreclosed riverfront lands at basement prices would experience a tidy windfall, if and when the State Department purchased the riverbed.

This strategy was a gem of duplicity - despite the many benefits that the project would, in fact, provide New Mexicans. Any arguments that the project would help provide the Republic of Mexico with its annual 60,000 acre-feet of water were flatly hollow. The 1906 treaty used 60,000 acre-feet as the absolute minimum that Mexico should receive. This number was based on the desire of both governments to maintain an acceptable division of waters in the anticipation of future urban development in the region. In reality, Mexico was never in danger of receiving less than the guaranteed amount. In fact, the controversy during the 1930s revolved around the fact that Mexico was taking *too much* water annually - about 128,000 acre-feet (U. S. Congress. House of Representatives. Committee on Flood Control).

Whatever Chávez and Phillips may have felt about the ethical issues involved in resource management, all the evidence points to a bit of a ruse on the part of the EBID. In private correspondence between the interested parties, there is no mention of any commitment to Mexico or the treaty obligations. Instead, the leadership of the EBID made clear that they wanted Chávez to "exercise every precaution in shaping [the] canalization bill" so as to keep it under the jurisdiction of the State Department (N. B. Phillips to Dennis Chávez, April 29, 1936. Dennis Chávez Papers, Box 84, Folder 19). The Irrigation District made no secret (at least not to Chávez) about whose "best interest" it was looking out for (Ibid). The Irrigation District warned Chávez that he had to "safeguard against any encroachment on the part of the Department of the Interior," and reminded him of the "appreciation of the people in the district" for his efforts – a euphemistic reminder that those who are elected do not have to be reelected (N. B, Phillips to Dennis Chávez, April 23, 1936, Dennis Chávez Papers, Box 84, Folder 19).

Chávez was more than willing to go along with their plan. As a member of the Senate Committee on Foreign Relations, he pushed to have the canalization project sold as a foreign relations measure. But Secretary of the Interior, Harold Ickes was loath to turn the project wholly over to the State Department. In many respects, this made perfect sense. After all, for over three decades the Department of the Interior had been gaining valuable expertise in the reclamation of arid lands. As far as the Department of the Interior was concerned, the State Department knew little (at most) about reclamation? When the EBID leadership caught wind of Secretary Ickes's reluctance to turn the project over to the State Department, it informed Chávez that it was "rather apprehensive" about the project falling under the control of the Bureau of Reclamation (N. B. Phillips to Dennis Chávez, July 18, 1935, Dennis Chávez Papers, Box 84, Folder 19). Phillips immediately wrote to Chávez in the "strictest confidence," advising that the senator resort to "rather unethical" tactics in bringing the project back under the complete jurisdiction of the State Department (N. B. Phillips to Dennis Chávez, July, 1935, Dennis Chávez Papers, Box 84, Folder 19). Whether Chávez followed Phillips' advice is not clear. Still, the negotiations continued, and in 1935 Chávez was able to elicit a lukewarm endorsement from Secretary Ickes, who coolly informed the House Committee on Foreign Affairs that the bill was "satisfactory from the standpoint of this Department" (House Committee on Foreign Affiars 1936: 46).

By 1935, all of the necessary political footwork had been done and each step of securing the project had fallen into place. In February, Congress appropriated 60,000 dollars to the IBC for investigation and planning. The investigation began in April, and the final report was submitted by the IBC to the State Department in December 1935 (International Boundary Commission. December 14, 1935). But a final report did not mean that the project was certain to be built. At the beginning of 1936, Chávez made his next move. Working with Congressman John Dempsey (D-NM), he drafted a resolution calling for the authorization of the Canalization Project. Knowing that any legislation concerning the project would be referred to the Senate Foreign Relations Committee, they decided to have Dempsey introduce the bill (H.R. 11768) in the House of Representatives. This strategy sent the bill right to Chávez, who sat on the Committee that made the final recommendation to Congress - all without any appearance of a conflict of interest (Vigil 2006).

In May 1936, Chávez submitted the committee's favorable report to the floor of Congress, recommending the passage of the bill, S. 3536. Secretary of State, Cordell Hull also endorsed the plan. Hull recognized that the project would, to some degree, lighten the burden of the State Department by fulfilling the U.S.s' treaty obligations to Mexico. In the end, their efforts paid off. The Canalization Project was finally authorized by Congress and signed by Roosevelt

in June 1936. This was a major victory for Chávez, Phillips, the EBID, and the State of New Mexico (Vigil 2006).

CONSTRUCTION OF THE CANALIZATION PROJECT

Construction of the Canalization project began with the American Dam and Canal at El Paso, Texas, on January 6, 1937. (Ibid). Surveys for the canalization features in New Mexico commenced in August, and construction in New Mexico began January 15, 1938 (Ibid). The entire Canalization Project was completed on July 1, 1942. The total cost of the project's construction was $2,996,052, and the effort employed an average of 220 workers for a total of 2,749,192 hours worked (International Boundary Commission, January 31, 1943: 55). This was no small effort. During the eight years of construction, engineers and labor crews moved dozens of miles of highways and roads and built twenty-seven bridges (U. S. Congress. House of Representatives, March 1936; W. W. Baker, "Final Report on The Construction of the Canalization Feature of the Rio Grande Canalization Project, January 31, 1943," 1-4, IBWC Technical Library). Through the Canalization Project, the federal government also acquired nearly 11,000 acres through outright purchase, eminent domain, and condemnation (Ibid, 15, 30-33). The project was a mammoth undertaking involving fourteen federal, state, and municipal organizations, three states, and two countries (Vigil 2006). It was the largest water-control project that New Mexico had ever seen.

The amount of federal spending on the Canalization Project was considerable, yet the benefits for New Mexicans proved uneven. It is probable that the leadership of the EBID, plus wealthy residents of the Mesilla Valley, both engaged in land speculation in anticipation of the State Department's subsequent land purchases. Land speculation within the EBID was enough of a problem to elicit several requests from Lawrence M. Lawson, commissioner of the IBC, to put an end to the practice (Ibid). Those individuals who were involved certainly gained much financially. Small landholders looking to get out of agriculture may also have benefited from the purchase. In theory, all the residents of the Mesilla Valley gained through the benefits of better irrigation and flood-control. And, of course, many New Mexicans found employment working on the project - a lifesaving opportunity for those financially devastated by the Great Depression. However, there were some losers – those individuals who found themselves inextricably caught between high taxes, construction payments, and low agricultural prices. These were the people who lost their land without compensation. They were real human beings with real lives, and they endured genuine crisis.

One winner all the way around, however, was Dennis Chávez. Arriving on the national political stage in 1931, just as the Canalization Project was being initially discussed, Chávez found himself in the right place at the right time. He understood this and took full advantage of the opportunities that the political, social, and economic conditions of the United States presented. The success of the project meant that he could deliver to the people of New Mexico millions of dollars in federal spending, as well as hundreds of jobs. His ability to deliver to his constituents, rich and poor, Anglo and Hispanic, all but guaranteed his continued reelection. And, indeed, after 1936 Chávez won reelection each time he ran. He was instrumental in the development of many large-scale water-control projects, such as the Conchas Dam, the El Vado Dam, and the Alamogordo Dam Projects. However, the Rio Grande Canalization Project, due its great international and interstate importance, gave Chávez the political power he needed to become the undisputed leader of the political life of New Mexico.

REFERENCES

David Chávez Jr. Gubernatorial Campaign Collection, Center for Southwest Research, General Library, University of New Mexico.

Dennis Chávez Papers, Center for Southwest Research, General Library, University of New Mexico.

Clark, I. G. 1975. The Elephant Butte Controversy: A Chapter in the Emergence of Federal Water Law. Journal of American History: 61 (1975): 1006-1033.

Elephant Butte Irrigation District Library and Archive, Las Cruces, NM.

Elephant Butte Irrigation District Records, 1906-1974, Archives and Special Collections Department, New Mexico State University Library, Las Cruces, NM.

Governor Richard C. Dillon Papers, New Mexico State Records Center and Archives, Santa Fe.

Governor Arthur T. Hannett Papers, New Mexico State Records Center and Archives, Santa Fe.

Governor James F. Hinkle Papers, New Mexico State Records Center and Archives, Santa Fe.

Governor John E. Miles Papers, New Mexico State Records Center and Archives, Santa Fe.

Governor Clyde Tingley Papers, New Mexico State Records Center and Archives, Santa Fe.

Hundley, N. 1966. Dividing the Waters: A Century of Controversy Between the United States and Mexico. University of California Press, Berkeley.

International Boundary and Water Commission, United States Section, Technical Library, El Paso, Texas.

International Boundary and Water Commission. 1981. Technical Summaries of Projects Along the International Boundary Between the United States and Mexico.

International Boundary Commission. 1935. Final Report: Control and Canalization of the Rio Grande, Caballo Dam, New Mexico to El Paso, Texas.

International Boundary Commission. 1943. Final Report on The Construction of the Canalization Feature of the Rio Grande Canalization Project, January 31, 1943.

Lahart, E. 1958. The Career of Dennis Chávez as a Member of Congress, 1930-1934. Unpublished M.A. Thesis, University of New Mexico, Albuquerque. 147 pp.

Lujan, R. 1999. Dennis Chávez and the National Agenda: 1933-1945. New Mexico Historical Review 74: 55-71.

Lujan, R. 1987. Dennis Chávez and the Roosevelt Era, 1933-1945. Unpublished Ph.D. Diss. University of New Mexico, Albuquerque. 573 pp.

Patterson, T.G., J.G. Clifford, and K.J. Hagan. 2000. American Foreign Relations: A History Since 1895. Houghton-Mifflin, Boston.

Robinson, M. 1979. Water for the West: The Bureau of Reclamation, 1902-1977. Public Works Historical Society, Chicago.

Rosenbaum, S.I. (ed.). 1938. Public Papers and Addresses of Franklin D. Roosevelt, Vol. 2. McMillan, New York.

United States Congress. 1906. Statutes At Large 34, Part 3.

United States Congress. 1933. Statues At Large 48, part 2.

United States Congress, House of Representatives. 1935. Committee on Flood Control. Control of Flood Waters on the American Side of the Rio Grande in Texas: 74th Cong., 1st sess., 25 February 1935.

United States Congress, House of Representatives. 1930. Report of the American Section of the International Water Commission United States and Mexico. 71st Congress, 2nd Session, House Document No. 359, 21 April 1930.
United States Congress, House of Representatives. 1936. Committee on Foreign Affairs. Rio Grande Canalization Project: Hearings Before the Committee on Foreign Affairs. 74th Cong., 2nd sess., 10 and 13 March 1936.
U. S. Department of State. 1931. Press Releases: January 3-June 27, 1931, Weekly Issues Nos. 66-91A, 1931.
U. S. Department of State. 1961. Treaties in Force. U. S. Government Printing Office, Washington, D.C.
Robinson, M. 1979. Water for the West: The Bureau of Reclamation, 1902-1977. Public Works Historical Society, Chicago.
Vigil, C. 2006. Dennis Chavez and the Politics of Water, 1931-1941. Unpublished M.A. Thesis, University of New Mexico, Albuquerque. 150 pp.

CORRESPONDENCE SHOULD BE ADDRESSED TO:
Chris Vigil
vigilch@law.unm.edu